5000 Years Marble History in Troia and the Troad

Petroarchaeological Study on the Provenance of White Marbles in West Anatolia

Dissertation

der Mathematisch-Naturwissenschaftlichen Fakultät

der Eberhard Karls Universität Tübingen

zur Erlangung des Grades eines

Doktors der Naturwissenschaften

(Dr. rer. nat.)

vorgelegt von

Dipl.-Geol. Judit Zöldföldi

aus Mohács (Ungarn)

Tübingen

2011

Tag der mündlichen Qualifikation:	29.11.2011
Dekan:	Prof. Dr. Wolfgang Rosenstiel
1. Berichterstatter:	Prof. Dr. Dr. h.c. Muharrem Satir
2. Berichterstatter:	Prof. Dr. Ernst Pernicka

CONTENTS

APPENDICES

LIST OF FIGURES

LIST OF TABLES

SUMMARY

This study presents the first archaeometric results on Trojan white marble artifacts, using a multitude of analytic techniques. These artifacts were provided by the Troia Project, led by the late Professor Korfmann, and date from the Prehistoric to the Roman Empire. The primary goal of the study was to determine the provenance of the raw materials from which these marble objects were made.

Previous archaeometric results on Turkish and Greek marbles showed that provenance questions are often difficult to answer, even if a number of methods are available to study the material. A review of the existing data revealed that the archaeometric data are incomplete and, in turn, some sources seemed to be missing or were not yet analysed in detail. In order to increase our knowledge of the local material, the characterisation of a great number of marbles from West Anatolia was carried out for provenance purposes.

During the provenance analysis, a number of methods were applied to the Trojan archaeological samples and on marbles of the nearby regions, especially in the Troad and neighborhood. Many traditional techniques were used, such as macroscopic and microscopic investigation, grain size analyses, chemical investigations (RFA, AAS), the use of stable isotopic ratios ($\delta^{18}O$ und $\delta^{13}C$), and, furthermore cathodoluminescence studies. In order to determine the mineralogical composition XRD and EMPA were used. Additionally, $^{87}Sr/^{86}Sr$ ratios were measured. The quantitative textural analyses (QTA) that were used from time to time since the 1990s; were applied to the Trojan and West Anatolian marbles, moreover this method was improved and refined for the purposes of determining the provenance of the marbles.

Despite the fact that marble is a common material in the Troad and neighboring area, scarcely any of the investigated raw material stems from these quarries, neither in the Prehistoric nor Hellenistic nor Roman periods. The raw material of the investigated archaeological objects of the Prehistoric times stems from quarries in Southwest Anatolia; a few of them can be categorized as imported goods from Paros and Naxos. The raw material of the building stones of the Hellenistic and Roman periods was transported predominantly from Marmara, while a few of them also stem from Paros and Thasos. However, one new marble type can be recognized: it originated from Karabiga, close to Troia on the mainland of the Biga Peninsula on the opposite side of Marmara Island.

As a “by-product” of the study, a decision tree was developed, primarily for the Trojan and related marble material that defines a logically ordered sequence of measurement techniques, depending on the results of preceding measurements. Thus, this decision tree can be used to minimize the amount of the sample that has to be removed for analyses and also reduce the costs involved while maximizing the chances of determination the place of origin.

Since marble raw materials are available for study in different forms, like powder or fragments and in some cases thin sections cannot be created for quantitative textural or cathodoluminescence analyses, sample-type-specific decision trees were constructed, based on applicable methods. These decision trees may turn to be useful in provenance studies of other white marble occurrences as well.

ZUSAMMENFASSUNG

In dieser Studie werden die ersten Ergebnisse der archäometrischen Untersuchungen von Artefakten und Baumaterialien aus weißem Marmor aus Troia/Türkei vorgestellt. Die untersuchten Objekte stammen aus einer Zeitspanne vom Chalkolithikum bis zur Römischen Kaiserzeit und wurden vom Troia Projekt (damals unter der Leitung vom Prof. Korfmann) zur Verfügung gestellt. Das primäre Ziel der Studie war es, die Herkunft der Rohmaterialien dieser Marmor-Funde zu bestimmen.

Vorherige archäometrische Untersuchungen an anatolischen und griechischen Marmoren zeigten, dass die Frage nach der Herkunft oft schwierig zu beantworten ist, obwohl zahlreiche Methoden zur Verfügung stehen. Eine erste Zusammenstellung der vorhandenen Daten ergab, dass die Informationen und Daten über das Rohmaterial Marmor unvollständig sind. Einerseits wurden noch nicht alle Marmorvorkommen untersucht, außerdem sind die angewandten Methoden von Lokalität zu Lokalität sehr unterschiedlich. Aufgrund dieser Problematik und um unser Wissen über die lokalen Materialien zu ergänzen, wurde im Rahmen dieser Arbeit die Charakterisierung einer großen Anzahl von Marmor-Lagerstätten aus West Anatolien, zu Zwecken der Provenienzforschung durchgeführt.

Um die Herkunft der Rohmaterialien der untersuchten Objekte aus Troia zu bestimmen, wurden eine Reihe von traditionellen Untersuchungsmethoden angewandt sowohl an den archäologischen Materialien (62 Proben) als auch an den Rohstoffen (239 Proben), wobei schwerpunktmäßig die Marmorvorkommen in der Troas und Umgebung aufgesucht, beprobt und untersucht worden sind. Die Untersuchungsmethoden reichten von makroskopischen und mikroskopischen Beobachtungen, Korngrößenanalysen, Kathodolumineszenz-Mikroskopie, Bestimmung der mineralogischen Zusammensetzung (XRD, EMPA), chemische Analysen (RFA, AAS) bis zur Bestimmung von stabilen Isotopenverhältnisse ($\delta^{18}O$ und $\delta^{13}C$). Weiterhin wurden die $^{87}Sr/^{86}Sr$ Verhältnisse bestimmt, gerade auch im Bezug auf die Frage, ob und in welchem Ausmaß diese Methode für die Herkunftsbestimmung von Marmoren angewendet werden kann. Desweiteren wurde die quantitative Struktur Analyse (quantitative texture analysis; QTA), welche erst seit den 1990er Jahren im Einsatz ist, zu diesem Zwecke benutzt, bzw. verbessert und verfeinert.

Trotz der Tatsache, dass Marmor ein sehr verbreitetes Material in der Troas und der näheren Umgebung ist, wurden diese Rohstoffe nicht für die Herstellung von prähistorischen Marmorobjekten und kaum zur Konstruktion von hellenistischen und römischen Bauten in Troia benutzt. Die Rohstoffe der untersuchten archäologischen Objekte der prähistorischen Zeit stammen meist aus Südwest-Anatolien, neben einigen wenigen Objekten, deren Rohstoffe aus Paros und Naxos von den Kykladen stammen. Die Baumaterialien aus der hellenistischen und römischen Zeit wurden überwiegend auf der Insel Marmara gebrochen, wobei auch Rohstoffe aus Paros und Thasos vorhanden sind. Weiterhin konnte eine Marmorsorte aus dem in der näheren Umgebung gelegenen Karabiga identifiziert werden. Diese Lagerstätte liegt auf dem Festland an der gegenüberliegenden Seite des Marmara Island in der Nähe von Troia.

Als ein "Nebenprodukt" der Studie wurden Entscheidungspfade entwickelt, die in erster Linie zur Bestimmung der Herkunft der trojanischen, archäologischen Materialien aus Marmor in Troia dienen, aber auch für weitere Herkunftsbestimmungen an Marmoren, insbesondere im Ost-Mediterranen Raum zur Verfügung stehen. Der Entscheidungspfad definiert eine logisch geordnete Folge von Analysenverfahren, abhängig von den Ergebnissen der vorangegangenen Erkenntnisse. Somit kann man die Probenmenge, welche für die Untersuchungen an den wertvollen archäologischen Objekten entnommen werden muss, minimieren. Darüber hinaus besteht die Möglichkeit, die anfallenden Kosten der Analytik zu senken. Andererseits werden die Chancen für eine sichere Herkunftsbestimmung deutlich verbessert.
Da die untersuchten Materialien in unterschiedlicher Form zur Verfügung standen, wie zum Beispiel als Fragmente oder als Pulver, konnten nicht alle Methoden bei jeder Probe verwendet werden. Die Kathodolumineszenz-Mikroskopie oder quantitative Struktur Analyse können zum Beispiel nicht an Pulver-Proben durchgeführt werden. Um dieses Problem zu lösen, wurden die spezifischen Entscheidungspfade konstruiert.

ACKNOWLEDGEMENTS

The study presented in the following dissertation began within the framework of a three years scholarship of the Graduiertenkolleg “Anatolien und seine Nachbarn” at the University of Tübingen.

I would like to express my gratitude to Prof. Muharrem Satır, the former Head of the Department of Geochemistry and the supervisor of my dissertation, for the constant advice and support during this time. I am also very grateful to Prof. Manfred Korfmann, the Director of the Troia Project at that time, for encouraging me to study the problem of the marble provenance in Troia and for kindly allowing me to analyze the material from the excavations at Troia. I am also very grateful to Prof. Brian Rose, who helped me collect marble material of the Hellenistic and Roman archaeological material in Troia. I would like to express my thanks to Prof. Ernst Pernicka to the valuable remarks on my thesis and for willingness to examine my thesis. And at this time, I would like to express my warmest thanks to my colleague and friend Dr. Balázs Székely for his continuous presence along the long way to the end of this dissertation.

I would also like to express my thanks to the Colleagues and Friends for their help and support. I owe deep gratitude to Dr. Heinrich Taubald (University of Tübingen, Institute of Geoscience) who discussed the results of geochemical and isotope-geochemical analyses with me and made very useful suggestions for this study. He also kindly read the text several times and made many useful remarks. Dr. Wolfgang Siebel (University of Tübingen, Institute of Geoscience) performed the strontium isotope analysis and discussed its results with me. Mária Tóth (Hungarian Academy of Sciences, Institute for Geochemical Research, Budapest) ran the XRD analyses and was always a great help in the interpretation of the data. Dr. Mathias Westphal and Dr. Michael Marks (University of Tübingen, Institute of Geoscience) helped me carry out and interpret the electron microprobe analysis. Dr. Zoltán Lantos (Eötvös University, Budapest) and Dr. Bernadett Bajnóczi (Hungarian Academy of Sciences, Institute for Geochemical Research, Budapest) kindly helped run the cathodoluminescence analysis.

I would like to offer my warm thanks to the staff of the Geochemistry Group, University of Tübingen, especially to Gisela Bartholomä, Gabriela Stoschek, Bernd Steinhilber, Elmar Reitter and Marcella Schuhmann who helped me prepare the samples and perform series of analyses. The technicians of the Institute of Geoscience, University of Tübingen, Jürgen

Mällich and Indra Gill-Kopp, who prepared the thin sections analysed in the dissertation. Ute Wahl and Helga Mozer the Secretaries of the Geochemistry Group, University of Tübingen who always offered me their kind help in matters concerning the organisation of my work in Tübingen.

To Dr. Mustafa Kibaroğlu (University of Tübingen, Institute of Geoscience), Dr. Altug Hasözbek (Izmir University) and Dr. Gürsel Sunal (Istanbul University) I owe my thanks for many interesting discussions concerning the geology of Turkey and for practical help in acquiring data concerning the geology of the region.
I would like to express my thanks to all the participants of the Troia Project, especially Dr. Peter Jablonka, Dr. Jens Nieling, Diane Thumm, Christel Bock, Utta Gabriel for the help in Troia and the support in collecting the archaeological material for my studies on the Troian material.

Numerous friends have offered me their precious help and time during the long period of study: Judit Nagy and Dr. István Dunkl, Heide Varjú and Prof. Dezső Varjú, Regina Lischka, Dr. Farkas Pintér, Dr. Katalin T. Biró, Dr. Zsolt Kasztovszky, Dr. Judit Mihály, Dr. Vera Szilágyi, Dr. Katalin Gmélin, Prof. Wolfgang Frisch, Prof. Torsten Vennemann, Dr. Jana Göbel, Ibolya Györösy.

Special thanks must go to my Family, my parents, my husband and my son for their continuous support and trust.

PART I

AIMS OF THIS STUDY

The last decades have seen a rapidly increasing number of archaeometric studies that aim at understanding the technological and societal context of classic buildings, statues and artifacts. Among others, the marble artifacts have always played an important role in such analyses. This work deals with a specific category of marbles, grouped under the name white marbles. With regard to this, the marbles taken into consideration for this study are those that can be defined as crystalline carbonate rocks and consist, almost exclusively, of calcite and/or dolomite. They generally have the best technical and physical characteristics and were used for thousands of years as the noble material par excellence in architecture and plastic arts. An in-depth scientific knowledge of the properties and provenance of marbles has become an indispensable tool for classical archaeology and art history. In order to be able to answer questions concerning the societal aspects, trade connections and historic contexts, identifying the quarries of the origin of these marbles is an important issue. Commercial relationships and trade routes as well as changes in preferred material varieties and artistic styles influenced the ways of construction and left their fingerprints on the artifacts that we can still study today.
Archaeological and archaeometric activity have various focal points concerning the preferential archaeological age, excavation site and target artifacts. One of the very few sites worldwide that provides a wide variety of ages and types of artifacts is certainly the unquestionably famous archaeological site of Troia, a dream for all scientists that considered working on archaeological material. Since the site itself has an extremely long history and the findings are so diverse, it offers a great deal of opportunities to explore the unanswered questions of this recognized and well-maintained archaeological site.
The marble artifacts and building remnants form a specific group of Trojan objects. The marbles used for production of cult objects, objects for daily use and construction during the various periods of the settlement may stem from different sources; therefore, their provenance analyses may shed light on these not yet well-known historical aspects.

The primary goal of this study is the provenance analysis of the raw materials of marble objects from Troia between the Chalcolithic to the Roman period**,** and to draw conclusions from the acquired knowledge. By completing the investigations of Trojan marbles, the following questions have to be answered:

- Which marble raw material was used during the long history of Troia?
- Did the Trojan people use marbles from local sources of the Troad and neighbouring area?
- In which quantity were the famous Marmara marbles used in Troia?
- Are there any other marbles that were transported over greater distances from Anatolia and/or the Mediterranean Region?
- Are there any differences between the raw materials that were used during different historical periods?
- Are the results in agreement or disagreement with the archaeological theories of the cultural and exchange contact of Troia?

Fortunately, some Trojan artifacts were available to be sampled with less destructive methods. I collected powder samples of the prehistoric objects and fragments from the Hellenistic and Roman periods. These samples are the very first ones taken for archaeometric studies from the excavation of Troia and all of them sampled individual, separate objects. Thus, all samples were handled as individual entities during the analysis and, consequently, the provenance of each object was determined separately.

A further secondary goal of the study, in other words, a by-product of these activities was the characterisation of marbles from West Anatolia. From an archaeometric point of view, in turn, this spin-off result may also become important for similar studies concerning the research at other archaeological sites of Antiquity, especially in Anatolia.

A SHORT REVIEW OF MARBLE PROVENANCE ANALYSES

It is of great importance for archaeological exploration to identify marbles based on scientific data, because this knowledge enables implications and, in some cases, helps in maintaining cultural heritage. For instance, sculptures of uncertain attribution can be related to a specific origin or area of production. Properly dated monuments can provide us with information about when certain quarries had been in use. The marble material found in sunken cargoes enables implications on ancient trade routes. From the restoration point of view it is important to locate the quarry of origin of the marble of a damage object in order to use the original material for the reparatory works or to create replacements or copies, etc.

A number of marble provenance attempts have led to unsatisfactory results, especially those based exclusively on macroscopic examination or on visual evidence such as the colour, brilliance or grain size of the stone. This failure to determine the real source is essentially due to the inability of recognizing the fact that samples of marble from the same quarry often have different provenance-bearing properties while, on the contrary, samples from different quarries, sometimes a long way from each other, are very similar. On the other hand, it is important to emphasize that these properties are essential for a successful provenance determination.

Identification that is more reliable can be achieved based on the mineralogical and petrographic study of thin sections; however, some are often difficult and time-consuming to perform. Chemical composition in marble samples may also lead to valuable information on provenance. For example, certain Anatolian marbles can be distinguished from their Greek counterparts based on sodium and manganese content (RYBACH & NISSEN 1965), but this criterion cannot be used to discriminate between Greek mainland marbles and those from the Cyclades. The limiting factor of (geo)chemical provenancing of marbles is the separation or overlapping of specific petrographic properties of the various geographical regions.

The approach based on measurement of the isotopic ratios of carbon and oxygen is one of the most successful marble provenancing methods, even if, in many cases, it cannot be the single determining factor. In its first appearance, published by CRAIG & CRAIG (1972), it was possible to distinguish Greek marbles from Attica from their counterparts in the Cyclades. Later MANFRA *et al.* (1975) succeeded to distinguish marbles from various localities in Anatolia. Despite the increasing stable isotopic database ($\delta^{18}O$ and $\delta^{13}C$; e.g., HERZ 1988b; GORGONI *et al.* 2002b), it became subsequently clear that neither macroscopic observation nor

petrographic and geochemical studies alone would enable conclusive identification of the famous marbles used in Antiquity, while a combination of methods seemed more promising. The first proposal came from RENFREW & SPRINGER PEACEY (1968), who suggested combining a cathodoluminescence study with a petrographic study of thin sections. Another early multidisciplinary contribution involving a combination of petrographic characteristics (average grain size, type of crystal shape and structure, semi-quantitative assessment of accessory minerals) and the determination of the calcium/strontium ratio was proposed by LAZZARINI *et al.* (1980a). This geochemical ratio was considered especially important in pure marbles.

Another important analytical contribution was made by CORDISCHI *et al.* (1983), with the proposal to use electron spin resonance (ESR, later also termed as electron paramagnetic resonance spectroscopy, EPR) on the traces of manganese in marbles. As the method was applied to an increasing number of marbles, the initially encouraging results also showed similar overlap as in other methods (LLOYD *et al.* 1985). Eventually this method became one of the potentially applicable ones that can be used in combination with other techniques.

From the late 1980s on, numerous research groups proposed differing combinations of methods to improve provenance decisions. MOENS *et al.* (1988) made an important proposal involving the application of a combination of analytical, petrographic (including the introduction of MGS – maximum grain size) and geochemical methodologies. Using the proposed methods of these authors the attribution of marble artifacts to their quarries of origin was considerably improved but the method was still not ultimately conclusive. Finally, BARBIN *et al.* (1989) reconsidered the use of cathodoluminescence with significantly improved equipment and coupled with the petrographic study of the same thin section; this led to the determination of accurate cathodomicrofacies for the main marble types of Antiquity. Some of the aforementioned analytical techniques were applied in monographic studies of important marbles, including those from Carrara (HERZ & DEAN 1986), Thasos (HERZ 1987) and the Cyclades (GERMANN *et al.* 1988), all of which still provide substantial help to archaeometrists.

Considerable interest has been aroused by the determination of the rare earth elements BARBIN *et al.* (1991a) carried out with various methods including INAA (MELONI *et al.* 1995) and ICP-MS (GREEN *et al.* 2002). However, the same unresolved problems again arise for these trace elements (repeatability of results, their comparability when obtained with different analytical methods, content variability at small and large scale, etc.). EPR was further developed with the creation of larger databases, but it still cannot be considered as a single-

method-solution. Initially, EPR was combined with certain petrographic characteristics (ATTANASIO & PLATANIA 2002; POLIKRETI & MANIATIS 2002; ATTANASIO 2003; ATTANASIO *et al.* 2006) that could be seen with the naked eye, such as the maximum grain size, MGS. However, in the lack of MGS standard procedure it was not possible to improve this combination of methods. Later EPR was used together with other analytical procedures such as the stable isotopic technique, and subjected to statistical processing (ATTANASIO *et al.* 2002b; ATTANASIO *et al.* 2006).

The aforementioned technique, the determination of the maximum grain size has a long tradition in marble provenancing. More than a century ago, the determination of MGS was carried out with the naked eye (e.g., LEPSIUS 1890), and for longer time it remained a visually estimated parameter. By the end of the 20th century, measurements were carried out using simple techniques on thin section (e.g., GERMANN *et al.* 1988; CRAMER 2004), later more sophisticated derivative procedures came into application (e.g., MOLLI & HEILBRONNER 1999; OESTERLING *et al.* 2007; SZÉKELY & ZÖLDFÖLDI 2009).

An important proceeding in the isotopic investigations is the introduction of strontium isotope measurements (PENTIA *et al.* 2002) based on the proposal of HERZ (1985). Its extensive use is hampered by the work-intensive preparation and by the high cost of the analyses.

The last dozen years have seen the appearance of some very important studies of important marble occurrences, including those by PESCHLOW-BINDOKAT & GERMANN (1981) on the marbles of Miletus and Herakleia on Lake Latmos, by ASGARI & MATTHWES (1995) on Proconnesian marble (Island of Marmara), by BRUNO *et al.* (2002) on the marbles of Thasos, by BRUNO *et al.* (2000) and HERZ (2000) on the marbles of Paros, by LAZZARINI *et al.* (2002b) on Aphrodisian marble, and by MATTHEWS *et al.* (1992), PIKE (1999) and GOETTE *et al.* (1999) on Pentelic marbles. Several new quarries have also been discovered and characterised in recent years including those of the Greek islands of Skyros and Fourni (LAZZARINI & CANCELLIERE 2000b) and Tinos (LAZZARINI & ANTONELLI 2003) and the marbles of Anatolia such as those of Ionia and Caria, including the region of Ephesos (KOLLER *et al.* 2009).

In conclusion, many studies designed to identify the marbles used in Antiquity led only to results that were partial and not always satisfactory from a scientific point of view. A conclusion of the critical review of the literature is that the greatest uncertainty is due to the neglect of some marble-producing areas of the Mediterranean. Often only the best-known ones were analysed, ignoring others that may have been insignificant for the Greek and Roman periods but that could well have been significant sources in prehistoric times.

Furthermore, many other quarries have been revealed that might have contributed to the contemporaneous marble production.

Prior to this study, the knowledge base of the archaeometric community about Anatolian quarries were limited to a few marble occurrences (Figure 1) such as Afyon, Marmara, Uşak, Aphrodisias, Ephesos, i.e. the most famous marble quarries from historical times. Furthermore, the available information on the marble quarries is also unequal: a few "classic" and some popular target-quarries have been analysed by numerous methods, while others were included in studies with a focus on a specific method.

However, we have to consider, that marble occurrences in Anatolia are by far more widespread, and exceed these "celebrities". Nearly everywhere, the surface of West Anatolia provides useful pieces of rock without any great effort: various types of marbles cover approximately one third of West Anatolia. The first strategic step was to define what criteria should be used in order to identify marble as occurrences and "quarries". The location of the quarry in relation to the nearest settlement or to the communication routes, its position in the landscape, its lay-out, the properties of the extracted rock, the method of quarrying, the kind of tools used, and the character of human activity in the area – these are, in brief, the kind of facts that provide information on various aspects of quarrying.

Despite the advantageous outcropping and preservation situation, generally, it can be assumed that not all the quarries of ancient times have survived to our day. In those places where blocks were extracted, or rather levered out, weathering and other natural processes may have disguised the original appearance of the quarry. For these reasons some quarries may now be unrecognisable (BRUNO *et al.* 2009). Furthermore, all traces of quarrying may have been lost due to the large-scale industrial extraction of the valuable raw material in the last decades.

An important stimulus to scientific investigation over the last two decades was provided by the establishment of a topic-specific association of involved scientists, the ASMOSIA (**A**ssociation for the **S**tudy of **M**arbles and **O**ther **S**tones in **A**ntiquity).

New methods have been proposed and many new marbles and quarries, both major and minor, have been characterised. ASMOSIA introduced an important tradition in their contributions: the publication of original observation data in large quantities. ASMOISA also initiated important research trends.

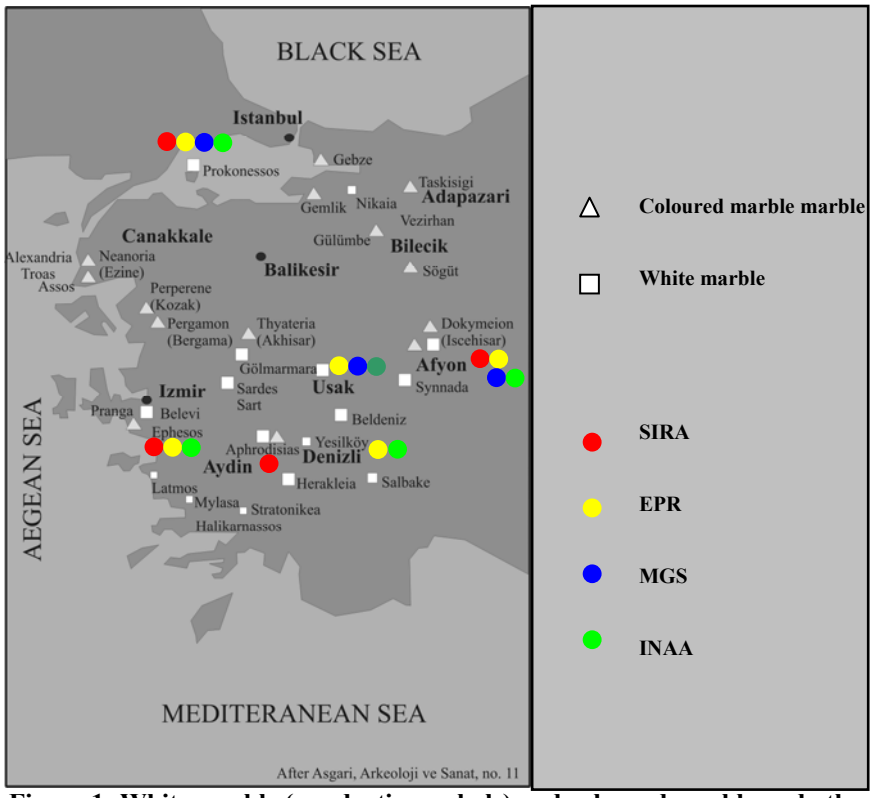

Figure 1: White marble (quadratic symbols) and coloured marble and other ornamental stone (triangle symbols) quarries in Western Anatolia (after ASGARI 1977). SIRA = stable isotopic ratio analyses; EPR = electron paramagnetic resonance; MGS = maximum grain size analyses; INAA = instrumental neutron activation analyses

PART II

ARCHAEOLOGICAL AND GEOLOGICAL OVERVIEW

1. The importance of marble provenance analyses of Trojan archaeological material

Regarding the remains from Antiquity, in museums or at archaeological sites the richness of marble statuary and buildings is amazing. Impressed by this richness, one can conclude that the marble was the most honoured material in Antiquity. The esthetical attractiveness of marble has always constituted an unquestionable aura of luxury. Despite the continuously changing types of societies and power constellations, marble has become more and more a symbol of official and private power, a means of expressing need for beauty, elegance, displaying wealth. It is a symbol of brilliance and luxury, its role had been recognised by society. Numerous very important great works were made of marble, which verifies its special role in the history of culture. Therefore, the high rank of this prestigious material from a historical point of view is generally acknowledged not only in history, but in cultural sciences, too.

Therefore, it is not surprising that researchers became more and more interested in the esthetical aspects of this material and its usage; they also turned their attention to technical and economical aspects. Numerous analyses deal with quarrying methods in the increasingly better-documented ancient quarries. Transport techniques and pathways and manufacturing techniques are at the centre of interest.

Furthermore, the provenance analysis also makes some implications on ancient trade relations as well as political and economical background of the construction activity possible. The quality of the applied material of archaeological objects gives us information about the economical and social situation of the population.

As Troia (**Fehler! Verweisquelle konnte nicht gefunden werden.**) was settled over 4000 years more or less continuously (3500 B.C. – 500 A.D.), this site offers an important and interesting reference point to study the above-mentioned hypothesis in Eastern Mediterranean archaeology. These excavations are very close to various marble quarries of the Troad that cover more or less the Biga Peninsula in Northwest Anatolia, including the marble quarries of the famous Ida Mountains (today Kazdağ Massif). Moreover, the well-known marble quarries of Proconnesos (today Marmara Island), whose quarries played a very important role in the

Hellenistic and Roman period in the Mediterranean region, are in the closest vicinity to Troia and a direct sea route is given. Therefore, the development of the usage of different marbles that was applied to produce the archaeological objects in Troia is of special interest to my research. The most important questions are:

* Where did the marbles that were used during the long history of Troia originate?
* Did the Trojan people use marbles from the local sources of the Troad and neighboring areas?
* In which quantity were the famous Marmara marbles used in Troia?
* Are there any marbles that were transported over greater distances?
* Are there any differences between the raw materials that were used during different historical periods?
* How is it possible to follow the trade and exchange system based on the scientific investigations of the provenance of the marble objects?

To broaden my investigation, and so have the possibility to give an overview of a larger interval of the marble usage in the Troad, Late Chalcolithic (4500 B.C. to 3500 B.C.) finds, excavated in the Kumtepe archaeological site 5 km northwest of Troia, were also analysed in the course of this work.

Figure 2: Position of Troia (© GoogleMap)

Figure 3: The remains in Troia today. (© Troia Project)

2. Archaeological overview of the Troia and of Kumtepe

In this chapter, I will present a short description on the development of the settlements of Kumtepe and Troia based on the publication by (KORFMANN & MANNSPERGER 1998; ASLAN *et al.* 2002; KORFMANN 2006) and the publication series of *Studia Troica* 1990-2010. Without going into the archaeological details, I would like to turn the attention to the find assemblages of a given period and to make comments on trade and exchange with other archaeological sites in the Eastern Mediterranean.

2.1. Prehistoric Times in Troia and the Troad

2.1.1. Late Chalcolithic Period in Kumtepe

The archaeological records demonstrate a new set of parameters in metallurgy, architecture and ceramics. In Kumtepe, it may be that there are Balkan/Thracian or Southeast European influences indicating a progressive migration from the north to the south. Findings suggest a movement of nomadic-pastoral tribes within the area and the infiltration of groups with differing traditions from Southeast Europe. Most probably mariners to and from the Aegean in the West brought cross-cultural exchanges. The artifact corpus indicates that the Chalcolithic community was part of wider northwestern and possibly southwestern Anatolian

cultural settings. The geography of this cultural area extends from the Eastern Aegean to Kumtepe, south to Lycia and east to the western border of the Konya plain.

2.1.2. The Bronze Age in Troia

Troia I (ca. 3000-2350 B.C.) belongs to the "Maritime Troia Culture" of the Early Bronze Age. It was the earliest settlement and had eleven building phases. It was a village with rough stone circuit walls, which were strengthened repeatedly (brown features in Figure 5). From this earliest level of Troia, metal needles, pins and awls were recovered. Figurines, adzes, hammer stones, grinders, querns and marble vases represented the ground stone industry, while the chipped stone industry is represented by flint tools. Obsidian from the Aegean island of Melos made its appearance for the first time at Troia in the chipped stone corpus.

Troia II (ca. 2550-2250 B.C.) the ″burnt city″ is one of the most impressive monuments of prehistoric archaeology. The southeast and southwest gates have typical entrance chambers (yellow features in Figure 5). A further gateway and a roofed colonnade separate the interior. Within lie large long houses with porches – the ″megaron″ style of building. The artifact repertoire of Troia II is legendary for its wealth. It is most important because it clearly demonstrates that exchange systems were well developed between Troia and other cities in Anatolia, the Cyclades and the Greek mainland. Troia had trade partners reaching out in all directions of the compass, and are masterpieces of artisanship such relicts, at this date, are rarely found outside of Mesopotamia and Egypt. The ground stone industry was enhanced by a steatite bowl, marble pestle and nephrite adzes. Industries established in Troia I continued with figurines.

Troia III (ca. 2250-2200 B.C.) It is assumed that the settlement was rather impoverished, with small houses and narrow streets. The artifact corpus is considerably poorer than in Troia II. The ground stone, chipped stone and bone industries show a continuation of artifacts associated with both Troia I and II.

Troia IV-V (ca. 2200-1700 B.C.) was known as "The Anatolian Troia Culture" and took place during the Early Bronze Age III and the beginning of the Middle Bronze Age. The material culture and probably the citadel continued to develop without serious interruption. Over the centuries, the settlement expanded to cover an area of 18,000 m^2. The artifact corpus continues in the tradition of the earlier periods and the ground stone, chipped stone and bone industries show few innovations. The final building-phase was destroyed by fire.

Troia VI (ca. 1700-1300 B.C.) is the beginning of the "Trojan High Culture" at the Middle to Late Bronze Age. This period is an important time for Troia because newcomers rebuild the

site. A completely new ducal or royal citadel was built covering an area of 20,000 m^2 (pink features in Figure 5). In size, and probably in importance, it surpassed the citadel previously known at Hisarlik and all others so far investigated in Asia Minor. Eight building phases were identified. The fortifications were built according to a new style: 552 m long and technically superior, consisting of gently sloping walls of ashlars masonry with offsets and massive towers. Behind the citadel wall, buildings in the interior were built on concentric terraces rising up towards the centre of the citadel. There were large, freestanding buildings, but these are only preserved around the edge of the Acropolis, behind the fortification wall. The final building phase of this period met its end due to a severe earthquake. The population was estimated at 7000. These findings place Troia among the larger trade and palatial cities of Asia Minor and the Near East in this period. Troia is linked into this trade network at a variety of levels. There were intense commercial and cultural links with the Aegean and with Mycenae, documented by Mycenaean pottery, which occurs ever more frequently as time goes on.

Troia VIIa (ca. 1300- 1200 B.C.) The remains of the houses of Troia VI, together with parts of the citadel walls, were repaired and re-used. There is no cultural break between Troia VI and Troia VIIa, but the buildings have a clear arrangement and are noticeably smaller and more cramped. There is an increase in the population.

2.1.3. Early Iron Age in Troia

Troia VIIb1, VIIb2 and VIIb3 (ca. 1200-1000 B.C.) The influence of the Balkan region is evident. In some respects, these phases show continuity from the preceded phases. Yet there are significant new cultural elements in both the lower and the upper levels. Handmade pottery suddenly re-appears after 1000 years of the potter's wheel. The lower parts of the walls are now faced with irregular, vertically placed stone slabs. How Troia VIIb1 perished is unclear. There was no destruction. Probably the settlement was taken over by a related cultural group. Phase VIIb2 was brought to an end by fire (red feature in Figure 5).

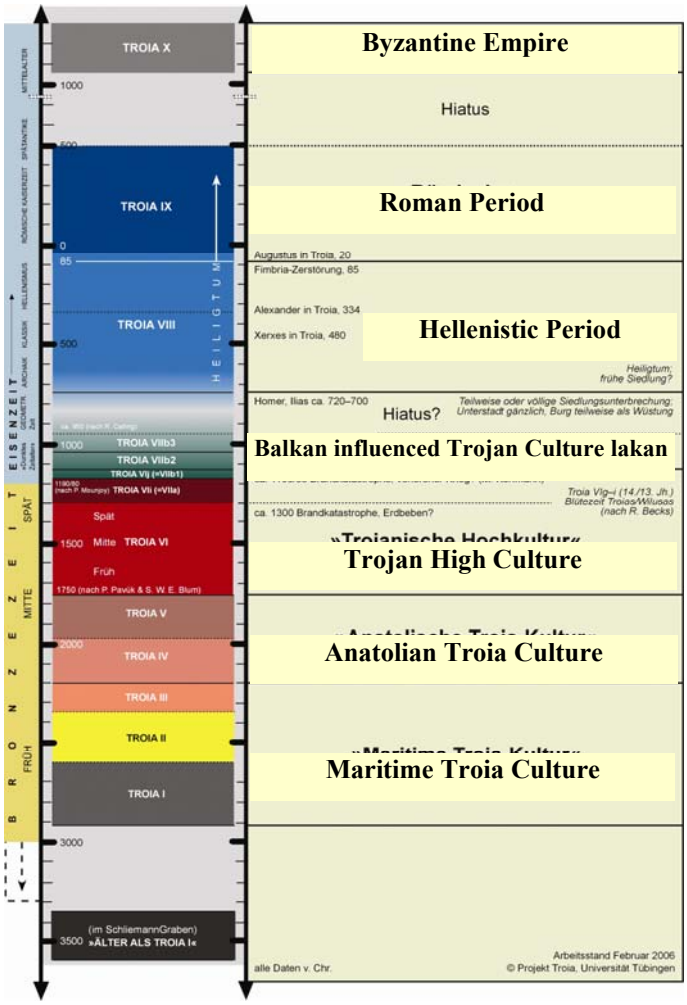

Figure 4: Stratigraphy of Troia. (©Troia Project)

2.2. The Hellenistic Period in Troia

Troia VIII (ca. 700 B.C. – 85 B.C.) Centuries later, at the time when Homer lived (8th century B.C.), most of the abandoned sites in Asia Minor, such as Troia were re-settled by Greeks. At first, it was a modest settlement, but later and especially from the beginning of the third century B.C., Troia was widely known as the ″Holy City of Ilion″. This period is characterised by the building of the sanctuary dedicated to Cybele to the southwest of Troia and of a temple to Athena inside the citadel (blue features in Figure 5). Of the temple itself, nothing remains apart from a few blocks from the substructures of the altars and some scattered marble components. When the temple was built, if not before, the central and most elevated buildings of Troia VI and VII were cut away.

The Athena Temple**:** The foundation trenches were dug ca. 240–230 B.C. and the carving of the superstructure was probably completed during the first half of the second century. The project appears to have been initiated by Antiochus Hierax, although it must have been completed with Attalid financial assistance. The closest architectural parallels are with Pergamon, Samothrace, and Macedonia, and they indicate a clear interaction among northern Aegean sanctuaries and their architects. There were probably metopes on all four sides representing a Gigantomachy, Ilioupersis, Amazonomachy, and Centauromachy, in deliberate imitation of the Parthenon in Athens. Two of the reliefs ascribed to the Ilioupersis cycle are identified as scenes of the death of Lykaon and Sarpedon. The plan of the Athena Sanctuary and, in particular, the layout of the temple, altar, and well were influenced by the tradition of the Locrian maidens, which had been revived at approximately the same time the temple was being designed. Consequently, both the architecture and the sculpture of the Sanctuary effectively exploited the Homeric associations of the site. The blocks of the archaic temple were apparently reused in the construction of the Hellenistic Athenaion, which explains the first temple's absence in the archaeological record (ROSE 2003).

The Athenaion appears to have sustained comparatively little damage in the Fimbrian attack during the Mithridatic wars, and the Augustan renovation was not extensive. The bronze inscription on the architrave of the temple, generally assumed to be that of Augustus, is here reassigned to Julian the Apostate. The archaeological evidence assembled here sheds considerable light on the reliability of the accounts of Hellenistic and Roman Ilion by Strabo, Appian, and Livy (ROSE 2003).

The Athena Temple Portico: A portico bordered the sanctuary on the east, south, and west sides; the north side was left unenclosed so as not to hinder the breathtakingly beautiful view of the Dardanelles. It was probably built during the Augustan renovation.

The Bouleuterion: It is clear that the ground behind and to the west of the Bouleuterion sloped up sharply toward the temenos of Athena. Many of the blocks of the building were shaped from marl. Marl was consistently used for the foundations of Troia VIII and IX buildings. DÖRPFELD unearthed statuary bases of Augustus and Tiberius within the Bouleuterion and therefore assigned the building to the early Roman Imperial period. ROSE (2003) declared that the foundation might have been associated with the early Hellenistic Bouleuterion of Ilion. It is clear that at some point in the late Antiquity the building was damaged, thereby making repairs to the roof and upper walls necessary. Several blocks of limestone were inserted and several inscribed blocks were used in the reconstruction of the walls. In 85 B.C., the Romans destroyed the site Troia and so all the buildings.

2.3. The Roman Period in Troia

Troia IX (85 B.C. – 500 A.D.) Later Ilion or Ilium The Temple of Athena was rebuilt; it was developed especially under the rule of Emperor Augustus whose imperial family honoured Troia as the supposed home of their ancestors (Aeneas). The preserved ruins of the monument include (blue features in Figure 5):

(1) long sections of the massive foundations supporting the porticoes and surrounding walls of the 9,500 m^2 rectangular sacred precinct;

(2) sport and bath complex with mosaic floors (no longer preserved);

(3) large theatre situated in a natural hollow to the northeast of the temple hill. At the beginning of the 4th century A.D., Constantine the Great at first planned to build his capital at Ilion and construction work began. Ilion received its water supply from the foothills of Mount Ida by means of aqueducts and clay pipes.

(4) altars and an assembly-hall, the Odeion, a small, roofed theatre from the period of Augustus and rebuilt under Hadrian, were located on the southern slope of the ruins of ″Sacred Ilios″. The columns of the scene were fashioned from grey marble while those in the eastern and western wings were a pinkish brecciated marble. The orchestra of the Odeion is fairly deep and surrounded by a limestone wall that was originally faced with marble and topped by a low marble cornice. ROSE (1993) found evidence for at least three phases of construction for the scene. (i) The first stage was wooden and its date is difficult to determine since the surrounding area was cut by subsequent rebuilding and by the Dörpfeld-Blegen trenches. However, it must date before the Hadrianic period. Its orientation conforms to the Roman city plan; it is likely that the Odeion was part of the Augustus renovation of the city. (ii) The second phase was the most elaborate. The stage itself was still wooden, but the rear now featured an aediculated façade of two stories – Ionic below and Corithian above. Grey marble columns with pinkish brecciated columns in the wings formed both stories and broken pediments crowned the central aediculae. Much of the marble revetment for the back wall of the second scene was found collapsed behind it and the range of marble represented is extraordinary: Brecciated marble from nearby Ezine, cipollino, pavonazetto, africano, and Proconnesian white marble were all recovered. Engaged pilasters mixed reeded and regular fluting, and there were opus sectile panels featuring white, purple, yellow and green marble arranged in geometric shapes. This was clearly an expensive building to erect. At a later point, the theatre was substantially damaged and repaired.

(5) Children of Claudius inscription: The Inscription to Claudius is a marble Doric architrave

and frieze (discovered by Rose in 1993). It was carved in one piece, which contains part of a dedication to the emperor Claudius.

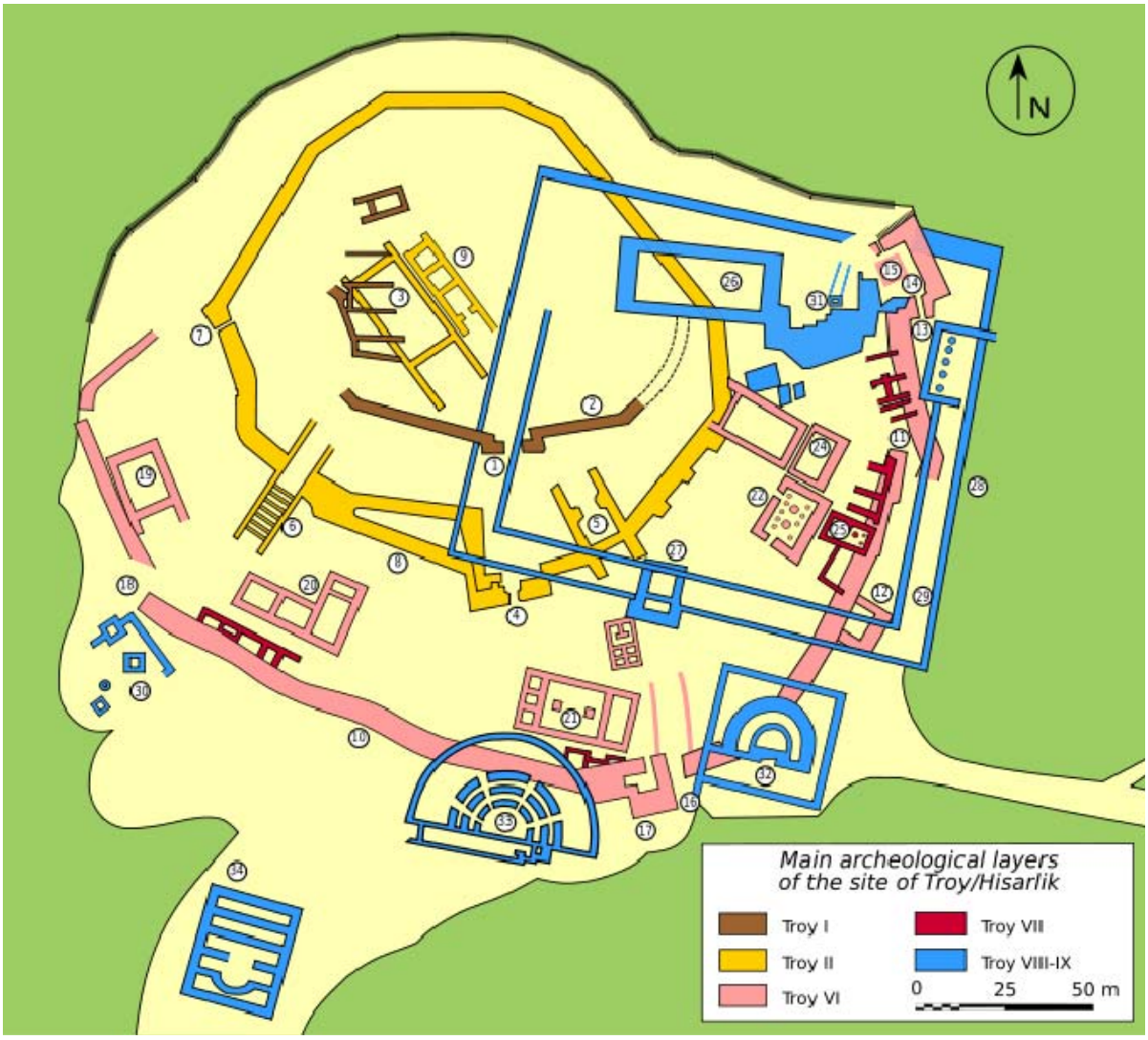

Figure 5: Plan of the archaeological site of Troy. 1 – Gate, 2 – City Wall, 3 – Megarons, 4 – FN Gate, 5 – FO Gate, 6 – FM Gate and Ramp, 7 – FJ Gate, 8 – City Wall, 9 – Megarons, 10 – City Wall, 11 – VI. S Gate, 12 – VI. H Tower, 13 – VI. R Gate, 14 – VI. G Tower, 15 – Well-Cistern, 16 – VI. T Dardanos Gate, 17 – VI. I Tower, 18 – VI. U Gate, 19 – VI. A House, 20 – VI. M Palace-Storage House, 21 – Pillar House, 22 – VI. F House with columns, 23 – VI. C House, 24 – VI. E House, 25 – VII. Storage, 26 – Temple of Athena, 27 – Entrance to the Temple (Propylaeum), 28 – Outer Court Wall, 29 – Inner Court Wall, 30 – Holy Place, 31 – Water Work 32 – Bouleuterion, 33 – Odeon, 34 – Roman Bath. (Data from http://www.goddess-athena.org/Museum/Temples/Troy/Troy_Plan.html).

3. Tectonic setting of Anatolian marbles

Turkey forms an east-west bridge between Europe and Asia and also straddles the geologic boundary between Gondwana and Laurasia along a north south transect. It was not a single entity until the early Tertiary, when several continental fragments with independent Paleozoic and Mesozoic geologic histories were assembled during a complex sequence of events leading to the collision of Gondwana and Laurasia (OKAY & TÜYSÜZ 1999; OKAY *et al.* 2008). Figure 6 shows the sutures and major continental fragments in Turkey and the surrounding regions. There are six major lithospheric fragments in Turkey: the Strandja, the İstanbul and the Sakarya Zones, the Anatolide-Tauride Block, the Kırşehir Massif and the Arabian Platform. The first three - Strandja, İstanbul and Sakarya Zones – are collectively known as the Pontides and show Laurasian affinities. They were only slightly affected by the Alpide orogeny and preserve evidence for Variscan and Cimmeridge orogenies. The Pontic terranes were amalgamated into a single terrain by the mid-Cretaceous times. The Anatolide-Tauride Block south of the Pontides shows Gondwana affinities but was separated from Gondwana in the Triassic and formed an extensive carbonate platform during the Mesozoic. The Pontides (Strandja, İstanbul and Sakarya Zones) are separated by the İzmir-Ankara-Erzincan Suture from the Kırşehir Massif and the Anatolide-Tauride Block, the latter is in contact with the Arabian Platform along the Assyrian-Zagros Suture (Figure 6).

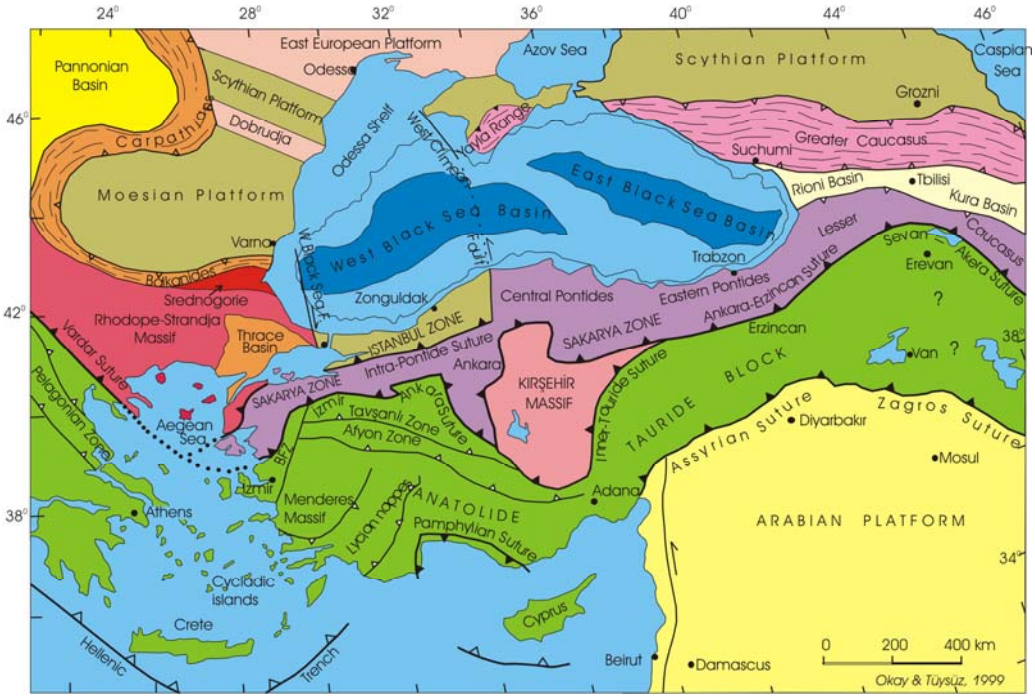

Figure 6: Tectonic map of the northeastern Mediterranean region showing the major sutures and continental blocks. (OKAY & TÜYSÜZ 1999).

Although separated by the Assyrian Suture, the Anatolide-Tauride Block shows a similar Paleozoic stratigraphy to that of the Arabian Platform, and hence to the northern margin of Gondwana. The Anatolide-Tauride terrane was intensively deformed and partly metamorphosed during the Alpine orogeny; this lead to the division of the Anatolides-Taurides into several zones based on the type and age of metamorphism. The Kırşehir Massif, which consists mainly of metamorphic and granitic rocks with Cretaceous isotopic ages, is in contact with the Anatolide-Tauride Block along the controversial Inner Tauride Suture. The Intra-Pontide Suture represents the former plate boundary between the Sakarya, İstanbul and Rhodope-Strandja Zones (SENGÖR & YILMAZ 1981; SENGÖR *et al.* 1982; OKAY 1989b; OKAY & KELLEY 1994; OKAY *et al.* 1994; OKAY & TÜYSÜZ 1999; OKAY *et al.* 1996; OKAY 2008).

I will briefly present the relevant geological features of the major geological units, which include marbles in different quantities and qualities that were sampled and investigated in this study. They are the Rhodope-Strandja Massif (especially Cetmi Melange) and the Sakarya Zone (including the Kazdağ Range, Karakaya Complex and Armutlu-Ovacik Zone), both located north of the Izmir-Ankara-Suture and collectively labeled "***Troad and neighboring areas***" (Figure 7) in Northwest Anatolia in this work. South of the Izmir-Ankara-Suture, hereafter "***Middle and Southwest Anatolia***", the Anatolide-Tauride Block (including the Menderes Massif and Central-Anatolide-Tauride Block) was sampled and will be discussed in this study.

Figure 7: Major units of the investigated area that will be discussed in this study.

3.1. Geological overview of the Troad and neighbouring areas with respect to marble

3.1.1. Rhodope-Strandja Massif

The Strandja Zone of Turkey represents the eastern continuation of the Rhodope Massif of northeastern Greece and southeastern Bulgaria. Stratigraphically, it consists of a basement of highly deformed metamorphosed rocks in amphibolite facies intruded by late Carboniferous extensional Permian granites (OKAY *et al.* 2001). This basement is erratically overlain by a Triassic transgressive sequence, comprising continental to shallow marine metasediments (AYDIN 1974; CAGLAYAN *et al.* 1988; OKAY *et al.* 2001; SUNAL *et al.* 2006; SUNAL *et al.* 2008). Recently, SUNAL et al. (2006) showed that the orthogneisses that are intrusive into the metasediments are late Carboniferous in age (between 300 and 315 Ma). The metasedimentary units in the basement lack fossils and thus their age was inferred from regional tectonic correlations. CAGLAYAN *et al.* (1988) proposed a Paleozoic age for the basement rocks. OKAY *et al.* (2001) inferred that country rocks of the Kırklareli pluton are late Variscan in age and TÜRKECAN & YURTSEVER (2002) estimated their age as Precambrian. This sequence extends into the Middle Jurassic of the Bulgarian part of the Strandja Zone (CHATALOV 1988). The Rhodope area is also characterised by the occurrence of melange-like units in the allochthonous nappes of northern Greece and eastern Bulgaria, where unmetamorphosed Mesozoic series locally occur as scattered klippen over the crystalline basement. The Late Jurassic – Early Cretaceous period corresponds to an important deformational regime involving all the previous units (Austrian phase or Balkanic orogeny s.l., (GEORGIEV *et al.* 2001). The deformation is sealed by Cenomanian conglomerates and shallow marine limestones followed by Senonian arc-related magmatic rocks. All these previous units were finally affected by the Alpide orogeny s.l., creating a new generation of northward-oriented thrusts in the latest Cretaceous–Oligocene. In the Turkish part of southern Thrace, sediments of the Cenozoic Thrace basin that obscure the structural relations between the Strandja Zone and the southern Biga Peninsula cover the Strandja Zone.

3.1.2. Sakarya Zone

The Sakarya Zone is an east-west oriented continental fragment, about 1500 km long and 120 km wide, between the Anatolide-Tauride Block to the south and the İstanbul and Strandja zones and the eastern Black Sea to the north (Figure 6). It includes the Sakarya Continent (SENGÖR & YILMAZ 1981) as well as the Central and Eastern Pontides, which show a similar

stratigraphic and tectonic development (OKAY 1989a). The crystalline basement of the Sakarya terrane can be broadly divided into three types:

– A high-grade Variscan metamorphic sequence of gneiss, amphibolite, marble and scarce metaperidotite; the high-grade metamorphism is dated to the Carboniferous (330-310 Ma) by zircon and monazite ages from the Kazdağ, Pulur and Gümüşhane Massifs (TOPUZ *et al.* 2004a; TOPUZ *et al.* 2004b; TOPUZ *et al.* 2006; TOPUZ *et al.* 2008; OKAY & SATIR 2006; OKAY *et al.* 2006).

– Palaeozoic granitoids with Devonian, Carboniferous or Permian crystallization ages (DELALOYE & BINGÖL 2000; OKAY *et al.* 2002; OKAY *et al.* 2006; TOPUZ *et al.* 2007).

– A low-grade metamorphic complex (the lower Karakaya Complex) dominated by Permo-Triassic metabasite with marble and phyllite. The Lower Karakaya Complex represents the Permo-Triassic subduction-accretion complex of the Palaeo-Tethys with Late Triassic blueschists and eclogites (OKAY & MONIE 1997; OKAY *et al.* 2002), accreted to the margin of Laurussia during the Late Permian to Triassic.

3.1.2.1. Kazdağ Range

The Paleozoic continental basement of the Sakarya Zone (Figure 8) consists of granitic and metamorphic rocks (OKAY *et al.* 1996). The metamorphism was at high-grade-amphibolite facies to granulite facies with local anatexis. This zone had a complex thermo-tectonic history, with Mid-Carboniferous (Hercynian), Late Triassic (Kimmeridgian), and Oligo-Miocene (Alpine) thermal events. The basement of the Biga peninsula between Edremit Bay and the Sea of Marmara is composed of calcschist, metaquartzite, schists, serpentinites, and marble. They are well exposed in the tectonic window of the Kazdağ Ranges.

3.1.2.2. Karakaya Complex

The Paleozoic basement is tectonically overlain by the Karakaya Complex, which consists in some regions, such as Manyas and on the island of Marmara, of Permo-Triassic carbonates (OKAY *et al.* 1996). They are several hundred meters thick and have undergone high-pressure, greenschist-facies metamorphism (Figure 9).

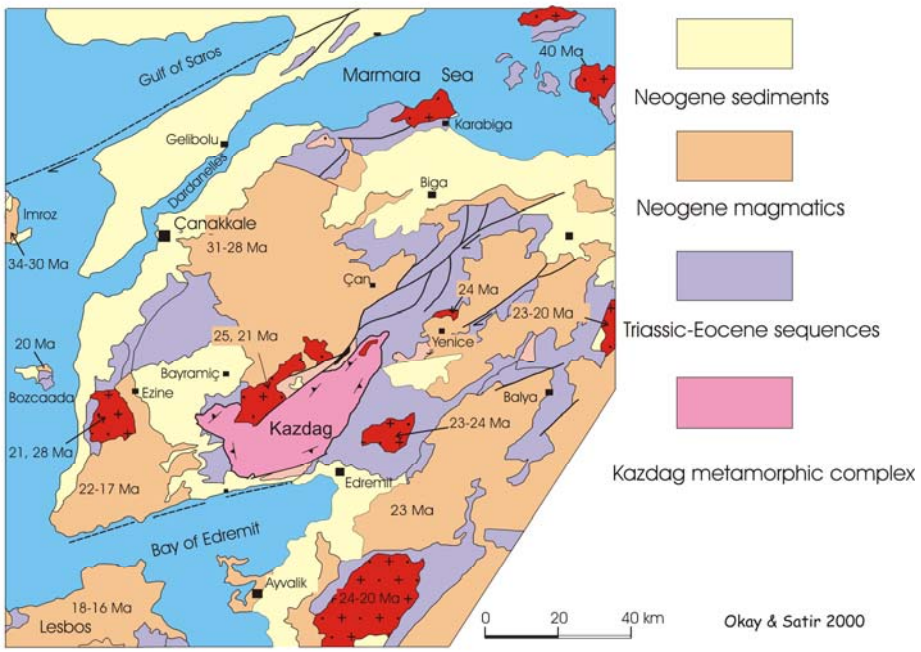

Figure 8: Simplified geological map of the Biga peninsula (OKAY & SATIR 2000)

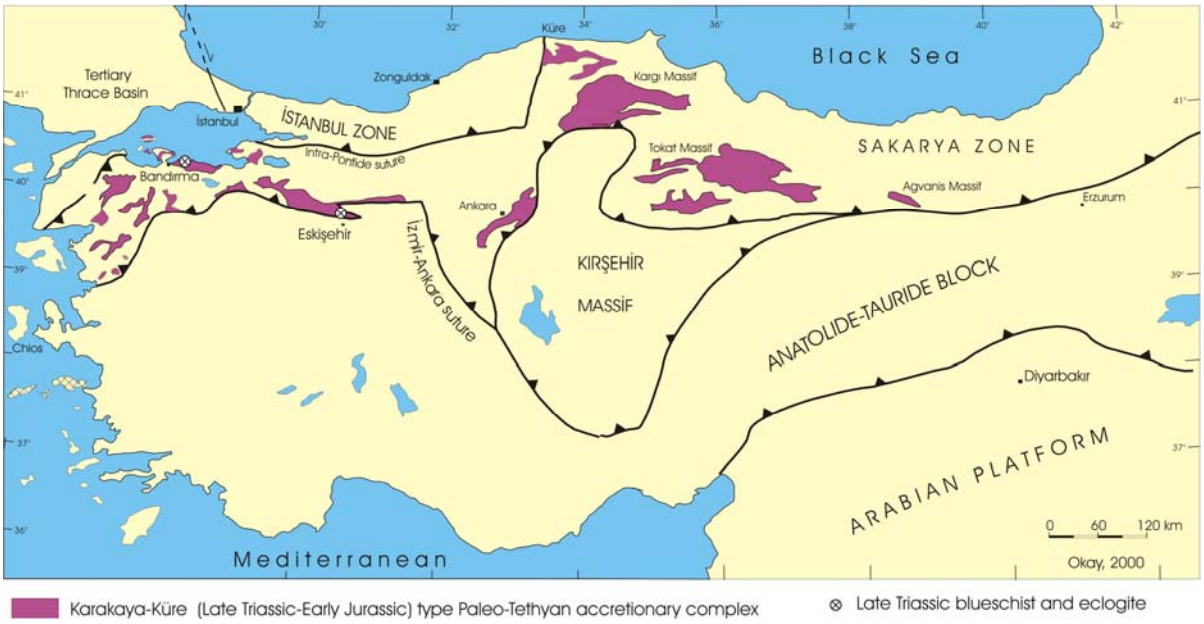

Figure 9: Distribution of the Karakaya Unit in Turkey (violet fields). The crystalline basement is also shown on the map. (OKAY 2000)

3.1.2.3. Armutlu-Ovacık Zone

The basement of the Armutlu-Ovacık Zone, near Iznik Lake (Figure 10), consists of metavolcanite, graphite-schist and metaclastics interbedded with recrystallised limestones (GÖNCÜOGLU & ERENDIL 1990; OKAY *et al.* 2008). These are overlain by a Permo-Triassic marble sequence. This unit passes upward into white, recrystallised, cherty limestones (GÖNCÜOGLU & ERENDIL 1990). Metamorphic sequences include both a low-grade metavolcanic-metaclastic-carbonate unit and a high-grade sequence of amphibolite and gneiss. A complex geology coupled with scarce biostratigraphic data, lack of isotopic ages and poor exposure resulted in a wide variety of contradictory models for the evolution of the Armutlu Peninsula (e.g., USTAÖMER & ROBERTSON 1994; ELMAS & YIGITBAS 2005; OKAY 2008).

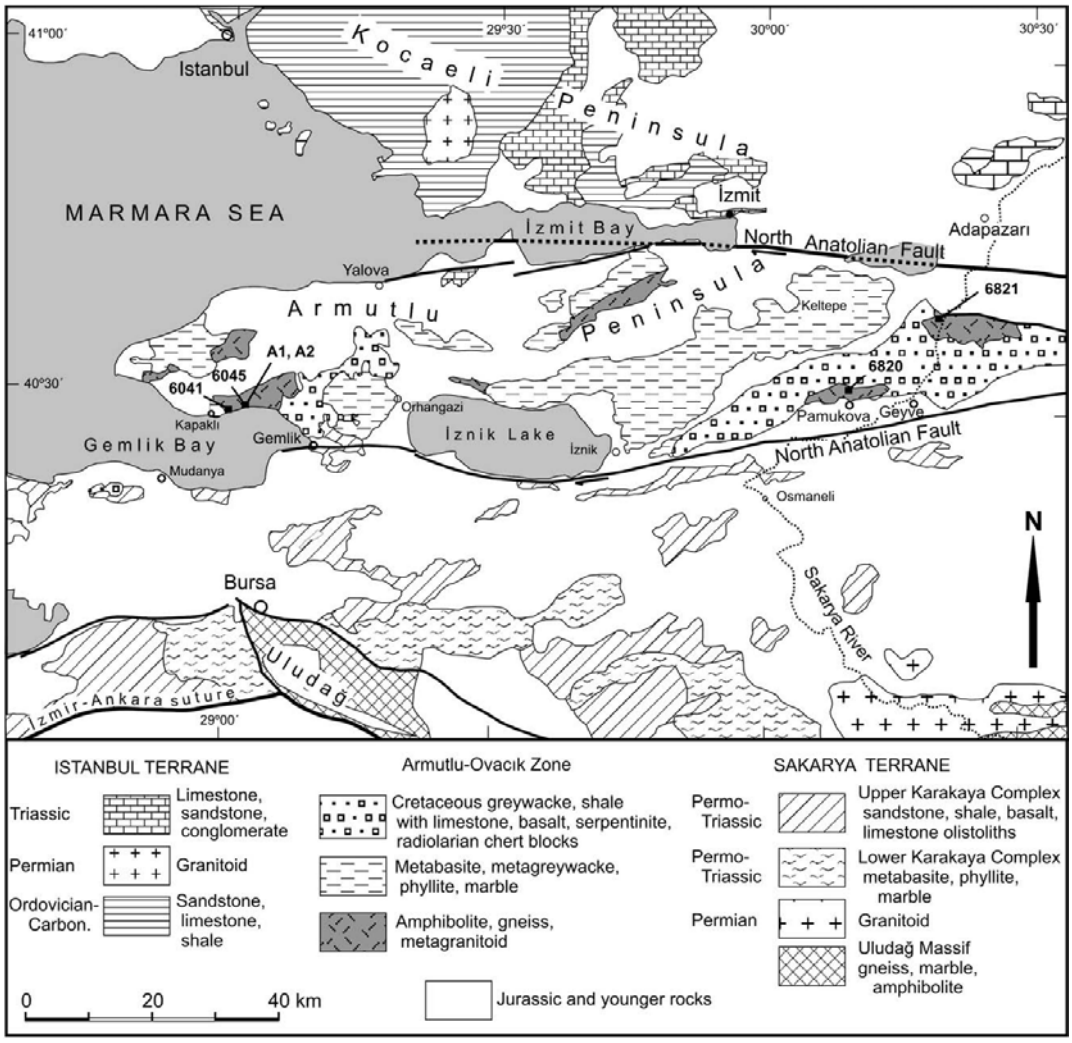

Figure 10: Geological map of the Armutlu-Ovacik Zone (after (OKAY *et al.* 2008).

3.2. Geological overview of Middle and Southwest Anatolia in respect of marble

The Anatolide-Tauride Block forms the bulk of middle and southern Turkey and, in contrast to the Pontide continental fragments, shows a similar Paleozoic stratigraphy to the Arabian Platform and hence to that of Gondwana (MONOD *et al.* 2003). During the obduction, subduction and continental collision episodes in the Late Cretaceous-Paleocene, the Anatolide-Tauride Block was in the footwall position and therefore underwent much stronger Alpide deformation and regional metamorphism than that observed in the Pontide zones. During the Senonian, a massive body of ophiolite and an accretionary complex were emplaced over the Anatolide-Tauride Block. The northern margin of the Anatolide-Tauride Block underwent HP/LT (high pressure / low temperature) metamorphism at depths of over 50 km under this oceanic thrust sheet. Erosional remnants of this thrust sheet of ophiolite and accretionary complex occur throughout the Anatolide-Tauride Block. In the Turkish geological literature, the accretionary complex is often referred to as ophiolitic mélange. However, it generally lacks a matrix and is structurally more similar to an imbricate thrust stack. With the inception of continental collision in the Paleocene, the Anatolide-Tauride Block was internally sliced and formed a south to southeast verging thrust pile (OKAY 2008). The compression continued until the Early to Mid-Miocene in western Turkey and is continuing in eastern Anatolia even today. The lower parts of the thrust pile to the north were regionally metamorphosed, while the upper parts to the south form large cover nappes. This leads to a division of the Anatolide-Tauride Block into zones with different metamorphic and structural features in a similar manner to the subdivision of the Western Alps into Helvetics and Penninics, albeit with a different polarity. There are three main regional metamorphic complexes (Figure 6): A Cretaceous blueschist belt, the Tavşanlı Zone to the north, two Barrovian-type metamorphic belts, the Afyon Zone from the Paleocene age and the Menderes Massif of Eocene age farther south (OKAY 2008).

3.2.1. Menderes Massif

The Menderes Massif forms a large metamorphic terrane (Figure 11 and Figure 12). It is bounded on the north and northwest by the ″İzmir-Ankara ophiolite zone″ (SENGÖR & YILMAZ 1981) and on the south by the Lycian Nappes (DE GRACIANSKY 1972). To the east and northeast the border is poorly defined. To the west the Menderes Massif extends across the Aegean Islands to the Pelagonic zone of the Hellenides (DÜRR 1975; DÜRR *et al.* 1978). It is part of the Alpine orogen in Turkey and comprises an inner crystalline core and a

surrounding schist belt. It is mainly composed of gneissic granites, migmatites, mica-schists and marble succession. In several previous studies, the gneissic granites and amphibolite-grade micaschists were described as the Precambrian core. The metapelites with marble lenses and emery-bearing massive marbles were defined as the Paleozoic-Mesozoic cover series of the Menderes Massif (DÜRR 1975; SENGÖR & YILMAZ 1981; SENGÖR *et al.* 1984; SATIR & FRIEDRICHSEN 1986; HETZEL *et al.* 1998). In the Tire region, the Menderes Massif is represented by a thick metasedimentary sequence including marble intercalations from the Triassic-Jurassic age (GÜNGÖR & ERDOGAN 2001, 2002).

The Mesozoic sequence of the southern Menderes Massif mainly consists of massive platform-type neritic marbles. The uppermost part of the Mesozoic sequence is characterised from bottom to top by emery-bearing marbles, rudist-bearing marbles, reddish pelagic marbles and flysch-like rocks. This sequence was metamorphosed to greenschist-facies conditions (SATIR & TAUBALD 2001; ÖZER *et al.* 2001). The rocks of the Menderes Massive experienced complex polymetamorphism. The most intensive metamorphism that led to anatexis is certainly pre-Alpine (AKKÖK 1983; SATIR & FRIEDRICHSEN 1986; CANDAN & KUN 1991; DORA *et al.* 1992). The Alpine metamorphism shows a progressive increase in grade from the schist belt toward the core (BASARIR 1970, 1975; DÜRR 1975; CAGLAYAN *et al.* 1980; AKKÖK 1983; EVIGREN & ASHWORTH 1984; ASHWORTH & EVIGREN 1985; SATIR & FRIEDRICHSEN 1986; BOZKURT 1996; BOZKURT & SATIR 2000), which is followed by a late Alpine retrograde metamorphism present in the core and schist belt. This event, called Main Menderes metamorphism, buried the Menderes Massif beneath the Lycian Nappes during Paleogene collision.

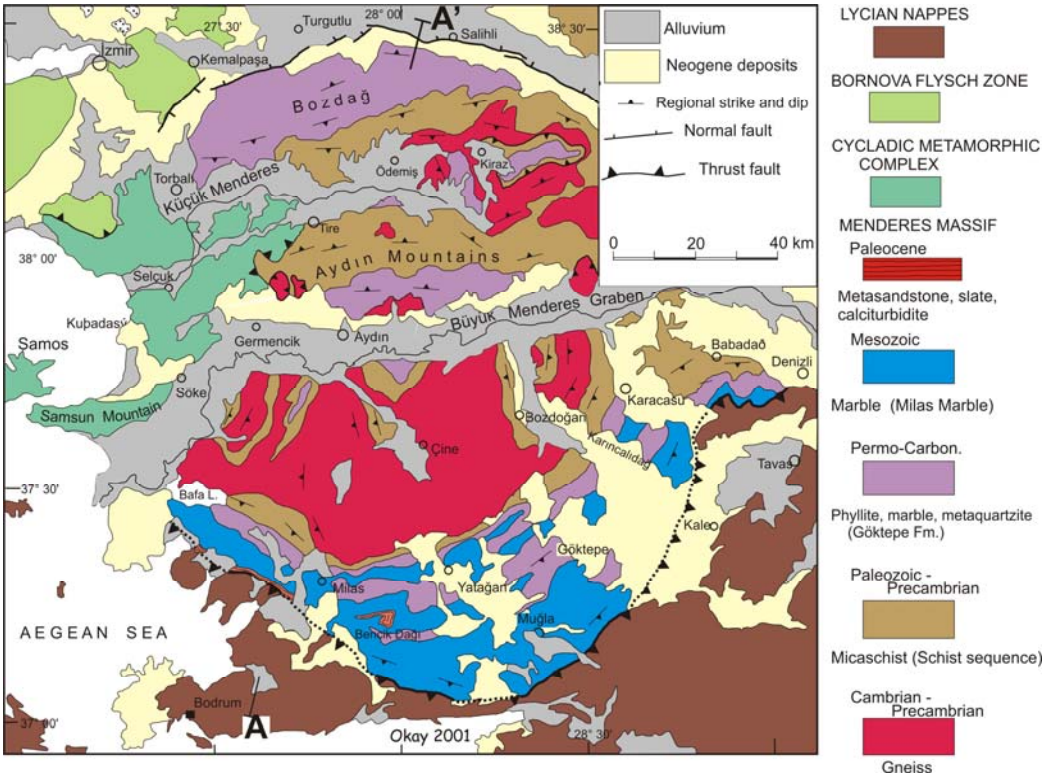

Figure 11: Geological map of the Menderes Massif (OKAY 2001)

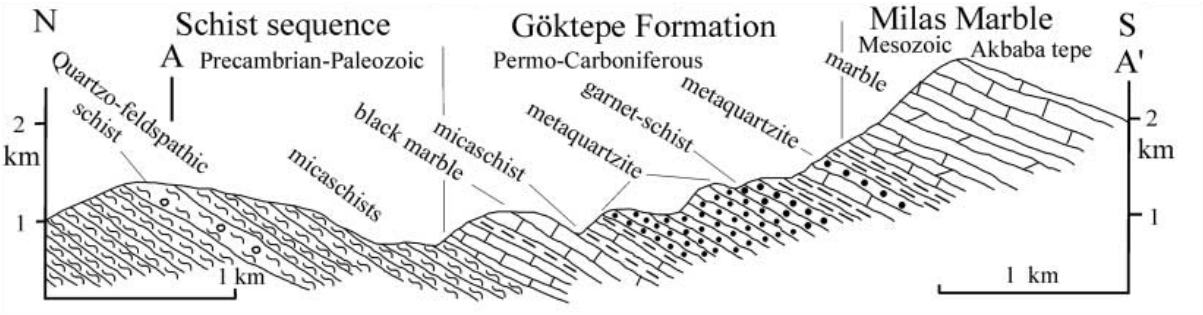

Figure 12: Geological cross section of the Menderes Massif (OKAY 2001).

3.2.2. Central-Anatolide-Tauride Block

The next geological unit to be presented is the Central-Anatolide-Tauride Block. Permo-Carboniferous clastic rocks, limestones and minor tuffs are the lowest formations exposed in the Afyon Zone (Figure 13). They progress up to the Lower Triassic shallow-water clastics and dolomites, which are succeeded by Middle-Triassic platform carbonates, overlain by pelagic micrites, radiolarian cherts and siliceous shales (OKAY *et al.* 1996). The Afyon Zone has undergone greenschist-facies regional metamorphism (ÖZCAN *et al.* 1988).

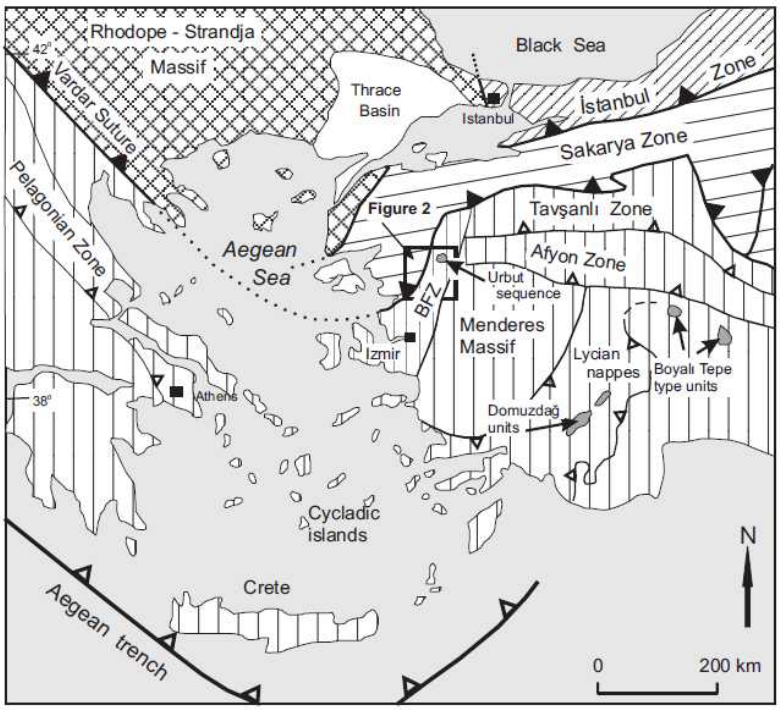

Figure 13: Tectonic map of the East Mediterranean Region showing the correlation of the geological units of West Anatolia and the neighbouring area (OKAY & ALTINER 2007)

4. Short remarks on Greek marbles

The continuation of the Menderes Massif into Greece (Figure 13) is the Attic-Cycladic Complex (JAKOBSHAGEN 1986). Nearly all the important marbles of classical Greece, except for those from Thasos, originated from this area, including the marbles of the Cyclades and Attica. The structures were formed during the Mesohellenic orogeny, about 45-40 Ma ago. Metamorphism was largely high pressure / low temperature. A later metamorphism resulted in thermal domes, as at Naxos about 25 Ma years ago, with the emplacement of granitic rocks in Attica in the west to Samos and Kos in the east. Marble is commonly found in the metamorphic sequences surrounding the thermal domes. The marble of Thasos is part of the belt that surrounds the Rhodope Massif, which consists of igneous and metamorphic rocks of medium to high grade, Precambrian to Mesozoic in age. The marbles of the Peloponnesus, as at Doliana and Mani, are generally low-grade metamorphic and were later overprinted by a high-pressure metamorphism. The marbles have Mesozoic to Cenozoic origin and are highly deformed, emplaced as nappe structures. Because widespread regional metamorphism is lacking and the deformation is more intense due to very large nappe transport (80-100 km), these marbles are not as uniform in texture or as widespread in this area as those of the Attic-Cycladic Complex are.

PART III

SAMPLING AND ANALYTICS

5. Sampling

5.1. Archaeological samples from Troia

Generally, I preferred to sample fragments of the archaeological objects themselves, however, in some cases, only pulverized (drilled) samples were available. Many of the archaeological samples contain undesirable components of the surface layer that may hinder examination of the specific features of interest; therefore, this contamination had to be removed prior to the analysis. In the case of fragments, cleaning was carried out in the laboratory. In the case of smaller archaeological objects (especially from the Neolithic to Bronze Age) it was not possible to take whole fragments, but only a small amount of powder. Therefore - after removing weathered layers on the surface with hydrochloric acid - a microdrilling machine (type Proxxon MICROMOT 40/E+) with diamond cutters and drills was used. The samples were preferably taken from a deeper layer to avoid contamination or the effects weathering and restoration or conservation practices.

In this work, 27 archaeological objects from the Neolithic to Bronze Age periods were investigated. A list of the investigated marble samples is presented in Table 1. The structure of the table is as follow: The first column *"Areal"* lists the coordinates where the objects were found during the excavation, *"Archaeological unit"* is the identification number of the objects; *"Year"* states the year of excavation. In addition, the table includes a short description of the findings as determined by the archaeologist and – if it is possible – the context in which the objects were found. They are differentiated into three groups: (1) the group *"Korfmann"* includes the objects that were excavated in Troia under the supervision of Professor M.O. Korfmann between 1988 and 1999, (2) the group *"Blegen"* includes objects excavated in Troia by Blegen and (3) the group *"Kumtepe"* contains objects excavated at Kumtepe in correlation to the Troia excavation lead by Korfmann. Figure 20 shows a plan of Troia I trough VII with the sampled Bronze Age marble objects and drawings of some selected objects. For drawings and photographs of the analysed objects in this study, cf. Appendix A.

In addition, 35 marble samples were taken from Trojan monuments dated to the Hellenistic and Roman periods (Table 2 and Figure 15). These include samples from the Athena Temple (PBA1-6; hereafter referred as to AT) dated to 280 B.C., the Athena Temple Porticoes (PBA7-10; ATP) dated to 230 B.C., the ″Sanctuary″ of the Roman Altar (PBA11-13; SRA) and the Blue Marble Building of the Bath (PBA14-16; BM) dated to the 3rd century B.C., the North Building Threshold of the Sanctuary (PBA17-18; SAN) and the seat of the Bouleuterion (PBA19-21; BOU) dated to the 2nd century B.C., the "Children of Claudius Inscription" (PBA22; CCI) dated to 53 A.D., architectural elements (PBA23-25; ODE) and columns (PBA26-29; ODE) from the Odeion dated to the early 2nd century A.D., the Nymphaeum base moulding (PBA30-31; BM) and the base moulding (PBA32-33; BM) of the Bath dated as to the late 2nd century B.C. as well.

Table 1: List of the investigated marble samples from Neolithic to Bronze Age of Kumtepe and Troia

Areal	Archaeological unit	Year of excavation	Description	Context
Korfmann				
D8	1844	1994	Polish stone	Troia IV
K8	730	1992	Fragment	
Z7	732	1994	Round stone	Troia VI / VII ?
D3	30	1988	Polish stone fragment	
D9	106	1989	Fragment	
E8	354(44)	1996	Bracelet fragment	Troia VIIb2
E4	640(149)	1993	Marble disc fragment	
G6	42(1)	1997	Fragment	
D7	48	1990	Pendant fragment	
E4/5	100	1988	Alabaster bowl fragment	
D8	1755	1994	Polish stone	Troia IV
E4/5	95	1988	Polish stone	
K12	B38	1989	Marble fragment of a bowl	
E9	1297	1997	Marble fragment	Troia VII
Y8 (1)	100	1998	Pendant	
K17	1138	19xx	Disc	
A8	491	1995	Marble knob	Troia VI
D3	449	1995	Bowl fragment	
D2	190	1990		
I9	393	1993	Marble pendant	Troia VI
Blegen				
91/44 (7)			Idol fragment	
T-44/58 (4)			Fragment	
T-8/14 (3)			Polish stone	
T23 (5)			Fragment	
Kumtepe				
F28	990	1995	Marble bowl fragment	
F29	460	1995	Marble bowl fragment	
F28	958/1	1995	Marble bowl fragment	

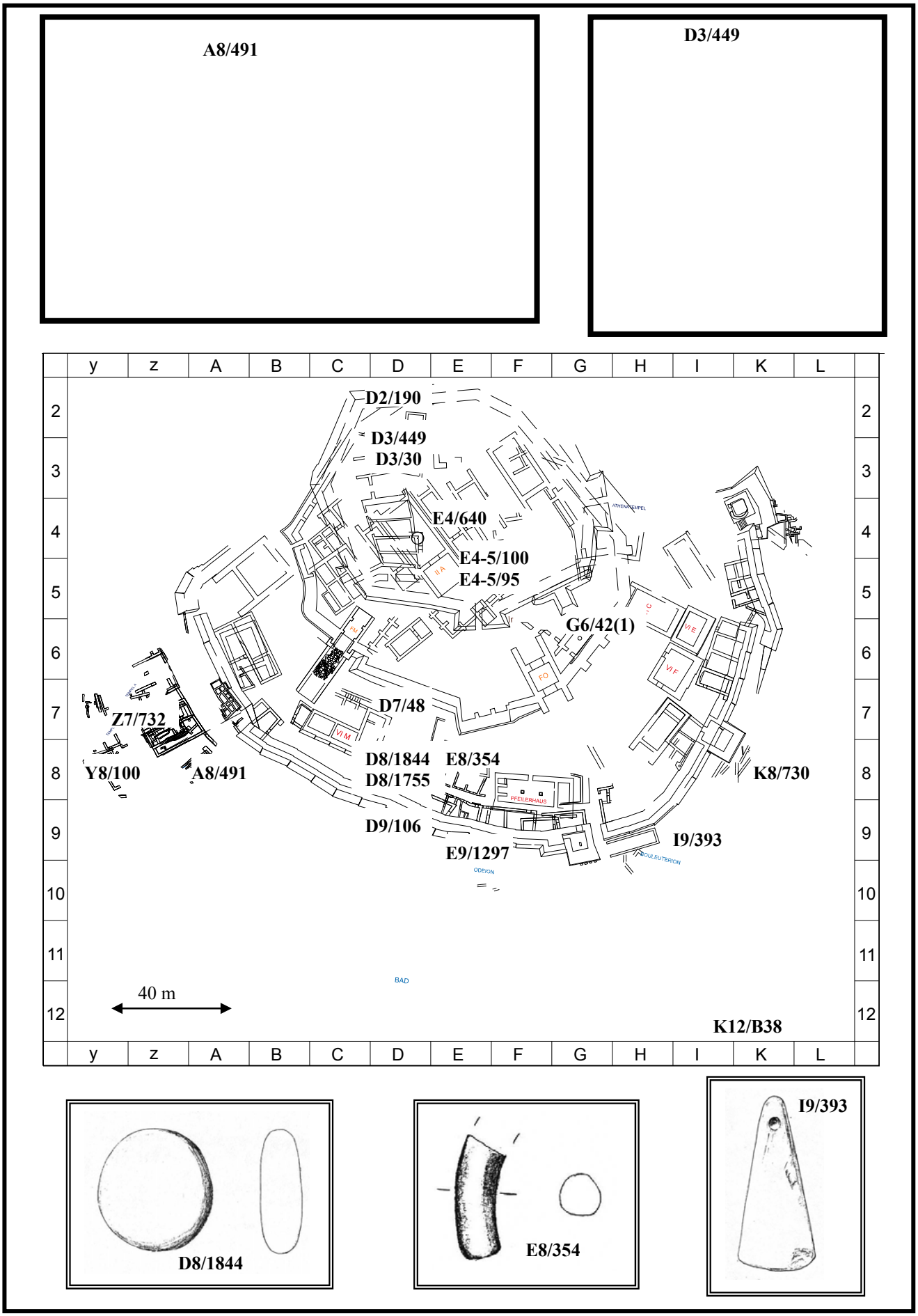

Figure 14: Plan of Troia I to VII with sampled of Bronze Age marble objects and drawings of some selected objects. (© Troia project)

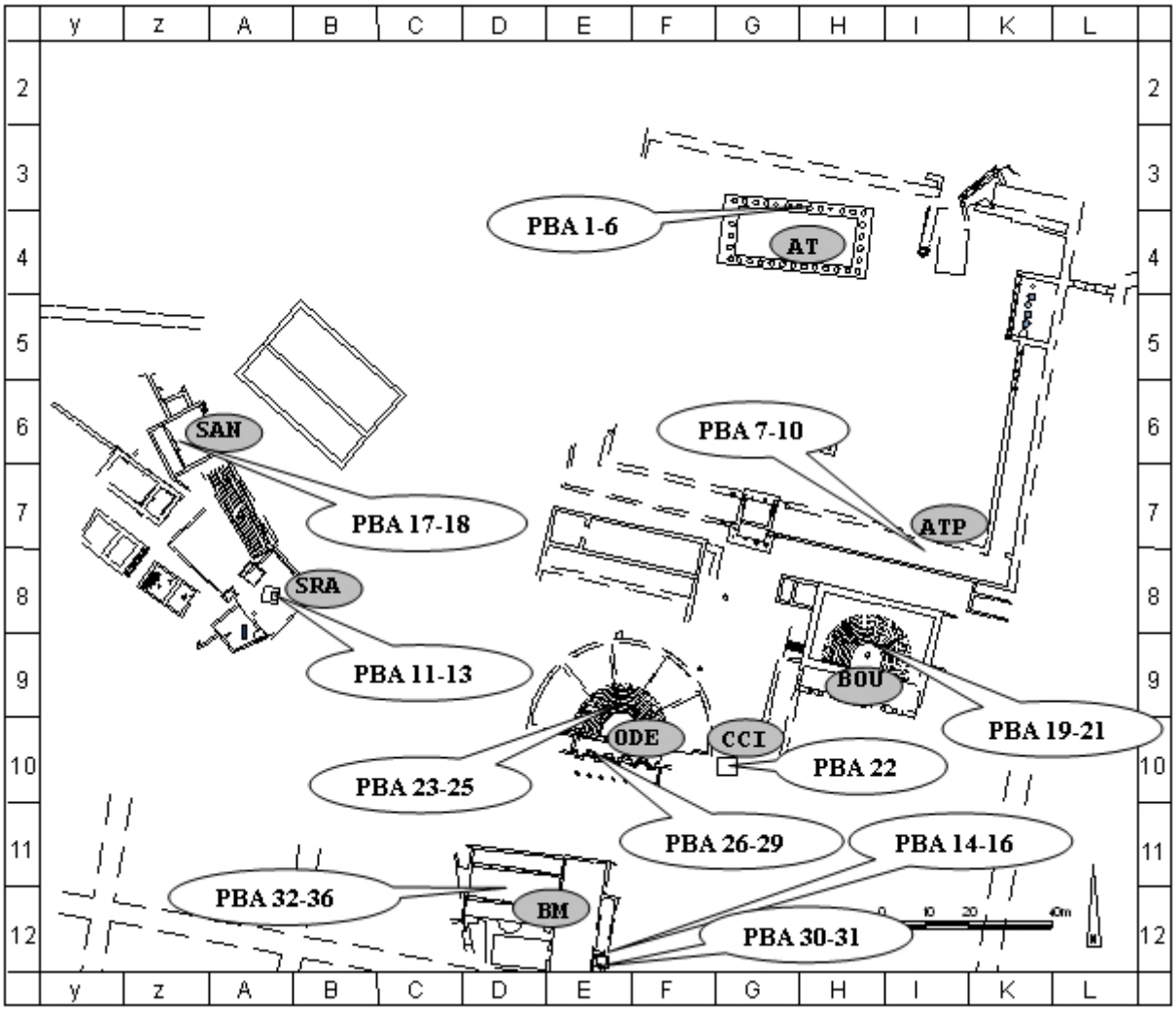

Figure 15: Plan of Troia VIII and IX (after Troia project) with sampling. AT = Athena temple; ATP = Athena Temple Portico; BOU = Bouleuterion; SAN = Sanctuary; SRA = Sanctuary Roman Altar; BM = Bath moulding; ODE = Odeion; CCI = Children of Claudius Inscription

Table 2: List of the investigated samples dating to the Hellenistic and Roman periods

Sample	Monument	Abbreviation	Part of the monument	Archaeological dating	More details
PBA1	Athena Temple	AT	Metope	280 B.C.	(FILGIS & MAYER 1992; ROSE 1995)
PBA2	Athena Temple	AT	Metope with giant (A236)	280 B.C.	
PBA3	Athena Temple	AT	Cornice with palmette	280 B.C.	
PBA4	Athena Temple	AT	Doric capital (A231)	280 B.C.	
PBA5	Athena Temple	AT	Ceiling coffer	280 B.C.	
PBA6	Athena Temple	AT	Ceiling coffer (A226)	280 B.C.	
PBA7	Athena Temple Portico	ATP	Doric frieze	230 B.C.	
PBA8	Athena Temple Portico	ATP	Doric frieze	230 B.C.	
PBA9	Athena Temple Portico	ATP	Doric frieze	230 B.C.	
PBA10	Athena Temple Portico	ATP	Doric frieze	230 B.C.	
PBA11	Sanctuary, ″Roman altar″	SRA	Base moulding	3rd century B.C.	(FILGIS & MAYER 1992; ROSE 1994; KORFMANN 1994)
PBA12	Sanctuary, ″Roman altar″	SRA	Base moulding	3rd century B.C.	
PBA13	Sanctuary, ″Roman altar″	SRA	Base moulding	3rd century B.C.	
PBA14	Bath	BM	Blue marble building, base moulding	3rd century B.C.	(FILGIS & MAYER 1992; ROSE 1994; KORFMANN 1994)
PBA15	Bath	BM	Blue marble building, base moulding	3rd century B.C.	
PBA16	Bath	BM	Blue marble building, base moulding	3rd century B.C.	
PBA17	Sanctuary	SAN	North building threshold	2nd century B.C.	(ROSE 1993, 1995)
PBA18	Sanctuary	SAN	North building threshold	2nd century B.C.	
PBA19	Bouleuterion	BOU	Seats	2nd century B.C.	(KORFMANN 1994; ROSE 1993, 1994, 1992)
PBA20	Bouleuterion	BOU	Seats	2nd century B.C.	
PBA21	Bouleuterion	BOU	Seats	2nd century B.C.	
PBA22	Children of Claudius Inscription		Dedicatory Inscription	53 A.D.	(ROSE 1994)
PBA23	Odeion	ODE	Architectural element	early 2nd century A.D.	(KORFMANN 1994; ROSE 1992, 1994)
PBA24	Odeion	ODE	Architectural element	early 2nd century A.D.	
PBA25	Odeion	ODE	Architectural element	early 2nd century A.D.	
PBA26	Odeion	ODE	Column	early 2nd century A.D.	
PBA27	Odeion	ODE	Column	early 2nd century A.D.	
PBA28	Odeion	ODE	Column	early 2nd century A.D.	
PBA29	Odeion	ODE	Column	early 2nd century A.D.	
PBA30	Bath	BM	Nymphaeum base moulding	late 2nd century A.D.	(FILGIS & MAYER 1992; ROSE 1994; KORFMANN 1994)
PBA31	Bath	BM	Nymphaeum base moulding	late 2nd century A.D.	
PBA32	Bath	BM	Moulding	late 2nd century A.D.	
PBA33	Bath	BM	Moulding	late 2nd century A.D.	
PBA34	Bath	BM	Moulding	late 2nd century A.D.	
PBA35	Bath	BM	Moulding	late 2nd century A.D.	

5.2. Geological samples

Apart from general information about some famous marble quarries like Marmara (Proconnesos), Afyon (Dokimeion), and Babadağ (Aphrodisias) there was no comprehensive database of the Anatolian quarries (prior to this study), and there is no written record of the exploitation of the quarries in different historical time periods. Therefore, in order to determine the provenance of the Trojan marble objects, the first step was the systematic sampling of the surrounding area. The samples have to characterize the quarries, while the quarries or occurrences belonging to the same district have to characterize the petrologic-geochemical properties of the given geological unit. Therefore, all the varieties from one site were collected (crystal size, colour, stripped) along vertical and horizontal cross sections.

More than 300 geological samples were taken from Anatolian marble quarries near Troia, especially in the Biga peninsula and around the Marmara Sea, for the investigation. The samples were collected from standing rock walls, both from natural outcrops and from quarry walls. Debris was not sampled to avoid deeply weathered material. Only fresh rocks were collected. The sample size was generally larger than 15-20 cm^3.

5.2.1. Geological samples of marble quarries from the Troad and neighboring areas

5.2.1.1. Rhodope-Strandja Massif

Two marble localities, namely Karabiga (hereafter referred as to KB) and Bergaz (BRG), were investigated in the Rhodope-Strandja Massif. (Abbreviations are shown in Figure 16).

5.2.1.2. Sakarya Zone

Several marble locations in the tectonic window of the Kazdağ Ranges area were sampled: Ayazma (AYA), Yeniçe (YEN), Serhat (SRH) and Altınoluk (ALT). Samples were collected from the Permo-Triassic carbonates of the Karakaya Complex (OKAY *et al.* 1996), from Manyas (MAN), Mustafa Kemalpaşa (MKB), Bandirma (BDR) and on the island of Marmara (MRM, ancient Proconnesos) as well as from the Permo-Triassic marble sequence of the Armutlu-Ovacık Zone, such as Orhangazi (ORH). White, recrystallised cherty limestones from Iznik (IZN) were also sampled. The samples localities are shown in Figure 16 and Figure 17.

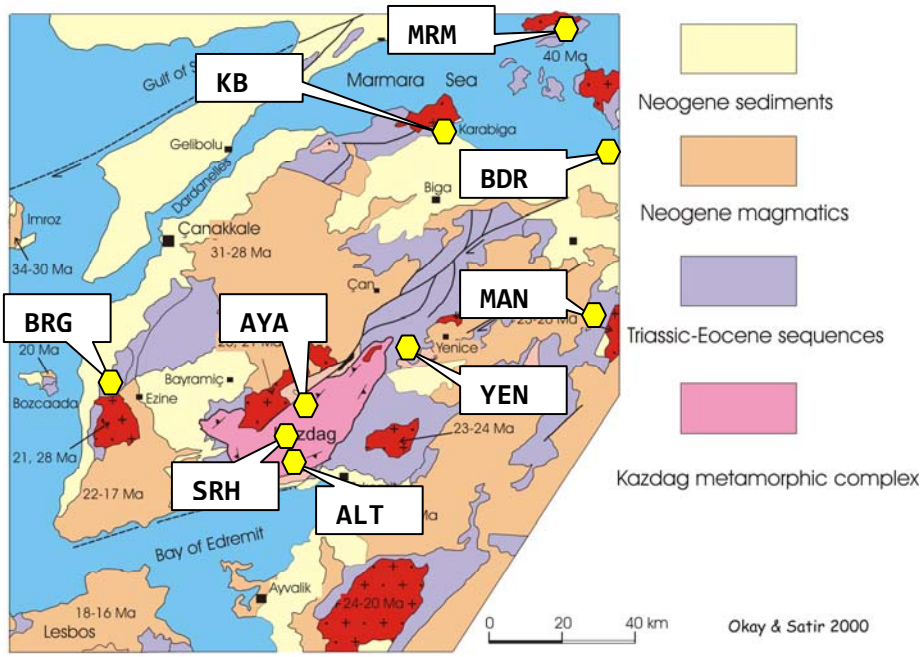

Figure 16: Simplified tectonic map of the Biga Peninsula (Okay & Satir 2000), NW-Turkey with sampled marble locations: KB = Karabiga, AYA = Ayazma, YEN = Yenice, BRG = Bergaz, SRH = Serhat, ALT = Altınoluk, MAN = Manyas, BDR = Bandirma, MRM = Marmara.

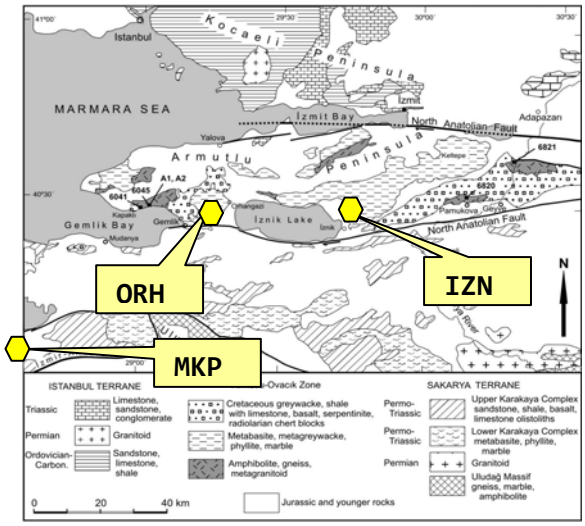

Figure 17: Simplified tectonic map of the Armutlu-Ovacik Zone in NW-Turkey (OKAY et al. 2008) with sampled marble locations: ORH = Orhangazi, IZN = Iznik and MKP = Mustafa Kemalpaşa.

5.2.2. Geological samples of marble quarries from Middle and Southwest Anatolia

The recently sampled quarries (Figure 18) of the southern Menderes Massif, which consists of Mesozoic massive platform-type neritic marbles, are Milas (MLS), Yatağan (YTG), Muğla (MGL), Uşak (USK), Babadağ (BBD, ancient Aphrodisias) and Denizli (DEN, ancient

Hierapolis). Samples from Afyon (AFY, ancient Dokimian) represent marbles of the Afyon Zone (Figure 19).

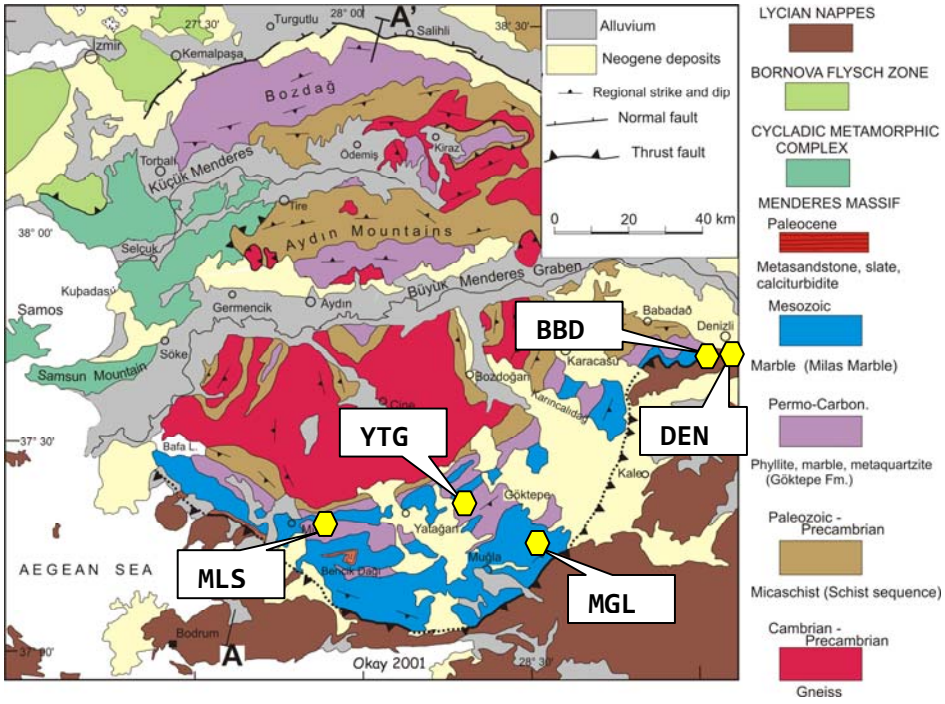

Figure 18: Simplified geological map of the Menderes massif (OKAY 2001) with sampled marble locations: MLS = Milas, YTG = Yatağan, MGL = Muğla, BBD = Babadağ, DEN = Denizli.

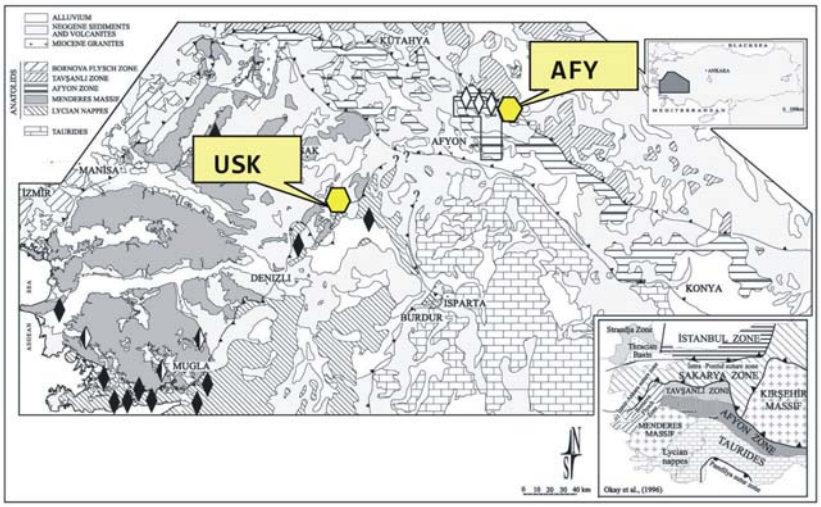

Figure 19: Simplified geological map of Middle Anatolia with sampled marble locations:AFY = Afyon, USK = Uşak.

6. Applied techniques

Owing to the remarkable similarity of their macroscopic appearance and physico-chemical properties, the identification of white marbles in order to assess their provenance can be a considerably difficult task. It must also be stressed that different marble types may originate from the same quarry, while different quarries may produce hardly distinguishable specimens. It is evident that tracing the origin of a marble sample requires an in-depth study of its physical, chemical and geochemical characteristics.

Several scientific methods were applied in order to distinguish antique marble quarries in the last century, but no single technique allows clear characterisation of white marbles. Therefore, a multi-disciplinary approach seems to be most promising. For an initial grouping of samples macroscopic features, such as colour and smell, and microscopic properties such as texture, grain size analyses and staining technique were used. The determination of minor and trace elements was carried out using different chemical techniques (XRF, AAS, ICP-MS) Electron microprobe (EMPA) and X-ray diffraction (XRD) were applied to characterise the mineral phases existing in the marble. Furthermore, $^{18}O/^{16}O$ and $^{13}C/^{12}C$ isotopic ratios were measured and finally, for the fine division of still ambiguous samples, cathodoluminescence and $^{87}Sr/^{86}Sr$ isotope analyses were used. The newly developed quantitative texture analysis (QTA) method was investigated on a large scale and methodical development took place. New parameters have been established.

In the following, a short description of the principles of each method, a summary of the previous works of the method and the analytical details that are relevant for this study are described.

6.1. Petrographical studies

Petrographic studies include ground observation; the microscopic study of samples, the microscopic analysis of thin sections in both normal and polarised light and in some cases the examination of X-ray diffraction spectra.

Even the purest of the metamorphic marbles contain some accessory minerals. The most common are quartz in small rounded grains, scales of colourless or pale-yellow mica (muscovite and flogopite), dark shining flakes of graphite, iron oxides and small crystals of pyrite. Many marbles contain other minerals that are usually silicates of lime or magnesia. Diopside is very frequent and may be white or pale green; white bladed tremolite and pale-

green actinolite also occur. The feldspar encountered may be a potassium variety but is more commonly a plagioclase (sodium-rich to calcium-rich) such as albite, labradorite or anorthite. Scapolite, various kinds of garnet, vesuvianite, spinel, forsterite, periclase, brucite, talc, zoisite, wollastonite, chlorite, tourmaline, epidote, chondrodite, biotite, titanite and apatite are all possible accessory minerals. Small amounts of pyrrhotite, sphalerite and chalcopyrite may also be present.

These minerals represent impurities in the original limestone that reacted during metamorphism to form new compounds. The aluminas represent an admixture of clay; the silicates derive their silica from quartz and from clay; the iron came from limonite, hematite or pyrite in the original sedimentary rock. In some cases, the original bedding of the calcareous sediments can be detected by mineral banding in the marble. The silicate minerals, if present in any considerable amount, may colour the marble e.g., green in the case of green pyroxenes and amphiboles; brown in that of garnet and vesuvianite and yellow in that of epidote, chondrodite and titanite. Black and grey colours result from the presence of fine scales of graphite. Bands of calc-silicate rock may alternate with bands of marble or form nodules and patches, sometimes producing interesting decorative effects, but these rocks are particularly difficult to finish because of the great difference in hardness between the silicates and carbonate minerals.

Nevertheless, petrographic studies and in particular the examination of thin sections remain fundamental in this field. This is because it is capable of providing detailed information regarding the type and extent of metamorphism, the texture of samples and the presence and nature of accessory minerals. Microscopic examinations primarily regard the texture and structure of isotropic or oriented rocks, which may be classified according to one of the many types of orientation. It is possible to determine the average value and the difference in the dimension of grains, identifying homogenous (homeoblastic) structures and those in which the grain sizes vary greatly (heteroblastic or porphyroblastic structures). Other important information regarding the shape and contours of the grains can be utilised, giving rise to quite complex and distinct typologies. The examination of optical properties, including the refractive index, colour, extinction and pleochroism is the key method for identifying accessory minerals and subsequently evaluating their concentrations, both qualitative and semi-quantitative. The use of X-ray diffraction spectra is often important in order to determine the quantity of dolomite. Many of the properties that have been mentioned are

relatively constant in a single marble formation and as such are particularly useful for determining origin.

6.1.1. Optical microscopic investigation

6.1.1.1. Analytical details

Thin sections are cut to a thickness of a few tenths of a millimetre (10-30 µm) such that they are transparent or semitransparent in visible light. They must have flat and parallel surfaces. They are mounted between glass plates with a mounting agent of known refractive index, or they are uncovered and polished. Using the latter, it is possible to use the same thin section for microprobe and cathodoluminescence investigation, as well.
For the initial grouping of samples, macroscopic features, such as colour and smell, and microscopic properties, such as texture, grain size analyses and staining technique, were used with the aid of a polarising microscope.

6.1.1.2. Previous studies

The first attempts to apply scientific methods to the study of marble go back to the work of G.R. LEPSIUS, published in 1890. He introduced the methods of petrography and, in particular, the microscopic study of thin sections into the field (LEPSIUS 1890). This was the only method utilised for many years and it remains important even today. In the first half of the twentieth century, it was gradually joined by the use of X-ray diffraction spectra, with which the identification of the most significant mineral phases could be made. One of the most relevant studies was published by CAPEDRI & VENTURELLI (2004) and includes the mineralogical composition of more than 75 samples from antique marble quarries.

6.1.1.2.1. Grain size determination

Very often expressions such as medium grained, coarse grained, fine-grained, etc., are used to describe the grain size of marbles. Here, in the Table 3, I summed up the categories after WIMMENAUER (1985) with an indication of size used for carbonate rocks.

Table 3: Classification of grain size for carbonatic rocks (WIMMENAUER 1985)

Classification	Grain size (mm)	Grains pro cm²
giant grained	33-	<<1
very coarse grained	10-33	<1
coarse grained	3.3-10	$1\text{-}10^1$
medium grained	1.0-3.3	$10^1\text{-}10^2$

small grained	0.3-1.0	10^2-10^3
fine grained	0.1-0.3	10^3-10^4
very fine grained	0.01-0.1	10^4-10^6
compact	< 0.01	$>10^6$

6.1.2. Maximum grain size analysis (MGS)

One of the most common used parameters in marble provenance analyses is the maximum grain size (MGS). However, until some years ago, in most cases neither numerical results nor descriptions of the methods used to determine this very important parameter were published on this topic. In the last years, some authors listed detailed results in their works (ZÖLDFÖLDI & SATIR 2003; CRAMER 2004; UNTERWURZACHER *et al.* 2005; ATTANASIO *et al.* 2006; MORBIDELLI *et al.* 2007; ZÖLDFÖLDI & SZÉKELY 2004; 2005b, 2008; SZÉKELY & ZÖLDFÖLDI 2009). ATTANASIO *et al.* (2006) published the most comprehensive database of maximum grain size with more than 1300 samples. Their measurement of marble grain size is generally based on the microscopic examination of the thin sections. Since a large number of samples needed to be measured, they used a simpler, faster method. A cut and polished sample surface was treated with HCL 2N for approximately 30 seconds in order to display the edges of the crystalline grains more clearly. After rinsing and drying the sample, the crystalline grains, or at least the largest of them, were observed with the aid of a normal reflecting microscope, equipped with a polarising filter. In this way, the value of the MGS (maximum grain size), the maximum dimension of the largest microcrystal present in the sample, was measured in mm with the aid of a graduated eyepiece. In some cases, the observation value depends on the direction of the surface cut of the polished section. Therefore, it is often useful to compare the results from two different sections, with cuts that are perpendicular to each other. ATTANASIO *et al.* (2006) carried out a series of controls that show that the classical thin section method and the described method provide MGS results that are in agreement to within 10%. This is not true when an estimate of the average value of the crystalline grain size is necessary. Extremely small crystals are difficult to observe due to reflection from the polished surface, which reduces the accuracy of the results.

CRAMER (1998) used a different approach for the investigation of the Telephos fries marbles. In his study, he measured the parameters of the grains along a traverse in the thin section. Of these grains, the longest diameters and, perpendicular to those, the width of each grain was measured. In his approach, for some cases the "mean grain size" (the "mittlere Kornanschnitt") was also derived, i.e. the measured distance was divided by the number of the grains that was crossed by the track of the traverse. This procedure can result in a smaller

grain diameter than with the first procedure. A similar procedure was applied in CRAMER (2004). However, the measurements were not carried out directly in the microscope. Average grain size (AGS) was calculated by dividing the measured distance by the number of the crossed grains along several measuring traverses on the enlarged image of the thin section. To determine the maximum grain size (MGS), the three biggest punches in each case were measured. The quotient from MGS and AGS can be a measure of the heterogeneity or homogeneity of the crystal lattice structure. Recognizing the ambiguity of the MGS parameter, Cramer used the second largest grain as an important property. The values of the second largest grain are of course lower. However, due to statistical reasons, they describe the heterogeneous grain structure better, because an isolated big grain cannot accidentally bias the values. Thus, the values often turn out to be larger in the second method, which offers a more realistic picture.

Figure 20 shows the ranges of maximum grain size (MGS) that were presented in the above-mentioned publications. In addition to the samples of ATTANASIO *et al.* (2006), about 300 MGS values determined by Cramer (2004) were compared with those published by ZÖLDFÖLDI & SZÉKELY (2003, 2004; 2005b, 2008) and SZÉKELY & ZÖLDFÖLDI (2009). However, we must keep in mind that different methods were used to determine MGS values; therefore, the results of the investigation are very inconsistent. Figure 20 shows some of the occurrences that were investigated by Attanasio and Cramer. For example, in the case of Aphrodisias (today Babadağ), Attanasio measured MGS between 0.2 to 4.5 mm, while Cramer measured MGS between 1.6 to 4 mm. Similarly, in the case of Proconnesos (today Marmara), Attanasio measured MGS between 0.5 and 3.5 mm, but Cramer between 0.3 to 3.2 mm.

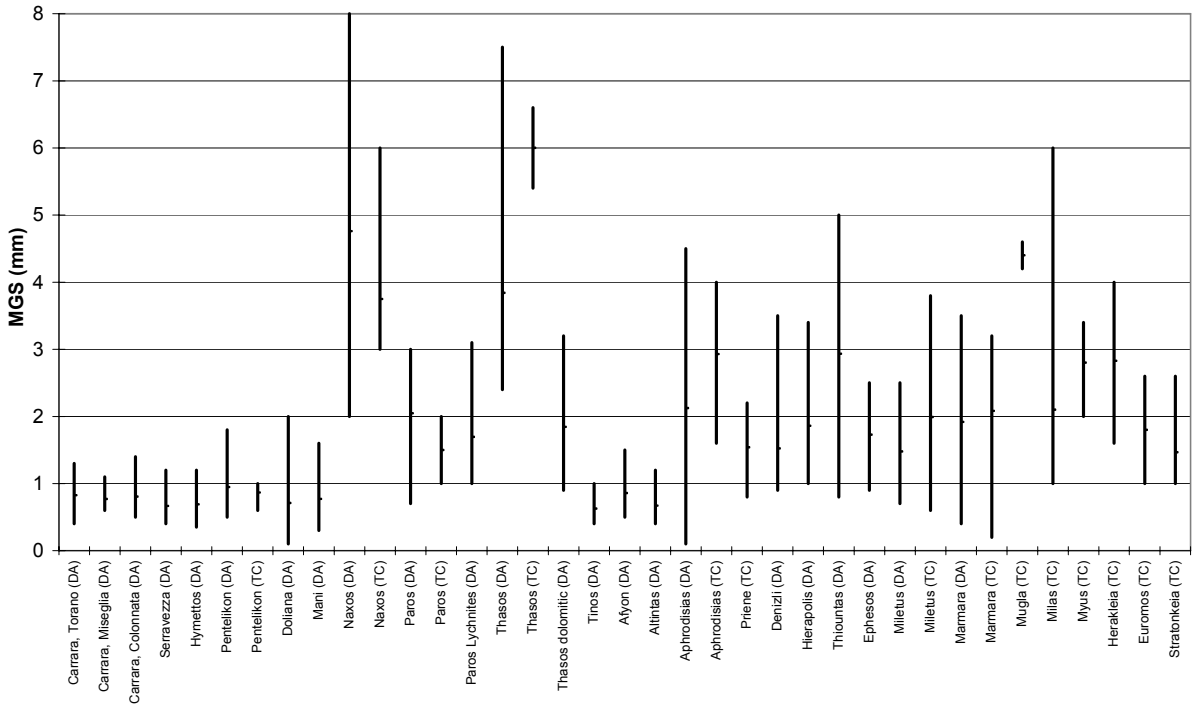

Figure 20: Range of the maximum grain size (MGS) for the investigated quarry districts based on the databases of ATTANASIO *et al.* 2003 and 2006 (labelled as DA on the X-axis), CRAMER 2004 (labelled as TC on the X-axis).

6.1.3. Quantitative texture analysis (QTA)

6.1.3.1. The principles of the method

As mentioned above, texture is a crucial property of marbles, since it is strictly related to the specific petrogenetic history of various geological units. The quantitative textural analysis (QTA; PERUGINI *et al.* 2003), and the combination of the quantitative fabric analysis (QFA; SCHMID *et al.* 1999a; QFA; SCHMID *et al.* 1999b) and extraction of fractal properties (fractal analysis: FA) of the calcite grain boundaries was applied to the Western Anatolian and Trojan white marbles in the framework of this study.

Some contributions to the development of this method and results of the investigation have been published by the author and her co-authors in several articles (ZÖLDFÖLDI & SATIR 2003; ZÖLDFÖLDI & SZÉKELY 2003, 2004; ZÖLDFÖLDI & SZÉKELY 2005a, b, 2008; SZÉKELY & ZÖLDFÖLDI 2009). This section gives a summary based on these works and focuses on quantitative textural analysis (QTA), the evaluation of the textural properties on the marble samples by means of quantitative fabric analysis (QFA) and fractal analysis (FA).

In the raster approach (FA), the thin section is taken as an image, and image-processing tools are applied to extract features that are specific to the sample. After completing this step, the grain boundaries were automatically traced from manually and digitally enhanced images composing the grain boundary data set. This data set was then analysed: Parameter extraction based on 2D geometrical features were performed (QFA, vector-based approach). From the geometric point of view, in addition to the grain size determination, three parameter groups for classification were integrated:

- Measured grain parameters: long axis, short axis, perimeter, area, convex hull parameters (perimeter and area)
- Derivative grain parameters: axial difference, orientation of the long axis, perimeter/area ratio, shape factor
- Whole-image parameters: fractal dimension (box counting and information dimension), maximum grain size.

The method is described in more detail in Appendix B.1.

6.1.3.2. Previous studies

Quantitative texture analysis (QTA), which includes quantitative fabric analysis (QFA) and fractal analysis (FA), is one of the most recently introduced methods in the study of marble and it is still in the development phase. It has demonstrated its great potential for establishing the provenance of unknown marbles. In particular, the study of the size, shape and boundaries of calcite grains provides basic information on the tectono-metamorphic evolution of the different kinds of marble (LAZZARINI *et al.* 1980b; COLI 1989; MOLLI & HEILBRONNER 1999; PIERI *et al.* 2001; OESTERLING *et al.* 2007). Conspicuous textural differences of white marble samples are observed. The grain size distribution and shape is primarily determined by the facies of the rock: This thermo-chronological evolution of the hosting formation leaves its unique fingerprints not only on the chemical composition and isotopic signal, but on the fabric as well.

The importance of this method is due to the fact that material from classical petrography is, at least partly, qualitative and despite its diagnostic importance it is difficult to use alongside quantitative methods of data treatment that exploit the discriminating ability of numerical variables. The variability in grain size is extremely useful and widely used in localizing the origin of marble. This is because granulometry (particle size analysis) is quantitative and is easily definable in terms of the maximum and minimum grain diameter. The introduction of methods that transform morphological information into numerical variables immediately

renders the information more useful and important for the study of origin, despite the laborious methodology. The importance of QFA lies in the fact that it has given a rigorous numerical character to petrographic information for the first time; this method has a central role in the study of the origin of marble even today. The quantitative study of texture (quantitative fabric analysis or QFA) is in essence the numerical analysis of microscopic images obtained with thin sections. The necessity of quantitative fabric analysis of white marbles is rather obvious, if we take into account the striking diversity of the texture of marble samples. The statistical treatment of data has demonstrated that the most important variables obtained from the analysis of texture are the major axis of the grain (so-called maximum grain size or MGS and their distribution), the area of the grain (maximum grain area, MGA and their distribution) the relationship between perimeter and surface area, and the defined shape factor.

SCHMID *et al.* (1995) coined the term of quantitative fabric analysis (QFA) when they analysed marbles from different historic quarries, deriving various parameters in order to characterize the whole grain geometry. In addition to QFA, with respect to the grain boundary pattern as a whole, PERUGINI *et al.* (2003) applied the fractal analysis (FA) on the digital image of the marble thin sections. They coined the term of QTA for the combination of QFA and FA and analysed marbles from Carrara, Marmara, Penteli, Naxos, Paros and Thasos (n=28). At the same time we also applied this combined technique (ZÖLDFÖLDI & SZÉKELY 2003, 2004; ZÖLDFÖLDI & SZÉKELY 2005b; ZÖLDFÖLDI *et al.* 2005; ZÖLDFÖLDI & SZÉKELY 2008), though in our studies the box counting method was used for FA, while PERUGINI *et al.* (2003) applied the probability density function method (PDFM).

6.1.3.3. Relating the fractal dimension results with previous data

It is very difficult to relate the results of this study to those of the previous authors, because (1) except for Marmara marbles the previous workers did not analyse other West Anatolian marbles with this technique; (2) the present computing capacity is considerably better than that available to the previous authors and (3) the fractal dimension relevant analysis of PERUGINI *et al.* (2003) gives their results in units of pixels without defining its real extent. The latter problem does not influence the fractal dimension results in theory, but the considerably lower number of grains counted (Marmara samples can be compared) suggests that the resolution of the hand drawn outlining of PERUGINI *et al.* (2003) seems to be considerably lower than in this study.

It is important to note that both QFA and FA techniques are influenced by the creation of the data set at the smallest grain scale: A cut-off effect exists when outlining the crystal boundaries, because below a given size the observer cannot follow the boundary lines. Furthermore, the automated processing filters out the very small crystals. The grain size histograms should be evaluated with this fact in mind.

6.1.4. Electron microprobe investigation

6.1.4.1. The principles of the method

An electron microscope was used to examine mineral particles in detail, given the resolution obtainable by a beam of accelerated electrons produced by a heated tungsten filament and focused by an electromagnetic field. Two main methods were used: Scanning electron microscopy, with magnifications up to 50,000x (see details in GRUNDY & JONES 1976), and transmission electron microscopy (more about this in MCCONNELL 1977), with magnifications up to 250,000x. In the scanning electron microscope, the image is formed by backscattering of electrons from the specimen surface, which has previously been made conductive by coating it with carbon. This technique is most suitable for studying the different morphologies and microtextures of, for example, calcite grains in marble. Transmission electron microscopy can be used to study features of the atomic arrangement in minerals, since the wavelength of the electrons is less than the size of an atom. Very thin specimens are required; sufficiently small crystals can be produced by grinding or a small area may be thinned by ion-beam etching.

6.1.4.2. Analytical details

Minerals were analyzed using a JEOL 8900 electron microprobe at the Institute of Geosciences at the University of Tübingen, Germany. The emission current was 15 nA and the acceleration voltage was 15 kV.

6.1.5. X-ray powder diffraction (XRD)

One of the most common methods used to analyse the mineral composition of materials is powder diffractometry. The advantages of this method are multifold: Only some milligrams of the sampled material are required and it is particularly suitable when only powder samples are

available. Currently, mineral content of less than 1 w% can be detected quantitatively after calibration. In the case of pure white marbles, the dolomite content can be determined quickly.

6.1.5.1. The principles of the method

A brief description of the XRD method is given below. Macroscopic grains are made from many elementary crystals, which coherently diffract X-rays. Measurement is based on the detection of the intensity of the beam diffracted in the function of the diffraction angle. The diffractogram consists of a continuous background (instrument, amorphous phases) and high-intensity sharp peaks (Bragg-reflexions), which occur at characteristic angle-values. The position and the intensity of the reflections are determined by the real crystal structure and the model of diffraction. The position of the peaks can be described by Bragg´s Law ($n\lambda = 2d \sin \Theta$), which ascribes the contact between the crystal lattice, wavelength (λ) and the angle of incidence (Θ). Using these parameters, the lattice plain distance (d) is determinable. The determination of the phases (qualitative analysis) is carried out by comparing the measured d-values and intensities with international references (PDD – Powder Diffraction Data, ASTM – American Society for Testing Materials).

6.1.5.2. Analytical details

X-ray diffraction measurements to determine the main and accessory minerals were carried out with the *Siemens SRS 300* instrument on pulverized material at the Institute of Geosciences, University of Tübingen.

Further measurements were carried out at the Institute for Geochemical Research of the Hungarian Academy of Sciences (Budapest) with a Philips PW 1730 X-ray diffractometer (graphite monochromator and Cu tube) controlled by PC-APD software.

6.1.5.3. Previous studies

In the archaeometrical literature of XRD analysis of marble, apart from a few exceptions (FRANZINI *et al.* 1984; e.g., LAZZARINI & MARIOTTINI 1987; LAZZARINI *et al.* 1988; CRAMER 2004; FRANZINI *et al.* in print), typically only the presence of dolomite is mentioned, and no quantitative assessment is given.

6.2. Analysis of chemical composition

The determination of the chemical composition is one of the most frequently used analytical methods in archaeometry. In many applications, it has proved to be a capable of characterising widely different materials and artifacts in detail (HERZ & GARRISON 1998) providing conclusive information on their origin. The method has frequently been used to determine the provenance of white marble, therefore summarising its many aspects and the vast literature available is quite a difficult task. Without going into the chemical details, many different methods have been developed for trace element analysis: These include optical emission spectroscopy (OES), atomic absorption spectroscopy (AAS), X-ray fluorescence (XRF), electron microprobe (EMPA), neutron activation analysis (INAA), inductively coupled plasma mass spectroscopy (ICP-MS) and inductively coupled plasma atomic emission spectroscopy (ICP-AES). The various techniques have different levels of sensitivity and accuracy. This means that the comparison of data obtained by different methods is often problematic, as can be the case when different laboratories use the same techniques. In the meantime, the initial enthusiasm (e.g., RYBACH & NISSEN 1965) concerning the applicability of the method declined as increasingly sensitive geochemical methods became available.

The problems or general difficulties in using chemical analyses for marble provenance analyses arise for three reasons: (1) the scattering in element distribution within one marble quarry can be as high as between the various quarries. (2) Some of the applied methods (RFA, INAA) capture the chemistry of the entire material that can be strongly influenced by the random distribution of accessory minerals. Whereas the wet-analytic methods (ICP-MS, OES, AAS, etc.) primarily capture the element content, that is built in the calcite lattice, because these analyses are applied on the solution solved by acids. Furthermore, the type of acid used also influences the results because it affects the type and cooking degree of dissolution of accessory minerals (e.g. pyrite). (3) Not only different analytic techniques may lead to differing results when applied on the same marbles, but inter-laboratory comparisons carried out on the same marble material applying the same methods may also fail to provide comparable results.

6.2.1. X-ray fluorescence (XRF)

6.2.1.1. The principles of the method

X-ray emission spectrographic analysis (MAXWELL 1968; NORRISH & CHAPPELL 1977) is widely used. XRF analysis was used in this study in order to determine the bulk chemical composition of the geological and archaeological samples.

In X-ray fluorescence spectroscopy, the sample is exposed to a source of X-rays. As the high-energy photons strike the sample, they knock electrons out of their orbits around the nuclei of the atoms. As a result, an electron from an outer orbit (shell) of the atom will fall into the orbit of the missing electron. The relocated electron has an excess of energy that is expended as an X-ray fluorescence photon. This fluorescence is unique to the chemical composition of the sample. The detector collects the spectrum of the fluorescence and converts it to electrical impulses proportional to the energy of the various X-rays in the sample's spectrum. Since each element has a different and identifiable X-ray signature, counting the pulses in that sector determines the presence and concentration of the chemical element(s) in the sample.

6.2.1.2. Analytical details

The quantitative analyses of the major and trace elements were carried out using the wavelength dispersive XRF. Samples were powdered (grain size of the powder < 50 μ) in an agate mortar. LOI (loss of ignition), equivalent to the loss of weight, which occurs during ignition, results from the reactions of CO_2 (mostly from carbonates), H_2O (structural water of the clay minerals) and $Fe^{2+/3+}$ conversions. LOI is calculated after heating the samples to 1000 °C for one hour. The samples (1.5000 g) were mixed with 7.5000 g of Spectromelt Fluxing agent (MERCK A12, di-Lithiumtetraborat/Lithiumteraborat (66:34)) and melted using the OxiFlux-System of the Firm CBR Analyse Service at 1200 °C to obtain homogenous tablets.

Measurements were carried out at the Department of Geochemistry of the University of Tübingen using a Bruker AXS Pioneer X-ray Spectrometer (Rh X-ray tube, 4kW). The results were evaluated with the computer program ″Traces″, which uses 32 standards for calibration.

6.2.2. Atomic absorption spectroscopy (AAS)

6.2.2.1. The principles of the method

The technique makes use of absorption spectrometryto assess the concentration of an analyte in a sample. It relies heavily on the Beer-Lambert law.

In short, the electrons of the atoms in the atomizer can be promoted to higher orbitals for a short amount of time by absorbing a set quantity of energy (i.e. light of a given wavelength). This amount of energy (or wavelength) is specific to a particular electron transition in a particular element and, in general, each wavelength corresponds to only one element. This gives the technique its elemental selectivity. As the quantity of energy (the power) put into the flame is known and the quantity remaining on the other side (at the detector) can be measured, it is possible, from the Beer-Lambert law, to calculate how many of these transitions took place, and thus get a signal that is proportional to the concentration of the element being measured (more details in HEINRICHS & HERMANN 1990)

6.2.2.2. Analytical details

In atomic absorption spectroscopy (MAXWELL 1968; MCLAUGHLIN 1977), as with flame photometry, a solution of the sample is sprayed into a flame, causing the compounds present in the solution to dissociate into their constituent atoms. Monochromatic light of the characteristic wavelength for the element to be determined is shone through the flame, and the atoms of the element will absorb this light. The total amount of light absorbed is measured and, by comparison with standards, concentrations can be calculated. Each element needs a different lamp to produce its characteristic radiation, unless multi-element lamps are used, so that simultaneous multi-element determinations are not usually feasible. The method ideally requires 1 g of sample for a complete analysis, although 0.2-0.4 g would normally be sufficient.

6.2.3. Previous studies on chemical composition of marble

The first examples of the use of trace analysis for determining the origin of marble date back about 40 years. Applications on marble characterisation using spectroscopic methods are numerous and databases on the chemical composition of marbles are voluminous (ANDREAE *et al.* 1972; CONFORTO *et al.* 1975; GERMANN *et al.* 1980; GERMANN *et al.* 1988; JONGSTE *et al.* 1992; JONGSTE *et al.* 1995; MÜLLER *et al.* 1996; MÜLLER *et al.* 1999; AKCAY *et al.* 1999; LAZZARINI & CANCELLIERE 2000a; CAMPANELLA *et al.* 2001; LAZZARINI 2002; LAZZARINI *et al.* 2002a; e.g., LAZZARINI *et al.* 2002b; KRITSOTAKIS *et al.* 2003; GERMANN & CRAMER 2005; LAZZARINI & ANTONELLI 2003). LAZZARINI *et al.* (1980), MARGOLIS & SHOWERS (1988) and GORGONI *et al.* (1992) detected that some of the marble quarries are distinguishable by Ca:Sr ratios.

One of the standard methods for the determination of trace today is the neutron activation analysis (RYBACH & NISSEN 1965; CONFORTO *et al.* 1975; MELLO 1983; ODDONE *et al.* 1985; MELLO *et al.* 1988a; MELLO *et al.* 1988b; GRIMANIS & VASSILAKI-GRIMANI 1988; JONGSTE *et al.* 1992; MOENS *et al.* 1992; MELONI *et al.* 1993; JONGSTE *et al.* 1995; DULIU *et al.* 1999). This is a complex experimental technique and the associated analyses are often extremely time-consuming. Furthermore, a nuclear reactor to irradiate samples with a beam of slow neutrons must be available. Although INAA would appear to be less competitive than other methods, it has become established as the reference analytical tool for trace determination because it is capable of analysing a large number of elements simultaneously and with great accuracy to a concentration of less than one µg/g. The difficulties that are intrinsic to this method, as well as the high cost, have encouraged the development of alternative techniques.

Inductive coupled plasma mass spectrometry has currently become almost competitive with neutron analysis in terms of accuracy (MOENS *et al.* 1987; MELLO *et al.* 1988a; JONGSTE *et al.* 1995; ROOS *et al.* 1995). Recently, as many as 30 elements could be analysed; these include alkali, alkaline earth, rare earth and other heavy elements. This high number of variables has meant that use of multivariate statistical methods of analysis is indispensable in order to fully utilise the large amount of experimental material, which otherwise would be difficult to manage (MELLO *et al.* 1988a; MOENS *et al.* 1988). In this way, it was also possible to identify the most discriminating variables or traces, those that contributed less to the results or, for various reasons, showed excessive variability being eliminated. Due to these intrinsic reasons, the fact that there are many variables, trace analysis is the method that has developed a multivariate statistical approach for determining the origin of marble to the greatest degree, discriminant and cluster analysis being used predominantly.

The results obtained are as significant in the context of a single technique as when a multi-method approach is employed. Stable isotope data combined with trace element analysis being the most frequent. In this respect, the results published by MATTHEWS (1995) are particularly interesting, as are the works by Moens' group (MOENS *et al.* 1988). In Matthews' work it is demonstrated that the isotopic method and the trace element analysis have similar discriminant powers, while the combined use of these two methods can increase the success rate considerably, bringing the discrimination between three or four different provenance sites to between 91 and 99 % (ATTANASIO *et al.* 2006).

An approach that is slightly different from those already discussed is the attempt to solely use the analytical results of rare earth elements and a number of parameters deriving from them.

These include their total content, the relationship between light and heavy rare earth or alternatively the relationship between two specific elements such as lanthanum and ytterbium (MELONI *et al.* 1995). The importance and diffusion of neutron activation trace analysis is once again emphasised by the first results of a database published by MATTHEWS (1997). It presently refers to 183 samples from 8 different localities.

It should be emphasised that in recent years, a number of studies have emerged that have been critical of the capacity of trace element analysis to localise the origin of marble correctly (MANDI *et al.* 1995). These criticisms utili new data to resume and intensify previously expressed doubts. They centre on the great variability that trace analysis demonstrates, not just within one quarry, but also for a single block of marble. This variability is essentially due to the casual presence of accessory minerals that are rich in those specific elements under examination. This is the main reason why a number of authors attribute greater diagnostic significance to spectroscopic methods that are based exclusively on substitution impurities, like manganese, iron or strontium. The latter are not accessory traces but enter the carbonate lattice structure, residing in the positions usually occupied by the calcium ions.

6.3. Cathodoluminescence investigation (CL)

6.3.1. The principles of the method

This method is based on the cathodoluminescence of the marbles – that means the light emission after stimulation with electrons – which causes characteristic intensities and patterns depending on the concentration of manganese, iron and other trace elements. Here I should like to point out that the colour and intensity of the cathodomicrofacies depends on the intensity and durability of the stimulation. Therefore, to be able to compare the results, accurate information about the laboratory conditions and measuring parameters are essential. More details about the method are described in Appendix B.2.

6.3.2. Analytical details

Department of Environmental Geology, Eötvös Loránd University, Budapest

Cathodoluminescence experiments were performed on polished thin sections of marbles with the instrument *Nuclide ELM-3* at the Department of Environmental Geology, Eötvös Loránd University, Budapest, Hungary. The microscope was a monocular Olympus Pos one with an Olympus D Achromat 4X objective. A high sensitivity cold cathode CL-microscope was

used. Experiments were carried out between 10 and 30 keV accelerating voltage and 0.60 μA/mm² beam current density. In principle, all luminescence features can be recorded on photographic films. Long exposure times are necessary due to the low luminescence light intensity, which is additionally decreased by absorption through the microscope optics. According to the luminescence properties of different minerals, exposure times between 1 and 10 minutes are necessary. Coloured slides were taken with Kodak 400 and 800 ASA colour transparency film.

Institute for Geochemical Research, Hungarian Academy of Sciences

Further cathodoluminescence examinations were performed at the Institute for Geochemical Research (Hungarian Academy of Sciences) using a Reliotron 'cold-cathode' microscope operated at 5-7 kV accelerating voltage and 0.5 to 0.9 mA current. Additionally, thin sections were studied using a 'hotcathode' CL microscope HC1-LM operated at 14 kV acceleration voltages and a current density of ~10 mA/mm^2. Luminescence images were captured on-line during CL operations by means of an adapted digital video camera (KAPPA 961-1138 CF 20 DXC) with cooling stage.

6.3.3. Previous studies

Early reports of luminescent carbonates, particularly calcite, date back to the middle of the 19th century (BEQUEREL 1859, 1867). The first extensive experimental data on carbonate luminescence were provided in the 1920s (NICHOLS *et al.* 1928; TANAKA 1924). It was not until the 1960s that geologists began to utilize carbonate CL for petrographic studies (LONG & AGRELL 1965; SMITH & STENSTROM 1965; SIPPEL & GLOVER 1965). CL and Mn^{2+} and Fe^{2+} contents are used, often in combination with stable isotope data, to interpret the diagenetic environment, i.e., salinity, temperature, pH and Eh of the formation waters (MEYERS 1974; FRANK *et al.* 1982). There are few papers in the geological literature that consider elements other than Mn^{2+} and Fe^{2+} in the CL of carbonates even though solid state physicists have long known that there are many more elements that may activate, sensitize or quench luminescence even in natural carbonates (e.g., KRÖGER 1948).

Sedimentological, diagenetic and reservoir studies are the major fields of application of CL methods, but recently this application is also used for provenance studies. At present, more than 1000 samples of calcitic and dolomitic marbles from classical quarrying areas have been investigated with CL (BARBIN *et al.* 1989; BARBIN *et al.* 1991a; BARBIN *et al.* 1991b; BARBIN *et al.* 1992a; BARBIN *et al.* 1992b; HERRMANN & BARBIN 1993; BARBIN *et al.* 1995; BARBIN

et al. 1999; HABERMANN *et al.* 1996, 1998; MARSHALL 1988; LAPUENTE *et al.* 2000; LAPUENTE *et al.* 1999; MACHEL *et al.* 1991a).

6.4. Isotope geochemical analysis

6.4.1. Carbon and oxygen isotope analyses

6.4.1.1. The principles of stable isotope analysis

The isotopic composition of diverse materials or those with different origins is variable. In the case of marble, the variations are of the order of a few per mil. The reasons for these variations are related to what is known as isotope fractionation, particularly for light elements such as carbon and oxygen. Isotope fractionation is the reactivity of isotopes with different weights to the physical, chemical and biological processes that determined the formation of the material. The variation in the isotopic composition of carbon and oxygen in marble carbonates has a number of causes. These include the different ways in which the rock was formed; the isotopic composition of the water in contact with carbonate minerals during their formation and its subsequent history; the temperature at which metamorphism took place and successive aging processes.

In other words, marble from a certain locality, formed by means of a unique geological history, possesses isotopic characteristics that distinguish it from marbles with quite different geological histories, formed elsewhere. It is also reasonable to assume that the same process that led to the formation of a particular type of marble has also caused it to become relatively homogeneous within a certain area. This is affected by means of isotopic equilibrium during formation and metamorphism of the calcareous rock due to fluid phases. Both these hypothesis were shown to be correct and justify the use of the isotopic method. More details about the method and the basics are described in Appendix B.3.

6.4.1.2. Analytical details

6.4.1.2.1. Off-line stable isotope measurements

The isotopic analyses were carried out on the CO_2 extracted from marble samples by reaction with 100% phosphoric acid (H_3PO_4) at 25 °C in a vacuum extraction line (MCCREA 1950). The relative abundance of the ^{13}C and ^{18}O isotopes was determined with a *Finnigan Mat 252* isotope mass spectrometer at the Institute of Geosciences, University of Tübingen. The results

are expressed in terms of $\delta^{13}C$ and $\delta^{18}O$ in ‰ relative to the international reference standard PDB. Reproducibility for both carbon and oxygen was better than ± 0.1‰.

6.4.1.2.2. On-line stable isotope measurements

Extraction of CO_2 and stable isotope measurements were performed on a *Finnigan MAT 252* mass spectrometer, coupled with an on-line automated carbonate extraction system. The need for a high sample throughput at somewhat reduced accuracy to screen large numbers of samples has promoted the continuous flow technique. The *GasBench* is a continuous flow interface, feeding gas samples to the mass spectrometer. From carbonates, the CO_2 is prepared with phosphoric acid (103-105 %) in sealed He-flushed headspace bottles. After reaction and equilibration, a syringe is used to extract the sample He-CO_2 mixture and feed it to a sample loop. This sample loop sends the aliquot of the sample gas via a gas chromatograph where CO_2 is separated from other trace components to the mass spectrometer. Reproducibility for both carbon and oxygen was ± 0.2 ‰. All analyses are reported in the standard notation to PDB standard calcite.

6.4.1.3. Previous studies

When the method was introduced by CRAIG & CRAIG (1972), 170 samples from five different Greek quarries were measured and formed the database: The data relative to single samples are summarized within drawing all-inclusive contours around the extreme data points from each quarry. The initial results were very promising and encouraged many other researchers to apply the same method. There were several other quarry sites of interest to be tested along the Mediterranean region: The first in West Anatolia, where a large number of quarries were exploited during ancient times. MANFRA *et al.* (1975) plotted new data on the usual $\delta^{13}C$ / $\delta^{18}O$ diagram (Figure 22). This already gave a more confused frame for the growing database of marble isotopic compositions. Overlap started to appear and discrimination based on the simple hypothesis of unique isotopic values became more difficult.

In 1985, HERZ presented many new data and summarized the existing results. The field sources of quarry sites already sampled were better defined and many new historical sites were introduced (HERZ 1987, 1985). Herz´s diagram, reported in Figure 23, became the basis for every subsequent work on the isotopic determination of marble provenance.

After the above briefly mentioned studies, the marble isotopic reference diagram has been enlarged and updated several times in the past two decades. Comprehensive accounts were

published by GERMANN *et al.* (1980) and MOENS et al. (1992) in usual graphic form and are shown in Figure 24 and Figure 25. The databases of both Herz and Moens include most, but not all, the Mediterranean quarries of historical relevance and have became, over the years, the standard tools for the isotopic assignment of unknown marble samples.

GORGONI *et al.* (2002a) published a completely new, extensive database (Figure 26). This database is based upon 753 quarry samples (208 measured by Gorgoni and 545 from the literature) and 984 marble artifacts (414 measured by Gorgoni and 570 from the literature).

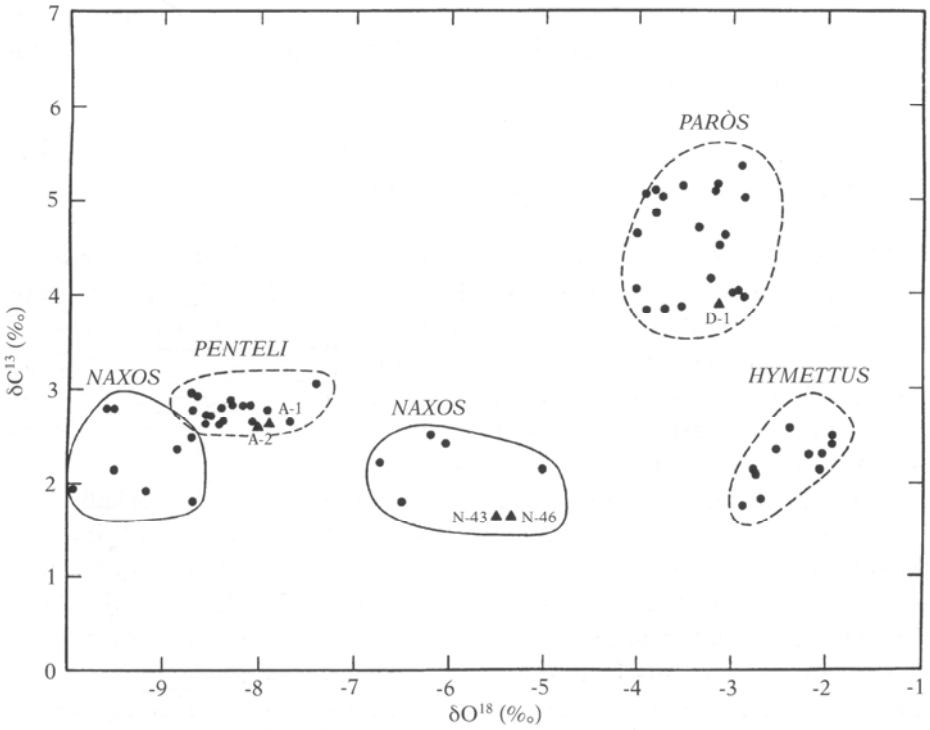

Figure 21: The isotopic databases published by Craig and Craig in 1972. Approximately 170 quarry samples were analysed.

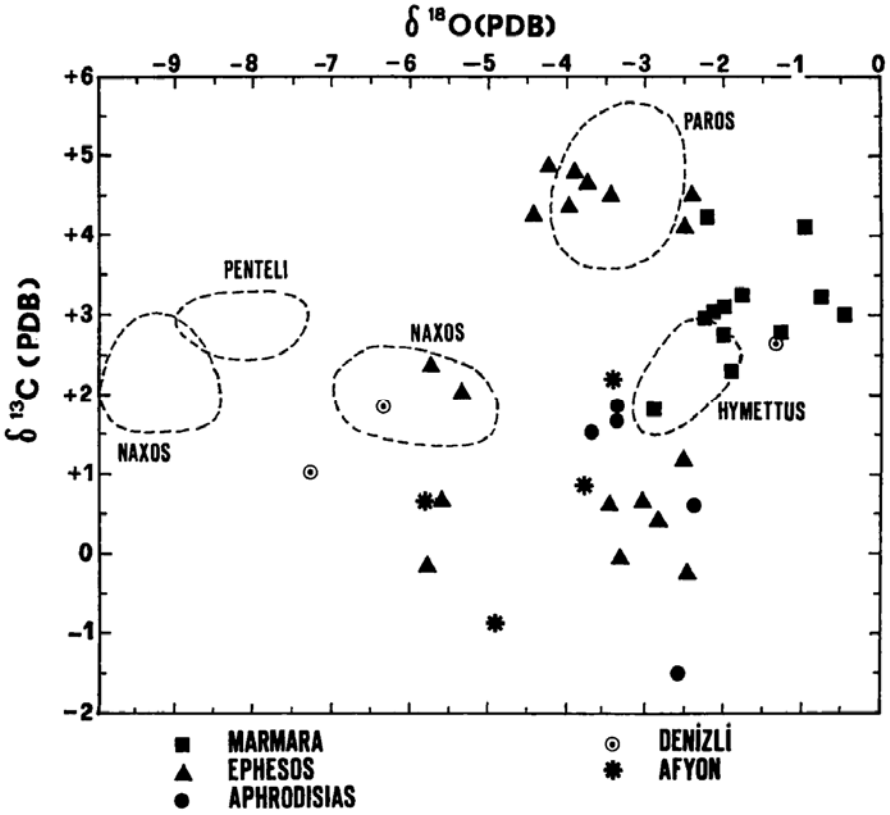

Figure 22: $\delta^{13}C/\delta^{18}O$ diagram of the marble samples from West Anatolia analysed by MANFRA *et al.* 1975. Encircled by dotted contour lines are the variations observed by CRAIG & CRAIG (1972) in ancient Greek marble quarries.

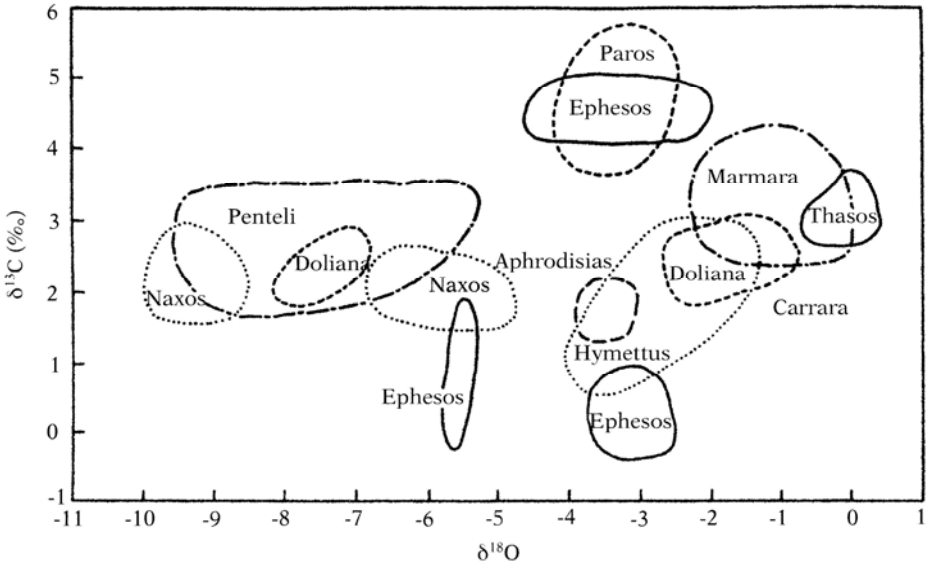

Figure 23: The isotopic databases published by Herz in 1985 and 1987. About 600 quarry samples were analysed.

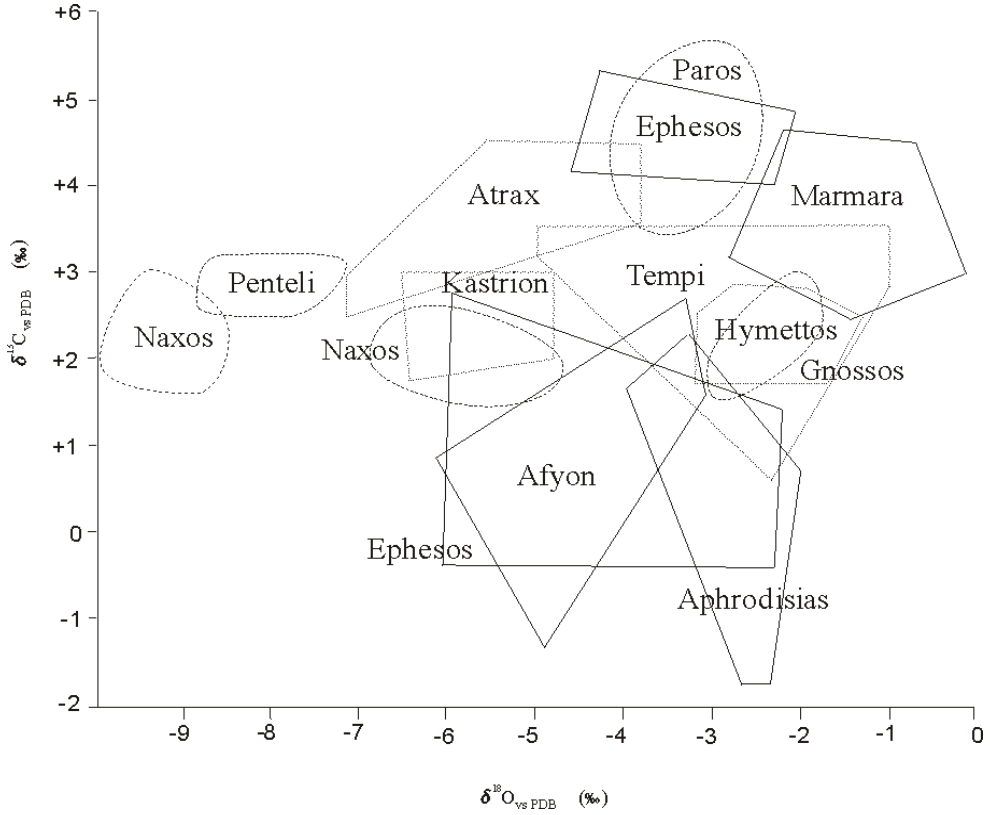

Figure 24: $\delta^{13}C/\delta^{18}0$ isotopic clusters of Greek and West Anatolian marbles after GERMANN *et al.* (1980), including data from CRAIG & CRAIG (1972) and MANFRA *et al.* (1975).

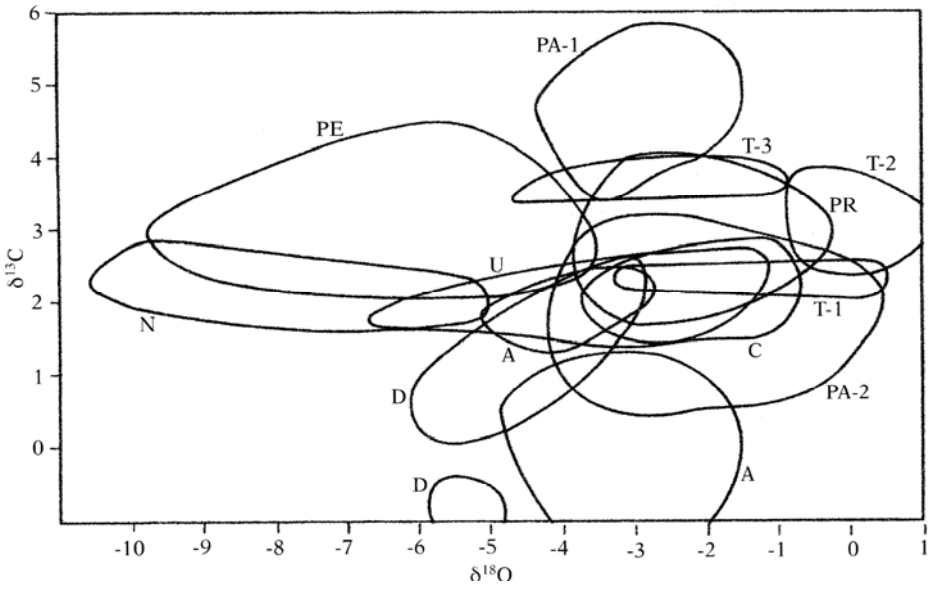

Figure 25: Isotopic database reported by MOENS *et al* in 1992. Quarry abbreviations are as follows: A=Aphrodisias, C=Carrara, D=Docimeum (=Afyon), N=Naxos, PA1=Paros-Marathi, PA-2=Paros-Chorodaki, PE=Pentelikon, PR=Proconnesos (=Marmara), T1, T2 and T3=Thasos, U=Uşak.

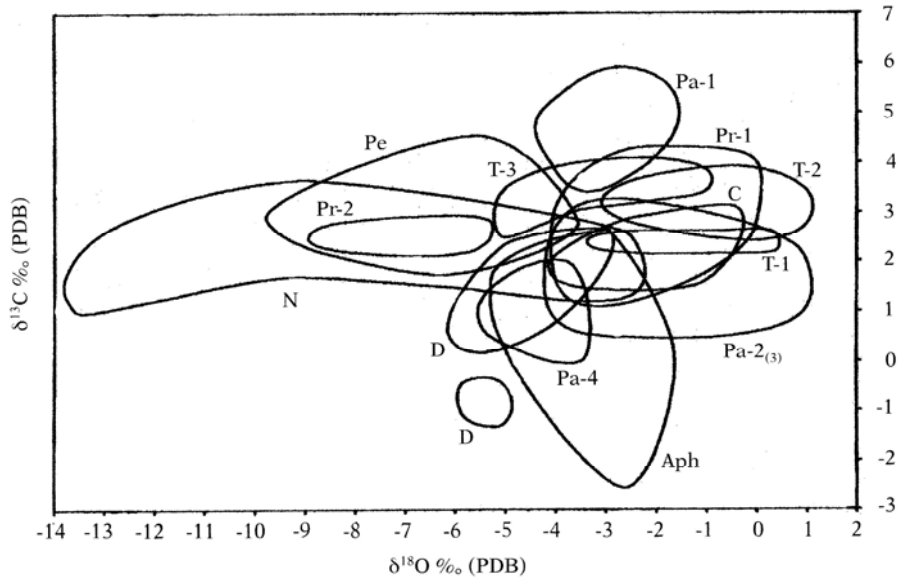

Figure 26: Stable isotopic database published by GORGONI *et al.* in 2002. Eight quarry sites subdivided into 11 groups are present in the database according the following abbreviations: Aph=Aphrodisias, C=Carrara, D=Docimium (Afyon), N=Naxos, Pa-1=Paros-Marathi or Lychnites, Pa-2=Paros Chorodaki, Pa-3=Paros-Haghios Minas, Pa-4 Paros Karavos, Pe=Pentelikon, Pr-1 and Pr-2 Proconnesos (Marmara), T-2=Thasos Aliki, T-3= Thasos Cape Vathy and Saliara (dolomitic marbles).

For this work, the database published by ZÖLDFÖLDI & SATIR (2003) is of particular interest: It examined the occurrences of the Biga peninsula in detail. Within this framework, the question ″where did the Trojans procure their marble from″ is especially interesting (Figure 27).

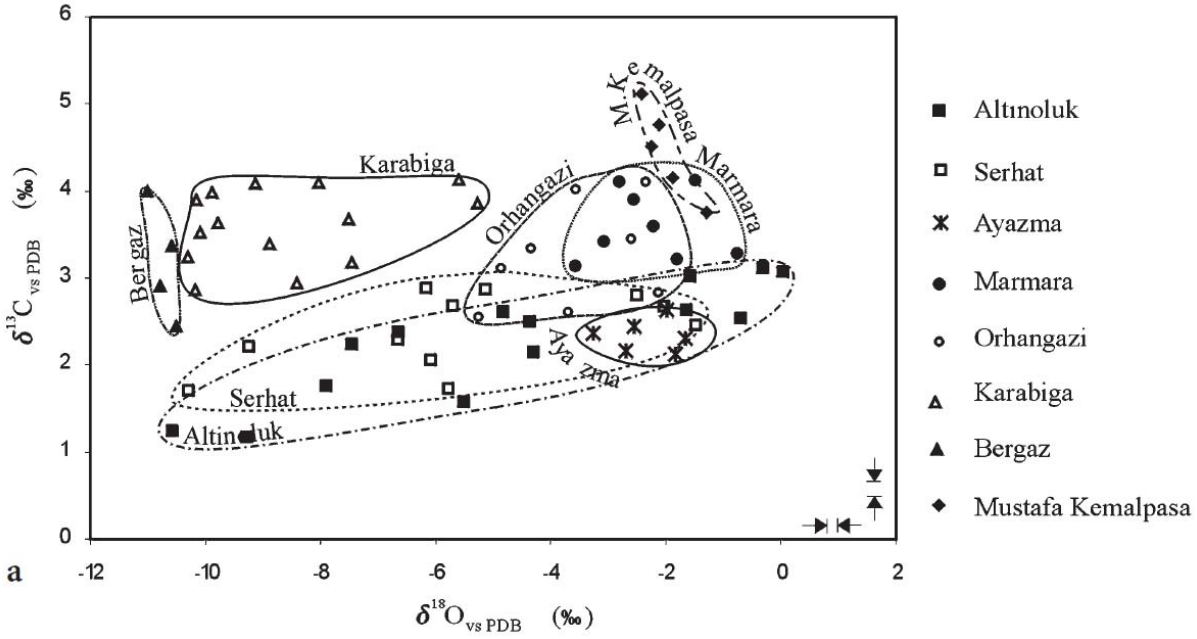

Figure 27: Database of the marble quarries in Northwest Anatolia published by ZÖLDFÖLDI & SATIR in 2003.

In addition, CRAMER (2004) published a database (embedded in a Marble Expert System) of more than 900 marble samples (both geological and archaeological).

Under a geographic point of view far from the Mediterranean and Troia, further historical stone quarries were investigated in the Eastern Alps. (ZÖLDFÖLDI *et al.* 2004a; ZÖLDFÖLDI *et al.* 2004b; ZÖLDFÖLDI *et al.* 2005; UNTERWURZACHER *et al.* 2005; ZÖLDFÖLDI & WEIGELE 2007). More recently, ATTANASIO *et al*. (2006) published a more detailed and descriptive database of the marbles of the Mediterranean Region. This includes 1346 marble quarry samples and takes care to distinguish samples within the individual quarries.

It must be added, however, that the use of summarising graphs, despite their obvious advantages in terms of simplicity and immediacy, means that the publication of detailed analytical data has been sporadic. Detailed results are rarely available in many cases and for this reason; statistical analysis of the data is difficult. A quick look at the figures clearly shows that the phenomenon of overlapping isotopic data between different localities appears to have increased greatly over the years with the number of sites sampled having increased. This result is not surprising, although it is less obvious that this overlap slowly increases with the number of samples measured for each locality. The reason is that an increase of the total number of samples gives rise, inevitably, to a larger number of marginal data points. The areas spanned by each quarrying site, drawn to include all the experimental samples, become larger and obviously tend to superimpose each other more. Another consideration is that graphs do not provide objective criteria for determining origin in the case of unknown samples with isotopic values that fall in the overlap region between two or more groups. Therefore, an internet-based interdisciplinary database, MissMarble was developed for archaeometric, art historian and restoration use by the author (ZÖLDFÖLDI *et al.* 2008a, b, 2009). The isotopic data of about 3000 quarry samples (Figure 32, ZÖLDFÖLDI *et al.* 2008b) including localities of the Eastern and Western Mediterranean region, of the ALCAPA region (Alps-Carpathian-Pannonian) and results of localities of the Indian subcontinent and Indochina available in the literature, published by ZÖLDFÖLDI *et al.* (2008b). More details about the MissMarble database are described in Appendix C.

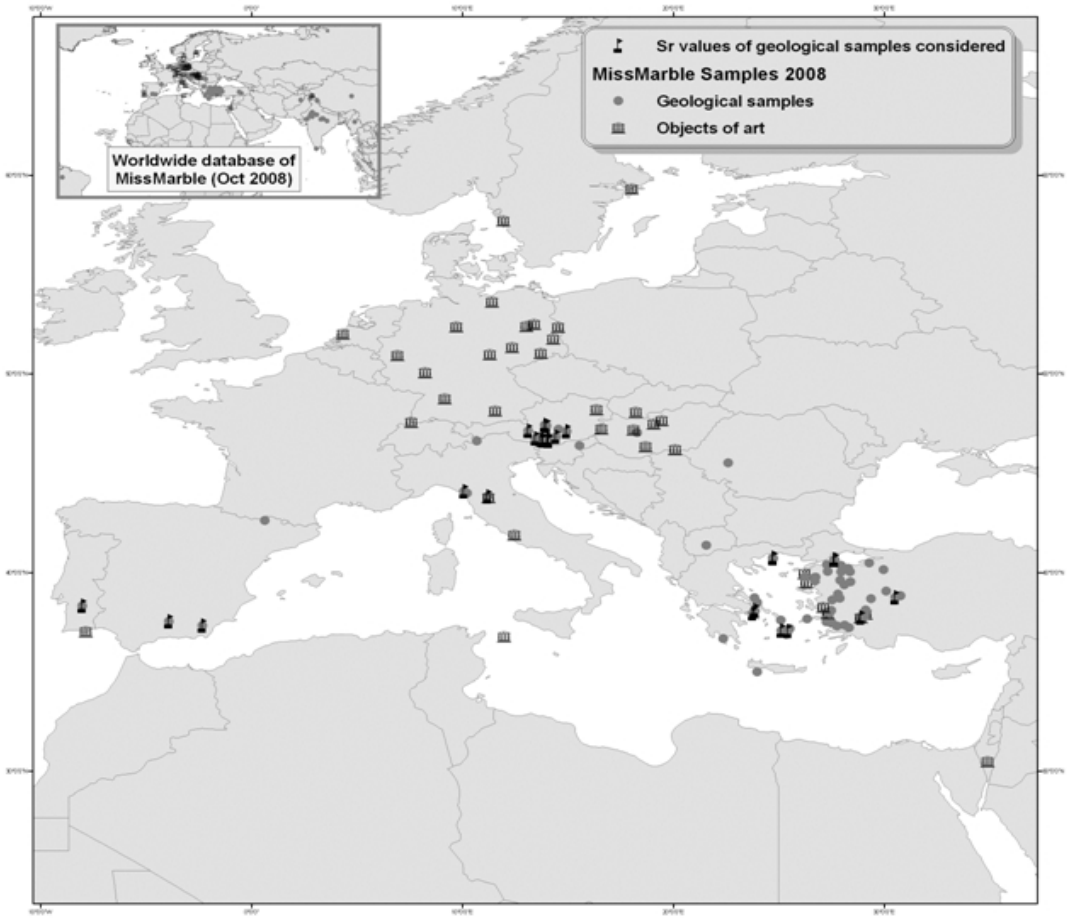

Figure 28: Spread of the existing data in the MissMarble database; the internet-based and interdisciplinary database, developed for archaeometric, art historian and restoration use (ZÖLDFÖLDI et al. 2009).

Nonetheless, stable isotopic ratio analysis is the most widely used method for determining the origin of marbles and very efficient to determine a small selection of quarries to be taken into consideration. In the last twenty years, the previously existing methods have been accompanied by a further series of even more sophisticated techniques: These include magnetic resonance, cathodoluminescence, laser reflectance and the quantitative analysis of texture. These methods are in different stages of development and have all demonstrated varying degrees of efficiency. Despite their efficiency, none of these techniques has replaced isotopic methods, or rather the integrated use of isotopic and petrographic data, in the study of marble. One of the most important advantages of the method is that only small powder samples are needed for the analyses (about 200 µg). This ″destruction″ is acceptable, even for museum people.

6.4.2. $^{87}Sr/^{86}Sr$ isotope analysis

6.4.2.1. The principles of strontium isotope analysis

This parameter is widely used in geological investigations, such as dating of minerals and rocks and/or inferring information about the genesis and evolution of geological materials. The range of $^{87}Sr/^{86}Sr$ ratios in nature is very wide. Generally, geological systems have significantly different $^{87}Sr/^{86}Sr$ ratios, depending on the initial value, the Rb/Sr concentration ratio and the age of the system. Strontium is a major component of seawater, with a concentration of 8 mg/l. This, combined with possible variations in the abundance of ^{87}Sr in the geologic realm due to the contribution of different amounts of radiogenic ^{87}Sr from ^{87}Rb decay, makes this element particularly interesting in marine geochemistry.

Sedimentary rocks composed of accumulated fossil carbonate shells can be dated and correlated with the use of high precision measurements of the ratio of $^{87}Sr/^{86}Sr$. The approximate $^{87}Sr/^{86}Sr$ variation in seawater at different geological times is known. Because Sr isotopes do not fractionate during metamorphism, the measurement of this ratio in marble could theoretically fix time constraints for the formation of the original carbonate.

Because of the great advantage of isotopic ratio analysis, principally the need for only small samples and homogeneity over large areas, we decided to investigate the $^{87}Sr/^{86}Sr$ isotopic ratios of the marbles. More details about the method and its basics are presented in Appendix B.4.

6.4.2.2. Analytical details

The whole-rock powders selected for Sr isotope analysis were dissolved for 24 hours in 1 ml 11.2 N ultra-pure HCl at 100°C. For isotope analysis, strontium was isolated on quartz columns by conventional ion exchange chromatography with a 5 ml resin bed of *Bio Rad AG* 50W-X12, 200-400 mesh. All isotopic measurements were carried out via Thermal Ionisation Mass Spectrometry at the Institute of Geoscience, University of Tübingen on a *Finnigan MAT 262* mass spectrometer equipped with 8 Faraday cups in static collection mode. Sr was loaded with a Ta-Hf activator on pre-conditioned W filaments and was measured in single-filament mode. The $^{87}Sr/^{86}Sr$ isotope ratios were normalised to $^{86}Sr/^{88}Sr = 0.1194$ for mass fractionation. Analyses of 28 separate loads of NBS 987 Sr standard during the course of this study (01-10/2000) gave $^{87}Sr/^{86}Sr$ of 0.710259 ± 0.000012 (± errors are 2σ of the mean). Total procedural blanks (chemistry and loading) were <300 pg Sr.

6.4.2.3. Previous studies

Using $^{87}Sr/^{86}Sr$ isotopic ratios for provenance determination of marbles used in Antiquity dates back to the work of HERZ *et al.* 1982. In that work he observed that strontium isotopic composition appeared to vary significantly between marbles from quarries located in different Mediterranean regions and therefore was suitable for use together with those parameters that had already shown to give good results (i.e. oxygen and carbon isotopic ratios). HERZ *et al.*'s conclusions, however, were based on few data, because, at that time, an adequate database of $^{87}Sr/^{86}Sr$ values did not exist. Those data showed that marbles from the Aliki quarry district of Thasos, Paros and Pentelikon could have significantly different $^{87}Sr/^{86}Sr$ values (HERZ 1987). HERZ & DEAN (1986) published new strontium isotopic data from Carrara, again showing their apparent ability to characterise and identify different marbles. Carrara quarries, in fact, displayed remarkably uniform $^{87}Sr/^{86}Sr$ values, which were different at least with respect to the values from Paros and Pentelikon.

These promising results, however, did not receive a large acceptance in the use of this technique as had occurred for oxygen and carbon isotope determinations, after CRAIG & CRAIG (1972) showed their usefulness in the identification of quarry sources of classical Greek and Roman marble artifacts. Most likely, the cost and labour-intensive nature of strontium isotopic analysis prevented the potential of $^{87}Sr/^{86}Sr$ ratio as an indicator for provenance to be accurately tested. CASTORINA *et al.* (1997) published the $^{87}Sr/^{86}Sr$ ratio of a large number of samples from some of the main quarry locations in the Mediterranean: Marmara, Carrara, Paros, Pentelikon, Doliana, Naxos and Aphrodisias. These authors reported that, although not conclusive as a means of distinguishing the different classical marbles, the strontium isotope ratios could provide a valuable contribution to solving particular cases of discrimination when combined with other methodologies. PENTIA *et al.* (2003) came to similar conclusions when presenting further data. They showed that discrimination was in some cases (such as Hymettus and Thasos-Aliki) improved using oxygen-carbon-strontium trivariate data sets compared to that obtained by using oxygen-carbon bivariate ones. Further $^{87}Sr/^{86}Sr$ ratios are presented by BRILLI *et al.* (2005) for white marbles collected from some of the most famous classical quarry areas of the Mediterranean: Carrara, Paros, Naxos, Pentelikon, Dokimeion, Hymettus, Thasos and Proconnesos. These ratios range from 0.7071 to 0.7092. The ranges of the different quarry areas are notably superimposed, but these results, together with petrographic and geochemical methods, could be used in marble provenance determination as an ancillary technique. Using the value of the $^{87}Sr/^{86}Sr$ isotopic ratio to solve contradictory or unknown assignments of marble artifacts will

become more and more common because of the worldwide growth of strontium isotope databases of marble quarries. Databases of the marble quarries in the Eastern Alps (ZÖLDFÖLDI *et al.* 2008b; ZÖLDFÖLDI & SZÉKELY 2009), the Iberian Peninsula (MORBIDELLI *et al.* 2007; ZÖLDFÖLDI *et al.* 2009; ZÖLDFÖLDI & SZÉKELY 2009) and the Indian subcontinent (ZÖLDFÖLDI 2009; ZÖLDFÖLDI & SZÉKELY 2009) are presently available (Figure 29 and Figure 30).

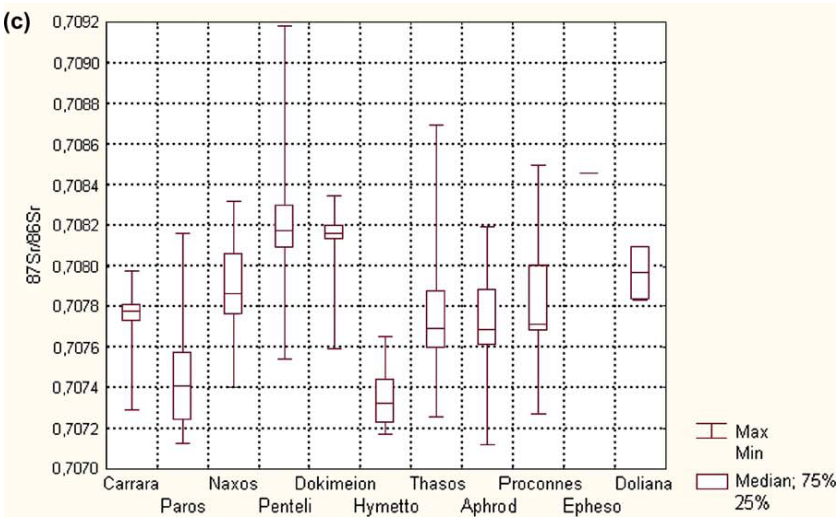

Figure 29: The $^{87}Sr/^{86}Sr$ ratios resulting from the data published by (BRILLI *et al.* 2005), including the collected data from the literature (CASTORINA *et al.* 1997; HERZ & DEAN 1986; HERZ 1987; PENTIA *et al.* 2003)

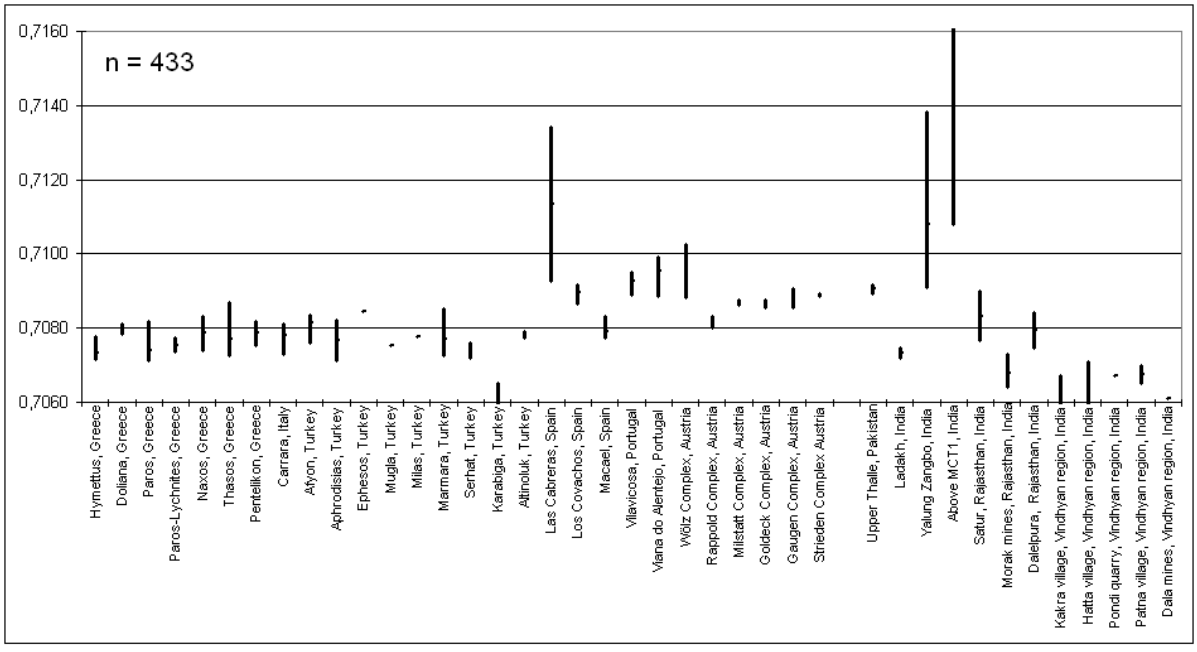

Figure 30: The $^{87}Sr/^{86}Sr$ ratios resulting from the data published by ZÖLDFÖLDI *et al.* (2008), including the collected data from the literature (BRILLI *et al.* 2005; CASTORINA *et al.* 1997; SCHUSTER *et al.* 2005a; PENTIA *et al.* 2003).

6.5. Other techniques

Further non-destructive methods were tested in order to prove the success of determining marble provenance. On the one hand, small angle neutron scattering (SANS) can be used to study the structural properties of certain materials. Its archaeological use is less common for the time being. However, interesting experiments were made trying to extend the methodology for determining marble provenance (LEN 2006). On the other hand, prompt gamma activation analysis (PGAA) was carried out in order to determine the bulk chemical composition non-destructively. Additionally, the broad lining method was applied. These three methods were initially applied in determining the provenance of marble in the framework of this study. Because the development of these methods regarding marbles is in progress and the results are available only for few selected occurrences, these methods were not involved in the provenance analysis of the Trojan marbles.

Recently, a new database of white marbles, based primarily on EPR (Electron Paramagnetic Resonance or ESR) spectroscopy and including some of the most important Greek, Turkish and Italian historical quarrying sites, was introduced (ATTANASIO *et al.* 1998; ATTANASIO 1999). In the field of marble provenance, the use of ESR spectroscopy, which detects, among others, the Mn^{2+} impurity ubiquitously present in marbles, dates back to the early 1980s (CORDISCHI *et al.* 1983). Since then, much more work has been carried out (LLOYD *et al.* 1988; MANIATIS & MANDI 1992; MANIATIS *et al.* 1995; POLIKRETI & MANIATIS 2002; POLIKRETI 2003; ATTANASIO 2003; ATTANASIO *et al.* 2006). Since its first introduction, the marble database has been considerably enlarged and updated (ATTANASIO 1999, 2003; ATTANASIO *et al.* 2002a; ATTANASIO *et al.* 2008a; ATTANASIO *et al.* 2008b; ATTANASIO *et al.* 2006). New samples, mainly from Anatolian quarries, were collected and measured. New, more suitable, standardization procedures were adopted and the measuring process has been modified and improved, particularly in the case of the petrographic or morphological variables, which were previously estimated simply on a qualitative basis and given as categorical variables (ATTANASIO *et al.* 1998).

The analytical and physico-chemical techniques discussed so far are without doubt the most widely used and efficient for determining the origin of unknown samples of white marble. They are not the only techniques that have been experimented with for this purpose, however. Among the numerous other methods, those that deserve mention are: xeroradiography, the

analysis of radiographic images (FOSTER & HERZ 1985), porosimetric studies (CASTRO 1995), colour spectrophotometry analysis (ZEZZA 1999), and work carried out on the angular distribution of light intensity by flat surfaces of marble samples (CARERI *et al.* 1992). This method was based on the use of portable laser equipment that recorded the absorbance/reflecting qualities of quarried marble, a parameter connected essentially to the type of structure, granulometry and composition (presence of carbonaceous/graphite substances) in a given marble. The method achieved good discrimination for some marbles and more or less nil for others. Since it proved to be of only partial usefulness right from the beginning, the decision was made not to proceed with the development of the methodology, although this decision may have been a mistake. Similar results have been recorded by BIRICOTTI & SEVERI (2004) using an optical non-destructive methodology.

The Inclusion-Fluid-Chemistry method is based on the "crush and leach" analysis of extractable total dissolved solids (TDS) from marbles and carbonate rocks in general (PROCHASKA & ATTANASIO 2009). The results from fluid inclusion investigations of carbonate rocks show that the fluid phase is usually relatively uniform with respect to its chemical composition. The composition of the extracted solutes depends on the depositional environment of the original carbonate rock (seawater, evaporation brines, primary dolomitization effects, etc.) and on the post-depositional alteration of the inclusion fluids in the marbles.

PART IV

RESULTS: CHARACTERIZATION OF ANATOLIAN MARBLE QUARRIES AND TROJAN MARBLE ARTIFACTS

7. Descriptive Approach

7.1. Macroscopic and microscopic description

7.1.1. Marbles from the Troad and neigbouring areas

7.1.1.1. Rhodope-Strandja Massif

Marbles from Karabiga (KB) are made of calcite and are grey to bluish grey in colour, coarse grained and homeoblastic in texture. The marbles from Bergaz (BRG) are mainly made of dolomite, are very fine-grained, white to yellowish-white in colour and have a homeoblastic texture, and mainly made of dolomite.

7.1.1.2. Sakarya Zone

Marbles from Ayazma (AYA) are white, coarse-grained and have a heteroblastic texture. Marbles from Yenice (YEN) and Serhat (SRH) are white to greyish-white in colour; have a heteroblastic texture and are made up mainly of calcite. Finally, the marbles from Altınoluk (ALT) are white to reddish-white in colour, have a heteroblastic texture and are calcitic. All three marbles come from the ***Kazdağ Range***.

Marmara (MAR) marbles from the ***Karakaya Complex*** are mainly made of coarse-grained calcitic marble, rarely white but in general characterized by grey stripes, which makes Marmara marbles so distinctive. Marbles from Bandirma (BAN) are very similar to those from Marmara. Marbles from Manyas (MAN) are white to yellowish-white in colour, coarse-grained and have a heteroblastic texture. The marbles from Mustafa Kemalpasa (MKB) are white to yellowish-white in colour, they have a heteroblastic texture and grains greater than 1 cm are imbedded in the fine- to medium-grained matrix.

Marbles from Orhangazi (ORH) belong geologically to the ***Armutlu-Ovacik Zone*** and are very similar to those of Marmara: They are coarse-grained calcitic marbles with grey stripes.

Marbles from Iznik (IZN) are white to greyish-yellowish-white, coarse-grained and have a heteroblastic texture.

7.1.2. Marbles from Middle and Southwest Anatolia

The marbles from the ***Menderes Massif*** differ in colour, texture and pattern depending on their stratigraphic levels. There are four major stratigraphic carbonate horizons in the cover successions along the southern flank of the Menderes Massif, where marbles are produced today and probably in antiquity. These carbonate horizons are in the Permo-Carboniferous, Triassic, Upper Cretaceous and the Paleocene levels (DÜRR 1975). The marble beds on the surface are (i) the Permo-Carboniferous black marble lenses interbedded with phyllites, (ii) the Triassic white to purple marbles found within mica schist beds, (iii) the Upper Cretaceous emery bearing white-greyish white marble beds and (iv) the Paleocene red coloured Agaean Bordeaux marble beds. In this work, I focused on the white marbles of the Triassic and Cretaceous. The Triassic white marbles (also known as "Milas marbles") are mainly made up of calcite, have a greyish-white weathered and white fresh colour and a granoblastic texture. There is no well-defined foliation plane observed within this marble bed but it occasionally includes eggplant coloured veins. Some samples include white dolomite spots of 1-5 cm, with a heteroblastic texture and varying grain size. Fine dolomite crystals with smaller grain size are present alongside the coarse calcite crystals. The marbles from Muğla are white-greyish in colour, granoblastic in texture and consist almost 100 % of calcite crystals. Samples from Babadağ are white to greyish-white marbles with a homeoblastic texture. Often grey layers can be observed in a white matrix.

Samples from Afyon (AFY, ancient Docimian), belonging to the ***Central-Anatolide-Tauride*** *block,* are white to yellowish-white, fine-grained marbles with a homeoblastic texture.

7.1.3. Trojan marbles

The samples of archaeological objects were perceived, in any case, as an individual. Therefore, in the next chapters, it is necessary to present the detailed results without making groups.

7.1.3.1. Prehistoric marbles

Kumtepe marbles exhibit different macroscopic features: Some of the samples are greyish-white, fine-grained marbles (F28/990), other are white in colour and medium to coarse-grained (F29/460), again others are reddish-white in colour and fine- to medium-grained (F28/958/1). Based on the macroscopic features, the provenance of the marbles has to be different. All these objects are soluble with HCL *(Appendix D.1.1)*.

The macroscopic features of the ***Bronze Age marble*** of Troia are summarized in *Appendix D.1.2.* The finds are not arranged in groups because the archaeological objects are from different areals that date to different archaeological ages, and in some cases the chronology is not clear. The marbles are all soluble in HCL. The colour varies between white to greyish-white, sometimes yellowish or reddish. The grain size varies from fine-grained to coarse-grained.

7.1.3.2. Hellenistic marbles

They are two typical raw materials among the building stones of the ***Athena Temple***: PBA1-4 are white marbles, with fine to medium grain size and a heteroblastic texture. PBA5 and PBA6 are white to greyish marbles with medium to coarse grain size and a heteroblastic texture. All these samples are soluble in HCL and produce strong odour during sampling. The marbles from the ***Athena Temple Portico*** can be grouped into two types: PBA7 and PBA8 are white to greyish-white marbles with medium to coarse grain size, a heteroblastic texture and strong odour during sampling (they are similar to the samples PBA5 and PBA6 from the Athena Temple). The other group, PBA9 and PBA10, are white and greyish-white with fine to medium grain size, a heteroblastic texture, but without the strong odour during sampling.
The marbles from the ***Sanctuary "Roman Altar"*** (PBA11-13) are macroscopically similar, white to yellowish-white in the colour, with medium to coarse grain size and heteroblastic texture, and produce a strong odour during sampling (*Appendix D.1.3.*).
The marbles from the ***Blue Marble Building of the Bath*** (PBA14-16) are dark grey; they have a fine grain size and heteroblastic texture. No odour was detected during sampling. The marbles of the ***North Building Treshhold of the Sanctuary*** (PBA17-18) are white in colour with fine to coarse grain size and a heteroblastic texture. A strong odour was produced during sampling. The marbles of the ***Bouleuterion*** (PBA19-21) are white to grey in colour with fine to coarse grain size and a heteroblastic texture. PBA19 produced a light, the other samples a strong odour during sampling (*Appendix D.1.3.*).

7.1.3.3. Roman marbles

The ***Children of Claudius Inscription*** (PBA22) was made of white marble, with fine to medium grain size and a heteroblastic texture; sampling produced a light odour. The marbles of the ***Odeion*** can be differentiated into two group, some of them are white to greyish-white with medium grain size, a heteroblastic texture and strong odour during sampling (PBA23-

26). Other samples (PBA27-29) are grey to dark grey with fine to medium grain size and light or absent odour. The marbles from the ***Nymphaeum base moulding of the Bath*** (PBA33-35) are white to greyish in colour, with fine to medium grain size and heteroblastic texture. Only two samples (PBA32 and PBA35) produced a strong odour during sampling (*Appendix D.1.4.*).

8. Mineral composition of the investigated marbles

8.1. Results of X-Ray-Diffraction (XRD) Analysis

8.1.1. Marbles from the Troad and neighbouring areas

8.1.1.1. Rhodope-Strandja Massif

The marbles from Bergaz (sample BE2) are fine-grained, dolomitic, white marbles. The marbles from Karabiga (KB) are calcitic marbles *(Appendix D.2.1.1*).

8.1.1.2. Sakarya Zone

The marbles from the ***Kazdağ Range*** are mostly calcitic. Samples especially from Altınoluk (samples ALT1D and ALT2A) on the southern part of the Kazdağ Massif and Yenice (sample KR1, *Appendix D.2.1.2.1*), contain quartz, kaolinite, dolomite, mica and chlorite as accessory minerals. Marbles from Serhat are calcitic, with accessory minerals such as quartz, dolomite and mica. Marbles from Ayazma are also calcitic with accessories like quartz and mica, but no dolomite was detected. Marbles from Yenice are calcitic with accessory minerals such as quartz, dolomite and kaolinite, while marbles from Bergaz have a high amount of dolomite with accessory quartz.

The marbles from the ***Karakaya Complex*** are calcitic. Manyas marbles include accessory quartz; Mustafa Kemalpasa marbles include accessory dolomite, quartz and plagioclase while Marmara marbles often contain dolomite, quartz and sometimes hematite, plagioclase and mica (*Appendix D.2.1.2.2.*).

The marbles from Orhangazi and Iznik from the ***Armutlu-Ovacik Zone*** are calcitic. Quartz, dolomite, plagioclase, mica and hematite are present as accessory minerals (*Appendix D.2.1.2.3.*).

8.1.2. Marbles from Middle and Southwest Anatolia

The marbles from the Milas are calcitic (*Appendix D.2.1.3.1.*), but dolomite also occurs as the major mineral component (MI1, MI3, MI11). Accessory minerals are quartz, mica and dolomite (if dolomite is not occurring as major component). Yatagan provides calcitic marbles with accessory quartz, plagioclase and mica. Muğla marbles are calcitic; almost all samples include quartz as accessory mineral, dolomite is present occasionally.

The marbles from the ***Central-Anatolide-Tauride block*** are always calcitic (*Appendix D.2.1.3.2.*). Dolomite appears in the investigated material neither as a major mineral nor as accessory mineral. Accessory minerals are quartz, mica, ancillary chlorite and plagioclase.

8.1.3. Trojan marbles

8.1.3.1. Prehistoric marbles

The marble objects from ***Kumtepe*** are primarily calcitic; but dolomite appears as a major mineral in the object F28/958/1 and as an accessory mineral in the object F29/460. Other accessory minerals are quartz and chlorite (*Appendix D.2.2.1.*).

The ***Bronze Age*** marble objects are calcitic with the exception of two pieces, namely E4/5/95 and T23/(5), which contain dolomite as a major mineral. Accessory minerals aside from dolomite are quartz, hematite, plagioclase, chlorite, kaolinite and christobalite. A more detailed description is presented in *Appendix D.2.2.2.*

8.1.3.2. Hellenistic marbles

The marble samples of the ***Athena Temple*** are calcitic, but dolomite is present as major mineral in the samples PBA2 and PBA3. Accessory minerals are dolomite, quartz, mica, chlorite, and hematite. The investigated material taken from the architectonical elements of the ***Athena Temple Portico*** are also calcitic. Dolomite is present as a major mineral in the samples PBA7 and PBA9 and as an accessory mineral in two additional samples. Quartz and mica are also present as accessories. The samples of the ***Sanctuary "Roman Altar"*** are calcitic marbles and include dolomite and quartz as accessory minerals. The samples of the ***Blue Marble Building*** of the Bath are composed of calcitic marble with quartz, mica and dolomite as accessory minerals. The investigated samples of ***North Building Treshhold of the Sanctuary*** are composed of pure calcitic marble (PBA18) and calcitic marble with quartz and dolomite as accessory minerals (PBA17). The investigated samples taken from ***Bouleuterion***

are calcitic marbles. Dolomite is present in all samples as an accessory mineral while quartz and mica are present in the sample PBA19 (*Appendix D.2.2.3.*).

8.1.3.3. Roman marbles

The raw material of the ***Children of Claudius Inscription*** is composed of calcitic marble with quartz and dolomite as accessory minerals. The investigated samples of the architectonical elements of the ***Odeion*** are made up of calcitic marble with dolomite as major component (PBA23 and PBA24) or as an accessory mineral (PBA26). Quartz is a common accessory mineral in all investigated samples, while mica and plagioclase are present infrequently. The samples of the columns of the ***Odeion*** are composed of calcitic marbles with dolomite and quartz as common accessory minerals. The raw material of the ***Nympheum base moulding*** (PBA30-32) is calcitic marble with dolomite, quartz and plagioclase as accessory minerals. The raw materials of the moulding of the Bath (PBA33-35) consist also of calcitic marble, with accessory minerals as quartz, sometimes dolomite and amphibole (*Appendix D.2.2.4.*).

8.2. Results of the electron microprobe investigations

Backscattered electron images (BSE) can give important information about the spatial relationships of adjacent phases and about zoning and inclusions within phases. BSE intensity is, to a first approximation, a function of the chemical composition: The brighter an area, the greater the mean atomic number of that area relative to adjacent areas. Therefore, to check the mineralogical composition and the arrangement of the different minerals within a sample, a selection of the samples were investigated with electron microprobe.

8.2.1. Electron microprobe investigations on marbles from the Troad and neighbouring areas

8.2.1.1. Rhodope-Strandja Massif

Using electron microprobe analyses, calcitic marbles from Karabiga seem to be very pure marbles, including small aggregates (some 10 µm) consisting of hedenbergite (Figure 31).

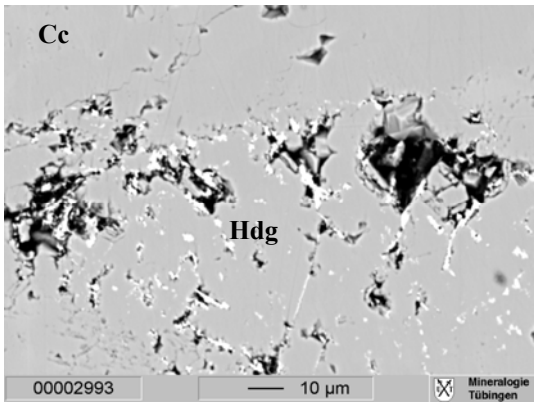

Figure 31: BSE image of the sample KB1A. Calcitic marble with hedenbergite (Hdg).

8.2.1.2. Sakarya Zone

Based on the investigation with BSE images, the marble samples of the ***South Kazdağ Range*** are calcitic with dolomite present to a greater or lesser amount. In the case of samples from Altınoluk (e.g., ALT2F, K12, K21) dolomite appears in agglomerates or scattered throughout the sample. Accessory minerals include apatite, which appears very frequently and is scattered throughout the sample (Figure 32 and Figure 33); magnetite, which is common on the scale of up to 50 µm (Figure 33 and Figure 35); elongated flogopite crystals on the scale of up to 50 µm (Figure 33 and Figure 35); sporadic occurrences of diopside (up to 100 µm, Figure 32), quartz (up to 20 µm, Figure 32 and Figure 34), titanite (up to 10 µm, Figure 32), perovscite (up to 10 µm, Figure 34), talc (or chlorite, 10 µm, Figure 34 and Figure 35) and rutile (up to 10 µm, Figure 35) can be observed. The ***North Kazdağ Range*** (e.g., AyazmaA) can be characterised due to the presence of elongated flogopite crystals (up to 200 µm), diopside (up to 60 µm) and apatite (up to 50 µm) in relatively high concentrations (Figure 36). Using the BSE method, the marbles of the ***Karakaya Complex*** are described as calcitic marbles, with accessory minerals such as apatite, paragonite, rutile and titanite in the sample MA3 from Marmara (Figure 37) and flogopite, pyrite, dolomite, muscovite and talc (or chlorite) in the sample BAN1B from Bandirma (Figure 38).

8.2.1.3. Marbles from Middle and Southwest Anatolia

Marble samples from Milas contain dolomitic layers composed of crystals on the scale of few tens of µm (MI3, Figure 39) or singular dolomite crystals up to 200 µm in size (MI2, Figure 40). Additionally apatite crystals (few µm) are scattered throughout the samples. Marbles from Muğla (Figure 41 and Figure 42) are calcitic and include accessory minerals such as dolomite (up to 50 µm), pyrite that grows on the boundary of calcite grains (up to 40 µm),

apatite that is scattered throughout the sample (only few µm in size) and anthophyllite (up to 20 µm). The marbles from the ***Central-Anatolide-Tauride block*** are very clean marbles. Only some small accessory minerals, such as apatite and pyrite, can be observed in the samples (Figure 43-67).

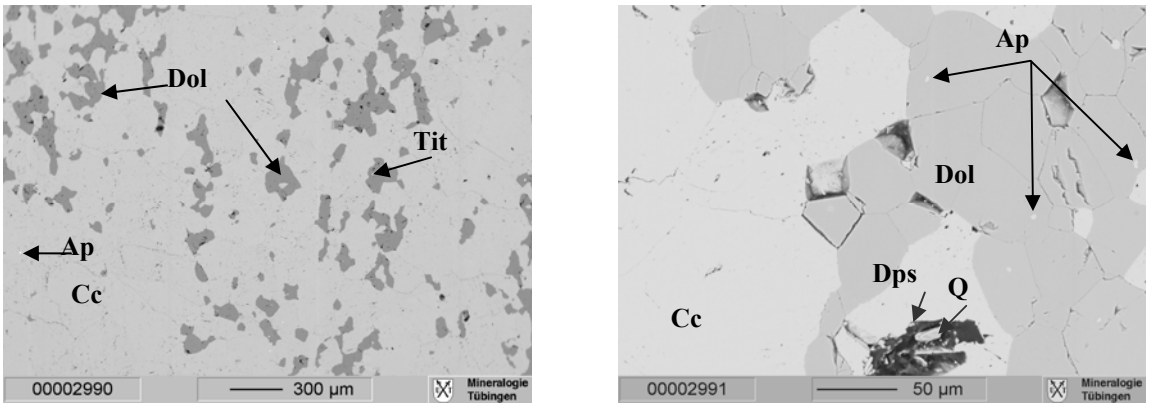

Figure 32: BSE image of sample ALT2F. It mostly consist of calcite (Cc), additionally dolomite (Dol), diopside (Dps), quartz (Q), apatite (Ap) and titanite (Tit) are present.

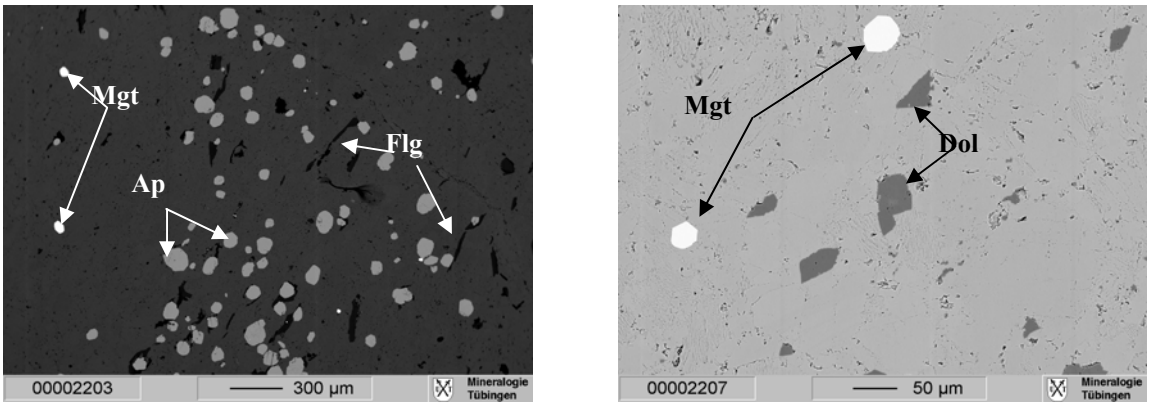

Figure 33: BSE image of sample K12. It mostly consists of calcite, additionally dolomite (Dol) isomorphic apatite (Ap) and magnetite (Mgt) and elongated flogopite (Flg) are present.

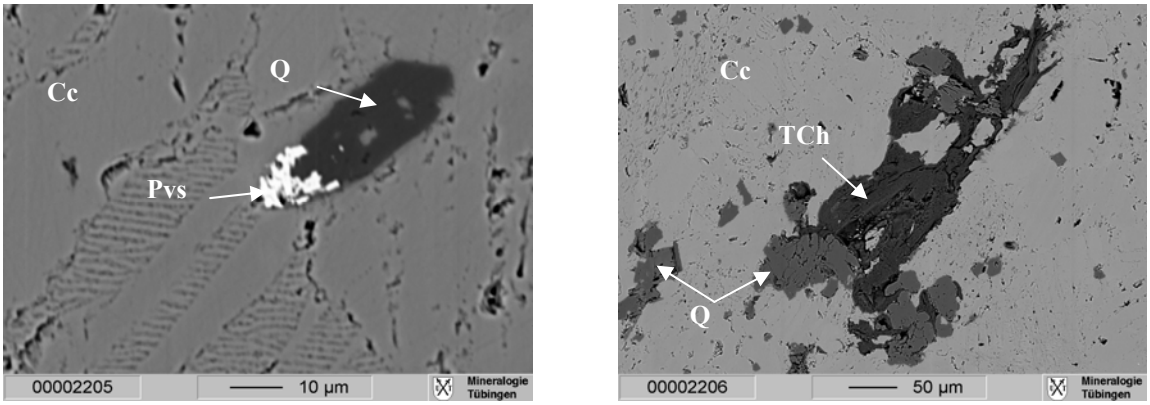

Figure 34: BSE image of sample K12. Calcitic marble with accessory minerals, perovskite (Pvs), quartz (Q), talc-chlorite (TCh)

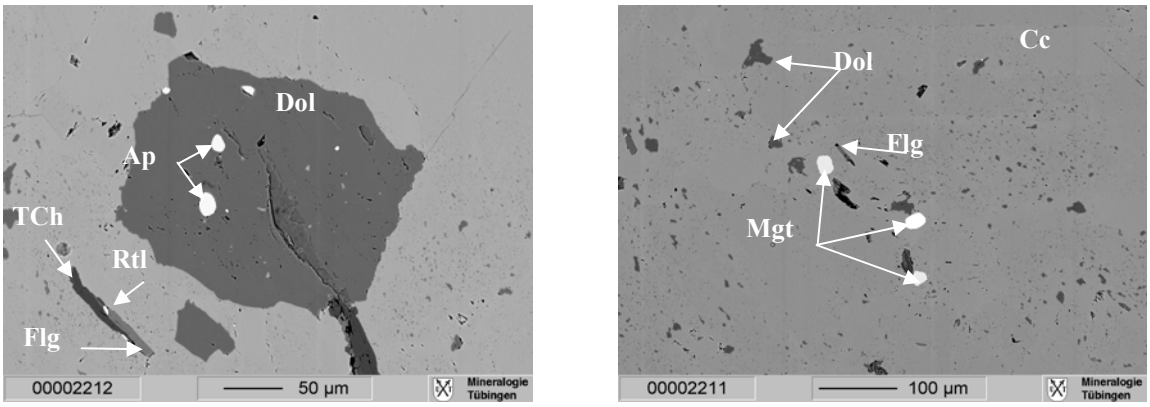

Figure 35: BSE image of sample K21. Calcitic marble with traces of dolomite (Dol), talc or chlorite (TCh), apatite (Ap), rutile (Rtl), flogopite (Flg) and magnetite (Mgt)

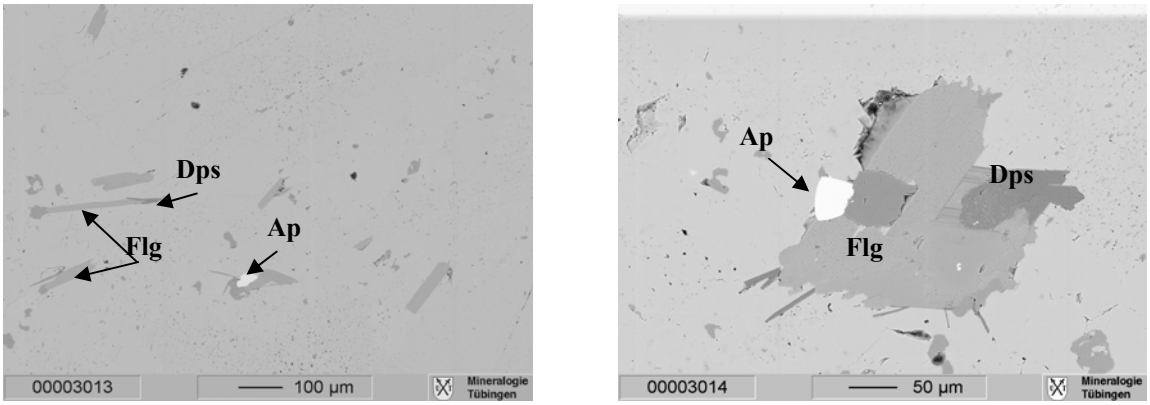

Figure 36: BSE image of sample AyazmaA. It mostly consists of calcite, but flogopite (Flg), diopside (Dps), apatite (Ap) are also present.

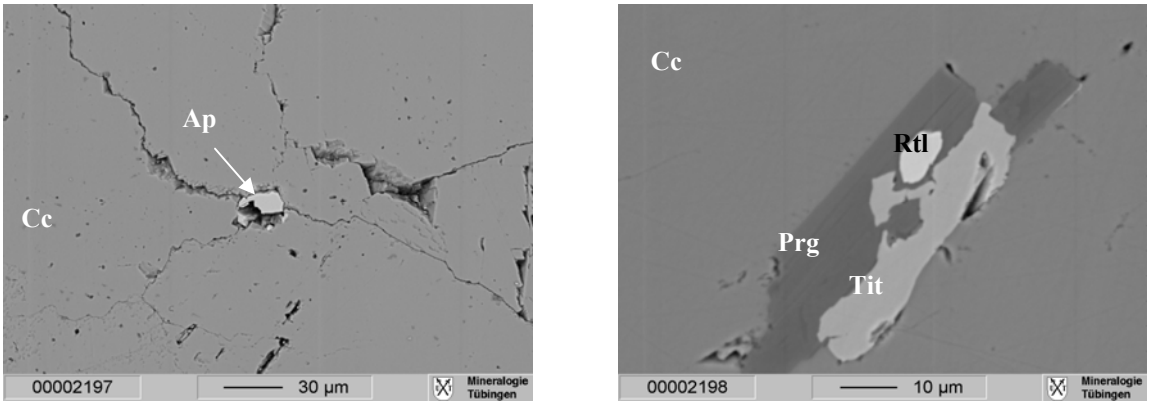

Figure 37: BSE image of sample MA3. Calcitic marble with traces of apatite (Ap), paragonite (Prg), rutile (Rtl) and titanite (Tit).

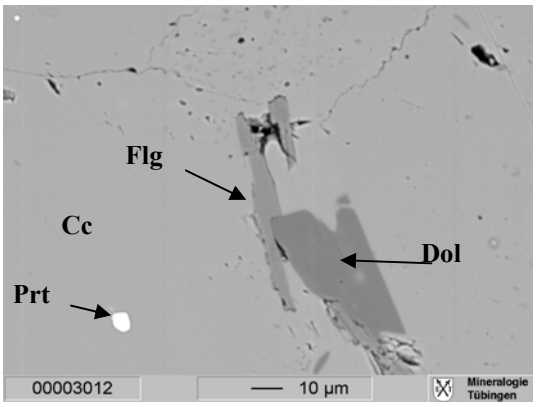

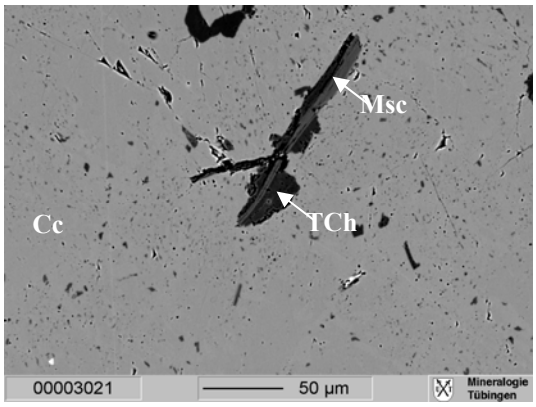

Figure 38: BSE image of sample BAN1B. Calcitic marble with traces of dolomite (Dol), flogopite (Flg), pyrite (Prt), tacl or chlorite (TCh) and muscovite (Msc)

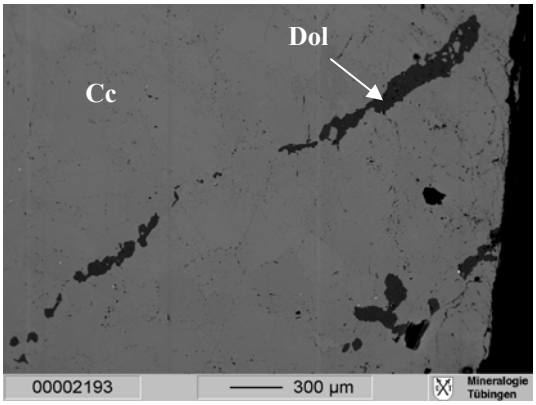

Figure 39: BSE image of sample MI3. It mostly consists of calcite with dolomitic veins (dark crystals)

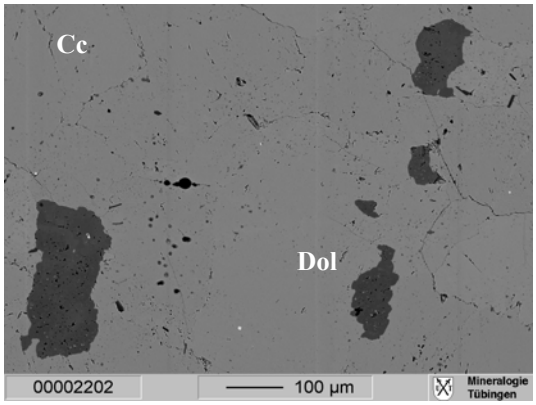

Figure 40: BSE image of sample MI2. In a calcitic matrix, dolomite crystals are present. Bright white splotches – probably pyrite – scattered throughout the sample

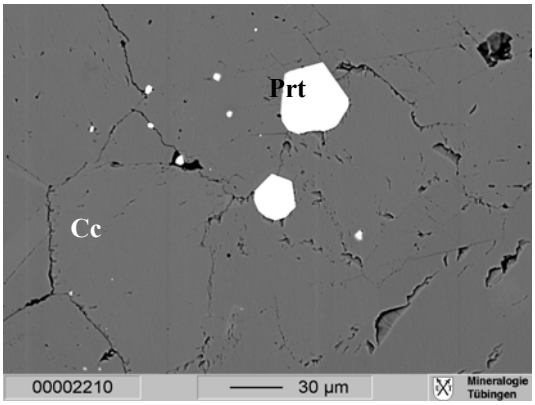

Figure 41: BSE image of sample M11. Bright isomorphic pyrites (Prt) sit on the boundary of the calcite crystals.

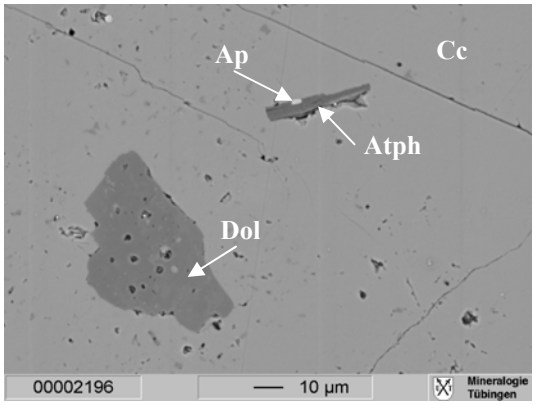

Figure 42: BSE image of sample M10. Calcitic matrix with dolomite (Dol), anthophyllite (Atph) and apatite (Ap).

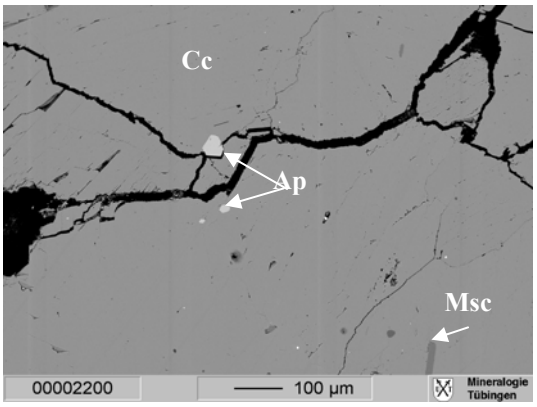

Figure 43: BSE image of sample BD4. Marble with calcitic matrix and small apatite crystals (Ap), mostly grown on the boundary of calcite crystals. Additionally muscovites (Msc) are present.

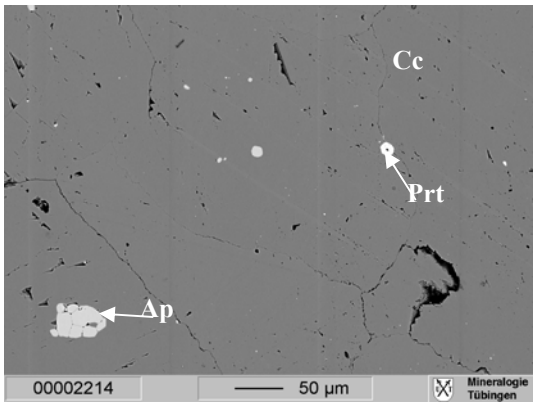

Figure 44: BSE image of sample BD6. Calcitic matrix with apatite (Ap) and pyrite (Prt) splotches scattered throughout the sample. An agglomerate of apatite crystals can be observed in the bottom left corner.

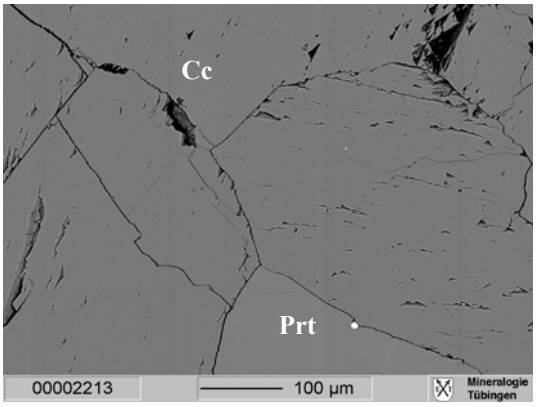

Figure 45: BSE image of sample A2. Very clean calcitic marble with only a few spots of pyrite (Prt) crystals.

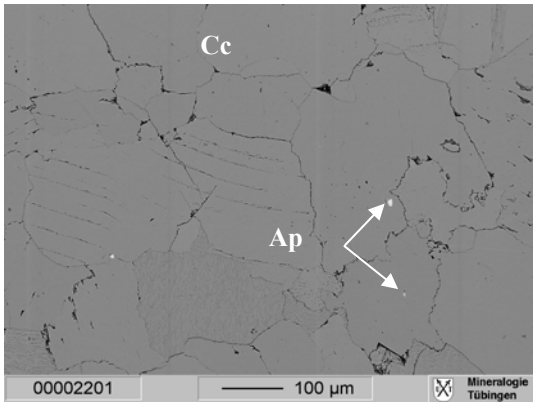

Figure 46: BSE image of sample A14. Very clean calcitic marble with only a few spots of apatite crystals (Ap).

8.2.2. Trojan marbles

Unfortunately, I did not receive permission to sample the Prehistoric marbles to make thin sections and it was not possible to perform electron microprobe investigations. Therefore, only the observations by electron microprobe of the marble samples of the Hellenistic and Roman period in Troia can be discussed here.

8.2.2.1. Hellenistic marbles

The material of the ***Athena Temple*** (e.g. PBA6, Figure 47 and Figure 48) is calcitic marble including single dolomite crystals (up to 100 µm), apatite (few µm), feldspar (up to 20 µm) and muscovite (up to 30 µm). Sample PBA9 represents the marbles from the ***Athena Temple Portico***. The agglomerates composed of kyanite, flogopite, feldspar and magnetite are

particularly interesting. These agglomerates are on the scale of 200 µm and are easily recognisable in the complete thin section (Figure 49 and Figure 50).

The material of the ***Sanctuary, North Building Threshold*** consists of calcitic marble with accessory minerals such as flogopite, pyrite, apatite and dolomite. The size of the accessory minerals did not exceed 50 µm.

The sample PBA19 (Figure 52), from the ***Bouleuterion*** has a calcitic matrix with agglomerates consisting of dolomite and muscovite on the scale of up to 600 µm. PBA21 (Figure 53) is also calcitic marble, including dolomite crystals whose size reaches 200 µm. Furthermore, flogopite, pyrite and apatite minerals are present.

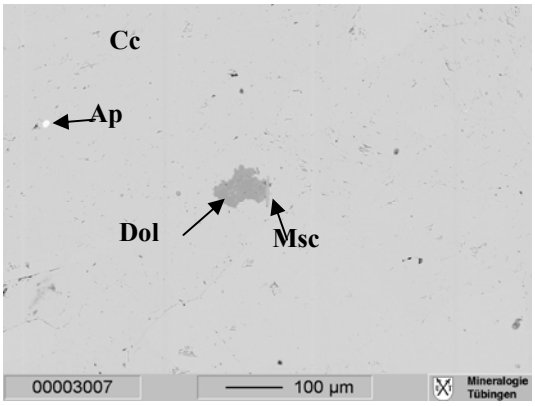

Figure 47: BSE image of sample PBA6. Calcitic marble with small amount of dolomite (Dol), muscovite (Msc) and apatite (Ap)

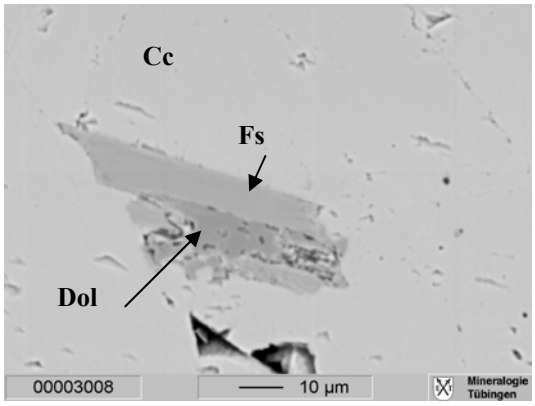

Figure 48: BSE image of sample PBA6. Traces of dolomite (Dol) and feldspar (Fs) in the calcitic matrix.

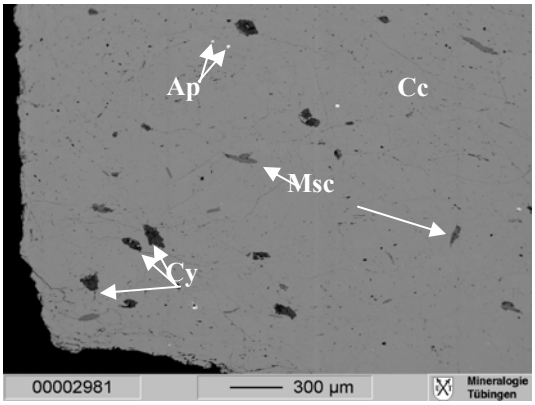

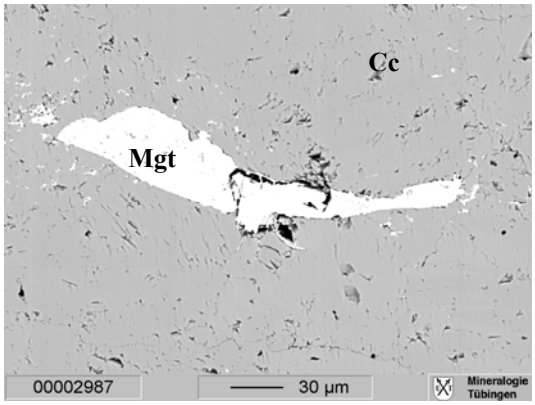

Figure 49: BSE images of sample PBA9. Calcitic marble with accessory minerals: dolomite (Dol), muscovite (Msc), apatite (Ap), cyanite (Cy) and magnetite (Mgt) on the scale of about 100 µm.

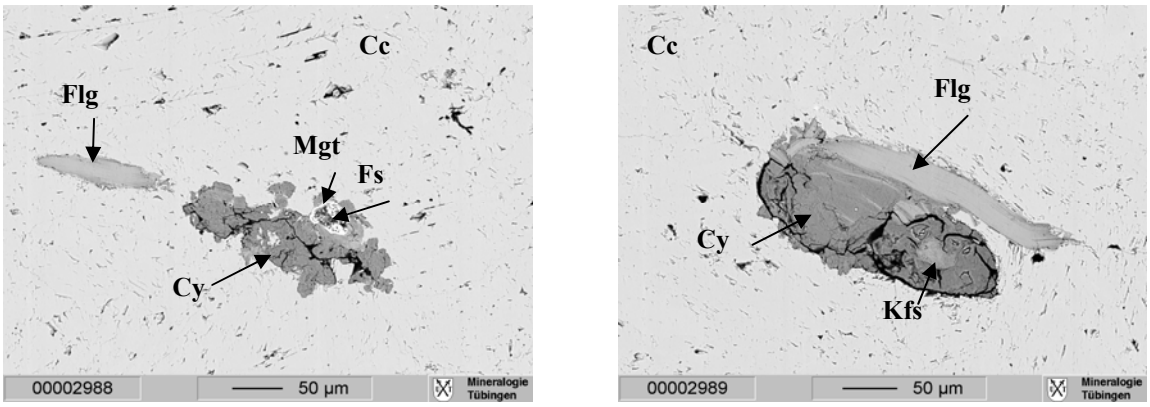

Figure 50: BSE images of sample PBA9. Calcitic marble with agglomerates of cyanite (Cy), magnetite (Mgt), flogopite (FLG), feldspar (Fs) and kalifeldspar (Kfs)

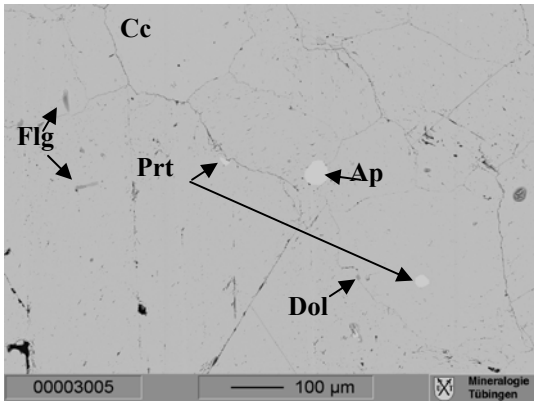

Figure 51: BSE image of sample PBA18. Calcitic marble with flogopite (Flg), pyrite (Prt), apatite (Ap) and dolomite (Dol)

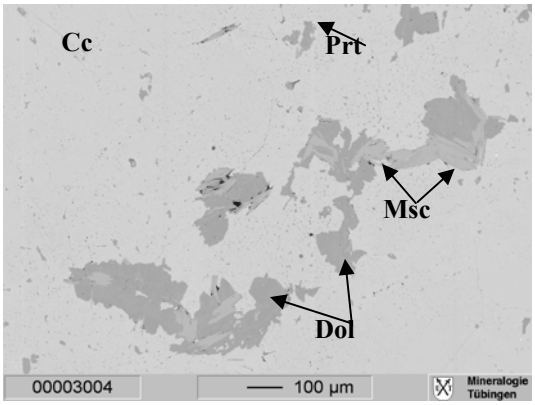

Figure 52: BSE image of sample PBA19. Calcitic matrix with dolomite (Dol) and muscovite (Msc) agglomerates. Traces of pyrite (Prt) can also be observed.

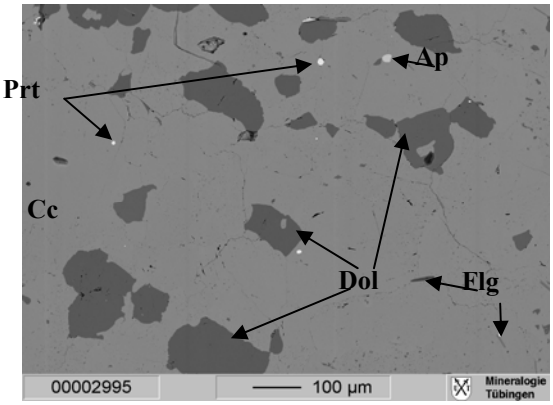

Figure 53: BSE image of sample PBA21. Calcitic matrix with dolomite (Dol), pyrite (Prt), apatite (Ap) and flogopite (Flg).

8.2.2.2. Roman marbles

The material of the ***Odeion*** is calcitic marble, with a small amount of apatite and dolomite. Apatites are on the scale of few µm and are scattered throughout the thin section. Dolomite crystals have an irregular shape, are sized about 30 µm and they are concentrated on the boundary of calcite crystals. Based on the microprobe investigation, the marbles from the

Bath moulding and ***Nympheum base moulding*** have different origins. Samples PBA30 and PBA31, belonging to the ***Nympheum base moulding***, are rich in dolomitic layers with accessory minerals such as apatite (few µm) and kyanite (up to 20 µm, Figure 55 and Figure 56). PBA32 from the Bath moulding is calcitic marble without traces of dolomite. Only very small apatite crystals are present in the sample (Figure 57).

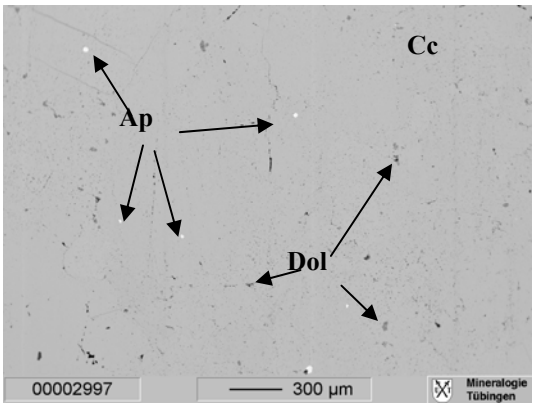

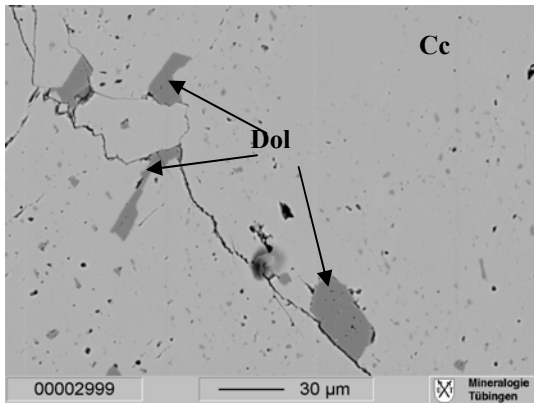

Figure 54: BSE images of sample PBA24. Calcitic marble with apatite (Ap) and dolomite (Dol) scattered throughout the sample (left). Dolomite crystals (Dol) are concentrated on the boundary of the calcite crystals (right).

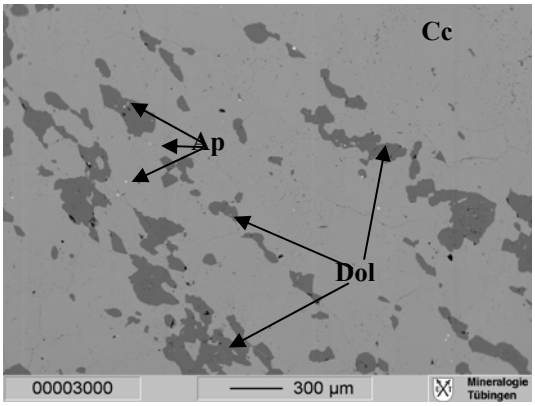

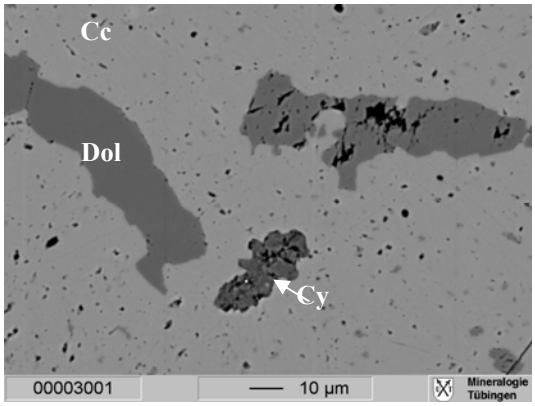

Figure 55: BSE images of sample PBA30. Calcitic marble with dolomitic layers (Dol). Apatite (Ap) crystals are scattered throughout the marble. Sporadically kyanite (Cy) can be observed.

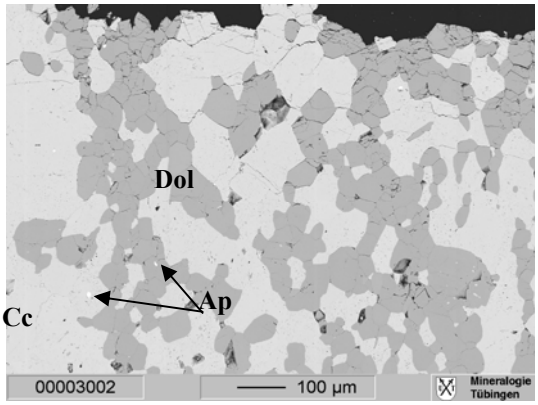

Figure 56: BSE image of sample PBA31. Marble wit high amount of dolomite (Dol) and apatite crystals that are scattered throughout the sample.

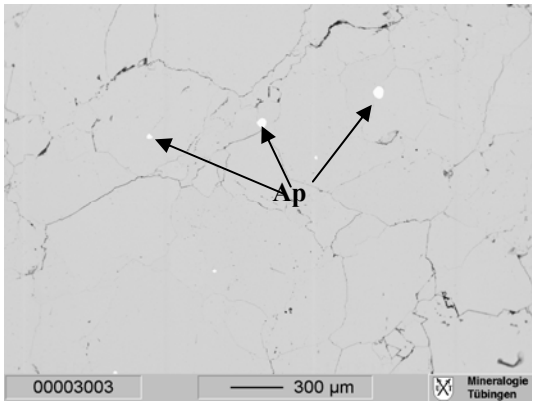

Figure 57: BSE image of sample PBA32. Calcitic marble with apatite (Ap).

8.3. Summary on the mineralogical investigation

8.3.1. Anatolian marbles

Based on the thin section observation with alizarin-red, XRD (*Appendix D.2.1*) and microprobe investigations, the marble is predominantly calcitic in most quarries. Apart from dolomite, many accessory minerals can be observed such as feldspar, muscovite, quartz, epidote, flogopite, graphite, apatite, perovskite, rutile, gypsum and opaque minerals (Table 4). Their abundance rarely exceeds 5% and the probability of their microscopic observation, therefore, strongly depends on the random choice of material used to make the thin sections. In the majority of the analysed Anatolian marbles, however, there is minor variation in the accessory minerals. First, two groups can be distinguish based on the dolomite amount in the samples. (i) The occurrences e.g., Marmara (2-8 wt%), Bandirma (up to 6 wt%), Altınoluk (5-12 wt%), Muğla (up to 4 wt%) and Milas (< 1 wt%) belong to the first group, (ii) the second group includes samples from the occurrences of the Taurides: Afyon, Uşak, Denizli, Babadağ; they do not contain dolomite (*Appendix D.2.1.3.*).

In some cases, many minerals are present, as in the marbles from Marmara (dolomite, apatite, flogopite, titanite, rutile, and pyrite), Altınoluk (dolomite, apatite, quartz, flogopite, diopside, titanite, perovskite, rutile, magnetite, and talk-chlorite) and Muğla (dolomite, apatite, perovskite, pyrite, gypsum, and talk-chlorite). Others are poor in accessory minerals, such as Afyon (apatite, epidote, and pyrite), Babadağ (apatite, quartz, muscovite, and pyrite), Karabiga (apatite, epidote) and Ayazma (apatite, flogopite, clay minerals).

8.3.2. Trojan marbles

The mineralogical composition of the Trojan samples is summarised in Table 5. Generally, the accessory minerals do not distinguish between the marbles. However, in some cases the mineral compositions can be helpful for provenance analysis, such as the presence of aluminum silicates, (e.g., kyanite). Trojan marble samples (***Athena Temple Portico***, `PBA9-10` and ***Bath, Nymphaeum base,*** `PBA30-31`) contain kyanite, which is not known in the Anatolian marbles investigated in this study. Additionally, almost all Trojan samples contain dolomite, so a provenance of the Tauride Block is very unlikely.

Table 4: Mineral composition of Anatolian marbles. ″+″ detected by XRD, ″x″ detected by microprobe

	Troad and neighbouring areas (North of the IAS)												**Middle and Southwest Anatolia** (South of the IAS)					
	Rhodope-Strandja Massif		Sakarya Zone								Armutlu-Ovacik Zone		Menderes Massif		Taurides			
			Kazdağ Range				Karakaya Complex											
	Bergaz	Karabiga	Yenice	Ayazma	Serhat	Altınoluk	Manyas	Mustafa Kemalpas	Marmara	Bandirma	Orhangazi	Iznik	Muğla	Milas	Afyon	Uşak	Denizli	Babadağ
Calcite	+++	+++	+++	+++	+++	+++	+++	+++	+++	+++	+++	+++	+++	+++	+++	+++	+++	+++
Dolomite	+++		++		+	++		+	+	+	+		+	+				
Apatite		x		x		x			x	x	x		x	x	x			x
Baryte														x				
Quartz	+		+	+	+	+	+	+	+		+		+	+	+	+		+
Mica				+							+				+			
Muscovite					+					+								+
Flogopite				x		x			x	x								
Diopside				x		x												
Epidote		x													x			
Titanite						x			x									
Perovskite						x							x					
Rutile						x			x									
Sphalerite														x				
Magnetite						x												
Pyrite									+	+			+	x	x			+
Hematite									+		+							
Kyanite																		
Hedenbergite		x																
Anthophyllite													x					
Feldspar								+	+									
Gypsum													+					
Talk-Chlorite						+				x			+					
Clay-Minerals			+	+		+												

Table 5: Mineral composition of marble used as construction material in Troia. ″+″ detected by XRD, ″x″ detected by microprobe

	NT	BA	Hellenistic Period						Roman Period			
	Kumtepe (only XRD)	Bronze Age marbles (only XRD)	Athena Temple	Athena Temple Portico	Sanctuary Roman Altar (only XRD)	Bath, Blue marble Building (only XRD)	Sanctuary, North Building Treshhold	Bouleuterion	Children of Claudius (only XRD)	Odeion	Bath Nymphaeum base	Bath Moulding
Calcite	+++	+++	+++	+++	+++	+++	+++	+++	+++	+++	+++	+++
Dolomite	+	+	+	+	+	+	x	+	+	+	+	
Apatite			x				x	x		x	x	x
Baryte												
Quartz	+	+	+	+	+	+	+	+	+	+	+	+
Muscovite			+	+		+		+		+		
Flogopite				x			x	x				
Diopside												
Epidote												
Titanite												
Rutile												
Sphalerite												
Magnetite				x								
Pyrite			+	+			x	+				
Hematite		+	+									
Cyanite				x							x	
Gypsum												
Feldspar		+		x						+		
Amphibole												+
Talk-Chlorite	+	+	+									
Clay-Minerals				+								

9. Textural analysis

9.1. Quantitative Texture Analysis (QTA)

Digitally enhanced images of marble thin sections were processed as input data to extract numerous parameters from the images themselves and from vectorized contours of grain boundaries of samples from Anatolian marble quarries and Trojan marble architectonical elements. Because only powder samples were available for the Prehistoric marble objects from Troia, this method could not to be used in order to determine the origin of these samples. As mentioned above, the MGS statistic can be highly biased by sample selection because the range of a distribution cannot be estimated from the distribution itself. Therefore, the 99% quantile is used here to characterise the maximum grain size property so that the lower 99% of the grains determine the value, termed as $MGS_{99\%}$. It is clear that the deviation of MGS and $MGS_{99\%}$ is influenced by the fractal properties of grain distribution: The higher the fractal dimension, the higher the $MGS/MGS_{99\%}$ ratio. Two data sets, histograms of the geometric parameters $MGS_{99\%}$ on the left side and grain area on the right side, are presented in the following section regarding the geological units. The numerical results of the QFA and FA are listed in the tables, again respective the geological units. The structure of the tables is the following: The columns are grouped in size-specific data (number of grains, MGS, $MGS_{99\%}$, the ratio $MGS/MGS_{99\%}$, MGA, $MGA_{99\%}$, $MGA/MGA_{99\%}$) and fractal dimension related data (D_{box}, SD_{box}, $Coeff_{box}$; the fractal-specific data are dimensionless).

The first apparent observation is that the number of grains present in the constant-sized thin section area varies strongly (140 to 4002 grains). Usually the resulting distributions are normalised for such a variation. However, since we are extracting the properties for comparative purposes, the ″fingerprinting″ technique is suitable and consequently no normalisation was applied. Thus, the distribution patterns are readily comparable.

Based on the distribution of the derived parameters the rock samples were grouped into distinct categories. These clusters represent different tectonic and geological units. Having defined the grouping criteria for the rock samples, this categorisation was then applied to the thin sections of archaeological artifacts determining the supposed provenance.

The method is clearly extremely laborious considering not only the fact that the images must be converted into drawings but also because the statistical treatment of data requires that many samples for each provenance site are available. The construction of a meaningful database is therefore extremely arduous. The importance of QTA lies in the fact that it has

given a rigorous numerical character to petrographic information for the first time; this method has a central role in the study of the origin of marble even today.

9.1.1. Marbles from the Troad and neighbouring areas

9.1.1.1. Sakarya Zone

Based of the length of the large axis and the grain area (Figure 58); note the logarithmic horizontal scale), marbles from the ***Kazdağ Range*** are characterised by a peaked distribution. The majority of grains group mainly near 300 μm size. Parallel to that they have a considerable percentage of larger and smaller grains as a consequence of the heteroblastic texture, whereas the MGS = up to 3.5 mm and $MGS_{99\%}$= up to 1.8 mm in the marbles from the South Kazdağ Range, and the MGS = up to 7.2 mm and $MGS_{99\%}$= up to 5.4 mm in the marbles from the North Kazdağ Range. The $MGS/MGS_{99\%}$ values are between 1.83 and 2.04 for the South Kazdağ Range marbles and 1.16 and 3.13 for the North Kazdağ Range marbles (Table 6).

Based on the length of the large axis and the grain area (Figure 59), marbles from the ***Karakaya Complex*** and ***Armutlu-Ovacık Zone*** are characterised by an extreme peaked distribution. The majority of grains group mainly near 300 μm size. Parallel to that they have a considerable percentage of larger and smaller grains because of the heteroblastic texture, with the MGS = up to 3.7 mm and $MGS_{99\%}$= up to 2.1 mm. The $MGS/MGS_{99\%}$ values are between 1.74 and 2.96 (Table 7).

Table 6: Data set for marbles of the Kazdağ Range

	Sample name	*N*	*MGS (μm)*	*$MGS_{99\%}$ (μm)*	*$MGS/MGS_{99\%}$*	*MGA (μm^2)*	*$MGA_{99\%}$ (μm^2)*	*$MGA/MGS_{99\%}$*	*D_{box}*	*SD_{box}*	*Coeff box*
Kazdağ-South	K15	1408	3357	1835	1.829	4586329	1380164	3.323	1.5851	0.2736	4.45
	K18	2471	3516	1464	2.401	5600829	916444	6.111	1.6382	0.0934	4.89
	K21	2763	2269	1016	2.233	2677303	388794	6.886	1.7018	0.1472	6.10
Kazdağ-North	K1	1948	2942	1759	1.673	3000754	1373589	2.185	1.5890	0.1315	4.16
	K2	2260	3938	1260	3.125	3813369	563370	6.769	1.6787	0.1514	5.19
	K3	1347	7164	2325	3.082	20834267	2172188	9.591	1.5733	0.1191	4.27
	K4	514	4390	3303	1.329	6785673	4878332	1.391	1.4420	0.1388	1.96
	K7	634	6246	5397	1.157	17633107	11802889	1.494	1.3982	0.1364	1.65
	AyaA	2589	4415	1462	3.019	11115754	947649	11.730	1.6482	0.0851	5.51

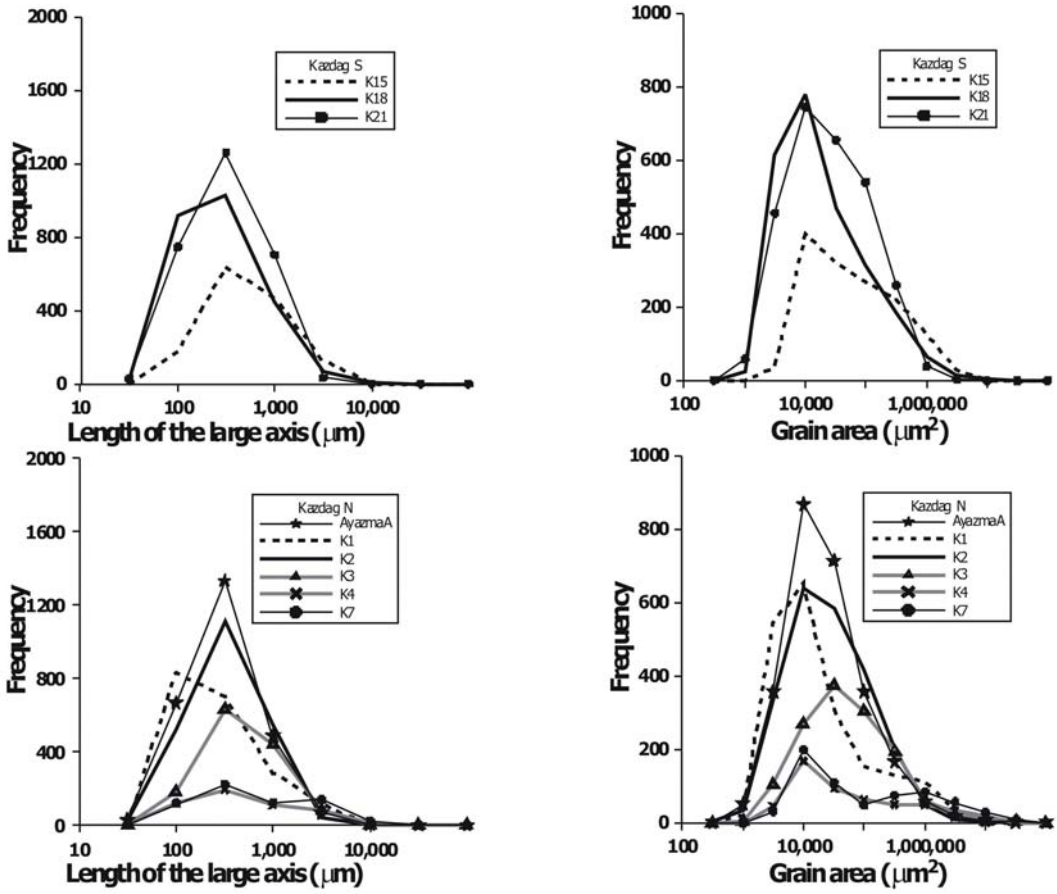

Figure 58: Distribution of the large axis (left side) and grain area (right side) of the various marble quarries of the Kazdağ Range.

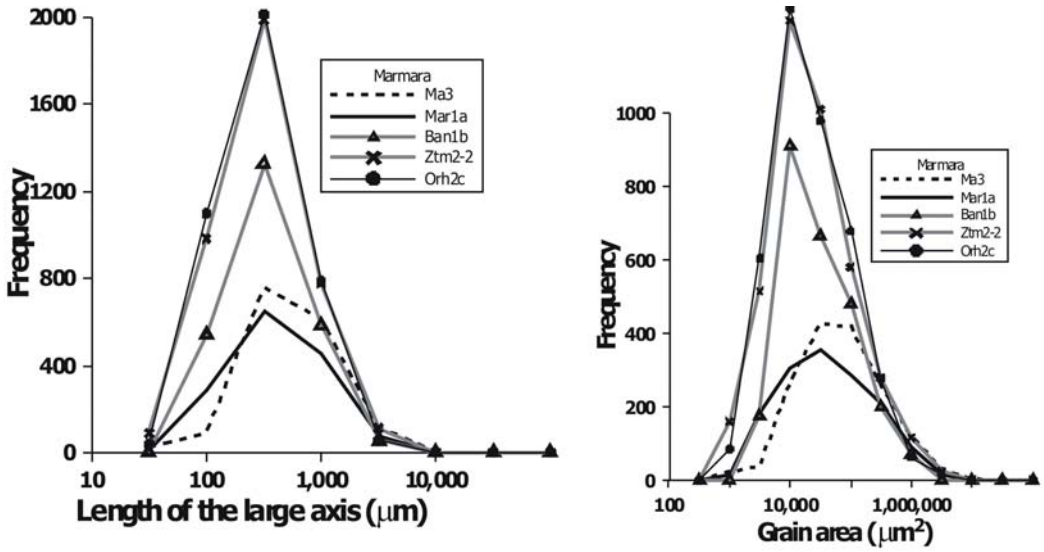

Figure 59: Distribution of the large axis (left side) and grain area (right side) of the various marble quarries of Marmara.

Table 7: Data set for marbles from the Karakaya Complex and Armutlu-Ovacik Zone

	Sample name	*N*	*MGS (µm)*	*$MGS_{99\%}$ (µm)*	*$MGS/MGS_{99\%}$*	*MGA ($µm^2$)*	*$MGA_{99\%}$ ($µm^2$)*	*$MGA/MGA_{99\%}$*	*Dbox*	*SDbox*	*Coeff box*
Karakaya	Ma3	1605	3695	2072	1.783	6093962	1734591	3.513	1.5842	0.2243	5.60
	Mar1a	1475	2757	1566	1.761	3762435	1118193	3.365	1.6016	0.2260	3.98
	BAN1b	2512	1990	1143	1.741	1383168	545388	2.536	1.6672	0.2348	4.88
	ZTM2-2	3952	3160	1360	2.323	4023047	810518	4.964	1.6679	0.1726	8.38
Armutlu Ovacik Zone	ORH2c	4002	3290	1113	2.956	3871332	542595	7.135	1.6735	0.2016	6.94

9.1.2. Marbles from Middle and Southwest Anatolia

Based on the length of the large axis and the grain area (Figure 60), the samples of the ***Menderes Massif*** show a flatter, sometimes bimodal distribution. These samples are typically homeoblastic, with relatively large grains; MGS = up to 3.1 mm and $MGS_{99\%}$= up to 2.0 mm in the samples from Milas and MGS = up to 6.0 mm and $MGS_{99\%}$= up to 5.3 mm in the case of the samples from Muğla. The $MGS/MGS_{99\%}$ values are between 1.54 and 1.57 for Milas and 1.12 and 1.82 for Muğla (Table 8).

Based on the length of the large axis, the grain area (Figure 61) and the texture, the marbles originating from the ***Central-Anatolide-Tauride block*** can be described as follows: A flatter, sometimes bimodal distribution of the large axis and grain area, especially in the case of Babadağ, while Afyon marbles are characterizsed by a flatter to slightly peaked distribution. These samples are typically homeoblastic, with relatively large grains: MGS = up to 3.3 mm and $MGS_{99\%}$ = up to 2.9 mm in the samples from Babadağ and MGS = up to 3.1 mm and $MGS_{99\%}$ = up to 2.7 mm in the case of the samples from Afyon. The $MGS/MGS_{99\%}$ values lie between 1.3 and 1.16 for Babadağ and 1.17 and 1.47 for Afyon (Table 9).

Table 8: Data set for marbles from the Menderes Massif

	Sample name	*N*	*MGS (µm)*	*$MGS_{99\%}$ (µm)*	*$MGS/MGS_{99\%}$*	*MGA ($µm^2$)*	*$MGA_{99\%}$ ($µm^2$)*	*$MGA/MGA_{99\%}$*	*D_{box}*	*SD_{box}*	*Coeff box*
Milas	Mi2	1013	3077	2000	1.539	3215470	1531565	2.099	1.5838	0.2603	5.02
	Mi3-2	1247	3018	1940	1.556	3509450	1467468	2.392	1.5490	0.2681	4.40
Muğla	M2-1	248	5777	4008	1.441	15627284	6114207	2.556	1.3881	0.1281	1.68
	M2-2	140	6004	5384	1.115	17421016	13708807	1.271	1.3651	0.0964	1.21
	M4	697	3324	2485	1.338	3228381	2293828	1.407	1.5211	0.3093	3.98
	M7	189	4929	4125	1.195	10468921	7893137	1.326	1.3997	0.1734	1.98
	M8	945	3683	2025	1.819	3644703	1386704	2.628	1.5484	0.3681	4.56

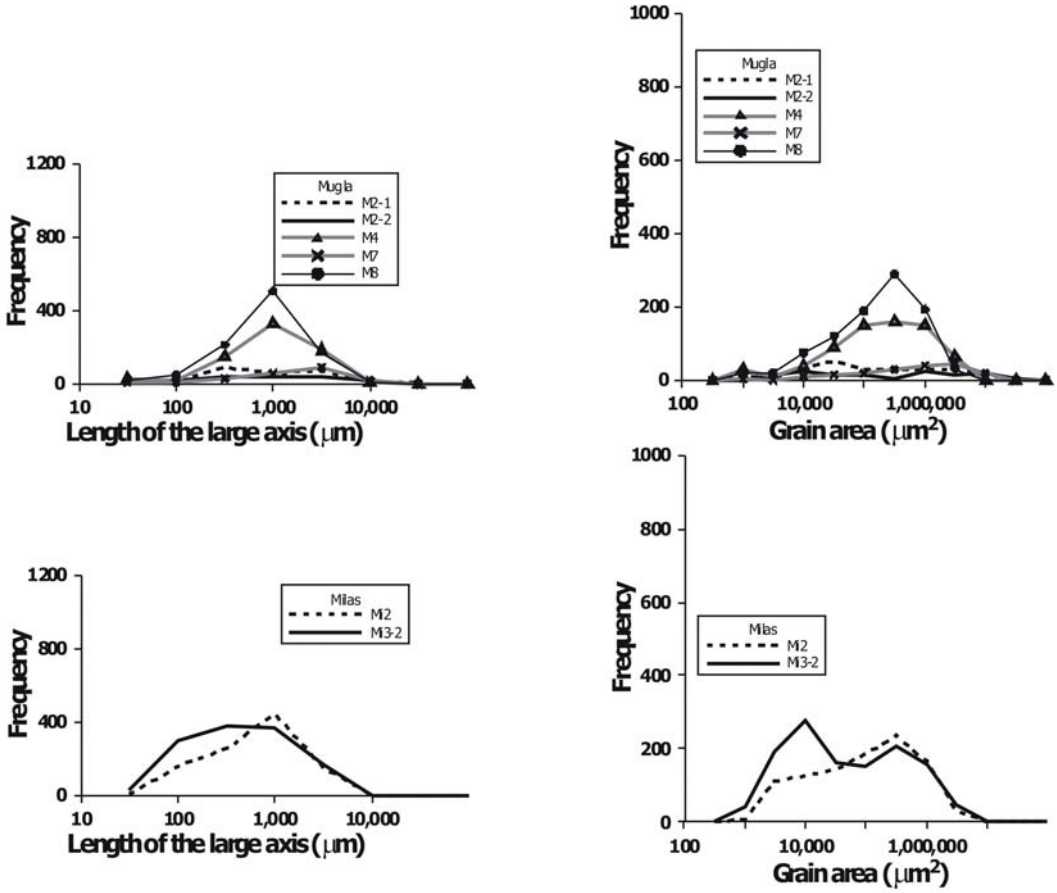

Figure 60: Distribution of the large axis (left side) and grain area (right side) of the various marble quarries of the Menderes Massif.

Table 9: Data set for marbles from the Central Anatolide-Tauride Block

	Sample name	*N*	*MGS (µm)*	*$MGS_{99\%}$ (µm)*	*MGS]/ $MGS_{99\%}$*	*MGA (µm²)*	*$MGA_{99\%}$ (µm²)*	*MGA/ $MGA_{99\%}$*	*Dbox*	*SDbox*	*Coeff box*
Afyon	A13	973	2756	1869	1.474	3393431	1088909	3.116	1.6233	0.2347	5.96
	A14	834	2655	1972	1.346	2792827	1358491	2.056	1.5925	0.2669	4.69
	A2	430	3138	2677	1.172	3550173	2652886	1.338	1.5280	0.2363	3.57
	A4-1	191	2756	1869	1.474	3393431	1088909	3.116	1.6233	0.2347	5.96
	A4-2	193	2655	1972	1.346	2792827	1358491	2.056	1.5925	0.2669	4.69
	A6-2	789	2816	2103	1.339	2436874	1615257	1.509	1.5848	0.2720	4.67
Babadağ	BD1	237	3323	2868	1.159	4438615	4156647	1.068	1.4751	0.1933	2.12
	BD4	790	3070	2620	1.172	5397256	3201846	1.686	1.4853	0.2095	3.15
	BD6	459	3021	2325	1.300	4517816	2364587	1.911	1.4805	0.3565	2.77

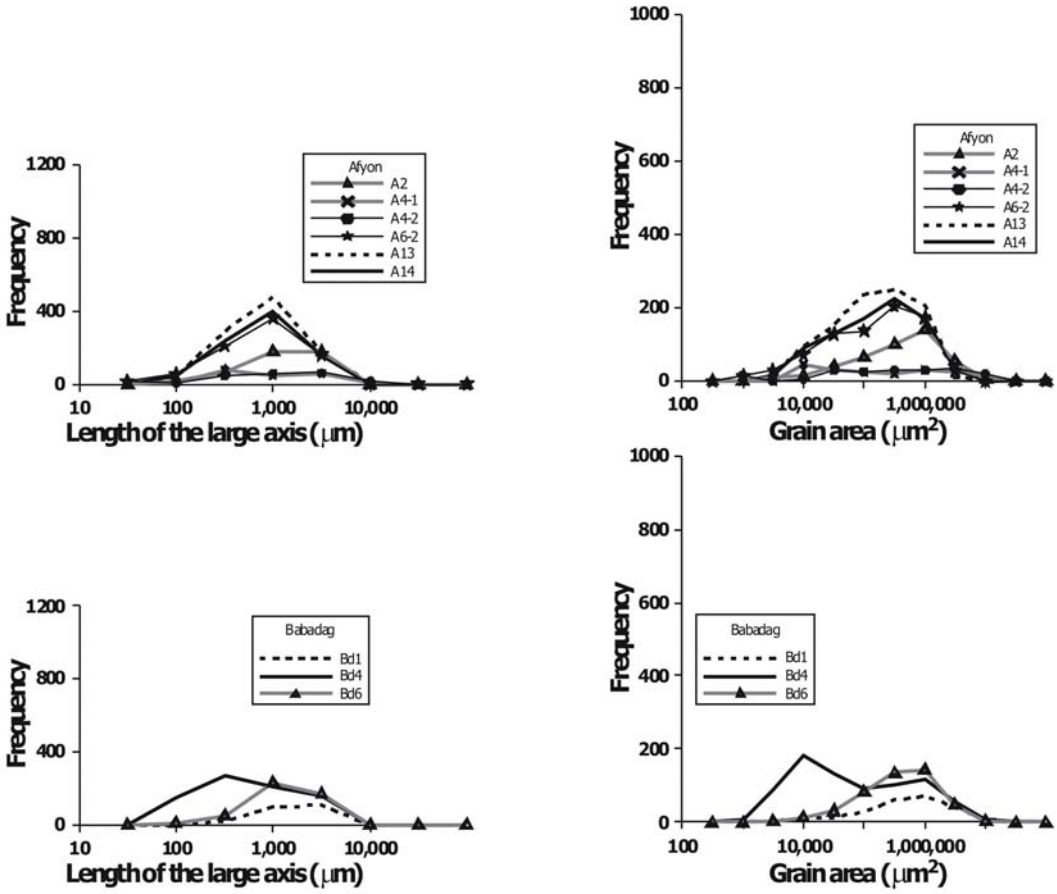

Figure 61: Distribution of the large axis (left side) and grain area (right side) of the various marble quarries of the Central Anatolide-Tauride Block.

Figure 62 presents the results of the fractal analysis in the form of a D_{box} vs. SD_{box} plot. The samples from different localities seem to group in definite clusters in most parts of the chart. The samples with higher S_D-values belong to the ***Sakarya unit***, while the ***Menderes Massif*** and ***Tauride Block*** are characterised by lower S_D-values. However, the marble samples from ***North Kazdağ Range*** from the Sakarya Zone, are scattered over the whole range of fractal dimension. This behaviour could be attributed to the special thermo-tectonic evolution of this geological formation. While other units from the Sakarya Zone suffered metamorphism at high-grade-amphibolite to granulite facies with local anatexis in Mid-Carboniferous (Hercynian), Late Triassic (Kimmeridge) and later Oligo-Miocene (Alpine) thermal events, the Ayazma marbles are the result of contact metamorphism due to plutonic activity represented by high temperature gradients.

Figure 63 shows the diagram D_{box} *vs.* $MGS/MGS_{99\%}$. The samples from the different tectonic units are separated without major overlapping. The oblique line separates the tectonic unit of Sakarya Zone (OKAY *et al.* 1996) with Laurasian affinities, classically referred to as the

Pontides and the units Anatolide-Tauride-Block (separated from the Sakarya Zone by the Izmir-Ankara-Erzincan Suture, OKAY *et al.* 1996).

Since the fractal dimension, D_{box} (together with S_{Dbox}) is found to be a characteristic separator of different tectonic units, the MGS/MGS$_{99\%}$ ratio, though only to a limited extent, seems to be useful for provenance analysis, as well. The geological units Sakarya Zone and Anatolide-Tauride-Block are separable in the D_{box} vs. MGS/MGS$_{99\%}$ chart along an oblique boundary. The samples from the Anatolide-Tauride-Block have more compact grain distribution (i.e., characterised by lower fractal dimension) and are located closer to the origin of the chart; the Sakarya Zone have a wider grain spectra, therefore involve greater D_{box} and MGS/MGS$_{99\%}$ values.

Because of the fractal nature of the grain size and the distribution of grain geometry parameters (Figure 59 - Figure 61), it is important to note that the resulting distributions of the measured parameters are usually non-Gaussian. Most of the distributions are asymmetric, therefore the standard deviation, etc., will be strongly distorted. In cases, however, the mean and standard deviation may be a good basis for clustering. In cases of uncooperative distributions, these parameters – in spite of their different behaviour – do not differ too much. Therefore, more sophisticated parameters (e.g., fractal dimension, high-resolution histogram) should be used as well to create individual groups of the samples.

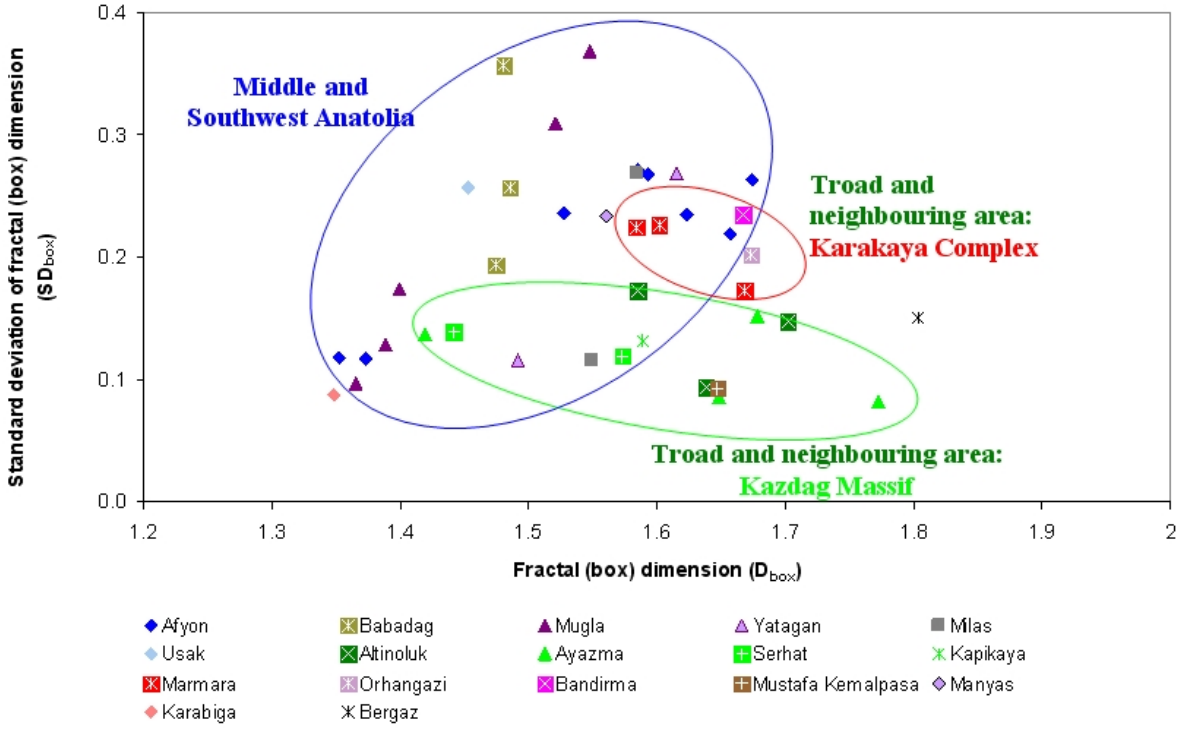

Figure 62: Cross plot of fractal dimension (D_{box}) vs. standard deviation of fractal (box) dimension of West Anatolian marbles.

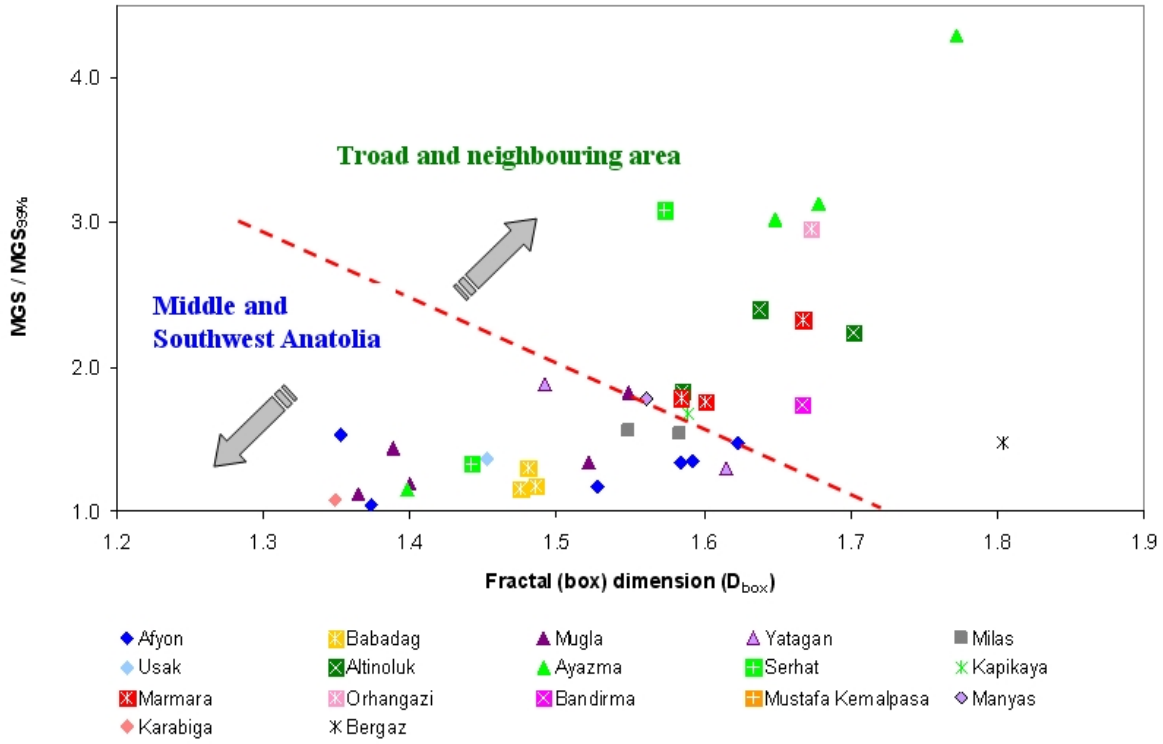

Figure 63: Cross plot of fractal dimension (D_{box}) vs. $MGS/MGS_{99\%}$. Note the separation line between the main geological units of West Anatolia.

9.1.3. Trojan marbles

I was not allowed to take chips of the Prehistoric marble objects from Troia; therefore this method could not be applied to these samples. However, samples of Hellenistic and Roman age were examined with this method, proving the usability of the parameters in determining the provenance of white marbles. There are no data available of non-Anatolian marble (or the method that was used is not described), therefore it was not possible to compare the parameters of the Trojan marbles with those of marbles outside of West Anatolia.

The distribution of the Trojan samples validates the applicability of this approach: The similarity of the samples PBA18, PBA19, PBA21, PBA24, and PBA32 to the marbles of the Karakaya Complex is obvious (Figure 64 and Figure 59). The samples are characterised by an extremely peaked distribution. The majority of grains group mainly at 300-350 µm size. Parallel to that they have a considerable percentage of larger and smaller grains because of the heteroblastic texture, whereas the MGS = up to 3.1 mm while $MGS_{99\%}$= up to 1.4 mm. The $MGS/MGS_{99\%}$ values lie between 1.57 and 2.22. However, the samples PBA30 and PBA31 show different distribution of the length axis, they are less peaked and the form of the curve is

different. The distribution of the grain area is different in the samples PBA30 and PBA31 from all other samples as well, and the form of the curve is staircase-shaped.

Figure 65 shows the comparison of the results of fractal analyses of the archaeological artifacts from Troia (represented as red stars). These results are very similar of to those of the marbles from the Sakarya Zone. None of the archaeological objects are made of marble from the Anatolide-Tauride-Block. Two of the Trojan architectonic elements (PBA18, PBA32) fall into the "Mixed Zone". Figure 66 shows the combined results of MGS/$MGS_{99\%}$ and fractal dimension (D_{box}) including the investigated marbles from West Anatolia and the Trojan marbles. On this diagram, the similarities between the marbles from the Sakarya Zone and Trojan marbles are obvious. Even if some overlapping between the marbles from Marmara and South-Kazdağ Region exists, the Trojan marbles seem to stem from Marmara.

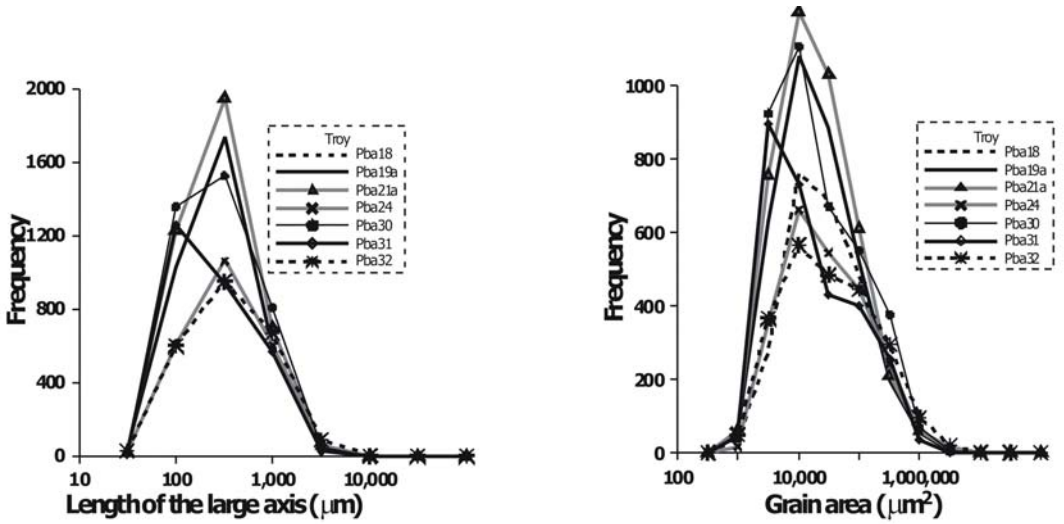

Figure 64: Distribution of the large axis (left side) and grain area (right side) of the Hellenistic and Roman marble objects from Troia.

Table 10: Data set for Hellenistic and Roman marble objects of Troia.

	Sample name	*N*	*MGS (µm)*	*$MGS_{99\%}$ (µm)*	*MGS/ $MGS_{99\%}$*	*MGA (µm²)*	*$MGA_{99\%}$ (µm²)*	*MGA/ $MGA_{99\%}$*	*Dbox*	*SDbox*	*Coeff box*
Troia	pba18	2543	1989	1259	1.580	1615702	612443	2.638	1.6656	0.2399	4.91
	pba19a	3431	1971	1006	1.959	1678418	403802	4.157	1.7062	0.1748	6.02
	pba21a	3947	2386	1077	2.215	2312397	488002	4.738	1.7028	0.1365	7.08
	pba24	2340	2913	1397	2.085	2742048	811289	3.380	1.6548	0.1590	5.34
	pba30	3744	1928	1015	1.899	1481513	425284	3.484	1.6829	0.2163	6.73
	pba31	2794	1519	965	1.573	687525	327134	2.102	1.6954	0.1704	4.77
	pba32	2327	3125	1475	2.118	4504683	874421	5.152	1.6269	0.2120	5.57
	pba6	1622	2602	1326	1.961	3161651	715216	4.421	n.d.	n.d.	n.d.

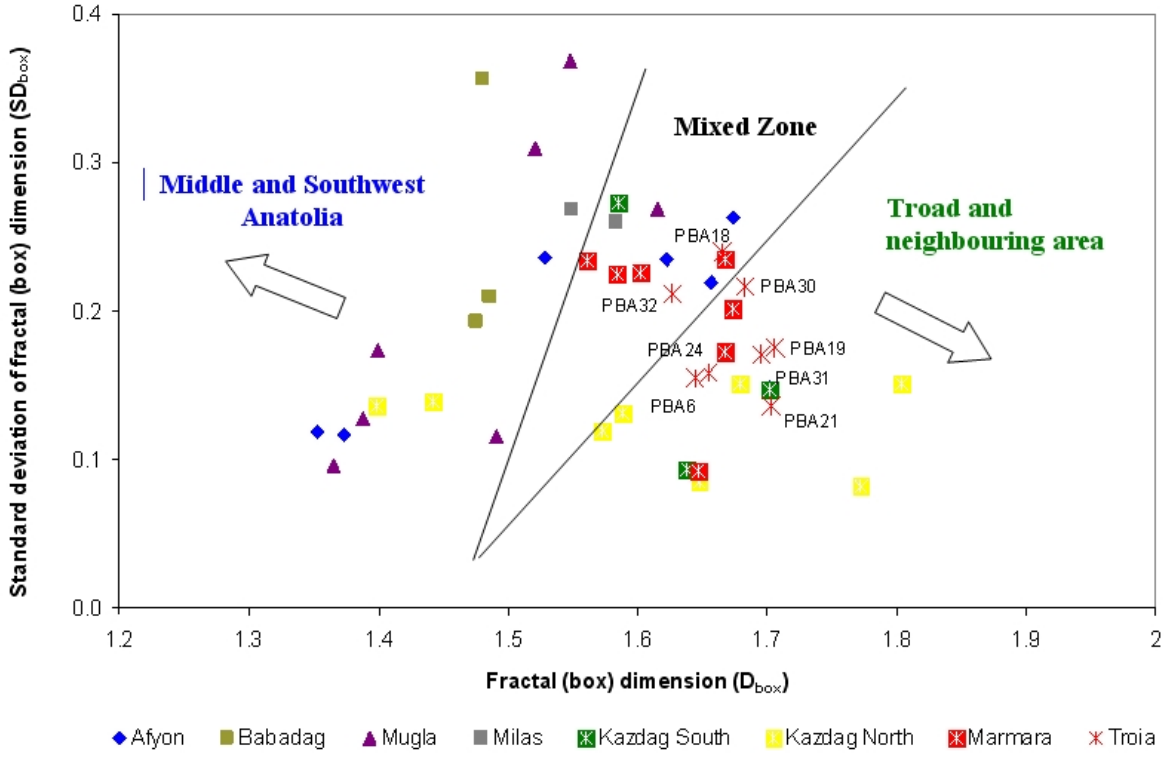

Figure 65: Cross plot of fractal dimension (D_{box}) vs. standard deviation of fractal (box) dimension, including the results of Trojan marbles.

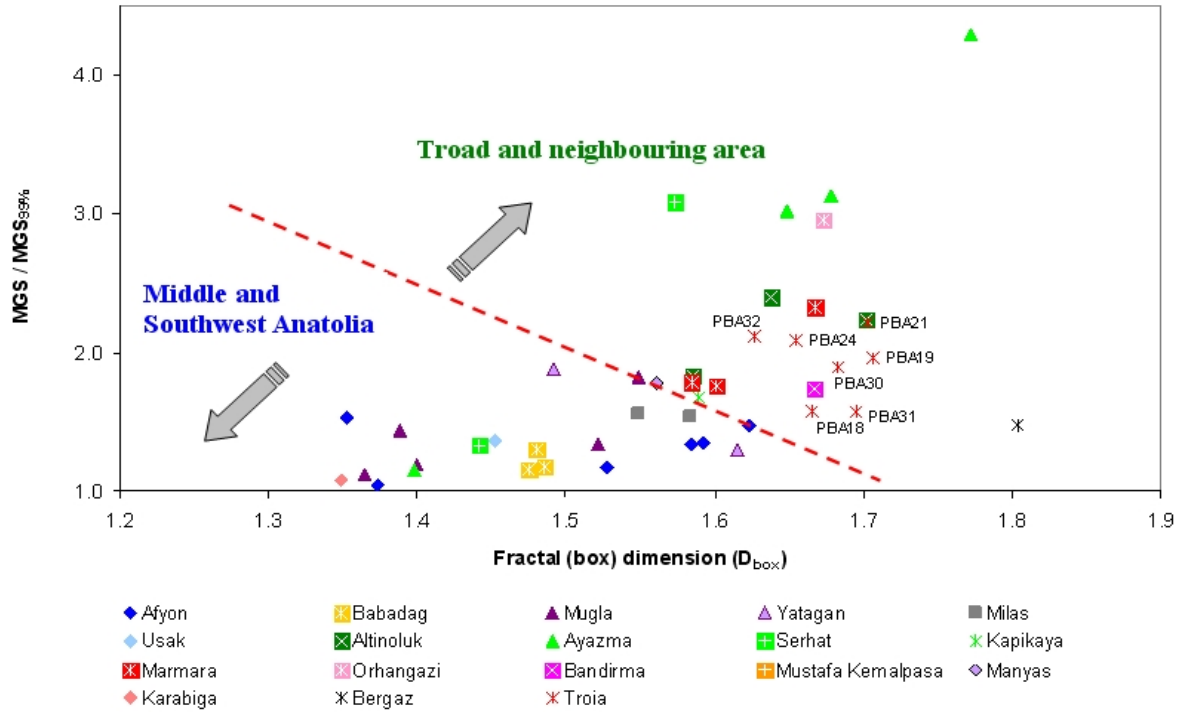

Figure 66: Cross plot of fractal dimension (D_{box}) vs. $MGS/MGS_{99\%}$ including the results of Trojan marbles.

10. Results of the chemical analysis

The concentration of major and minor elements was determined by XRF, AAS and ICP-MS analyses of the marble samples collected in the recent quarries of West Anatolia and of Trojan marbles.

10.1. X-ray Fluorescence Analyses (XRF)

Relatively large amounts of powdered material (1.5 g) are necessary to make the glass beads for XRF- measurements. Therefore, it was not possible to analyse the Trojan marbles by this method. In consequence, this section focuses on the chemical element concentration of Turkish marble samples *(Appendix D.3)*. Ranges in concentration are large for several elements, separated ranges are observed in some cases: While marble from Muğla has a significantly higher Fe_2O_3-concentration (0.2-0.6 wt%), the samples from Afyon have a typically low MgO-concentration (0.04-0.1 w%) and marbles from Altınoluk have typically higher MgO-concentration (0.5-4.3 w%). Marbles from Altınoluk and Muğla have relatively high Cr-content (Altınoluk: up to 258 µg/g and Muğla: up to 110 µg/g), but in Bergaz and Babadağ there are marbles with high Zn-content (Bergaz: up to 60 µg/g and Babadağ up to 30 µg/g). Furthermore, marbles from Afyon and Muğla have low Sr-concentrations (up to 102 µg/g and 93 µg/g, respectively); while marble from the Kazdağ Range (Altınoluk, Manyas, Serhat, Bergaz, etc.), Babadağ and Milas have higher Sr-concentrations (above 100 µg/g). Nonetheless, because the investigated marbles from Anatolia are very pure marbles, the influence of the accessory minerals on the bulk chemistry can be significant. These factors in addition to the relatively high amount of material needed to carry out XRF-measurements have led us to disregard this method for the future investigations.

Table 11: Summary of the chemical composition of the Anatolian marbles

		MgO (%)	Fe_2O_3(%)	Sr (µg/g)
Troad and neighbouring areas in Northwest Anatolia (North of the IAS)	Altınoluk	0.449-4.323	0.058-0.100	126-181
	Kazdağ-North	0.510-0.577	0.060-0.099	98-135
	Bergaz	0.742	0.077	110
	Manyas	0.66	0.067	117
	Mustafa KP	0.617	0.056	113
Middle and Southwest Anatolia (South of the IAS)	Afyon	0.04-0.112	0.059-0.065	48-102
	Babadağ	0.451-0.473	0.076-0.090	118-184
	Muğla	0.0516.171	0.068-0.512	64-93
	Milas	0.323-3.832	0.102-0.109	82-175

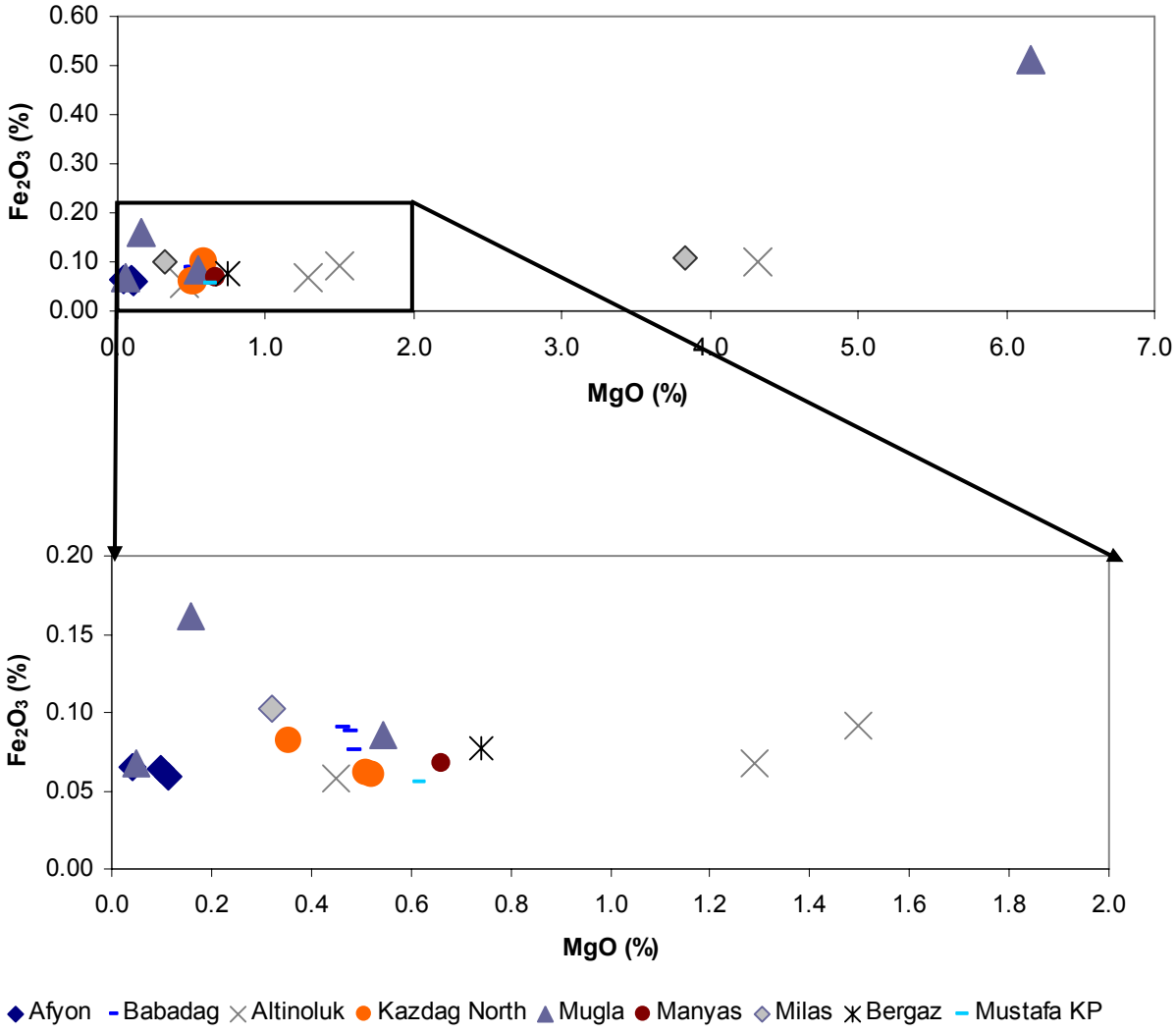

Figure 67: MgO vs. Fe_2O_3 bivariate plot, showing the differences of the chemical composition of the marble occurrences.

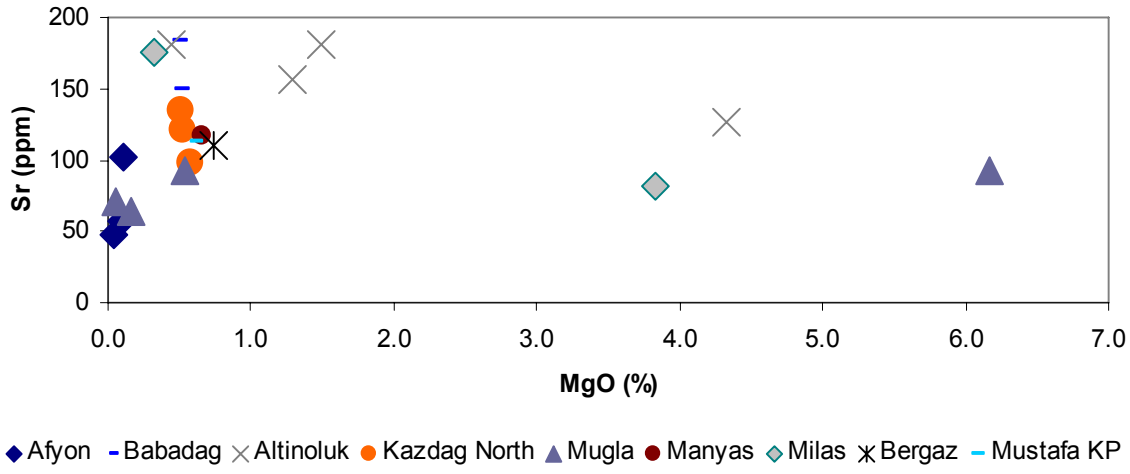

Figure 68: MgO vs. Sr bivariate plot, showing the differences of the chemical composition of the marble occurrences.

10.2. Atomic Absorption Spectrometry (AAS)

AAS was used to explore the acid-soluble components, in order to determine the concentration of the elements embedded in the calcite crystals.

The results of these tests are presented here: Marmara and Bandirma have a low Fe and Mn-concentration (Fe: up to 360 µg/g and up to 260 µg/g, Mn: up to 10 µg/g and up to 7 µg/g, respectively). The marbles from Ayazma have a lower concentration of Mn (up to 11 µg/g) and a raised Fe-concentration (up to 642 µg/g). The marbles from Iznik are characterised by higher Mn and Fe concentrations (up to 81 µg/g and up to 890 µg/g, respectively), similar to the marbles from Altınoluk, although the latter shows a lower Mn-concentration (up to 45 µg/g). Afyon, Babadağ and Milas have relatively high Mn (up to 62, 112 and 64 µg/g, respectively) and Fe concentration (up to 590, 846 and 466 µg/g, respectively), whereas the Fe values do not reach the values from Iznik and Altınoluk (see also *Appendix D.4*).

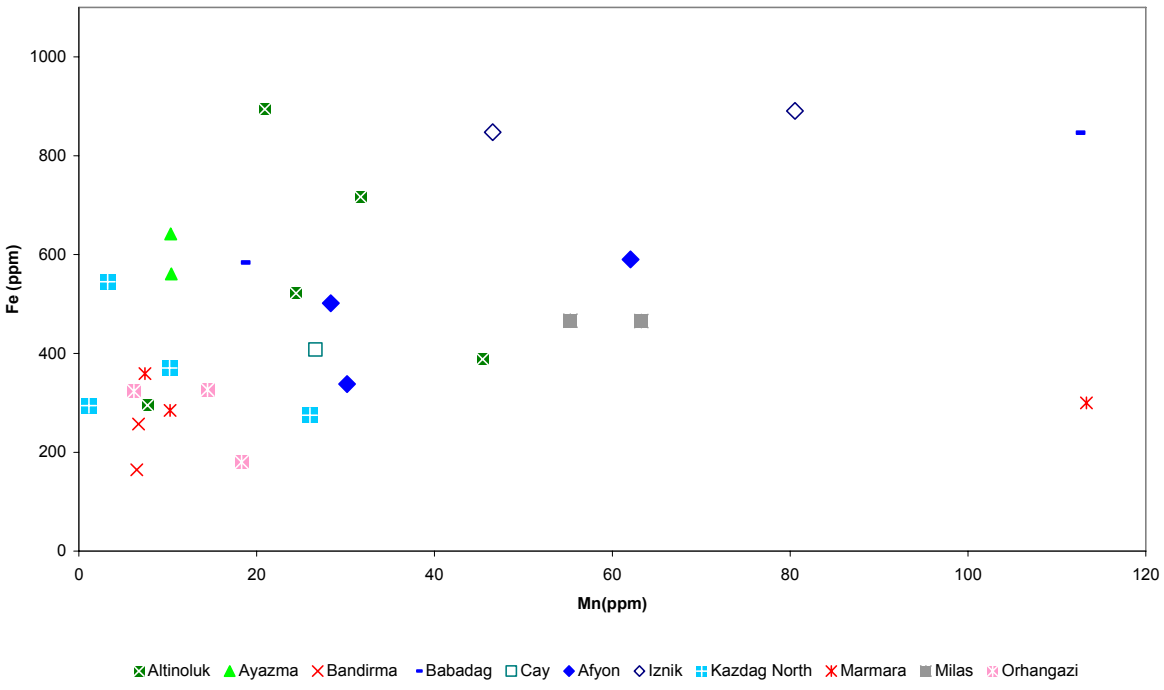

Figure 69: Fe vs. Mn bivariate plot showing the differences of the trace element concentration of the marble occurrences north of the Izmir-Ankara-Suture.

As I have already mentioned in the previous chapters, comparing analytical results of individual samples, measured with different methods in different laboratories is very difficult – in particular for chemical analyses. Therefore, I will first compare the results of the investigation on the Trojan materials using only the data from my own investigation.

At first sight, it is obvious that the Bronze Age marble objects from Troy have a larger dispersion than the objects of the Hellenistic and Roman periods. The Hellenistic and Roman objects were very probably made from raw materials from Marmara, Bandirma, Orhangazi and the northern Kazdağ Massif (with the possible exception of sample PBA33). However, the Prehistoric marble objects, which featured a larger dispersion, may have their origin in regions much further away, such as Afyon or Babadağ (antique Aphrodisias).

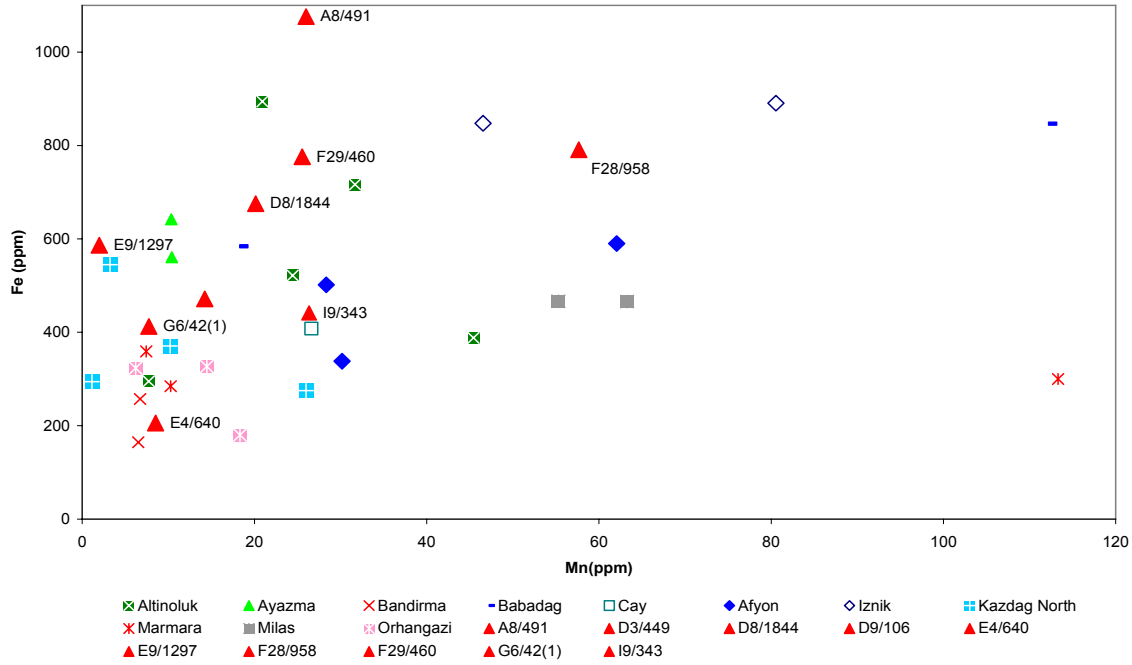

Figure 70: Fe vs. Mn bivariate plot showing the comparison of trace element concentration between the Bronze Age Trojan artifacts and the marble occurrences north of the Izmir-Ankara-Suture.

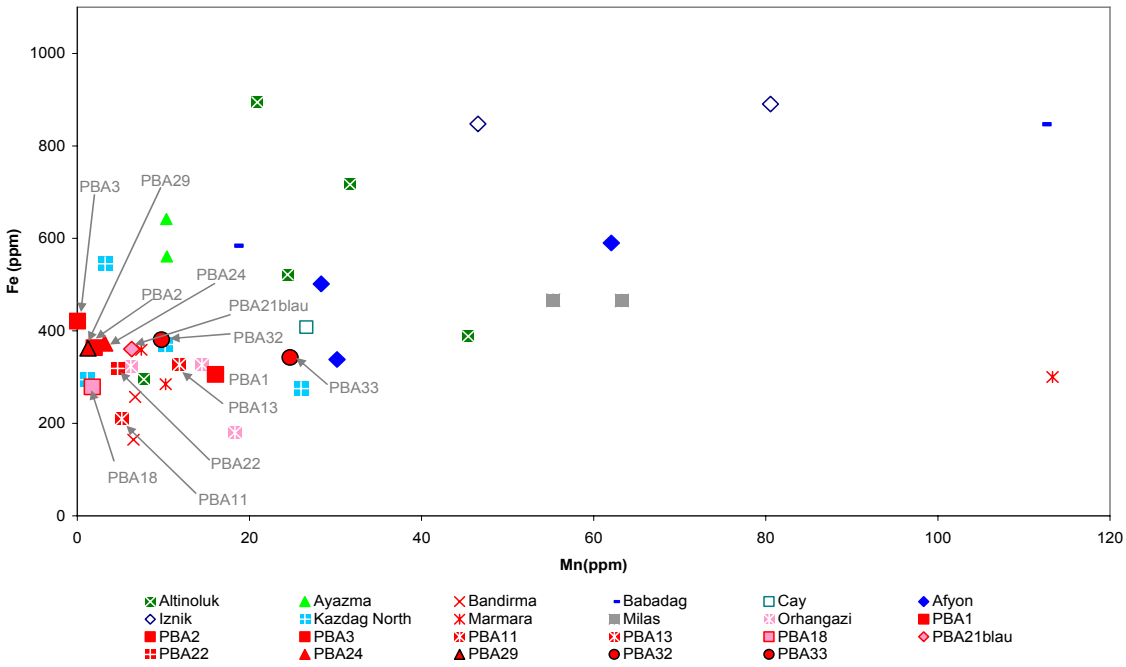

Figure 71: Fe vs. Mn bivariate plot showing the comparison of trace element concentration between the Hellenistic and Roman Trojan artifacts and the marble occurrences north of the Izmir-Ankara-Suture.

11. Cathodoluminescence analysis

In this chapter, I will describe the cathodomicrofacies of the samples of Anatolian and Trojan marbles. White marbles from Anatolia may be subdivided into three major families based upon their dominant luminescence colour. Calcitic white marbles have dominant orange or blue luminescence; depending of the trace element concentration and white dolomitic marbles predominantly show red luminescence. In addition, the luminescence intensity and distribution, the grain size and the texture are criteria permitting differentiations.

11.1.1. Anatolian marbles

11.1.1.1. The orange luminescence family

This family contains most of the calcitic marbles.

(i) Afyon (AFY) and Uşak (USK): Although these samples yield voidable pureness (Cc>98%) and macroscopic and microscopic homogeneity, the heterogeneous CL patterns show crystals with CL-zonation. A significant part of the rock forming calcite crystals has sharp-bordered, low-luminescent cores. The intensity of yellow-orange luminescence varies along small belts and there are also diffuse luminescent patches (Figure 72: A-D).

(ii) Muğla (MGL), Yatağan (YTG) and Milas (MLS): The rock forming calcite usually yields bright orange light, much more intense than the samples from Afyon. The central part of these crystals shows weaker intensity, but these patches form no developed cores, as in the case of the Afyon samples. The FeOOH inclusions are characteristic for these materials and they are observable in the CL patterns, as well (Figure 72: E-F).

(iii) Babadağ (BBD): The CL pattern of this marbles show a heterogeneous image. The calcite grains are different in intensity (dull to medium) and in color (black to orange, Figure 72: G-H).

(iv) Samples from Serhat (SRH): The CL patterns show homogenous images from the first generation calcite. Recrystallization on the boundary of the calcite crystals can be observed and sometimes secondary calcite fills the space between the primary calcite crystals (Figure 72: I-J).

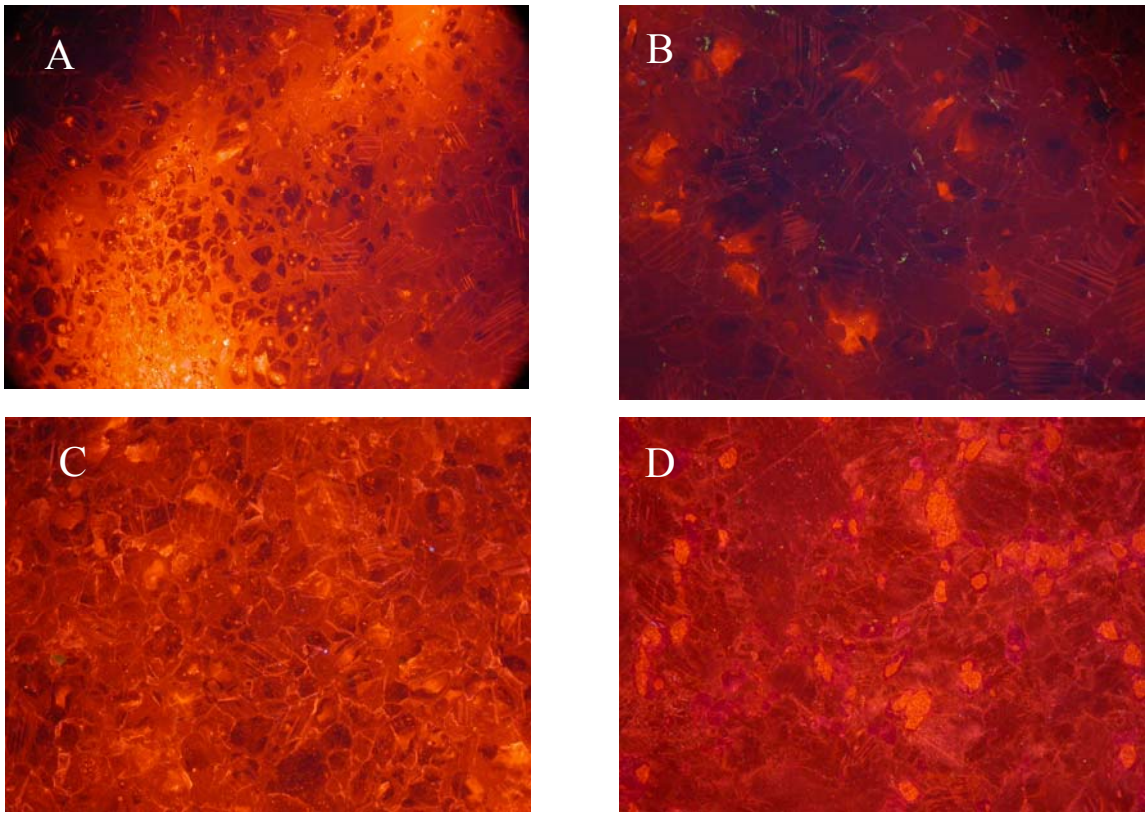

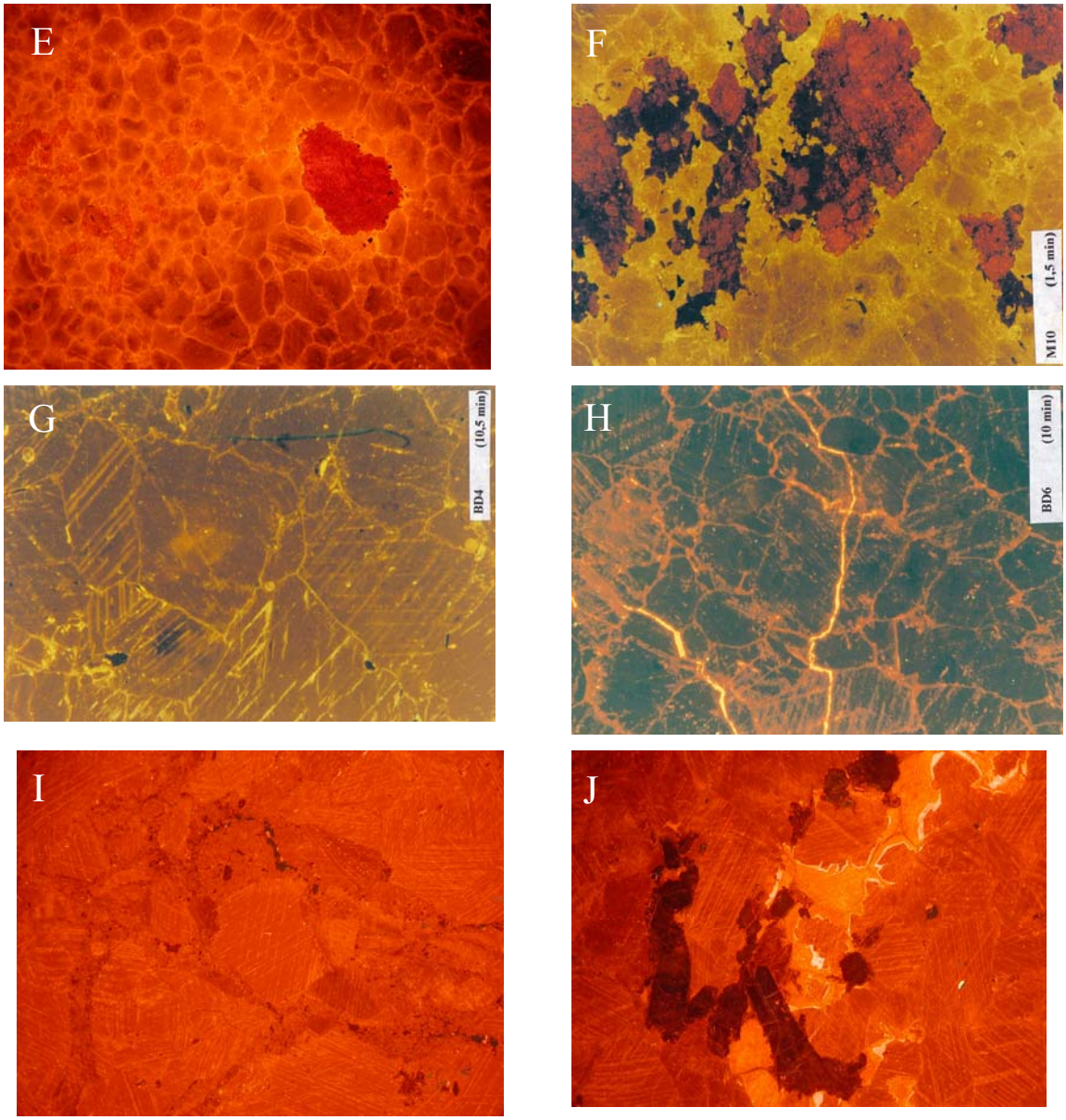

Figure 72: Typical CL patterns of marbles from Afyon (A,B,C), Uşak (D), Milas (E), Muğla (F), Babadağ (G,H) and Serhat (I,J).

11.1.1.2. The red luminescence family

This group is formed exclusively by dolomite bearing marbles. Several localities are reported in the literature (BARBIN *et al*. 1992) to have been quarried for dolomitic marbles. The most important is Thasos (Greece). Less well-known quarries with dolomite are at Crevola (Italy) and Villetta (France). A Cycladic area (Naxos-Mt Zeus), which is not considered to have been a quarrying area, also belongs to this family. At the mentioned localities, marbles can be found with dolomite content greater than 50 %. The investigated marbles in the studied area in Turkey have dolomite content below 10 %.

(v) Altınoluk (ALT): The CL patterns show clearly dolomite crystals arranged in belts. The size of dolomite crystals is always smaller than the size of the matrix-forming calcite. The CL colour of the dolomite is a strong red and the CL intensity is medium to bright. Some of the calcite crystals have a non-luminescent (black) core, similar to the Afyon samples. However, the boundaries of these cores are not so sharp. Small particles with intense bluish-white CL emission are probably quartz grains (Figure 73: A).

(vi) Bergaz (BRG): Dolomitic marble from Bergaz (dolomite content more than 90 %) shows red luminescence colour (Figure 73: B).

11.1.1.3. The non and dull luminescence family

The samples from Marmara (MAR), Bandirma (BAN), Karabiga (KB), Manyas (MAN), Mustafa Kemalpasa (MKB) and Orhangazi (ORH) typically show no or dull luminescence colour. This feature can be attributed to the low amount of Mn in these samples (Figure 73: C-F).

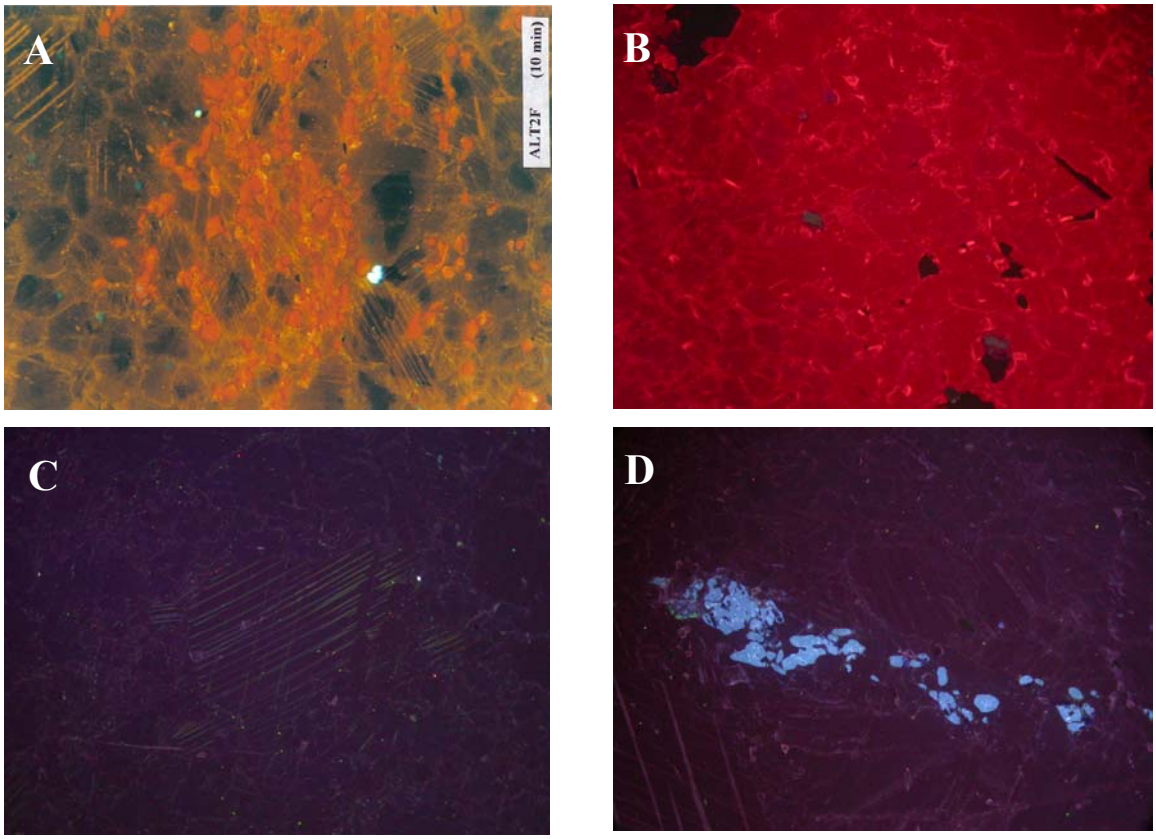

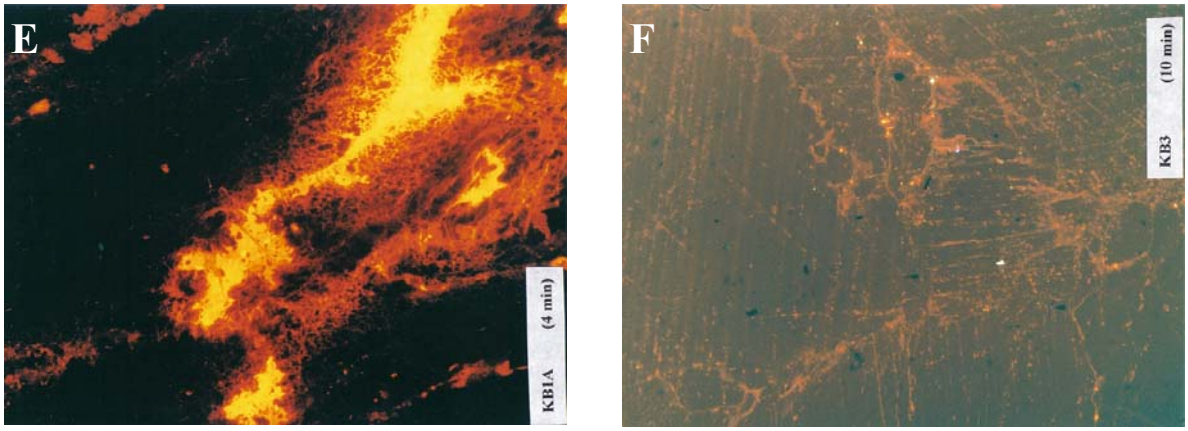

Figure 73: Typical CL patterns of marbles from Altınoluk (A), Bergaz (B), Marmara (C), Orhangazi (D) and Karabiga (E and F).

11.1.2. Trojan marbles

11.1.2.1. Prehistoric marbles

Because only drilled powder material was available from these artifacts, no CL-investigation was carried out.

11.1.2.2. Hellenistic marbles

The investigated archaeological samples of the Hellenistic Period of Troia (Athena Temple, AT), Athena Temple Portico (ATP), Sanctuary ″Roman Altar″ (SRA), Bath (BMB) with several phases) have no CL or dull CL intensity and show black to very dark blue colour. Only the sample PBA9 seems to be different from the other investigated samples, it has a light orange CL pattern.

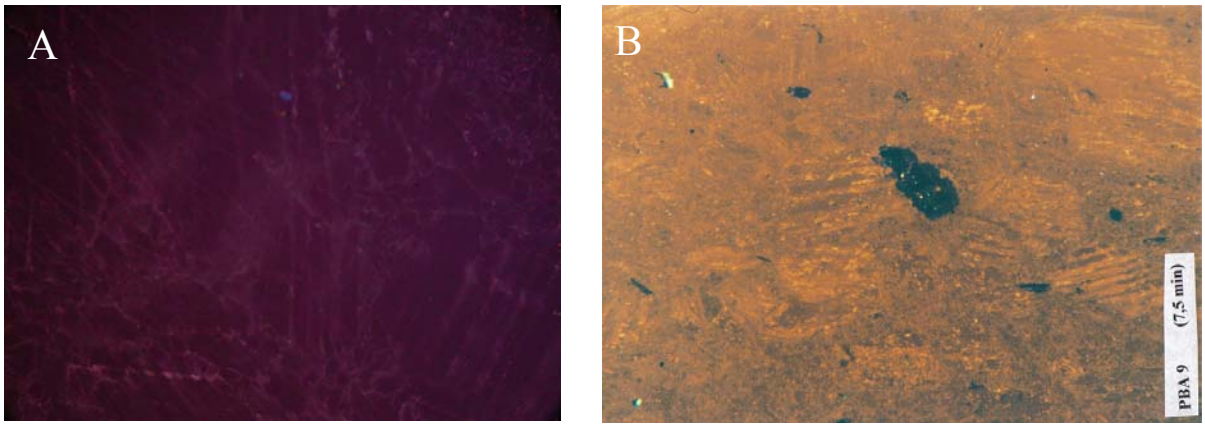

Figure 74: Typical CL patterns of marbles of the Hellenistic Period from Troia PBA4 (A) and PBA9 (B)

11.1.2.3. Roman marbles

Especially the samples PBA30 and PBA31 of the Nympheum base moulding of the Bath (BM) from Troia show heterogeneous images. The CL intensity varies from dull to bright. The CL colour is red in the case of the dolomite grains, which form strips. They are rounded and smaller than the calcite grains around them. The calcite grains generally show an orange colour, the intensity is dull to medium. The grains have no luminescence (black) cores, and the boundary of these cores is more or less sharp.

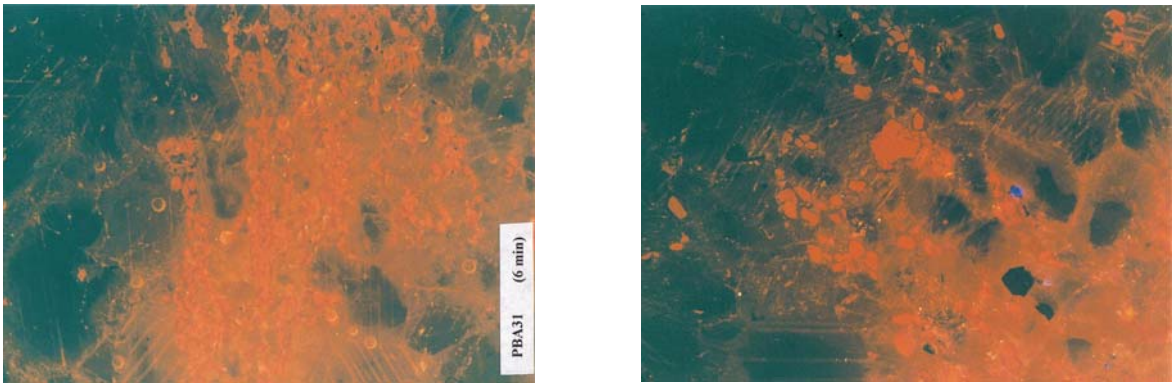

Figure 75: CL patterns of marbles of the Roman Period in Troia, PBA31

12. Carbon, oxygen and strontium isotope systematic

12.1. $\delta^{18}O$ and $\delta^{13}C$ isotopic investigation

The analysis of the isotopic ratios of carbon and oxygen is the most commonly applied method for the determination of the origin of marble. This is due to the discriminating ability of the two variables and due to their simplicity in terms of interpretation and use. However, as mentioned above, with an increasing number of measurements, it is more and more difficult to determine the origin of marble based on these two parameters alone, although a selection of the possible provenance is feasible in most of the cases.

Appendix D.5 provides the full list of all carbon and oxygen isotope ratios measured in the course of this work. In order to facilitate comparisons, graphical representations are given using a common scale.

In the following sections, the results of the stable isotope analyses are presented and discussed for each geological region. In this way, the role and discriminant power of isotopic data can be analysed in more detail and the possibility of intra-site discrimination will be discussed, as well. The general isotopic distribution of Anatolian marbles is illustrated in the Figure 76, based on my own measurements (239 data pairs) and data from the literature (538 data pairs, e.g., ATTANASIO *et al.* 2006; CRAMER 2004). They are many more results in the literature, however, it is unfortunate that the primarily data are often not published.

The data includes ratios from quarries, such as Afyon, Aphrodisias, Denizli, Ephesos and Marmara, which were analysed by several authors and within the framework of this study. Others, like Altintas, Miletus and Thiountas, were only analysed by other authors. On the other hand, samples from some marble quarries were analysed exclusively within the framework of this work. These are primarily the marbles of the Troad and neighbouring area: Altınoluk, Serhat, Ayazma, Bergaz, Karabiga, Mustafa Kemalpasa, Orhangazi, Manyas, but also Milas and Harmandali. (In the following figures in this chapter, the measurements that were carried out within the framework of this study are present with large symbols and labeled with bold letters in the legend).

Figure 76 clearly indicates that isotopic source fields of the different Anatolian quarries are largely overlapping. Figure 77 shows the statistical distribution of the $\delta^{18}O$ and $\delta^{13}C$ values (in ‰, relative to PDB) of the West Anatolian marble quarries, including 777 data pairs, of

which 239 samples were measured in the course of this work and 538 data were assimilated from the literature.

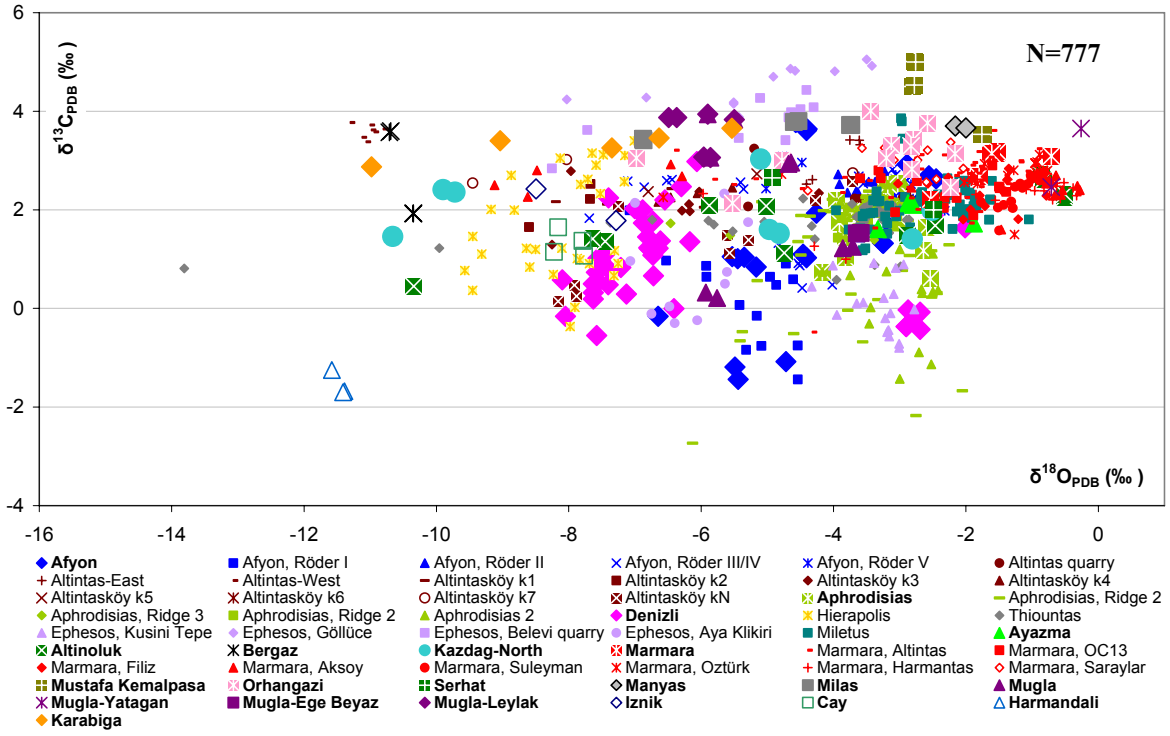

Figure 76: $\delta^{13}C$ versus $\delta^{18}O$ isotope ratios (in ‰; relative to PDB) of the marble quarries in West Anatolia. The large symbols in the diagram represent the measurements that were carried out in the course of this work. The occurrences that were investigated in the course of this work are labelled with bold letters in the legend (CRAMER 2004; ATTANASIO *et al.* 2006; ZÖLDFÖLDI *et al.* 2008b, a).

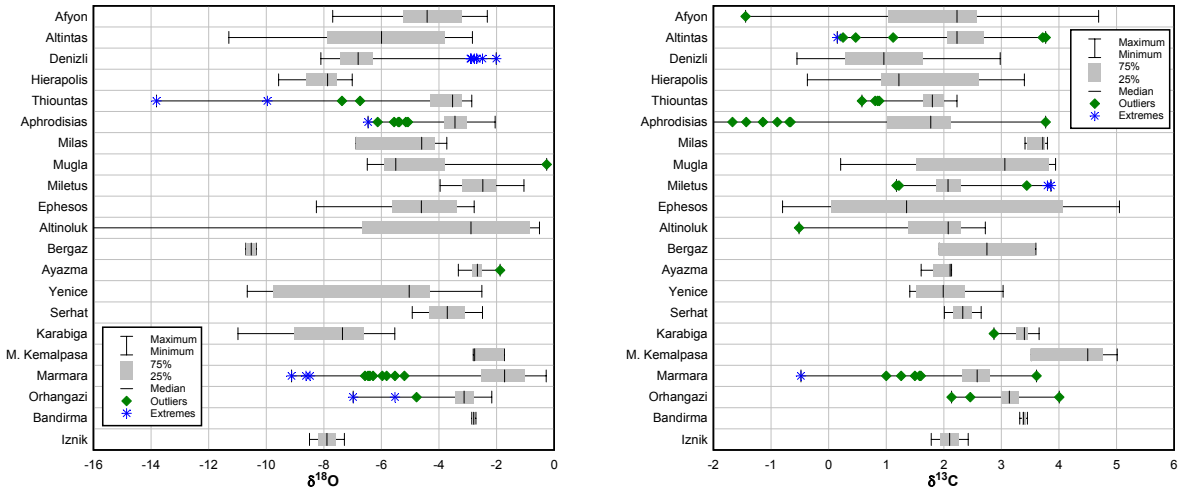

Figure 77: Distribution of the $\delta^{18}O$ and $\delta^{13}C$ values (‰, relative to PDB) of the West Anatolian marble quarries. The figure includes data from 777 samples, 239 samples were measured in the course of this work, 538 data were assimilated from the literature (CRAMER 2004; ATTANASIO *et al.* 2006).

12.1.1. Stable isotopic characterisation of marbles from the Troad and neighbouring areas

In the following section, each geological unit will be discussed in more details. Figure 78 shows the isotopic distribution of the marble samples from Troad and neighbouring areas in Northwest Anatolia, including 237 data points from 11 quarry areas. Seventy samples were analysed within the framework of this study, the data for 167 points (predominantly from Marmara) were taken from the literature (CRAMER 2004; ATTANASIO *et al.* 2006). The experimental data points are scattered over a relatively large area of the isotopic diagram, suggesting that discrimination of the different quarries might be difficult.

Some of the quarries show a more homogenous isotopic field, like Marmara, Orhangazi, Mustafa Kemalpasa and Ayazma, while others like Serhat and Altınoluk show a wide distribution of the isotopic results, especially in $\delta^{18}O$ values. This phenomenon was caused probably by contact metamorphism or fluid infiltrations.

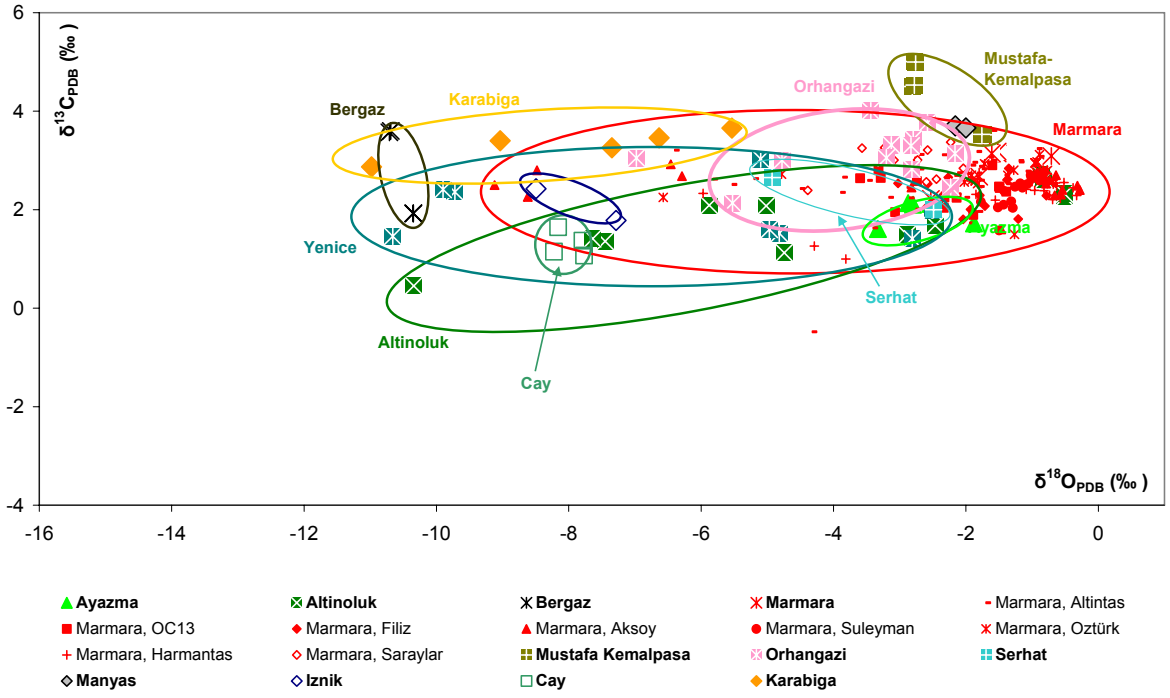

Figure 78: $\delta^{13}C$ versus $\delta^{18}O$ isotopic ratios (in ‰, relative to PDB) of the marble quarries from the Troad and neighbouring areas. The big symbols in the diagram present the measurements that were carried out within the course of this work. The occurrences that were investigated in the course of this work are labelled with bold letters in the legend (CRAMER 2004; ATTANASIO *et al.* 2006; ZÖLDFÖLDI *et al.* 2008b, a).

12.1.1.1. Kazdağ Range

Figure 78 shows the results (n=36) of the isotopic distribution of four localities (Altınoluk, Ayazma, Yenice, Serhat) from the Kazdağ Range of the Troad. All measurements were

carried out within the framework of this study. It was very important to investigate these occurrences because they are very close to Troia, and therefore they came into consideration for provenance for the Trojan artifacts. No previous works exists on these marbles. As previously mentioned, an interesting feature of the marbles from Yenice (Kazdağ-North) and Altınoluk is their elongated distribution due to the restricted $\delta^{13}C$ ratios and the large spread in $\delta^{18}O$ ratios (-10.66 ‰ < $\delta^{18}O$ < -2.51 ‰, SD=3.10 and -17.88 ‰ < $\delta^{18}O$ < -0.51 ‰, SD=4.75 respectively, see also Table 12). This comes from the lack of isotopic equilibrium with aqueous fluids or weathering. Exchange with metamorphic pore fluids, and equilibration with other country rock can also introduce high variations in $\delta^{18}O$ values (0.5 to 1.8 ‰), but only moderate to low variations in $\delta^{13}C$ values (0.2 ‰, HERZ 1988b).

Other occurrences have more a defined field on the isotopic charts, as in Ayazma (-3.33 ‰ < $\delta^{18}O$ < -1.88 ‰, SD=0.48). Generally, we must emphasize that overlap occurs between Altınoluk and Serhat. The experimental data points of Ayazma fall into the field, where most of the data are located. Therefore, without investigations of any other properties, the allocation of marbles originating from this locality is impossible.

12.1.1.2. Karakaya Complex

Data of 186 marble samples from 11 quarries from the Karakaya Complex northeast of Troia, are presented in the Figure 78 as well. Nine of the twelve quarries are on the Marmara Island, which is famous for its marble exploitation in Antiquity. Because of its status, it is one of the most investigated marble sources. Therefore, I concentrated my investigation on the other quarries (Mustafa Kemalpasa and Bandirma) and used the data available in the literature for comparison (167 samples, ATTANASIO *et al.* 2006; CRAMER 2004). When comparing the data of these occurrences one can immediately see the following features: The marbles from Mustafa Kemalpasa have more positive $\delta^{13}C$ values (up to 5.01 ‰, see also Table 12).

The discrimination of the quarries on Marmara Island is difficult. The marble from the Aksoy locality has a large share of $\delta^{18}O$ values (-9.12 ‰ < $\delta^{18}O$ < -0.28 ‰, SD=3.5). This seems to be a special feature when compared with other localities on Marmara Island. The reason for this feature was not investigated in this work. The other quarries show well-defined groups in the stable isotope charts, but the superposition of these results is strong and certainly requires the support of additional variables and multi-method analysis to obtain reliable assignments.

12.1.1.3. Armutlu-Ovacık Zone

Figure 78 includes the results of the stable isotopic investigation of two localities, Orhangazi and Iznik from the Armutlu-Ovacik Zone. Until now, no comparative data exist in the literature. The experimental data points have extensive isotopic superposition for Orhangazi and Marmara marbles. The marbles of Iznik show more negative $\delta^{18}O$ values than those from Orhangazi.

12.1.1.4. Rhodope-Strandja Massif

Figure 79 shows the stable isotopic results of the Rhodope-Strandja Massif, including seven data point from two quarry areas: Bergaz and Karabiga. These quarries were investigated exclusively in the framework of this study; no data are available in the literature. Bergaz shows a well-defined group with more negative $\delta^{18}O$ values (-10.71 ‰ < $\delta^{18}O$ < -10.35 ‰), while Karabiga shows relatively high $\delta^{13}C$ values ($\delta^{13}C$ > 3.5 ‰) compared to all other known marbles. This could be a provenance criterion for these marbles.

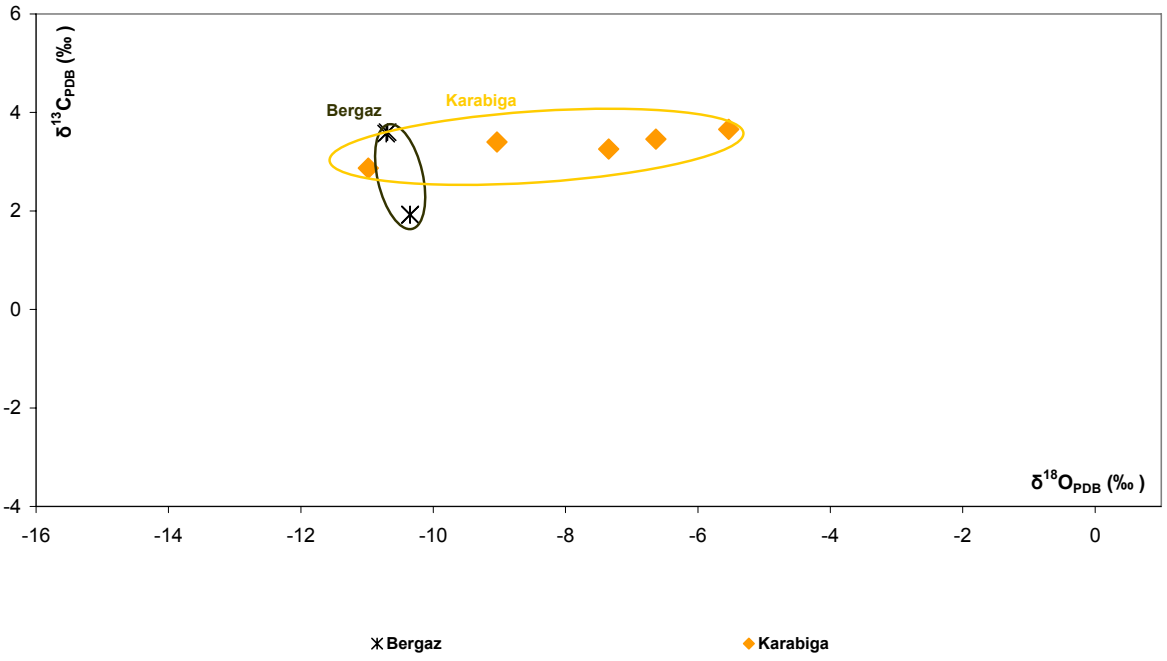

Figure 79: $\delta^{13}C$ versus $\delta^{18}O$ isotopic ratios (in ‰, relative to PDB) of the marble quarries belonging to the Rhodope-Strandja Massif in Northwest Anatolia. These measurements were carried out in the course of this work. No complementary data are available from these quarries.

12.1.2. Stable isotopic characterisation of Middle and Southwest Anatolian marbles

12.1.2.1. Menderes Massif

The isotopic plot in Figure 80 shows the results of 136 marble samples from 10 quarries (4 of them around Ephesos and 4 of them near Muğla). Twenty-six measurements were carried out in the framework of this study and 110 were collected from the literature (mainly ATTANASIO *et al.* 2006; CRAMER 2004).

Compared to the results from other West Anatolian marbles (see also Figure 76 and Figure 80) the relatively high $\delta^{13}C$ values are characteristic for Ephesos Göllüce (3.88 ‰ < $d^{13}C$ < 5.05 ‰, SD=0.39) and Ephesos Belevi quarry (2.84 ‰ < $d^{13}C$ < 4.43 ‰, SD=0.47), but also Muğla-Leylak (3.06 ‰ < $\delta^{13}C$ < 3.94 ‰, SD=0.42) and Milas (3.41 ‰ < $\delta^{13}C$ < 3.8 ‰, SD=0.18, see also Table 12).

In contrast, the samples from Muğla Yatağan have relatively positive $\delta^{18}O$ values (-0.71 ‰ < $\delta^{18}O$ < -0.26 ‰, unfortunately only two samples were available for investigation). The other two quarries, Kusini Tepe and Aya Klikiri, both near Ephesos, also showed a well-defined cluster in the isotopic plot, although they are strongly superposed with other quarries worldwide and therefore difficult to distinguish isotopically from other marbles.

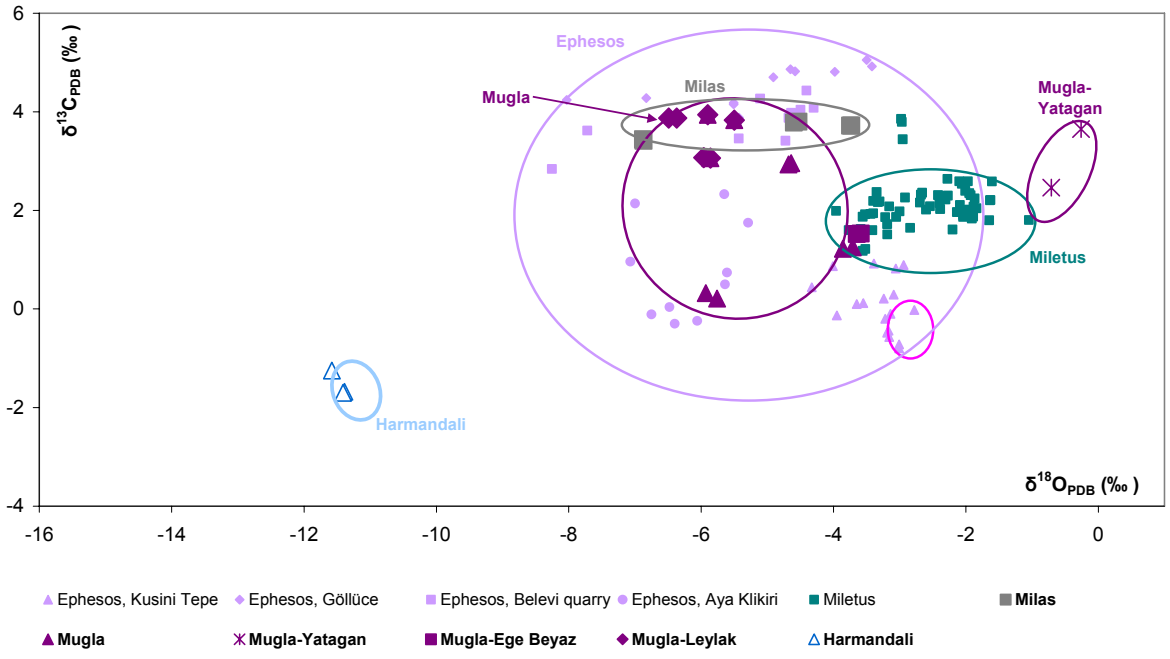

Figure 80: $\delta^{13}C$ versus $\delta^{18}O$ isotopic ratios (in ‰, relative to PDB) of the marble quarries from the Menderes Massif in Southwest Anatolia. The big symbols in the diagram represent the measurements that were carried out in the course of this work. The occurrences that were investigated in the course of this work are labelled with bold letters in the legend (CRAMER 2004; ATTANASIO *et al.* 2006; ZÖLDFÖLDI *et al.* 2008b, a).

A more detailed investigation of the marbles from Aya Klikiri and Kusini Tepe generally shows that the ranges of $\delta^{13}C$ values are more variable than in the case of other marbles, while the $\delta^{18}O$ values show less variability: -0.30 ‰ < $\delta^{13}C$ < 2.33 ‰ and -0.80 ‰ < $\delta^{13}C$ < 0.92 ‰ and -7.07 ‰ < $\delta^{18}O$< -5.29 ‰ and -4.33 ‰ < $\delta^{18}O$ < -2.78 ‰ respectively (see also Table 12). Additionally, the marbles from Aya Klikiri and Kusini Tepe have lower $\delta^{13}C$ values than the marbles of Göllüce and Belevi quarry and there is a trend in the $\delta^{18}O$ values.

12.1.2.2. Central-Anatolide-Tauride block

Figure 81 shows the results of 383 stable isotopic ratios measurements of six occurrences from the Central-Anatolide-Tauride block. Forty-one were measured in the course of this work and 342 data stem from the literature (mainly ATTANASIO 2003; ATTANASIO *et al.* 2006; CRAMER 2004; ZÖLDFÖLDI *et al.* 2008b). Comparing the results with other West Anatolian marbles the relatively low values of $\delta^{13}C$ appear in some samples from Aphrodisias (Min = -2.74 ‰), but relatively low $\delta^{18}O$ values appear in samples from Thiountas (Min = -13.81 ‰). The samples of Altintas can be arranged into two fields, one of them, the quarry of Altintas-West, with more negative $\delta^{18}O$ values (-11.30 ‰ < $\delta^{18}O$ < -10.80 ‰) and relatively high $\delta^{13}C$ values (3.38 ‰ < $\delta^{13}C$ < 3.77 ‰, see also Table 12). Remarkable are the fields of Denizli-I and Hierapolis, the modern and ancient quarry near Denizli. The samples from the modern quarry, Denizli-I, have slightly higher $\delta^{18}O$ values (-8.10 ‰ < $\delta^{18}O$ < -6.10 ‰) than the samples from Hierapolis (-9.57 ‰ < $\delta^{18}O$ < -7.01 ‰). On the other hand, no significant difference was recognisable in the $\delta^{13}C$ values. Additionally, there is another field were the samples of Denizli-II can be classified with considerably higher $\delta^{18}O$ values (up to 2.01 ‰). The more detailed investigation of the marbles from Afyon, reveals the similarity of the quarries Röder II and Röder V, concerning both $\delta^{13}C$ and $\delta^{18}O$ values. Röder I (also known as Bacakale) and Röder III/IV have more negative $\delta^{18}O$ values. Additionally the samples from Röder I have lower $\delta^{13}C$ values than all other marbles from Afyon.

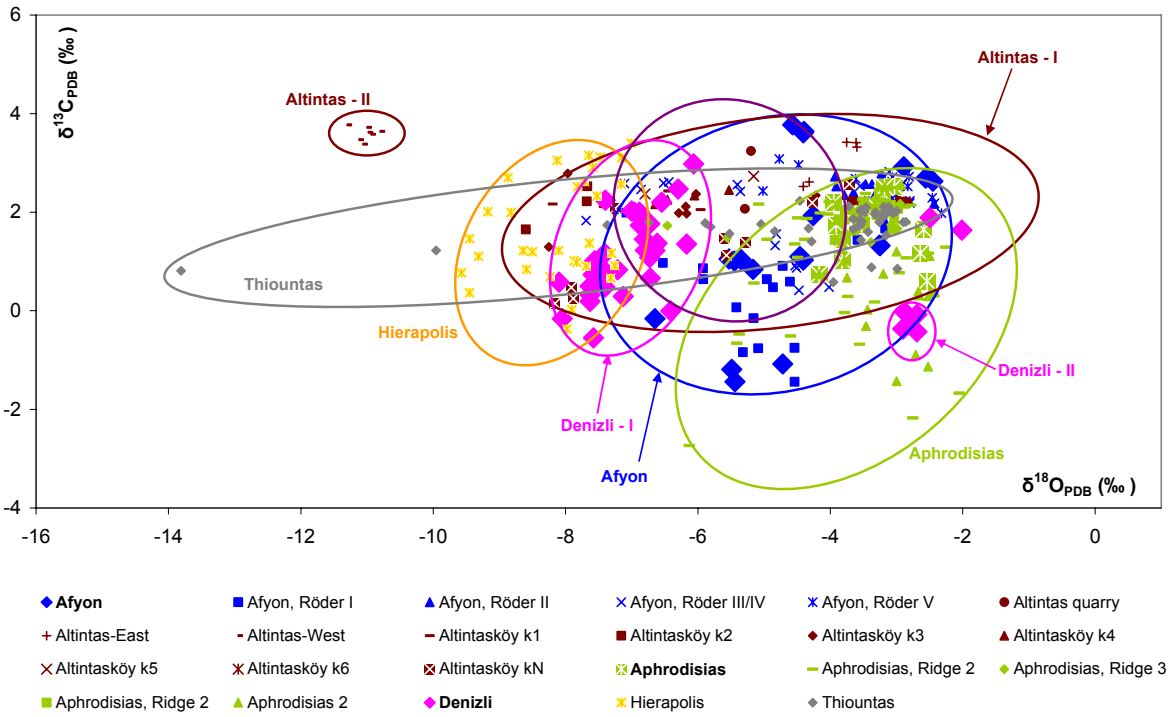

Figure 81: $\delta^{13}C$ versus $\delta^{18}O$ isotopic ratios (in ‰, relative to PDB) of the marble quarries from the Central-Anatolide-Tauride Block in Middle and Southwest Anatolia. The big symbols in the diagram present the measurements that were carried out in the course of this work. The occurrences that were investigated in the course of this work are labelled with bold letters in the legend (CRAMER 2004; ATTANASIO *et al.* 2006; ZÖLDFÖLDI *et al.* 2008b, a).

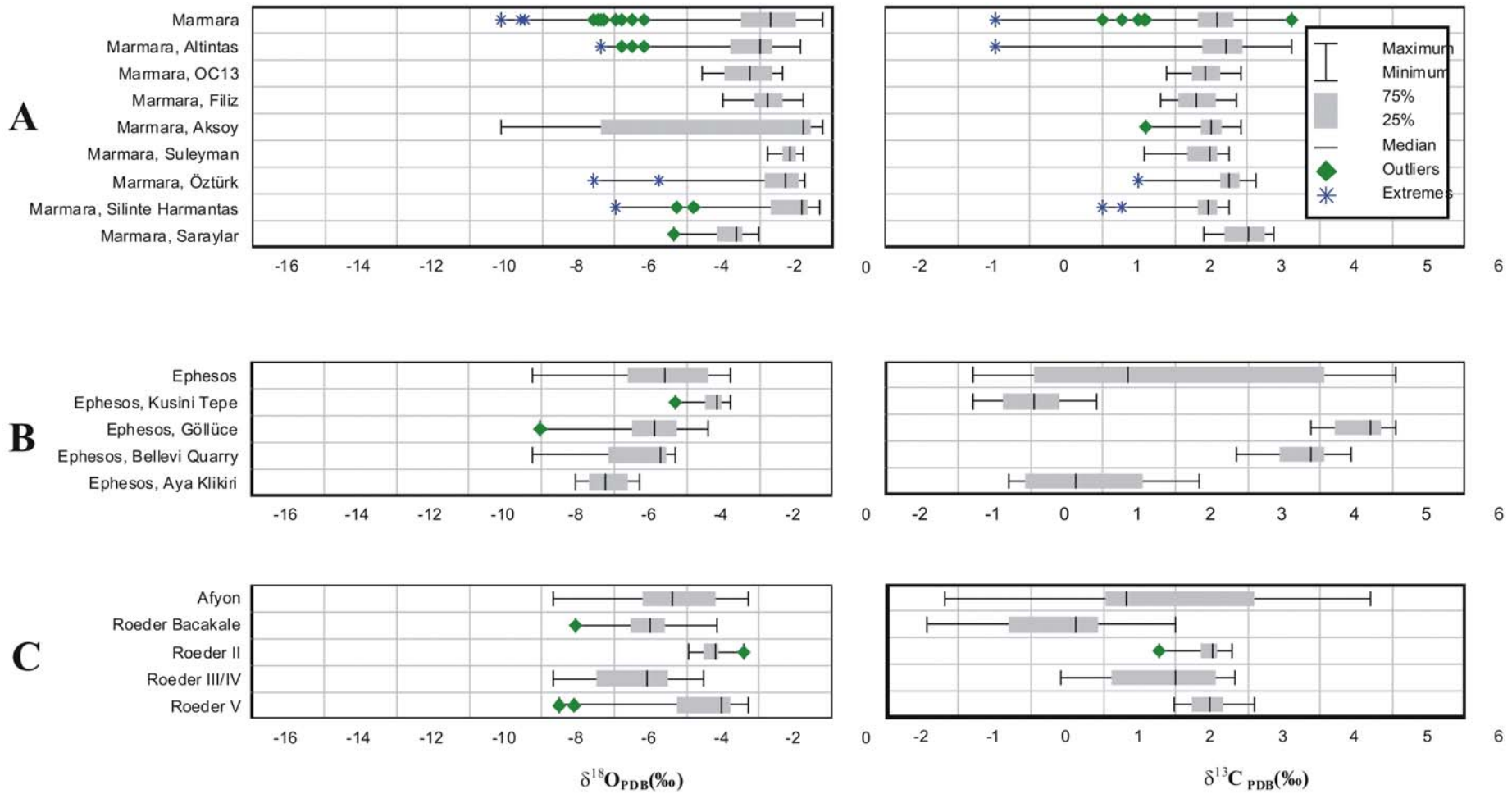

Figure 82: Intra-quarry distribution of the $\delta^{13}C$ and $\delta^{18}O$ values of marbles from Marmara (A), Ephesos (B) and Afyon (C). The figure includes data that were assimilated from the literature (CRAMER 2004; ATTANASIO *et al.* 2006).

Table 12: Statistical evaluation of the stable isotopic results of West Anatolian marbles

	Kazdağ Massif								Armutlu & Ovacik Zone				Rhodope-Stradja Massif			
	Altınoluk		Ayazma		Yenice		Serhat		Orhangazi		Iznik		Karabiga		Bergaz	
	$\delta^{13}C$	$\delta^{18}O$	$\delta^{13}C$	$\delta^{18}O$	$\delta^{13}C$	$\delta^{18}O$	$\delta^{13}C$	$\delta^{18}O$	$\delta^{13}C$	$\delta^{18}O$	$\delta^{13}C$	$\delta^{18}O$	$\delta^{13}C$	$\delta^{18}O$	$\delta^{13}C$	$\delta^{18}O$
n	15	15	6	6	9	9	2	2	13	13	2	2	5	5	2	2
Mean	1.73	-4.69	1.97	-2.66	2.00	-6.18	2.33	-3.71	3.14	-3.68	2.10	-7.89	3.68	-7.73	2.76	-10.53
Min	-0.51	-17.88	1.61	-3.33	1.41	-10.66	2.00	-4.93	2.13	-6.98	1.78	-8.49	3.66	-9.93	1.92	-10.71
Max	2.72	-0.51	2.13	-1.88	3.03	-2.51	2.65	-2.49	4.01	-2.16	2.42	-7.29	3.70	-5.54	3.60	-10.35
StDev	0.89	4.75	0.24	0.48	0.55	3.10	-	-	0.49	1.68	-	-	0.96	0.20	-	-

	Karakaya Complex															
	Marmara (all)		Marmara M.Altintas		Marmara OC13		Marmara Filiz		Marmara Aksoy		Marmara Suleyman		M. Kemalpasa		Bandirma	
	$\delta^{13}C$	$\delta^{18}O$	$\delta^{13}C$	$\delta^{18}O$	$\delta^{13}C$	$\delta^{18}O$	$\delta^{13}C$	$\delta^{18}O$	$\delta^{13}C$	$\delta^{18}O$	$\delta^{13}C$	$\delta^{18}O$	$\delta^{13}C$	$\delta^{18}O$	$\delta^{13}C$	$\delta^{18}O$
n	175	175	54	54	14	14	11	11	15	15	18	18	7	7	2	2
Mean	2.54	-2.08	2.60	-2.41	2.40	-2.35	2.31	-1.82	2.46	-3.19	2.38	-1.19	4.23	-2.34	3.39	-2.79
Min	-0.48	-9.12	-0.48	-6.40	1.89	-3.60	1.80	-3.03	1.60	-9.12	1.58	-1.77	3.52	-2.81	3.32	-2.86
Max	3.61	-0.28	3.61	-0.89	2.90	-1.39	2.84	-0.78	2.92	-0.28	2.75	-0.80	5.01	-1.73	3.45	-2.72
StDev	0.46	1.56	0.58	1.28	2.75	3.93	0.35	0.64	0.30	3.50	0.30	0.27	0.69	0.56	-	-

	Menderes Massif															
	Milas		Muğla		Muğla								Miletus		Ephesos	
					Muğla		Yatağan		Ege-Beyaz		Leylak					
	$\delta^{13}C$	$\delta^{18}O$	$\delta^{13}C$	$\delta^{18}O$	$\delta^{13}C$	$\delta^{18}O$	$\delta^{13}C$	$\delta^{18}O$	$\delta^{13}C$	$\delta^{18}O$	$\delta^{13}C$	$\delta^{18}O$	$\delta^{13}C$	$\delta^{18}O$	$\delta^{13}C$	$\delta^{18}O$
n	7	7	19	19	9	9	2	2	2	2	6	6	60	60	50	50
Mean	3.62	-5.32	2.66	-4.74	2.19	-5.09	3.06	-0.49	1.53	-3.62	3.61	-6.01	2.12	-2.59	2.01	-4.78
Min	3.41	-6.88	0.21	-6.49	0.21	-5.93	2.46	-0.71	1.52	-3.65	3.06	-6.49	1.18	-3.96	-0.80	-8.26
Max	3.80	-3.73	3.94	-0.26	3.94	-3.71	3.65	-0.26	1.53	-3.59	3.94	-5.50	3.86	-1.05	5.05	-2.78
StDev	0.18	1.49	1.26	1.77	1.45	0.89	-	-	-	-	0.42	0.36	0.48	0.69	2.04	1.51

	Menderes Massif								Middle Anatolia							
	Ephesos								Denizli		Hierapolis		Thiountas		Aphrodisias	
	Kusini Tepe		Göllüce		Belevi Quarry		Aya Klikiri									
	$\delta^{13}C$	$\delta^{18}O$	$\delta^{13}C$	$\delta^{18}O$	$\delta^{13}C$	$\delta^{18}O$	$\delta^{13}C$	$\delta^{18}O$	$\delta^{13}C$	$\delta^{18}O$	$\delta_{13}C$	$\delta^{18}O$	$\delta^{13}C$	$\delta^{18}O$	$\delta^{13}C$	$\delta^{18}O$
n	18	18	11	11	11	11	10	10	41	41	31	31	44	44	122	122
Mean	0.07	-3.33	4.54	-5.12	3.76	-5.52	0.78	-6.20	0.95	-6.22	1.65	-8.09	1.74	-4.20	1.39	-3.51
Min	-0.80	-4.33	3.88	-8.03	2.84	-8.26	-0.30	-7.07	-0.55	-8.10	-0.37	-9.57	0.58	-13.81	-2.74	-6.46
Max	0.92	-2.78	5.05	-3.42	4.43	-4.30	2.33	-5.29	2.98	-2.01	3.40	-7.01	2.23	-2.86	3.77	-2.05
StDev	0.56	0.41	0.39	1.38	0.47	1.43	0.99	0.64	0.89	1.84	1.04	0.76	0.38	2.02	1.06	0.77

	Middle Anatolia											
	Altintas		Afyon		Afyon							
					Röder I		Röder II		Röder III/IV		Röder V	
	$\delta^{13}C$	$\delta^{18}O$	$\delta^{13}C$	$\delta^{18}O$	$\delta^{13}C$	$\delta^{18}O$	$\delta^{13}C$	$\delta^{18}O$	$\delta^{13}C$	$\delta^{18}O$	$\delta^{13}C$	$\delta^{18}O$
n	58	58	87	87	16	16	16	16	15	15	18	18
Mean	2.33	-6.20	1.89	-4.59	0.39	-5.09	2.45	-3.32	1.83	-5.27	2.46	-3.73
Min	0.15	-11.30	-1.44	-14.61	-1.44	-7.08	1.78	-3.93	0.42	-7.69	1.98	-7.51
Max	3.77	-2.84	4.69	4.40	1.99	-3.17	2.78	-2.43	2.82	-3.11	3.08	-2.32
StDev	0.79	2.51	1.22	2.48	0.97	0.99	0.24	0.38	0.84	1.35	0.30	1.52

12.1.3. Stable isotopic characterisation of the Greek marbles

In this section, the isotopic data of marbles from the Eastern Mediterranean in the neighbouring region of Anatolia are summarised. This region cannot be excluded from the comparison in the course of the provenance analyses of the archaeological object from Troia, because of the very intense exchange between Anatolian and Greek civilisations in that historical period. A more detailed description of the quarries belonging to this geographical region and information about each sample are available in ATTANASIO (2003), ATTANASIO *et al.* (2006), CRAMER (2004), and in the MissMarble database (ZÖLDFÖLDI *et al*. 2008b).

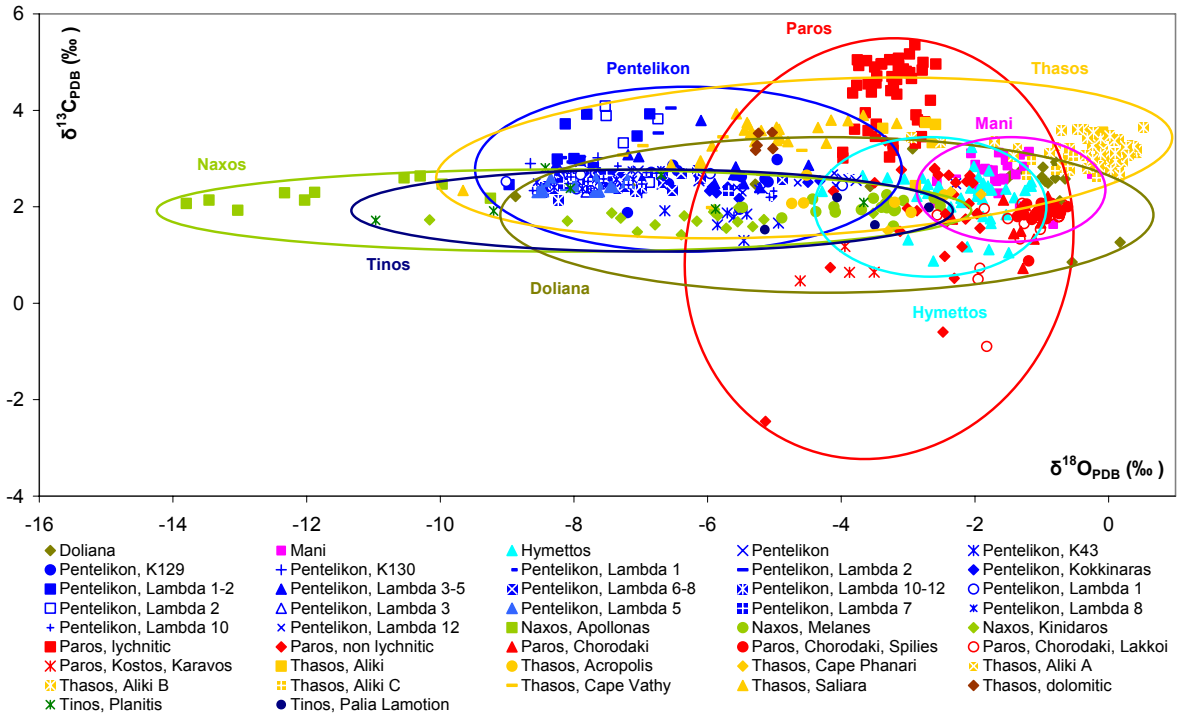

Figure 83: $\delta^{13}C$ versus $\delta^{18}O$ isotopic compositions (in ‰, relative to PDB) of the marble quarries of Greece. (ATTANASIO 2003; ATTANASIO *et al.* 2006; CRAMER 2004 and ZÖLDFÖLDI *et al.* 2008b).

12.1.4. Trojan marbles

Because of the enormous amount of the stable isotopic data on the East-Mediterranean marbles (more than 2000 data pairs), the comparison between raw materials and individual archaeological objects is not possible in one single diagram. Therefore, in order to keep track of the results, tree diagrams were used for comparison: The results of the archaeological objects were first compared to the marbles from Northwest Anatolia (marbles in the close neighbourhood of Troia), secondly, to Middle and Southwest Anatolia and finally to marbles from Greece.

The raw materials from different occurrences are presented as ellipses but the archaeological objects are treated at any time as individuals and are presented as single points in the diagrams.

12.1.4.1. Prehistoric marbles

12.1.4.1.1. Kumtepe marbles

When comparing the stable isotope ratios of the archaeological objects of Kumtepe with the results of the geological occurrences, it becomes obvious that (minimum) two different materials were used for the production. F28/990 and F29/460 have similar stable isotopic ratios, while F28/958/1 has more negative $\delta^{18}O$ values (-13.55 ‰). Based on the stable isotopic ratios only Thiountas can be considered as provenance for the object F28/958/1, while the other two objects (F28/990 and F29/460) could made of marbles from Serhat, Marmara (maybe Karabiga, Orhangazi and Altınoluk) in Northwest Anatolia (Figure 84), Muğla, Thiountas, Afyon, Ephesos, Altintas (maybe Milas and Denizli) in Middle and Southwest Anatolia (Figure 85) and Doliana, Hymettus, Pentelikon and Thasos (maybe Paros and Naxos) in Greece (Figure 86).

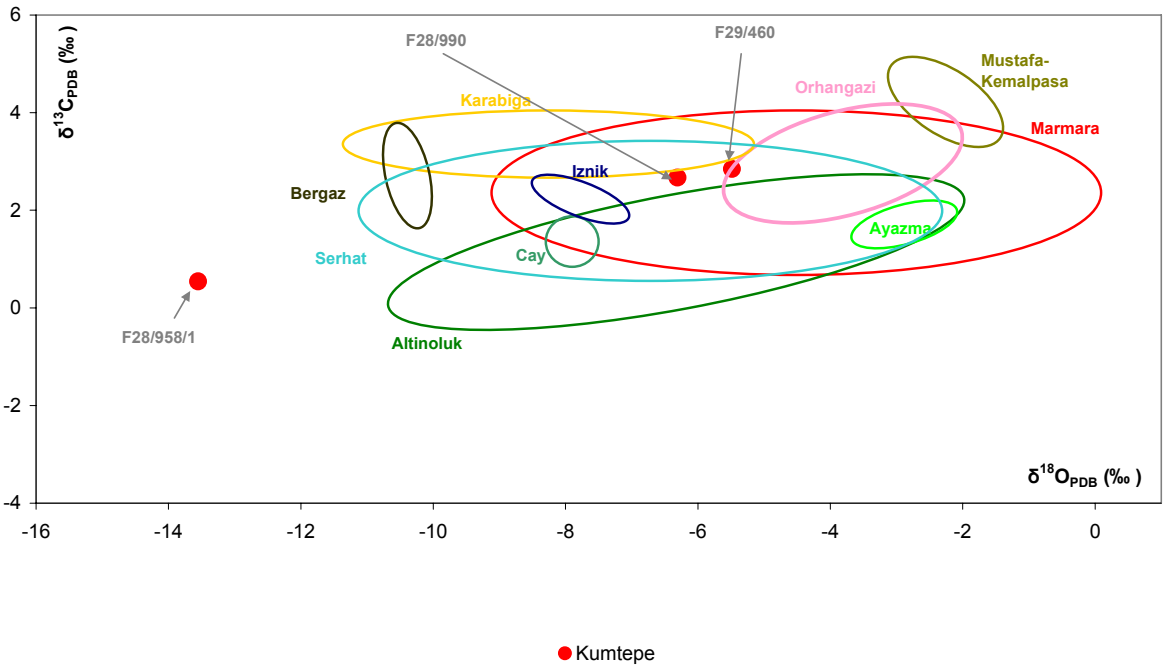

Figure 84: Data set of $\delta^{13}C$ vs. $\delta^{18}O$ isotopic compositions (in ‰, relative to PDB) of the archaeological samples of Kumtepe compared with the data set of marbles from the Troad and neighbouring areas.

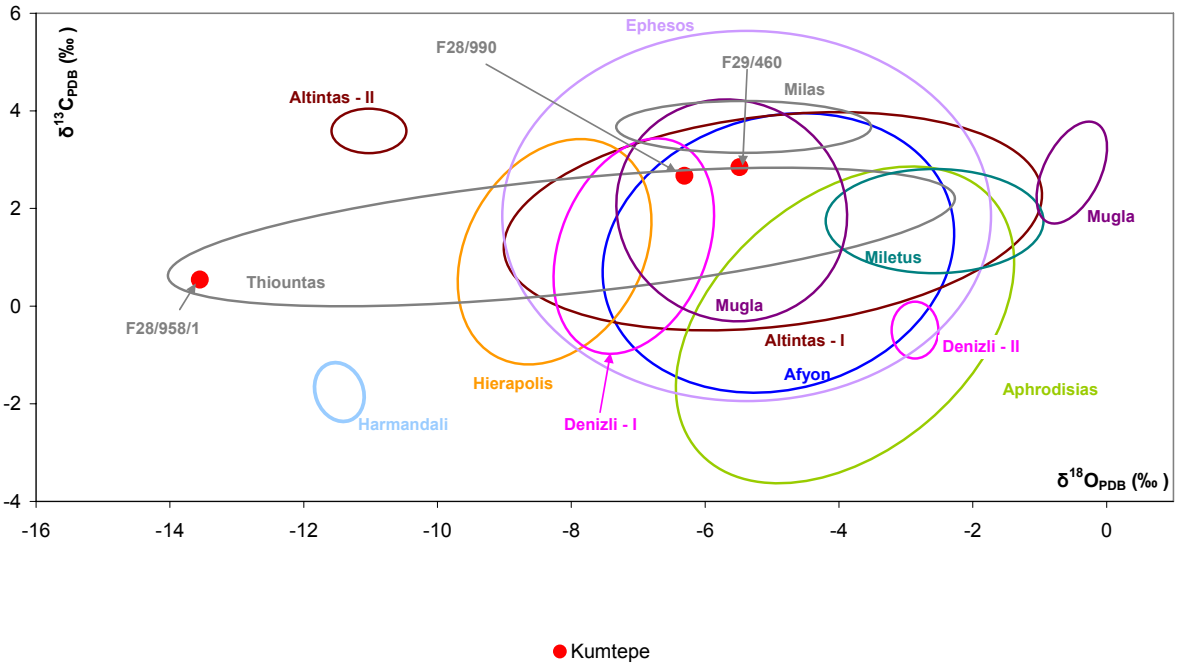

Figure 85: Data set of $\delta^{13}C$ vs. $\delta^{18}O$ isotopic compositions (in ‰, relative to PDB) of the archaeological samples of Kumtepe compared with the data set of Middle and Southwest Anatolian marbles.

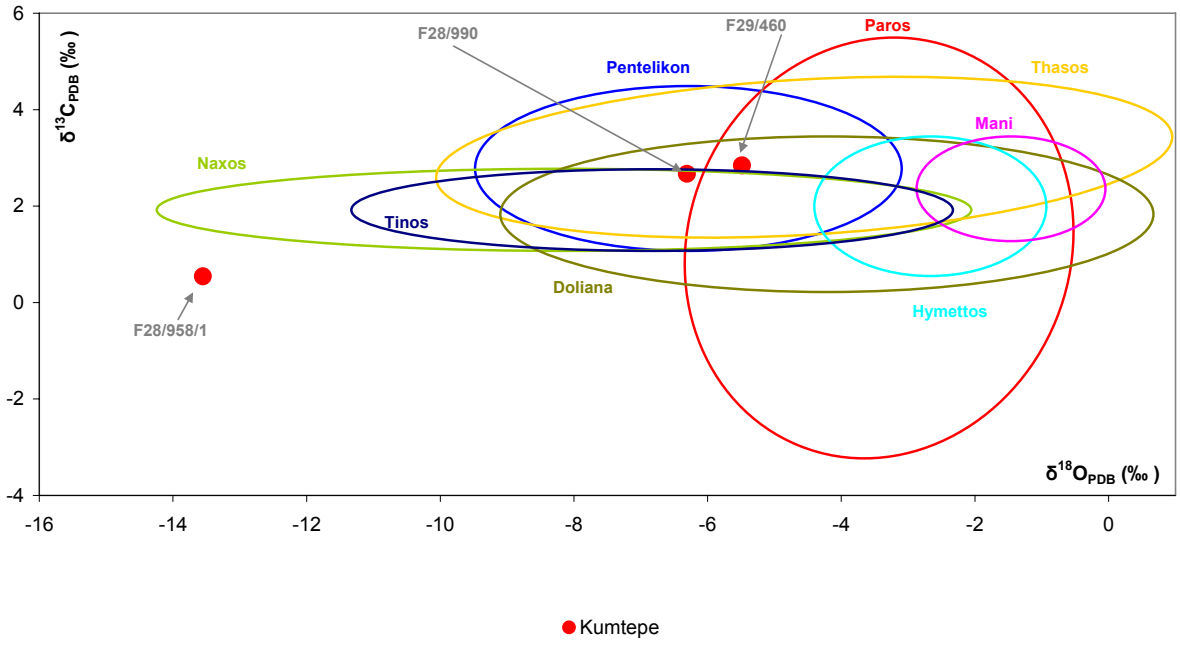

Figure 86: Data set of $\delta^{13}C$ vs. $\delta^{18}O$ isotopic compositions (in ‰, relative to PDB) of the archaeological samples of Kumtepe compared with the data set of marbles from Greece.

12.1.4.1.2. Bronze Age marbles

A comparison of the stable isotope ratios of the Bronze Age archaeological objects with the results of the geological occurrences makes it clear that the samples cannot be treated as a group because the results are widely spread. The possible provenances based on the stable isotope ratio analysis (see also Figure 87-Figure 89) are summarized in Table 13.

Table 13: Possible provenances of the raw materials of the Bronze Age objects from Troia

Areal	Northwest Anatolia	Middle and Southwest Anatolia	Greece
D8/1844	Marmara	Miletus, Ephesos, Aphrodisias, Afyon, Altintas	Hymettus, Mani, Paros, Doliana, Thasos (Naxos, Tinos)
K8/730	Altınoluk, Serhat, Marmara	Muğla, Ephesos, Aphrodisias, Afyon, Altintas, Thiountas	Paros, Doliana, (Naxos, Tinos, Pentelikon)
Z7/732	Altınoluk, Serhat, Marmara	Muğla, Ephesos, Aphrodisias, Afyon, Altintas, Thiountas, Denizli	Tinos, Naxos, Doliana, Pentelikon, Thasos, Paros
D3/30	Altınoluk, Serhat, Marmara, Orhangazi	Muğla, Afyon, Ephesos, Aphrodisias, Thiountas	Paros, Doliana, Naxos, Tinos, Pentelikon
D9/106	Karabiga, Serhat, Marmara	Hierapoilis, Ephesos	Pentelikon, Thasos
E8/354(44)			
E4/640(149)	Orhangazi, Marmara, Serhat	Muğla, Afyon, Ephesos, Aphrodisias, Milas	Pentelikon, Thasos, Doliana, Paros
G6/42(1)	-	Ephesos, Aphrodisias, Afyon, Altintas	Paros
D7/48			
E4/5/100			

D8/1755	Altınoluk, Serhat, Marmara	Muğla, Ephesos, Aphrodisias, Afyon, Altintas, Thiountas, Denizli	Tinos, Naxos, Doliana, Pentelikon, Thasos
E4/5/95	Altınoluk, Serhat, Marmara, Orhangazi	Miletus, Muğla, Afyon, Ephesos, Aphrodisias, Thiountas	Pentelikon, Naxos, Tinos, Doliana, Hymettus, Thasos, Paros,
K12/B38	Marmara	Muğla, Altintas, Miletus	Hymettus, Mani, Paros, Doliana, Thasos
E9/1297	Marmara, Serhat, Altınoluk	Muğla, Ephesos, Aphrodisias, Afyon, Altintas, Thiountas	Paros, Doliana, Naxos, Tinos, Pentelikon
Y8 (1) /100	-	Thiountas (?)	Naxos
K17/1138	Karabiga, Marmara, Serhat	Denizli, Milas, Muğla, Thiountas,, Afyon, Ephesos,	Pentelikon, Doliana, Thasos
A8/491	Serhat, Altınoluk, Cay	Thiountas, Hierapolis, Denizli, Ephesos, Altintas	Doliana, Tinos, Naxos
D3/449			
D2/190			
I9/393	Altınoluk, Serhat, Marmara, Iznik	Muğla, Ephesos, Aphrodisias, Afyon, Altintas, Thiountas, Denizli	Tinos, Naxos, Doliana, Pentelikon, Thasos
91/44 (7)			
T-44/58 (4)			
T-8/14 (3)	Orhangazi, Serhat, Altınoluk, Marmara	Miletus, Muğla, Afyon, Ephesos, Aphrodisias, Thiountas	Pentelikon, Naxos, Tinos, Doliana, Hymettus, Thasos, Paros,
T23 (5)	Orhangazi, Serhat, Altınoluk, Marmara	Miletus, Muğla, Afyon, Ephesos, Aphrodisias, Thiountas	Pentelikon, Thasos, Doliana, Paros

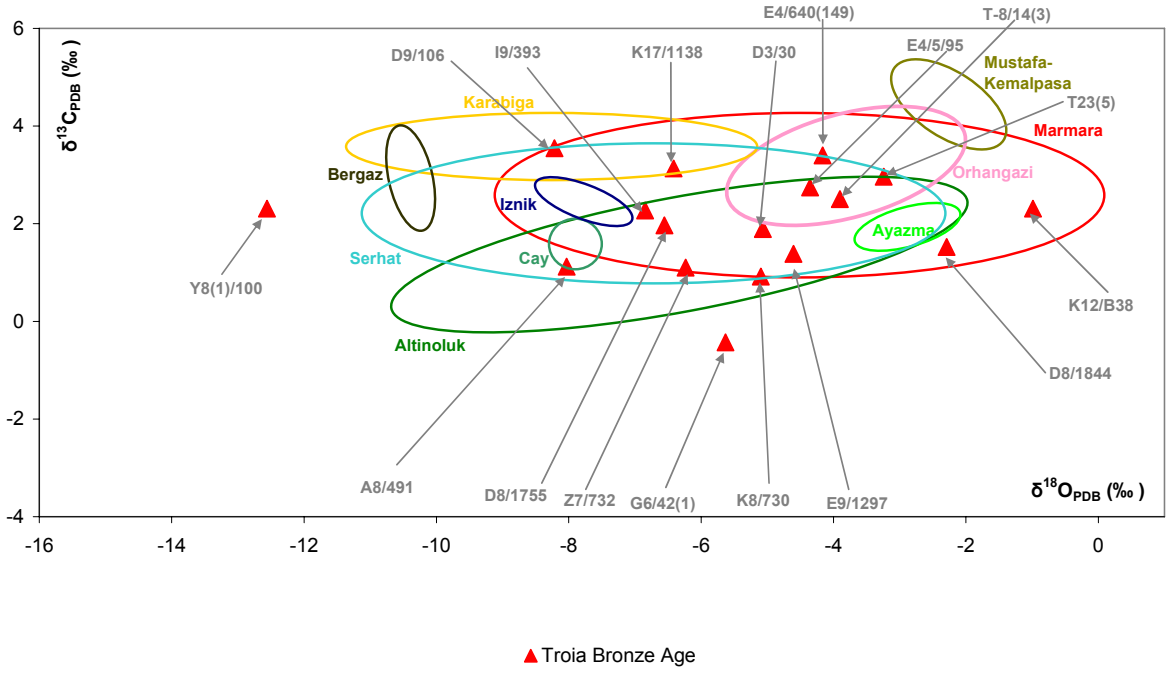

Figure 87: Data set of $\delta^{13}C$ vs. $\delta^{18}O$ isotopic compositions (in ‰, relative to PDB) of the Bronze Age archaeological samples of Troia compared with the data set of marbles from the Troad and neighbouring areas.

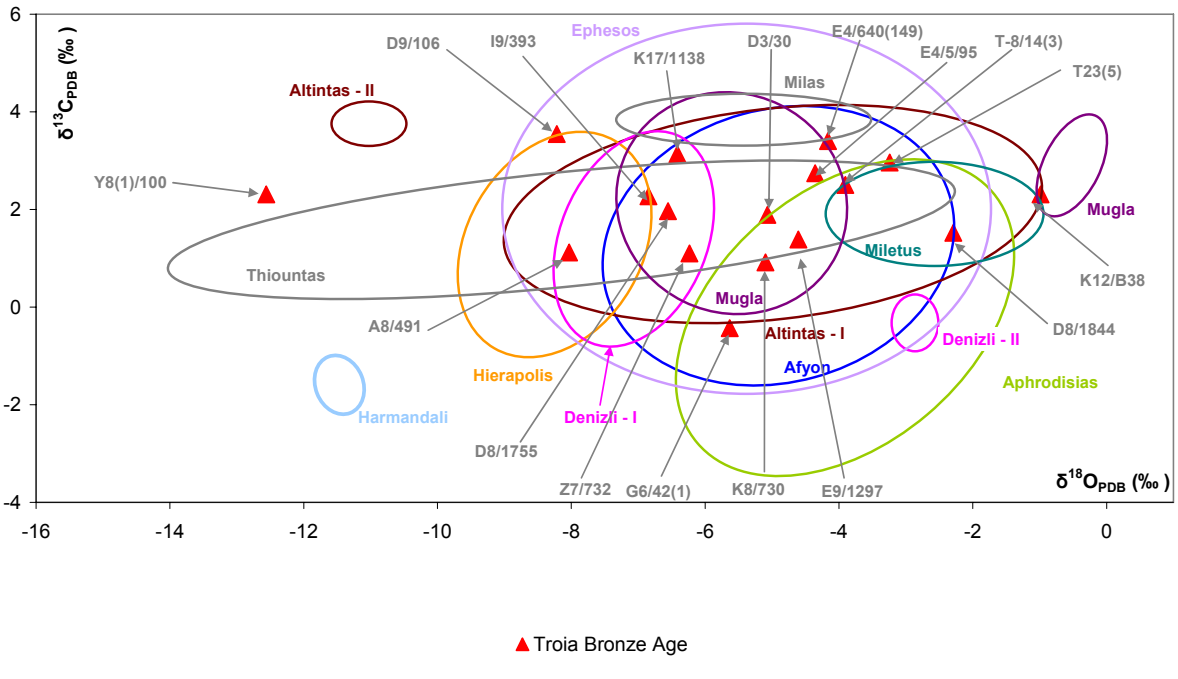

Figure 88: Data set of $\delta^{13}C$ vs. $\delta^{18}O$ isotopic compositions (in ‰, relative to PDB) of the Bronze Age archaeological samples of Troia compared with the data set of marbles from Middle and Southwest Anatolia.

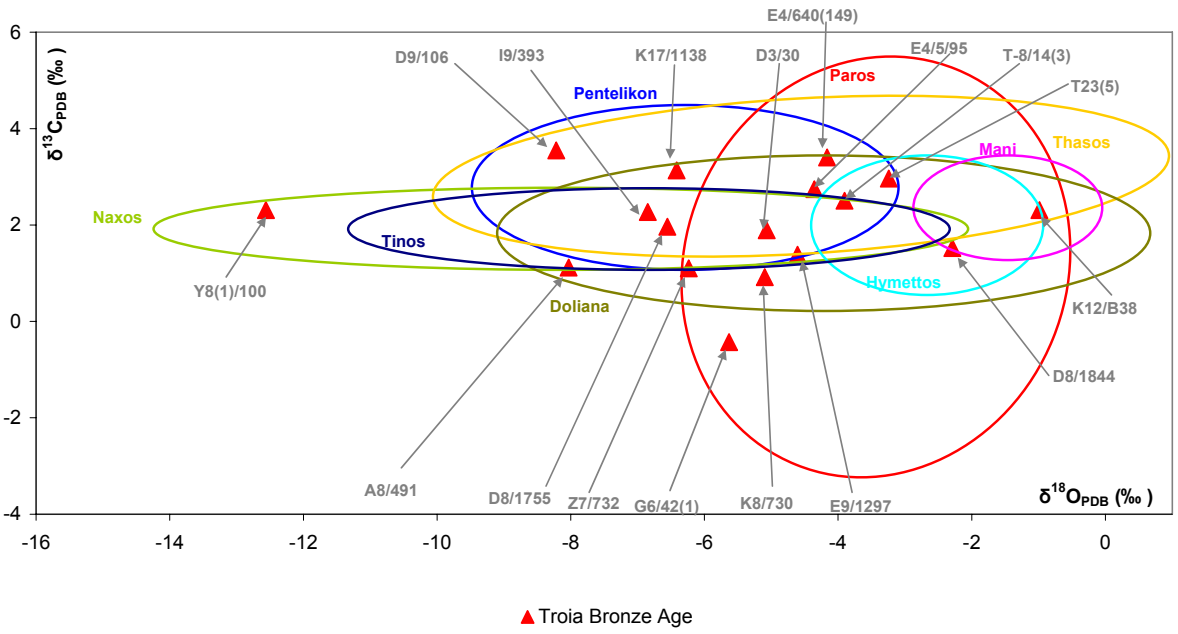

Figure 89: Data set of $\delta^{13}C$ vs. $\delta^{18}O$ isotopic compositions (in ‰, relative to PDB) of the Bronze Age archaeological samples of Troia compared with the data set of marbles from Greece.

12.1.4.2. Hellenistic marbles

Based on the stable isotope ratio analyses, the raw material of the ***Athena temple*** and ***Athena Temple Portico*** can be subdivided into several small groups. The samples PBA1, PBA6 and PBA7 have very similar results and probably come from Marmara, Orhangazi and Mustafa Kemalpasa (in Northwest Anatolia, Figure 90a), Ephesos and Altintas (in Middle and Southwest Anatolia, Figure 91a) or Thasos and Paros (in Greece, Figure 92a). PBA3 and PBA4 probably came from Marmara (in Northwest Anatolia, Figure 90a), Muğla, Altintas, Miletus (in Middle and Southwest Anatolia, Figure 91a) or Hymettus, Mani, Thasos, Doliana (in Greece, Figure 92a). PBA5 and PBA8 make up the next small group and may have originated from Altınoluk Serhat, Orhangazi, Marmara (in Northwest Anatolia, Figure 90a), Thiountas, Miletus, Aphrodisias, Ephesos, Afyon and Altintas (in Middle and Southwest Anatolia, Figure 91a) and Hymettus, Doliana, Paros, Thasos (in Greece, Figure 92a). PBA2 may have come from Marmara, Altınoluk, Serhat and Orhangazi (in Northwest Anatolia, Figure 90a), Milas, Muğla, Thiountas, Altintas and Afyon and Ephesos (in Middle and Southwest Anatolia, Figure 91a) and Doliana, Pentelikon, Paros and Thasos (in Greece, Figure 92a). PBA9 and PBA10 seem to be a separate group, and may have originated from Ephesos (in Middle and Southwest Anatolia, Figure 91a) or Pentelikon, maybe Thasos (in Greece, Figure 92a).

The material of the ***Sanctuary "Roman Altar"*** might have come from at least two different quarries based on the stable isotopic ratio analyses. PBA11 may have come from Altınoluk, Serhat, Marmara, maybe Karabiga (in Northwest Anatolia, Figure 90b), Denizli, Afyon, Thiountas, Muğla, Altintas, Ephesos (in Middle and Southwest Anatolia, Figure 91b) or Tinos, Naxos, Doliana, Pentelikon and Thasos (in Greece, Figure 92b). PBA12 and PBA13 could have originated from Marmara (in Northwest Anatolia, Figure 90b), maybe Altintas and Muğla (in Middle and Southwest Anatolia, Figure 91b) or Thasos (both PBA12 and PBA13) and Thasos, Doliana, Hymettus, Mani and Paros in Greece (PBA12, Figure 92).

Based on the stable isotopic ratio analyses, the raw material of the ***Blue Marble Building*** of the Bath seems to be quite homogeneous and could come from Marmara, Orhangazi or Mustafa Kemalpasa (in Northwest Anatolia, Figure 90b), Ephesos or Altintas (in Middle and Southwest Anatolia, Figure 91b) and Paros and Thasos (in Greece, Figure 92b).

The samples of the ***North Building Threshold of the Sanctuary*** show similar but not the identical stable isotope ratios. Sample PBA17 falls into the field of Marmara in Northwest Anatolia (Figure 90b), Muğla or Altintas in Middle and Southwest Anatolia (Figure 91b) or Paros, Mani, Doliana and Thasos in Greece (Figure 92b). Meanwhile PBA18 has similar stable isotope ratios to Marmara, Serhat, Altınoluk and Ayazma (in Northwest Anatolia, Figure 90b), Miletus, Aphrodisias, Ephesos and Altintas (in Middle and Southwest Anatolia, Figure 91b) or Hymettus, Mani, Thasos, Paros, Doliana (in Greece, Figure 92b).

Three of the four samples from the ***Bouleuterion*** (PBA19, PBA21B and PBA21W) showed similar stable isotopic ratios. Here I have to mention that PBA21B and PBA21W are two different samples that were taken from the same fragment: PBA21B was taken from the black part of the fragment and PBA21W from the white part of the fragment. Therefore, PBA21 could come from one of the following quarries, which is possible for both samples (PBA21B and PBA21W): Marmara, maybe Orhangazi and Mustafa Kemalpasa (in Northwest Anatolia, Figure 90b), Altintas or Ephesos (in Middle and Southwest Anatolia, Figure 91b) and Paros or Thasos, maybe Doliana, Hymettus and Mani (in Greece, Figure 92b). The same occurrences can be considered in the case of PBA19, as well. PBA20 has different stable isotopic ratios; noticeable is the high $\delta^{13}C$ value with 5.45‰. There are no quarries known with such high $\delta^{13}C$ value in Northwest Anatolia (Figure 90b), some extreme values of Ephesos can reach such high $\delta^{13}C$ values in Middle and Southwest Anatolia (Figure 91b). Marbles from Paros in Greece have such high $\delta^{13}C$ values, although their $\delta^{18}O$ values are somewhat higher (Figure 92b).

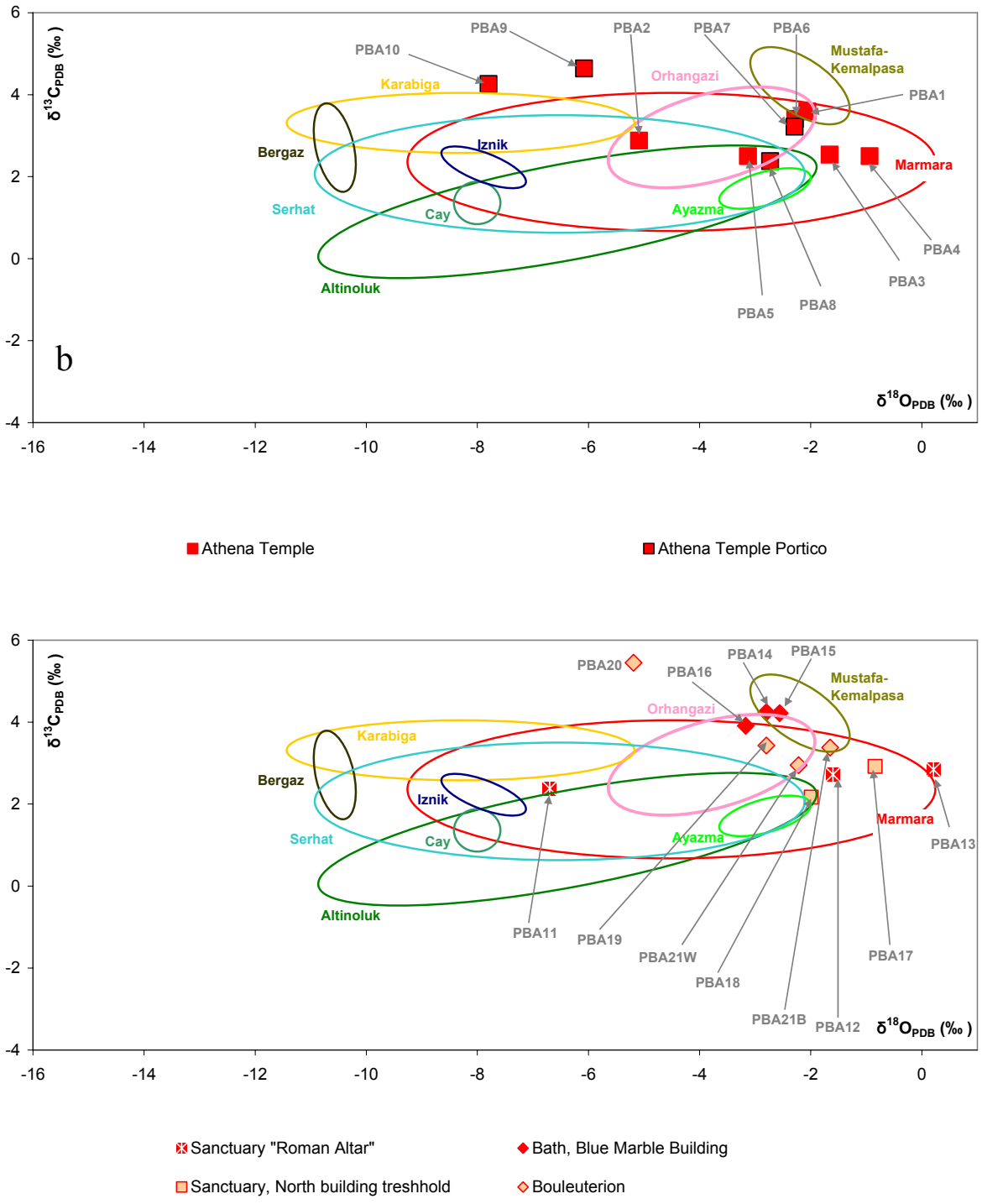

Figure 90: Data set of $\delta^{13}C$ vs. $\delta^{18}O$ isotopic compositions (in ‰, relative to PDB) from the Hellenistic Period in Troia compared with the data set of marbles from the Troad .neighbouring areas.

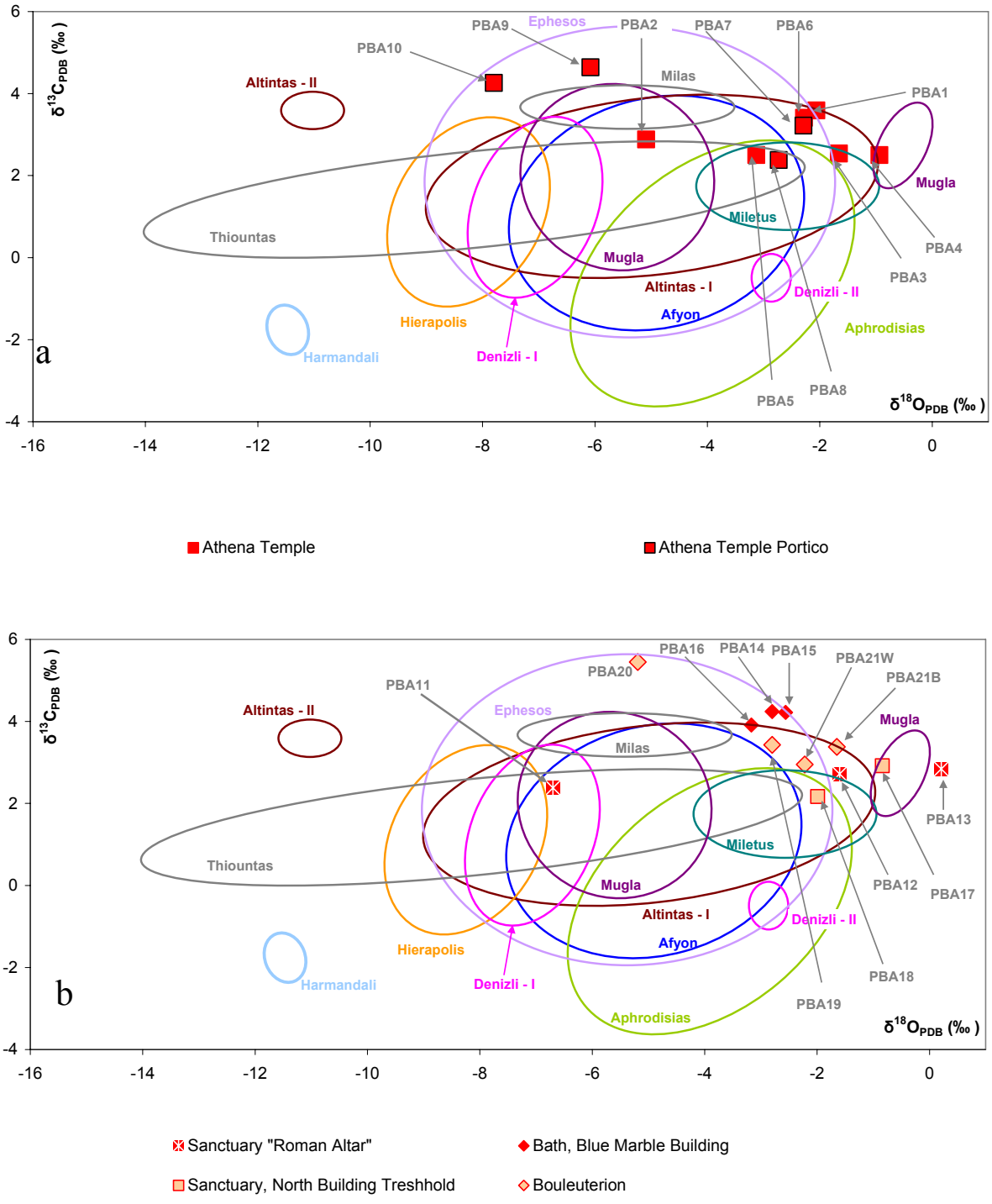

Figure 91: Data set of $\delta^{13}C$ vs. $\delta^{18}O$ isotopic compositions (in ‰, relative to PDB) from the Hellenistic Period in Troia compared with the data set of marbles from Middle and Southwest Anatolia.

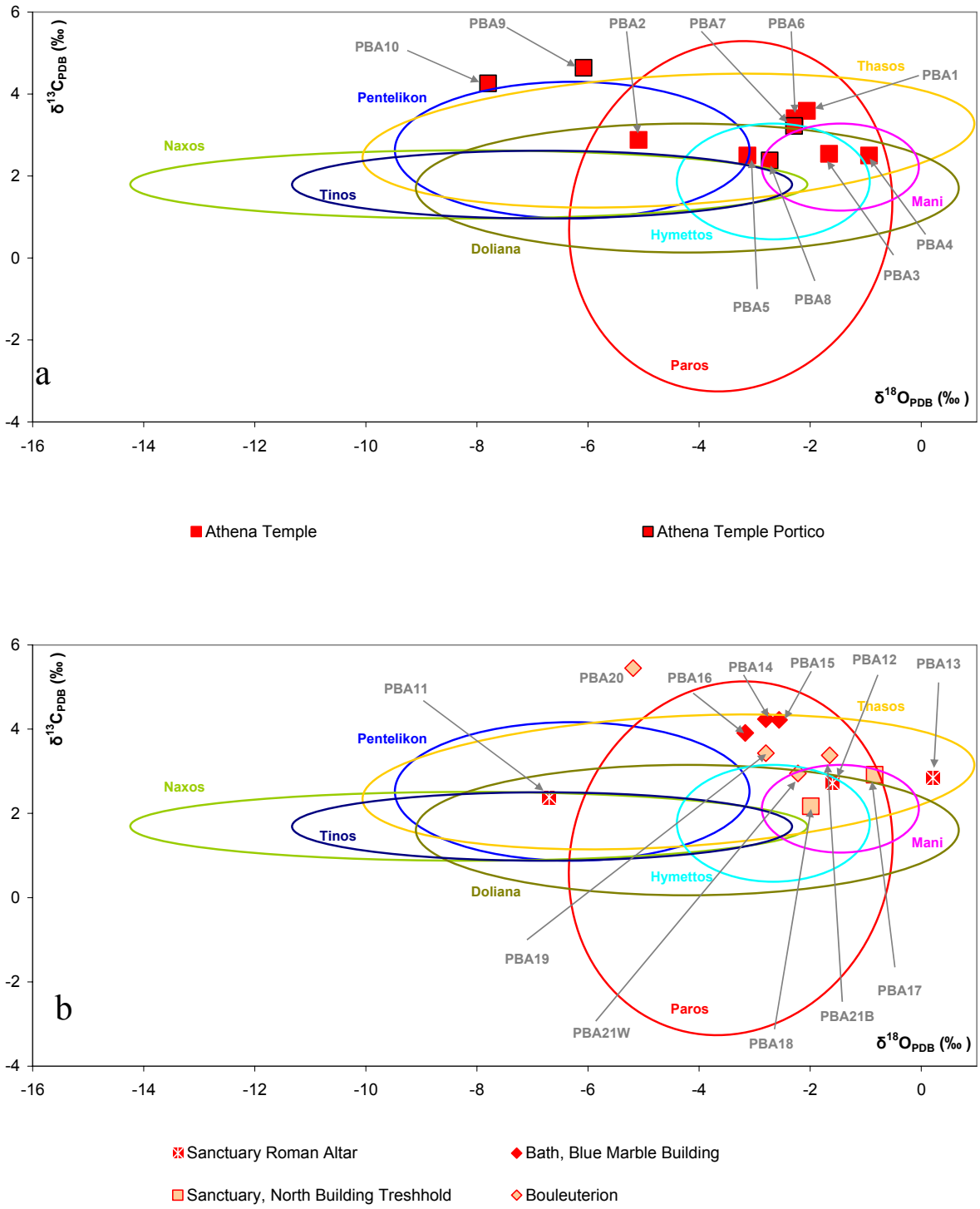

Figure 92: Data set of $\delta^{13}C$ vs. $\delta^{18}O$ isotopic compositions (in ‰, relative to PDB) from the Hellenistic Period in Troia compared with the data set of marbles from Greece.

12.1.4.3. Roman marbles

Based on the stable isotope ratios, the raw material of the ***Children of Claudius Inscription*** (PBA22) can stem from Marmara in Northwest Anatolia (Figure 93), Miletus, Aphrodisias, Hymettus, Ephesos in Middle and Southwest Anatolia (Figure 94), or Paros, Thasos, Doliana, Hymettus and Mani in Greece (Figure 95).

All of the raw materials of the ***Odeion***, the architectural elements as well as the columns, show similar stable isotopic ratios. The raw material could have originated from the quarries Marmara, maybe Serhat, Ayazma, Altınoluk or Orhangazi in Northwest Anatolia (Figure 93), Miletus, Aphrodisias, Ephesos, Altintas and Afyon in Middle and Southwest Anatolia (Figure 94), or Paros, Thasos, Hymettus, Doliana, Mani and maybe Pentelikon from Greece (Figure 95).

It seems that the material of the different architectural phases of the Bath, especially for the ***Nympheum base moulding*** and the ***moulding,*** were transported from different quarries. The samples from the Nympheum base moulding (PBA30 and PBA31) show similar stable isotopic ratios; the high $\delta^{13}C$ values (up to 5.45 ‰) are remarkable. Ephesos in Southwest Anatolia (Figure 94) and maybe Paros in Greece (Figure 95) can be considered as areas of provenance, while there are no quarries with such high $\delta^{13}C$ values in the Troad and neighbourhood areas (Figure 93). For the construction of the base moulding of the Bath, materials from new quarries were used (at least partly, based on the stable isotopic ratio analysis). The samples PBA33 and PBA34 make up a small uniform group. These samples have relatively high $\delta^{13}C$ values (3.09 to 3.23 ‰) and unusual negative $\delta^{18}O$ values (-10.92 to -11.2 ‰) for marbles from the Eastern Mediterranean Region. As provenance, Karabiga and Bergaz in Northwest Anatolia (Figure 93) and Altintas in Middle Anatolia (Figure 94) come into consideration. PBA32 has stable isotopic ratios similar to the marbles from Marmara, maybe Orhangazi or Mustafa Kemalpasa (in Northwest Anatolia, Figure 93), Altintas or Ephesos (in Middle and Southwest Anatolia, Figure 94) and Thasos or Paros, maybe Hymettus, Mani and Doliana (in Greece, Figure 95).

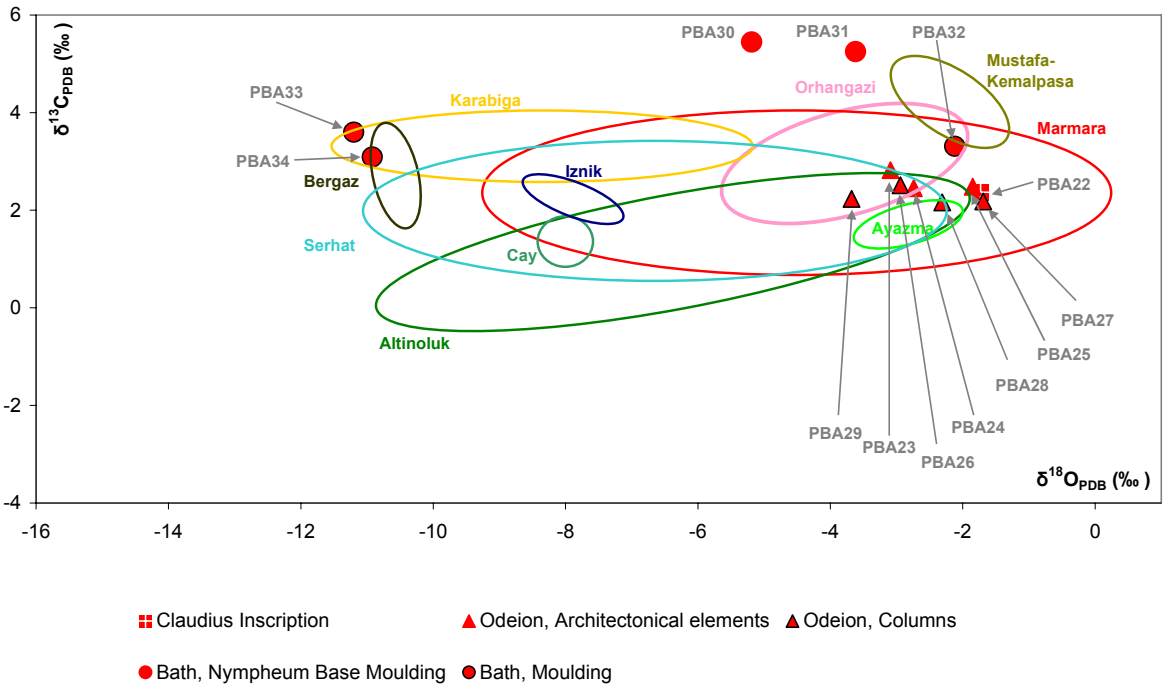

Figure 93: Data set of $\delta^{13}C$ vs. $\delta^{18}O$ isotopic compositions (in ‰, relative to PDB) from the Roman period in Troia compared with the Troad and neighbouring areas.

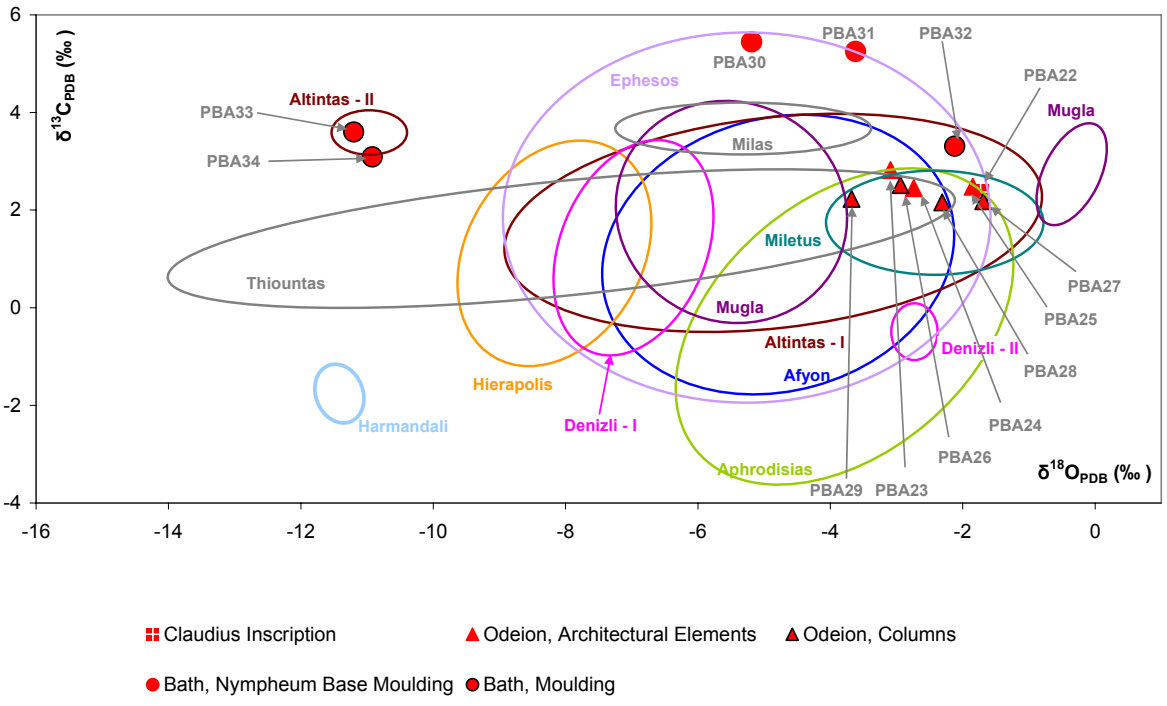

Figure 94: Data set of $\delta^{13}C$ vs. $\delta^{18}O$ isotopic compositions (in ‰, relative to PDB) from the Roman period in Troia compared with the data set of marbles from Middle and Southwest Anatolia.

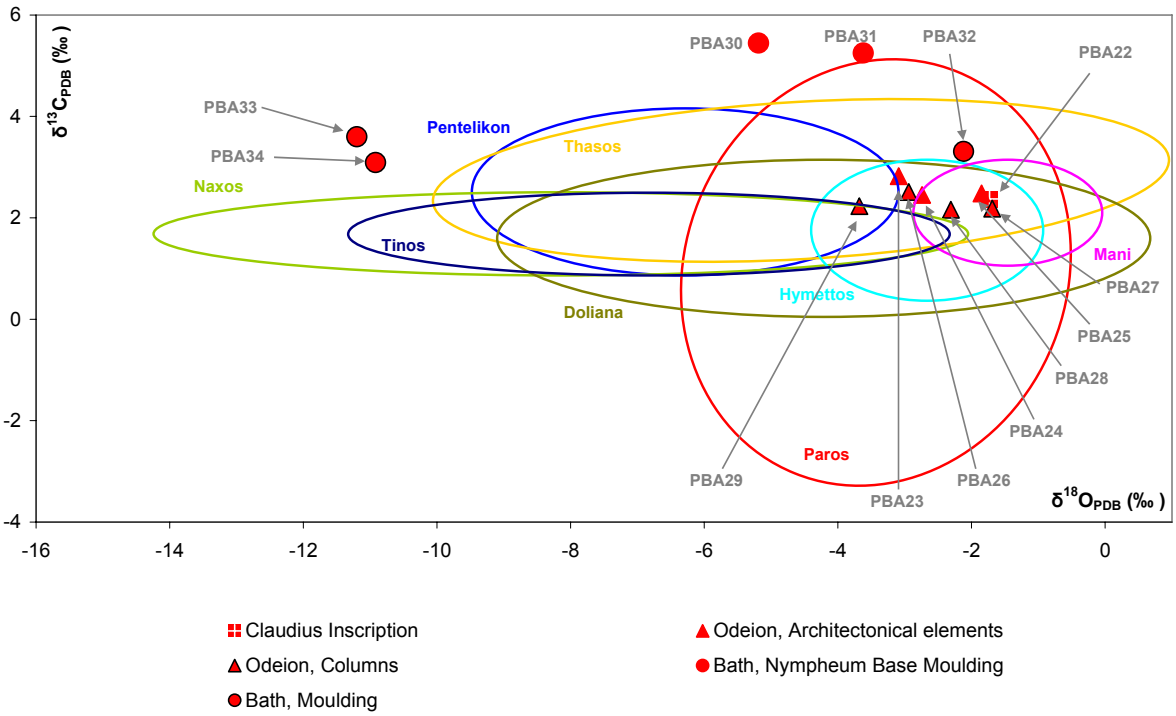

Figure 95: Data set of $\delta^{13}C$ vs. $\delta^{18}O$ isotopic compositions (in ‰, relative to PDB) from the Roman period in Troia compared with the data set of marbles from Greece.

12.2. $^{87}Sr/^{86}Sr$ isotope studies

12.2.1. Anatolian marbles

$^{87}Sr/^{86}Sr$ isotopic measurements were carried out on Anatolian marbles, especially on samples from Orhangazi, Karabiga, Marmara, North-Kazdağ Region, Altınoluk, Muğla and Milas. There were no comparative data previously available for these quarries. Marbles from the quarries Aphrodisias and Afyon were measured within the framework of this study and comparative data were available as well (BRILLI *et al.* 2005). The results were compared with the already published $^{87}Sr/^{86}Sr$ values of Greek and other marble occurrences used in Antiquity (PENTIA *et al.* 2002; BRILLI *et al.* 2005). *Appendix D.5* provides the full list of all $^{87}Sr/^{86}Sr$ ratios measured in the course of this study.

The $^{87}Sr/^{86}Sr$ isotopic ratios of the marble occurrences from Anatolia and Greece are presented in the box plot diagrams in Figure 96. Examining only the minimum and maximum values of the single quarries, one could conclude that these quarries strongly overlap. On the contrary, when we examine the same values using box plot diagrams, the differences are obvious immediately. This statistical method helps determine typical characteristics that describe the occurrences and the distinguishing power between the occurrences. Rocks reflect characteristic values typical for the occurrences, shown by 50 % boxes. Bigger boxes reflecting wider distributions are found in the case of Marmara and Karabiga. Smaller boxes, i.e. smaller spread, are found for Muğla, Aphrodisias and Afyon. The clear skew in the group-internal distributions of the quarries from almost all Anatolian marbles is remarkable. Exceptions would be Altınoluk and Muğla, from where, however, only a small number of suitable data was available for these quarries. The statistical evaluation resulted in proving that Aphrodisias marbles are the only outliers and extreme values only occurred for Afyon marbles. Furthermore, it is remarkable that the quarries north of the Izmir-Ankara-Suture show a very inhomogeneous picture. The quarries in this region are characterised by clear differences regarding the $^{87}Sr/^{86}Sr$ values of the single quarries. This is probably caused by the complex geologic history of the region. Karabiga samples show special behaviour with $^{87}Sr/^{86}Sr$ ratios between 0.705536 and 0.706651.

Generally, a trend can be recognised that the scattering of $^{87}Sr/^{86}Sr$ ratios of the Greek marbles is somewhat smaller than that of the Anatolian marbles (Figure 97). Comparing them to the ratios of the Anatolian marbles, it is obvious that skewness is lower, so the distribution is more similar to a normal distribution.

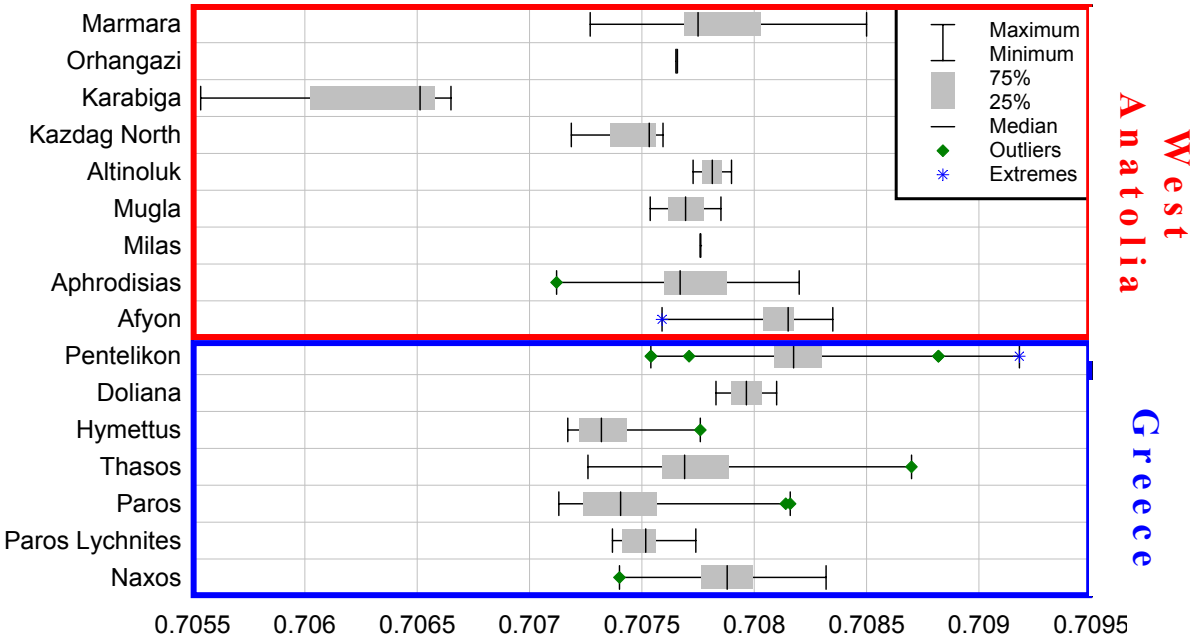

Figure 96: Distribution of the $^{87}Sr/^{86}Sr$ ratios of marbles from West Anatolia and Greece including data from BRILLI *et al.* (2005) and PENTIA *et al.* (2002).

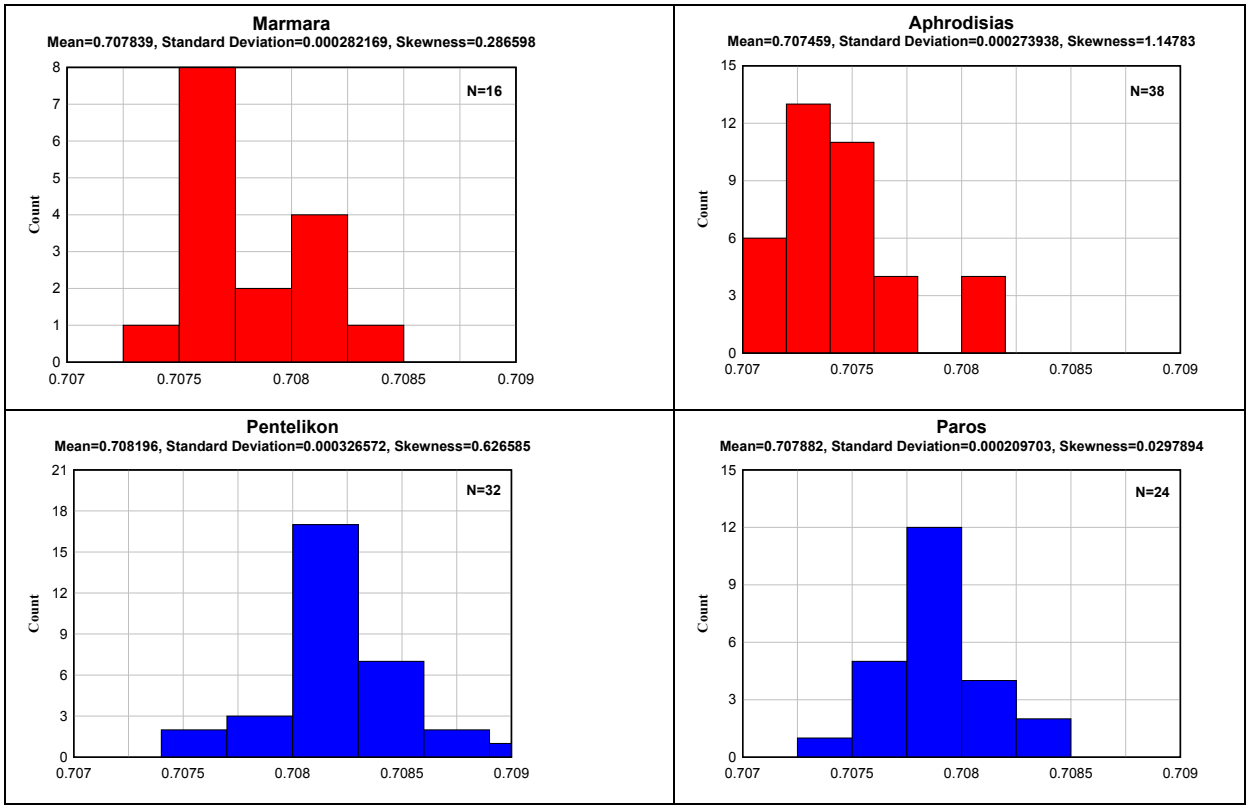

Figure 97: Distribution of the $^{87}Sr/^{86}Sr$ isotopic ratios within the quarries Marmara and Aphrodisias form West Anatolia; and Pentelikon and Paros form Greece including data from BRILLI *et al.* (2005) and PENTIA *et al.* (2002).

Figure 98 shows the $^{87}Sr/^{86}Sr$ ratios of marbles worldwide compared with the data from the Eastern Mediterranean Region (Anatolia and Greece). Generally, the occurrences from the

Eastern Alps and Iberian Peninsula have higher $^{87}Sr/^{86}Sr$ ratios, with the exception of the Wölz Complex in Austria and Macael in Spain. However, the marbles from the Indian Subcontinent generally have lower $^{87}Sr/^{86}Sr$ ratios than all other known marble quarries. Even if the marble occurrences of the Alps, Iberian Peninsula or other quarries far away form Troia were not relevant in this study, I would like to turn the attention to the powerful tool, studying provenance using $^{87}Sr/^{86}Sr$ ratios of an archaeological or art historical objects treasured in museums or private collections with unknown or assumed origin.

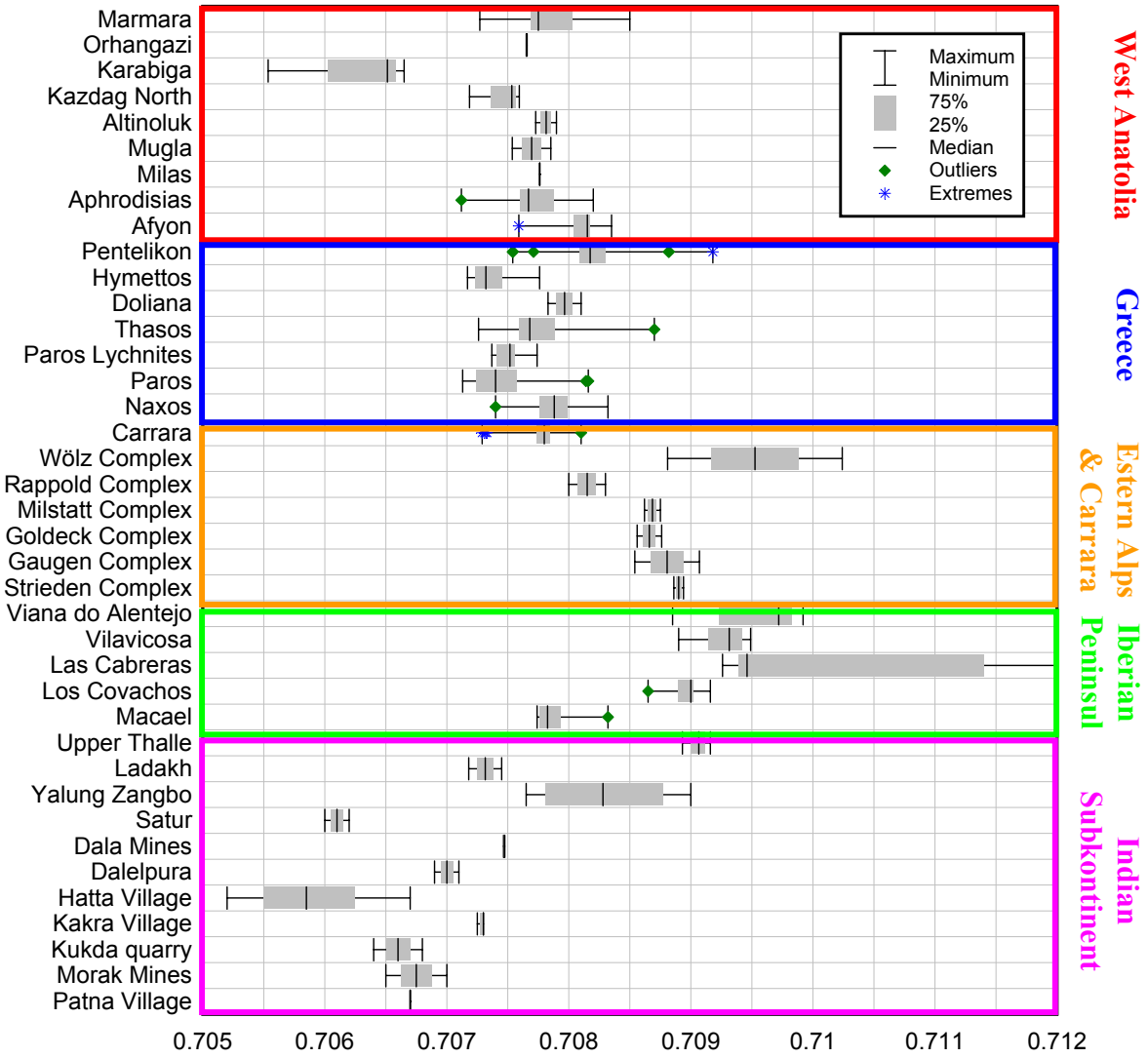

Figure 98: Distribution of the $^{87}Sr/^{86}Sr$ ratios of the marbles worldwide including data measured in the framework of this study and from various authors (KUMAR *et al.* 2002; PENTIA *et al.* 2002; ZÖLDFÖLDI & SATIR 2003; BRILLI *et al.* 2005; SCHUSTER *et al.* 2005b; LIU *et al.* 2006; MORBIDELLI *et al.* 2007).

12.2.2. Trojan marbles

12.2.2.1. Hellenistic marbles

The $^{87}Sr/^{86}Sr$ isotopic ratios of the Hellenistic marble building stones from Troia have shown, that most of the samples have similar Sr-isotopic ratios (PBA8, PBA18, PBA19 and PBA21;

Figure 99) with the exception of PBA9, which has different values ($^{87}Sr/^{86}Sr$ = 0.707253±0.000006).

Comparing the $^{87}Sr/^{86}Sr$ ratios of the Hellenistic marbles to the isotopic ratios of the marble occurrences of the Eastern Mediterranean, the probable provenance of the samples PBA8, PBA18 and PBA21 could be Marmara, Orhangazi, Muğla, Aphrodisias, and Thasos. PBA19 could originate from Paros or Kazdağ-North. PBA9 has much lower $^{87}Sr/^{86}Sr$ isotopic ratios and may have been transported from Paros or Hymettus.

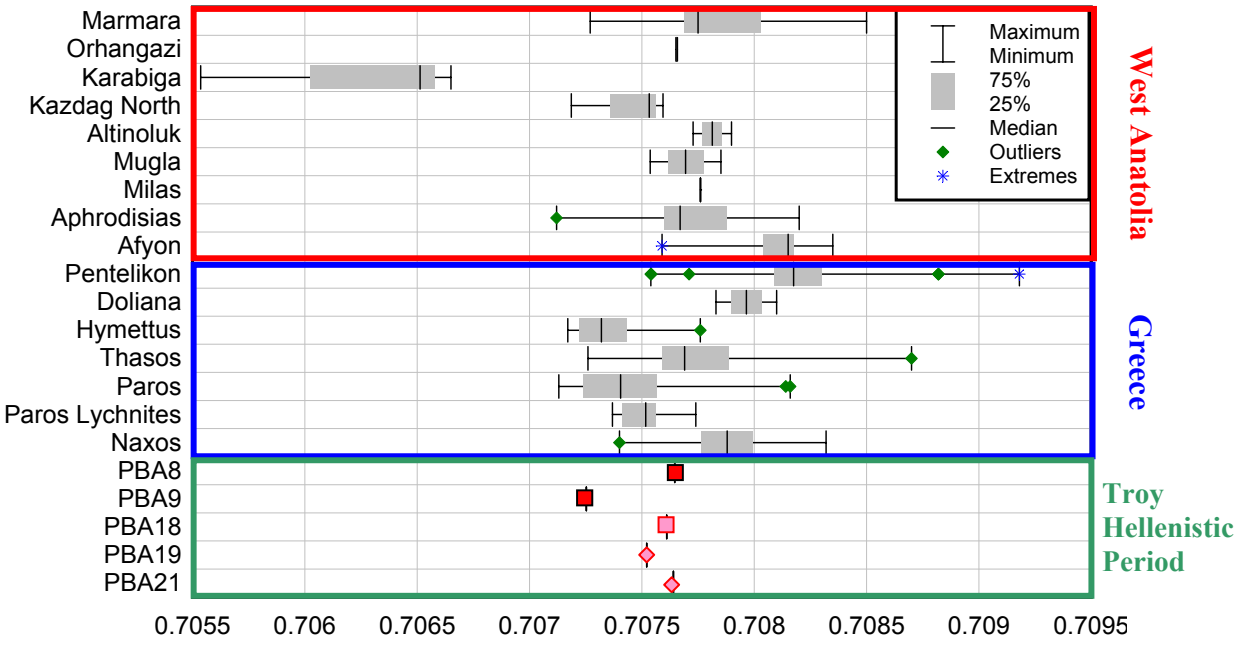

Figure 99: $^{87}Sr/^{86}Sr$ isotopic ratios of archaeological samples of the Hellenistic Period of Troia compared to those from Anatolia and Greece (including data from PENTIA *et al.* 2002; ZÖLDFÖLDI & SATIR 2003; BRILLI *et al.* 2005).

12.2.2.2. Roman marbles

The $^{87}Sr/^{86}Sr$ isotopic ratios of the Roman marble building stones from Troia show that the majority of the samples (PBA22, PBA24, PBA26, PBA30 and PBA32) have similar $^{87}Sr/^{86}Sr$ ratios (Figure 100), while sample PBA33 has considerably lower values (0.706802 ± 0.000008). A comparison of the $^{87}Sr/^{86}Sr$ ratios of the Hellenistic marbles with the isotopic ratios of marble occurrences of the Eastern Mediterranean suggests that the probable provenance of the samples PBA22, PBA24, PBA26, PBA30 and PBA32 could be Marmara, Orhangazi, Muğla, Aphrodisias, and Thasos. Such low values, as in the case of the sample PBA33, are generally not known for the marbles of the Eastern Mediterranean Region except

for the marbles from Karabiga. In this case, we can conclude that the raw material probably came from Karabiga.

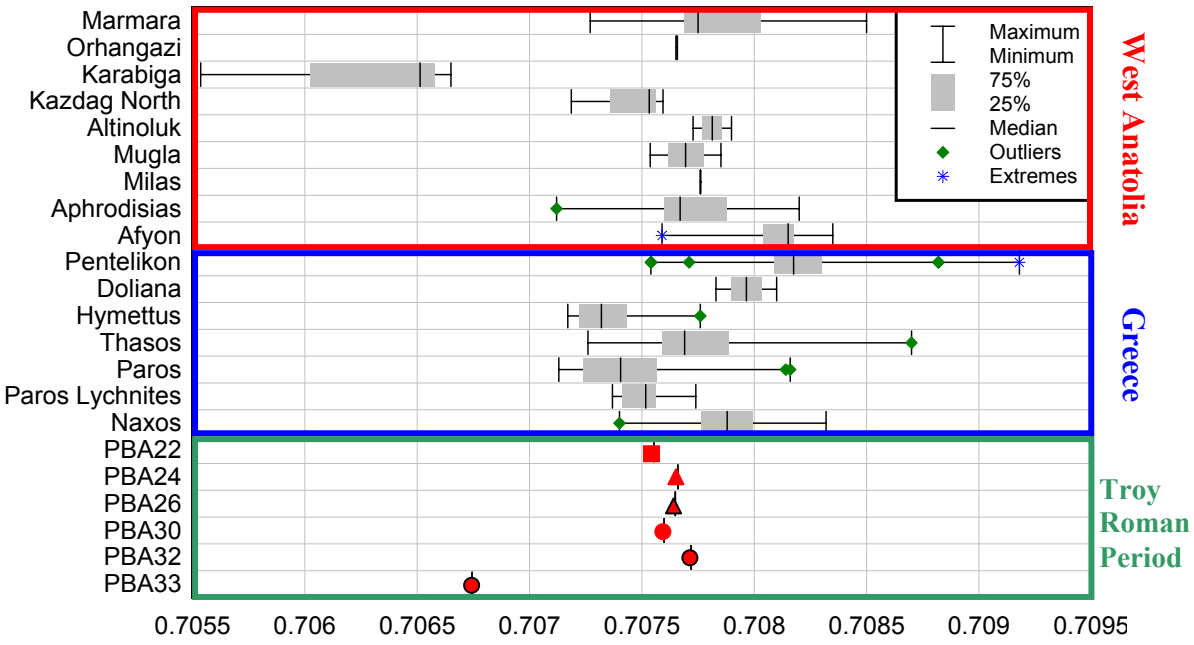

Figure 100: $^{87}Sr/^{86}Sr$ isotopic ratios of archaeological samples of the Roman Period of Troia compared with those from Anatolia and Greece (including data from PENTIA *et al.* 2002; ZÖLDFÖLDI & SATIR 2003; BRILLI *et al.* 2005).

12.3. Trivariate assignment method of the isotopic investigation

To answer the provenance question, and get more reliable information of the isotopic results, 3D diagrams were constructed. The trivariate assignment methods using isotopic signatures ($^{87}Sr/^{86}Sr$, $\delta^{13}C$ and $\delta^{18}O$) of Anatolian, Greek and Trojan marbles was used in this study to establish their provenance among of bivariate plots ($\delta^{13}C$, $\delta^{18}O$). Comparing the two methods, the trivariate method allows a better selectivity and a much more secure assignment of provenance. The major difficulty of the trivariate method is the scarcity of data in the literature, where all three isotopic values are published on the very same sample (e.g., PENTIA *et al.* 2002; ZÖLDFÖLDI & SATIR 2003; MORBIDELLI *et al.* 2007). Altogether, the isotopic signature of 122 marbles can be used for these trivariate diagrams, including the 36 samples from Anatolia that were investigated in this study. However, I have to emphasize again that the most important advantage of this combination is the very small amount of the sample that is needed for investigation.

12.3.1. Anatolian marbles in comparison to other Mediterranean marbles

Significant differences can be observed using the 3D diagrams ($^{87}Sr/^{86}Sr$, $\delta^{13}C$ and $\delta^{18}O$) of the marbles in the Eastern Mediterranean Region (Figure 101). One of the most valuable results of this plot is that the marbles within a specific geological unit can be distinguished, such as the marbles from the Kazdağ Range. Also the marbles from Marmara, Aphrodisias, Pentelikon and Hymettus, which overlap in the bivariate diagrams ($\delta^{13}C$ and $\delta^{18}O$) can be distinguish with high plausibility. On the other hand, the marbles from Marmara and Thasos cannot be distinguished with certainty.

An unambiguous differentiation can be made when the isotopic signature of the Eastern Mediterranean marbles to those of the Iberian Peninsula are compared (Figure 102), with the exception of the marbles from Macael, Spain. Furthermore, marbles of Marmara, Hymettus, and Pentelikon are distinguishable from the marbles of Carrara, although the stable isotopic values ($\delta^{13}C$ and $\delta^{18}O$) of these quarries overlap significantly. Trivariate diagrams using $^{87}Sr/^{86}Sr$, $\delta^{13}C$ and $\delta^{18}O$ seem to be very promising; therefore they will be used in the provenance determination of the Trojan marbles in the next section.

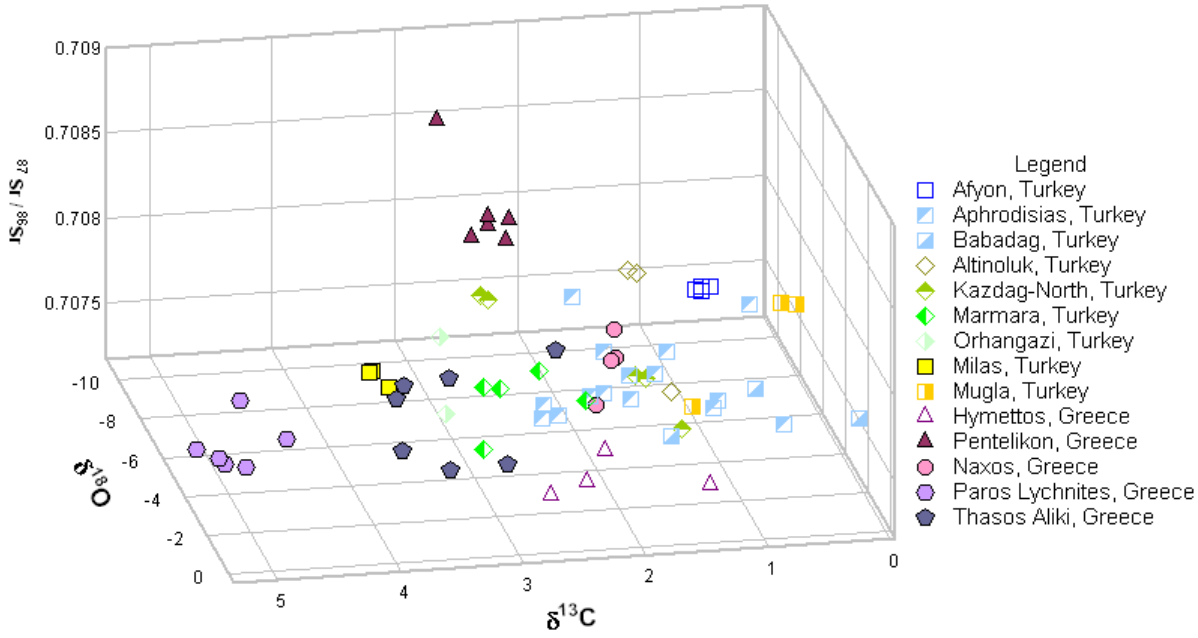

Figure 101: Trivariate assignment methods using isotopic signatures ($^{87}Sr/^{86}Sr$, $\delta^{13}C$, $\delta^{18}O$) of Anatolian and Greek marbles (including data from PENTIA *et al.* 2002).

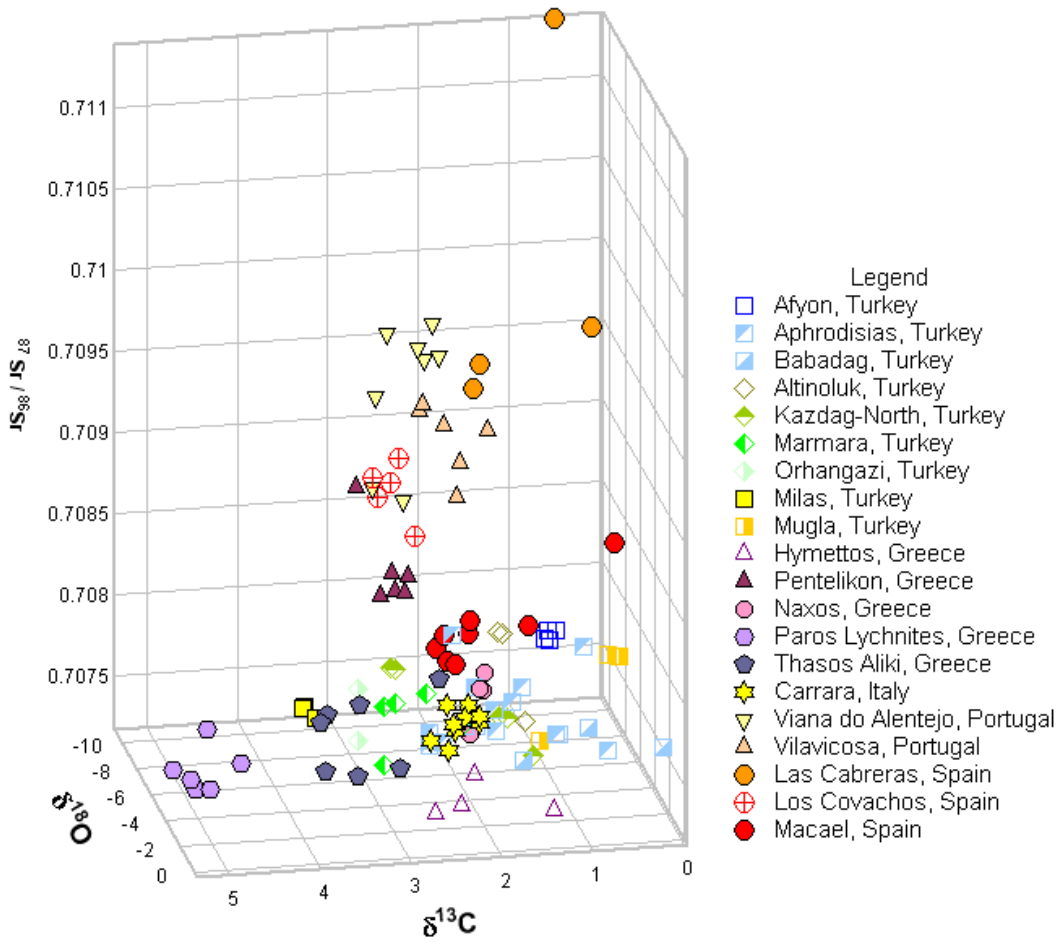

Figure 102: Trivariate assignment methods using isotopic signatures ($^{87}Sr/^{86}Sr$, $\delta^{13}C$, $\delta^{18}O$) of Anatolian, Greek and other Mediterranean marbles (including data from PENTIA *et al.* 2002; MORBIDELLI *et al.* 2007).

12.3.2. Trojan marbles

12.3.2.1. Hellenistic marbles

Combining the results of oxygen, carbon and strontium isotopic measurements ($^{87}Sr/^{86}Sr$, $\delta^{13}C$ and $\delta^{18}O$) of the Trojan archaeological objects with the 3D diagrams, I concluded that sample PBA9 has to originate from Paros (Greece). Furthermore, the samples PBA8, PBA18, PBA21 should originate from Marmara. However, the raw material of PBA19 must have been quarried in Thasos.

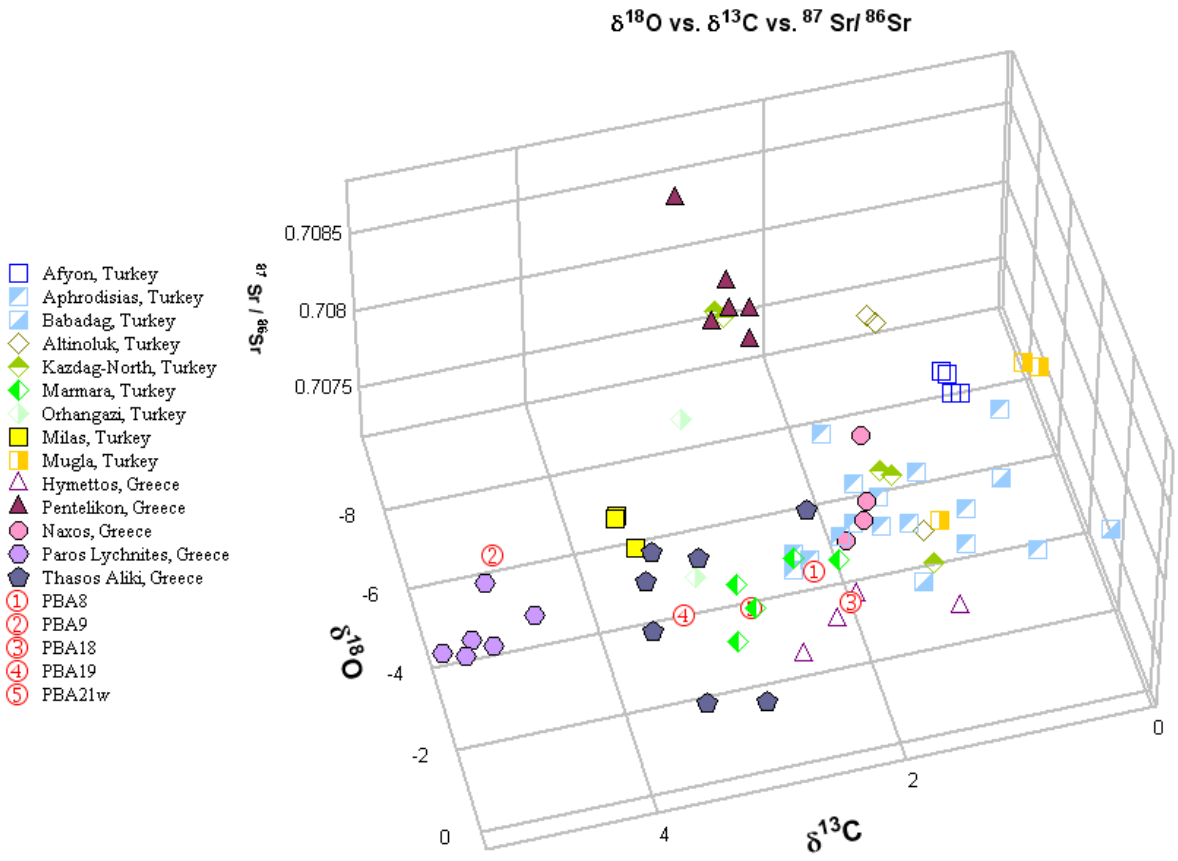

Figure 103: Trivariate method using $\delta^{13}C$, $\delta^{18}O$ und $^{87}Sr/^{86}Sr$ isotopic results. The red numbers represent the marble objects of the Hellenistic period of Troia.

12.3.2.2. Roman marbles

Combining the results of oxygen, carbon and strontium isotopic measurements ($^{87}Sr/^{86}Sr$, $\delta^{13}C$ and $\delta^{18}O$) of the Trojan archaeological objects with the 3D diagrams, I reached the conclusion that sample PBA30 stems from Paros (Greece), and sample PBA33 derives from Karabiga. The samples PBA24 and PBA26 seem to have the very same raw material and probably originate from Marmara. The raw material of the sample PBA22 is similar to that of the samples PBA24 and PBA26, and the origin from Marmara is the most probable. On the other hand, sample PBA32 falls within the range of Thasos, however, due to the partial overlap, the possibility that this material originated from Marmara cannot be excluded.

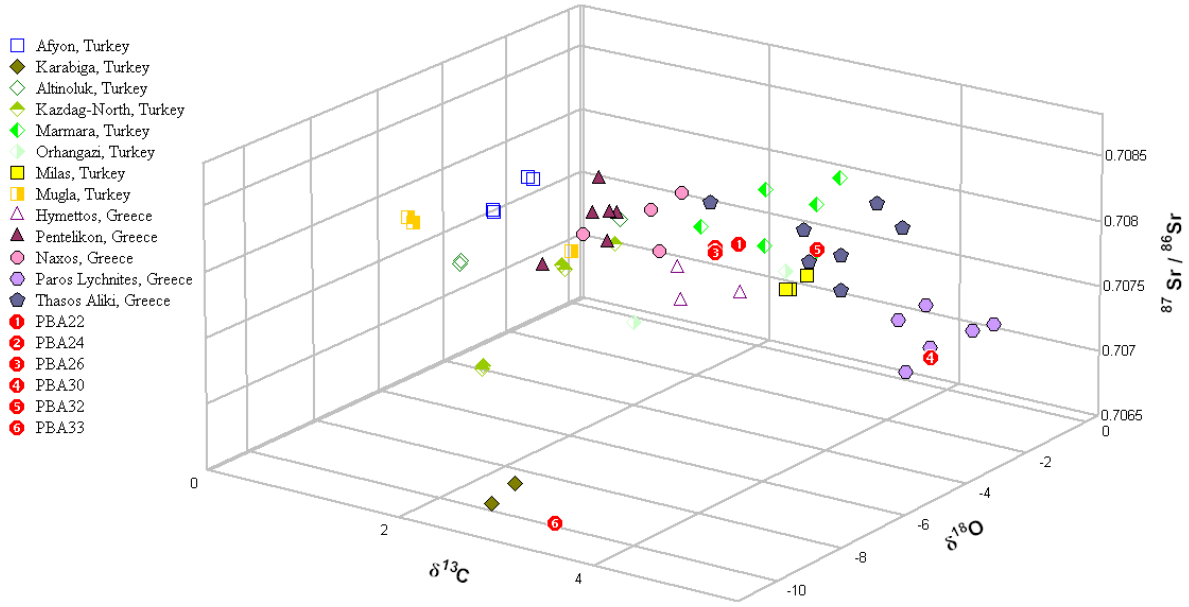

Figure 104: Trivariate method using $\delta^{13}C$, $\delta^{18}O$ und $^{87}Sr/^{86}Sr$ isotopic results. The red numbers represent the marble objects of the Roman period of Troia.

13. MissMarble: Measurement and Information System of Samples of Marble

The multitude of raw materials and the numerous techniques that have been applied in this study initialised the development of the MissMarble database. The aim of this project was to develop a scientific and technological interdisciplinary and easily accessible data base management system with user friendly interfaces for data entry, quality control, storage, continuous dissemination, and exchange. This is needed to develop innovative, efficient and practical ways of processing, archiving, and disseminating the large volume of data. MissMarble was developed by the author of this thesis and two colleagues, Péter Hegedűs and Balázs Székely (ZÖLDFÖLDI *et al.* 2008, see also *Appendix C*). **All the data generated in the course of this work have been added and are available online in the MissMarble database (**www.missmarble.de**).**

The database aims to characterise historic and recent marble quarries, as well archaeological and art historical marble objects, and makes the information available to all other people involved in the field of archaeometric research and preservation of marble artifacts. We have developed a software solution based on client/server architecture. The server-side engine can be installed both on Windows and Linux systems, while the client software is Windows-based. The client software connects to the server via Internet connection.

The data content of the database follows the principles previously laid down. Beside the sample description (geographic location and catalogue data) the database includes information on colour and fabric, physical properties, chemical composition, mineralogical composition (both macroscopic and instrumental), isotopic data, and textural analyses like fractal analytical and quantitative textural properties, etc. Most of these properties are suitable as filtering criteria to provide query tools and data grouping possibilities. Furthermore, a sophisticated geographical hierarchy is defined in the system, so the samples can be organised into a logical geographic context as well.

PART V

INTERPRETATION AND DISCUSSION

By collecting data and investigating samples from Western Anatolian marble quarries that, until now, did not come into consideration in archaeometric research, an immediate need of data integration emerged. The application of traditional and less common methods on this sample set showed the mosaic-like character of the existing results measured on classic marbles. By integrating the available and newly acquired data, the decision on possible provenance of analysed Trojan artifacts gradually became feasable. The first object of which the provenance could be identified was the Bronze Age Trojan vessel (D3/449) based on a sequence of measurements, including isotopic and chemical analyses. However, this scheme was not satisfying in the case of marble knob (A8/491). Thus, as other authors previously suggested, the combination of various, preselected methods might not fulfill the requirements. Proceeding with other samples parallel to Trojan and West Anatolian marble samples, a logical sequence of measurements was formulated. In this scheme, some samples showed that the final decision could not be achieved, because the real source of origin was not yet identified. This fact motivated me to follow this research direction. Subsequently to the determination of the provenance of the primary objects, the scheme was further developed.

At this stage, I have arrived at a very critical point, namely, how to interpret the multiple investigations and results. In the subsequent chapters, beside an interpretation of the results, I present a combination of techniques that can be applied to distinguish West Anatolian marbles from different quarries.

As the results from the previously presented analyses show, the grouping of samples from West Anatolian marbles (taken from antique and recent quarries) and Trojan marbles (samples of archaeological objects) is possible if a combined technique based on macroscopic and microscopic investigation, quantitative textural analyses, chemical analyses, cathodoluminescence microscopy and stable and radiogenic isotope geochemistry is used. None of these methods alone can distinguish the marbles from different quarries; a combination of several methods is needed in order to reasonably determine the provenance.

In order to define a standard way to proceed with artifacts, a decision tree was created. A decision tree is a decision support tool that uses a tree-like graph or model of decisions and their possible consequences, including utility. Decision trees are commonly used in operations research, specifically in decision analysis, to help identify a strategy most likely to reach a goal. Amongst decision support tools, decision trees have several advantages: (i) Decision trees are simple to understand and interpret. People are able to understand decision tree models after a brief explanation. (ii) They have value even with little hard data. Important insights can be generated based on experts describing a situation (its alternatives, probabilities) and their preferences for outcomes. (iii) Decision trees use a white box model. White box is - in contrast to a black box - a subsystem whose internals can be viewed. This is useful during testing, where a system is examined to make sure that it fulfils its requirements. If a model provides a given result, the explanation for the result is easily replicated.

14. Distinguishing Anatolian marbles

14.1. Distinguishing Anatolian marbles – if powder samples are available for investigation

Figure 105 shows the decision tree for distinguishing Anatolian marbles – if powder samples are available for investigations. This decision tree consists of six decision levels – 6 phases. In ***Phase I,*** the marble samples from various quarries were grouped based on their $\delta^{18}O_{PDB}$ values. Two main groups can be distinguished. Group "A" includes the quarries Altınoluk [ALT], Bergaz [BRG], Yenice [YEN], Karabiga [KB], Cay [CAY], Iznik [IZN], Hierapolis [HP], Denizli [DEN], Thiountas [THI], Altintas-II [ATS-II] and some samples from Marmara-Aksoy [MRM-Aksoy]. Group "B" consist of marbles from Marmara [MRM], Orhangazi [ORH], Serhat [SRH], Altınoluk [ALT], Yenice [YEN], Ayazma [AYA], Mustafa Kemalpasa [MKP], Afyon [AFY], Muğla [MGL], Babadağ [BBD], Milas [MLS], Miletus [MLT], Ephesos [EPH] and Altintas-I [ATS-I].

In ***Phase II,*** $\delta^{13}C_{PDB}$ values were considered and can be used to refine the groups. This information separates group "**A**" into three subgroups: "**A1"** is composed of marbles from Altınoluk [ALT], Hierapolis [HP] and Denizli [DEN] with $\delta^{13}C_{PDB}$ values lower than 1 ‰. Group "**A2**" – characterised by $\delta^{13}C_{PDB}$ values between 1‰ and 3‰ – includes the majority of the quarries of group "**A**", as well as marbles from Altınoluk [ALT], Bergaz [BRG], Yenice [YEN], Cay [CAY], Iznik [IZN] and Thiountas [THI]. However, some samples from

Hierapolis [HP] and Denizli [DEN], primarily assigned to group "**A1**", also fall into this group ("**A2**"). Group "**A3**" includes marbles with $\delta^{13}C_{PDB}$ values higher than 3 ‰. It includes marbles from Bergaz [BRG], Karabiga [KB], and Altintas-II [ATS-II]. In the other branch, $\delta^{13}C_{PDB}$ values again separate three groups: Group "**B1**" ($\delta^{13}C_{PDB}$ values higher than 4 ‰) consists of marbles from Mustafa Kemalpasa [MKP] and Ephesos [EPH]. Group "**B2**" characterised by $\delta^{13}C_{PDB}$ values between 0 ‰ and 4 ‰, includes many quarries: Marmara [MRM], Orhangazi [ORH], Serhat [SRH], Altınoluk [ALT], Yenice [YEN], Ayazma [AYA], Afyon [AFY], Muğla [MGL], Babadağ [BBD], Milas [MLS], Miletus [MLT], Ephesos [EPH] and Altintas-I [ATS-I]. Group "**B3**" includes marbles with $\delta^{13}C_{PDB}$ values lower than 0 ‰; they are from Altintas-I [ATS-I], Afyon [AFY], Ephesos [EPH], Denizli [DEN] and Babadağ [BBD]. I have to emphasize that in this phase some overlapping occurs, e.g., marbles from Ephesos can fall into all three categories: Samples from Altintas [ATS-I], Babadağ [BBD], Afyon [AFY], Ephesos [EPH] and Denizli [DEN] fall into two groups, "**B2**" and "**B3**".

The next decision level – ***Phase III*** is based on strontium isotopic results. $^{87}Sr/^{86}Sr$ ratios separate Bergaz [BRG], Yenice [YEN] and Cay [CAY] ($^{87}Sr/^{86}Sr < 0.7076$, group "**A2a**") from Altınoluk [ALT], Hierapolis [HP], Denizli [DEN], Thiountas [THI], Iznik [IZN] and some samples from Marmara-Aksoy [MRM-Aksoy] ($^{87}Sr/^{86}Sr > 0.7076$, group "**A2b**"). Additionally, $^{87}Sr/^{86}Sr$ ratios separate the marbles from Karabiga [KB] ($^{87}Sr/^{86}Sr$ ratios < 0.707, group "**A3a**") from Bergaz [BRG] and Altintas-II [ATS-II] ($^{87}Sr/^{86}Sr$ ratios > 0.707, group "**A3b**"). In the other branch, "B2" can be subdivided into 3 groups based on $^{87}Sr/^{86}Sr$ ratios: Group "**B2a**" includes marbles from Ayazma [AYM], Yenice [YEN] and Serhat [SRH] with $^{87}Sr/^{86}Sr$ ratios less than 0.7076, group "**B2b**" includes marbles from many quarries, such as Marmara [MRM], Orhangazi [ORH], Altınoluk [ALT], Muğla [MGL], Babadağ [BBD], Milas [MLS], Miletus [MLT] and Ephesos [EPH]. This group ("**B2b"**) is characterised by $^{87}Sr/^{86}Sr$ ratios between 0.7076 and 0.7078. Group "**B2c**" includes marbles from Afyon [AFY] and Altintas-I [ATS-I] with $^{87}Sr/^{86}Sr$ ratios greater than 0.7078. Additionally, $^{87}Sr/^{86}Sr$ ratios separate marbles from Ephesos [EPH], Denizli [DEN] and Babadağ [BBD] ($^{87}Sr/^{86}Sr <$ 0.708; group "B3a") from marbles of Afyon [AFY] and Altintas-I [ATS-I] ($^{87}Sr/^{86}Sr >$ 0.7078; group "**B3b**").

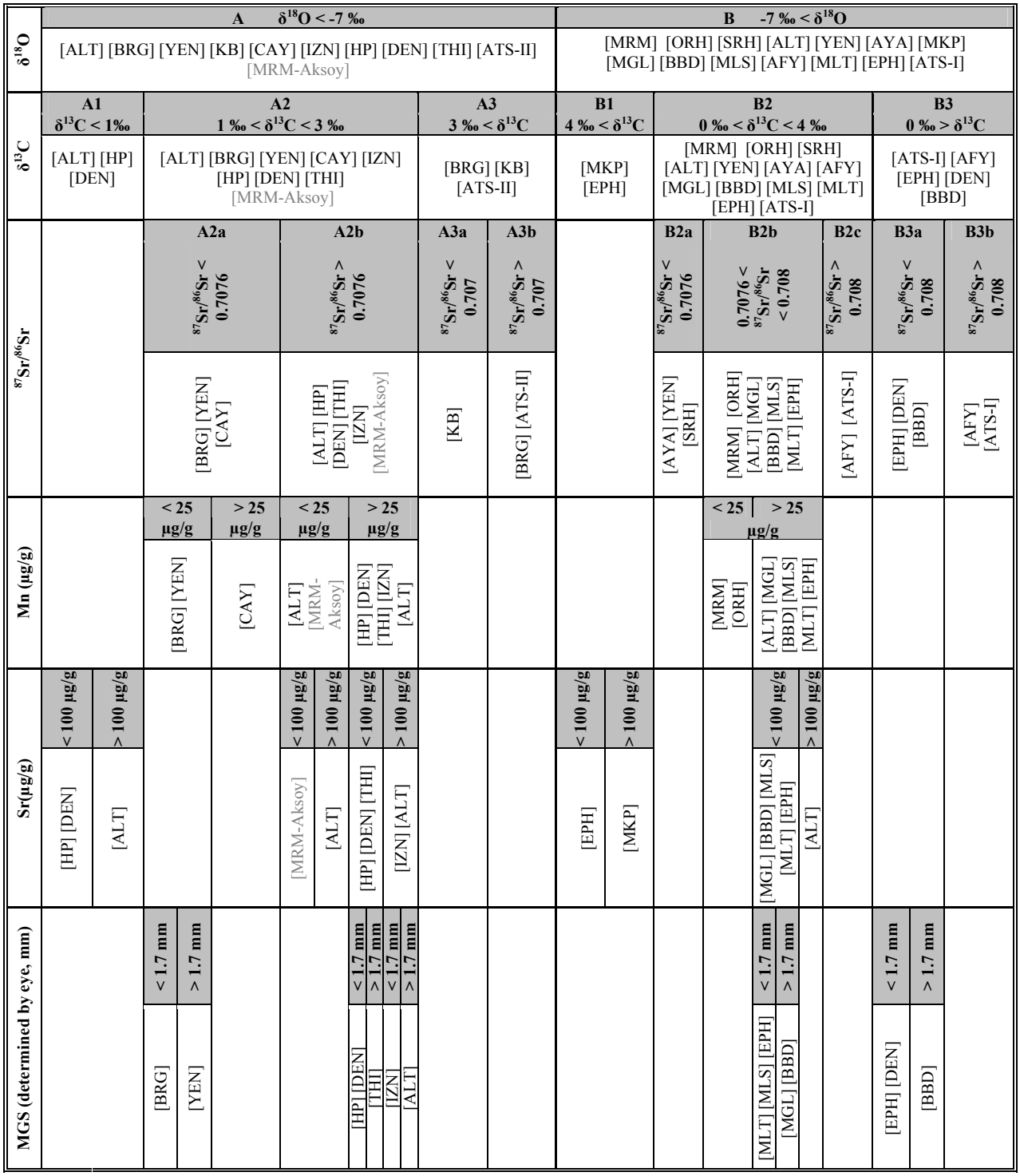

Figure 105: The decision tree consists of 6 decision levels in order to distinguish Anatolian marbles – if powder samples are available for investigation. This decision tree is based on stable isotopic investigations $\delta^{18}O$ in Phase I and $\delta^{13}C$ in Phase II, $^{87}Sr/^{86}Sr$ isotopic ratios (Phase III). Mn concentration (Phase IV) and Sr concentration (Phase V). Additionally MGS, determined by eye, were also taken into consideration (Phase VI).

The next decision level – ***Phase IV*** considers the Mn concentration of the investigated marbles. Based on this criterion, group "**A2a**" can be refined and subdivided into two clusters: Marbles from Bergaz [BRG] and Yenice [YEN] have Mn concentration less than 25 µg/g and marbles from Cay [CAY] have Mn concentration greater than 25 µg/g. Similarly, marbles from Altınoluk [ALT] and Marmara-Aksoy [MRM-Aksoy] have Mn concentration less than 25 µg/g and marbles from Hierapolis [HP], Denizli [DEN], Thiountas [THI], Iznik [IZN] and Altınoluk [ALT] have Mn concentration greater than 25 µg/g.
In the other branch, only the group "**B2b**" can be refined based on the Mn concentration. Marbles from Marmara [MRM] and Orhangazi [ORH] have Mn concentration less than 25 µg/g, while marbles from Altınoluk [ALT], Muğla [MGL], Babadağ [BBD], Milas [MLS], Miletus [MLT] and Ephesos [EPH] have Mn concentration greater than 25 µg/g.

In the next decision level – ***Phase V*** the Sr concentration of the investigated marbles are included. The group "**A1**" can be subdivided into two clusters: Marbles from Hierapolis [HP] and Denizli [DEN] have Sr concentration less than 100 µg/g, while marbles from Altınoluk have more than 100 µg/g. The subgroup of the "**A2b**" with a Mn concentration less than 25 µg/g includes marbles from Marmara-Aksoy [MRM-Aksoy] and Altınoluk [ALT]. The final decision or differentiation between the two sites can be made based on the Sr concentration. Marmara-Aksoy has Sr concentration less than 100 µg/g, while the values for the marbles from Altınoluk [ALT] are greater than 100 µg/g. Additionally, Hierapolis [HP], Denizli [DEN] and Thiountas [THI] can be separated from Iznik [IZN] and Altınoluk [ALT]; the first group has Sr concentrations less than 100 µg/g and the second group greater than 100 µg/g. In the other branch, the marbles of group "**B1**" can be separated; marbles with a Sr concentration greater than 100 µg/g originate from the quarries of Mustafa Kemalpasa [MKP] and those containing less than 100 µg/g from Ephesos [EPH]. Furthermore, Altınoluk [ALT] with Sr concentration greater than 100 µg/g reaches its final decision, while all other marbles of the subgroup have less than 100 µg/g. They are Muğla [MGL], Babadağ [BBD], Milas [MLS], Miletus [MLT] and Ephesos [EPH]. At this point, I have to mention that the marbles from different geological units have already been distinguished, even if some quarries could not reach their final decision. The quarries Thiountas, Hierapolis and Denizli are located a few kilometres apart, and the quarries Afyon [AFY] and Altintas-I [ATS-I] are also located very close to each other. Further, the quarries Muğla [MGL], Babadağ [BBD], Milas [MLS], Miletus [MLT] and Ephesos [EPH] all belong to the Menderes Massif.

To come to more decisions, the visually determined maximum grain size can be used. To do so, the grain size of the object has to be examined during sampling. The best way for this is to use a digital slide calliper measuring 10 of the putative biggest grains. This criterion can be use to further distinguish the samples and is therefore included as ***Phase VI***. In the end, Bergaz [BRG] and Yenice [YEN] can be separated; marbles from Bergaz have MGS less than 1.7 mm, while those from Yenice are greater than 1.7 mm. Similarly, marbles from Hierapolis [HP] and Denizli [DEN] have MGS less than 1.7 mm, while those from Thiountas are greater than 1.7 mm. Furthermore, marbles from Iznik [IZN] have MGS less than 1.7 mm, but the samples from Altınoluk are greater than 1.7 mm. In the other branch, the subgroup including many marbles from the Menderes Massif can be separated into two clusters: Marbles from Miletus [MLT], Milas [MLS] and Ephesos [EPH] are characterised by MGS less than 1.7 mm, and marbles from Muğla [MGL] and Babadağ [BBD] by MGS greater than 1.7 mm. Finally, the marbles from "**B3a**" group can be distinguished: Marbles from Ephesos [EPH] and Denizli [DEN] have MGS less than 1.7 mm, while marbles from Babadağ [BBD] have MGS greater than 1.7 mm.

14.2. Distinguishing Anatolian marbles – if marble fragments are available for investigation

Figure 106 shows the decision tree for distinguishing Anatolian marbles if marble chips/fragments are available for investigation. This decision tree consists of five decision levels – 5 phases. In ***Phase I,*** the marble samples from various quarries were grouped on the strength of their texture based on fractal analyses (FA). Two main groups can be distinguished: Group "**A**" includes the quarries Marmara [MRM], Orhangazi [ORH], Bandirma [BDR], Serhat [SRH], Ayazma [AYA], Bergaz [BRG], Altınoluk [ALT] and Afyon [AFY]. Group "B" includes Muğla [MGL], Babadağ [BBD], Milas [MLS], Afyon [AFY] and Ayazma [AYA]. Generally, one can say that group "**A**" principally includes marble samples of quarries belonging to the geological units north of the Izmir-Ankara-Suture (except of Afyon), while the quarries that belong to group "**B**" are primarily located south of the tectonic line (except of Ayazma).

In ***Phase II,*** the grain size analyses, especially $MGS_{99\%}$, were considered and can be used to refine the groups. This information separates group "**A**" into two subgroups: "**A1"** is composed of marbles from Bergaz [BRG] and Afyon [AFY] ($MGS_{99\%}$ < 1.6 mm) and "**A2**" is

composed of marbles from Marmara [MRM], Orhangazi [ORH], Bandirma [BDR], Serhat [SRH], Altınoluk [ALT] and Ayazma [AYA]. The samples of the group "**A2**" have $MGS_{99\%}$ greater than 1.6 mm. In the second branch, $MGS_{99\%}$ separates Milas [MLS] and Afyon [AFY] ($MGS_{99\%}$ < 2.0 mm, group "**B1"**) from Muğla [MGL], Babadağ [BBD], Ayazma [AYA] and Karabiga [KB] ($MGS_{99\%}$ > 2.0 mm, group "**B2**").

Phase I	FA	A D>1.55 and SD > 0.24													B D<1.55 and SD < 0.24										
		[MRM] [ORH] [BDR] [SRH] [ALT] [BRG] [AYM] [AFY]													[MGL] [BBD] [MLS] [AYM] [AFY] [KB]										
Phase II	$MGS_{99\%}$	A1 < 1.6 mm		A2 > 1.6 mm											B1 < 2 mm			B2 > 2 mm							
		[BRG] [AFY]		[MRM] [ORH] [BDR] [SRH] [ALT] [AYM]											[MLS] [AFY]			[MGL] [BBD] [AYA] [KB]							
Phase III	$\delta^{18}O$	A1a <-10.5	A1b >- 7	A2a -10.5<δ18O<-5.5		A2b δ18O > -5.5												B2a δ18O < - 4			B2b δ18O < - 4				
		[BRG]	[AFY]	[SRH] [ALT]		[MRM] [ORH] [AYM] [BDR] [SRH] [ALT]												[MGL] [BBD] [KB]			[BBD] [AYA]				
Phase IV	$\delta^{13}C$					δ13C< 2		2.0<δ13C<3			3<δ13C				δ13C<3		δ 13C > 3		0<δ 13C		0>δ13C		0<δ13C		0>δ13C
						[SRH] [ALT]		[AYM][ALT] [SRH] [MRM][ORH]			[MRM] [ORH]				[AFN]		[MLS] [AFY]		[BBD] [MGL] [KB]		[BBD]		[BBD] [AYA]		[BBD]
Phase V	$^{87}Sr/^{86}Sr$			< 0.7076	> 0.7077	> 0.7077	< 0.7076	< 0.7076	> 0.7076								< 0.7077	> 0.7077	> 0.7070	< 0.7070			< 0.7076	> 0.7076	
				[SRH]	[ALT]	[ALT]	[SRH]	[AYM] [SRH]	[MRM] [ORH]								[MLS]	[AFN]	[BBD] [MGL]	[KB]			[AYA]	[BBD]	

Figure 106: The decision tree consists of 5 decision levels in order to distinguish Anatolian marbles based on quantitative textural analyses (fractal analyses in Phase I and grain size analyses in Phase II), stable isotopic investigation ($\delta^{18}O$ in Phase III and $\delta^{13}C$ Phase IV) and $^{87}Sr/^{86}Sr$ isotopic ratios (Phase V).

The next decision level – ***Phase III*** is based on $\delta^{18}O$ values. Group "**A1**" is subdivided into two clusters: Group "**A1a**" includes marbles from Bergaz [BRG] that have $\delta^{18}O$ values lower than -10.5 ‰ and "**A1b**" includes marbles from Afyon [AFY] that have $\delta^{18}O$ values higher than -7 ‰. Group "**A2**" is subdivided into two clusters as well: Group "**A2a**" (-10.5 ‰ < $\delta^{18}O$ < -5.5 ‰) includes marbles from Serhat and Altınoluk and group "**A2b**" ($\delta^{18}O$ > -5.5 ‰) includes marbles from Marmara [MRM], Orhangazi [ORH], Bandirma [BDR], Altınoluk [ALT], Ayazma [AYA] and Serhat [SRH]. The other branch of the decision tree, group "**B2**" can be subdivided into two groups: "**B2a**" includes marbles that have $\delta^{18}O$ values lower than 4 ‰, such as the samples from Muğla [MGL] and Karabiga [KB] and group "**B2b**" contains marbles that have $\delta^{18}O$ values higher than -4 ‰. Ayazma [AYA]. Marbles from Babadağ [BBD] overlap both groups.

In the next decision level – ***Phase IV*** – the $\delta^{13}C$ values were taken into consideration. This criterion subdivides group "**A2b**" into three clusters: Serhat [SRH] and Altınoluk [ALT] belong together into the group that has $\delta^{13}C$ values less than 2 ‰. If the $\delta^{13}C$ values are higher than 3 ‰, the marble quarries Marmara [MRM] and Orhangazi [ORH] can be separated. However, many samples belong to the third group (2 ‰ < $\delta^{13}C$ < 3 ‰), Ayazma [AYA], Altınoluk [ALT], Serhat [SRH], Marmara [MRM] and Orhangazi [ORH], and so there is some overlap between the groups. The other branch can be partially subdivided. Group "**B1**" is divided into two groups: If $\delta^{13}C$ is less than 3 ‰, most of the Afyon marbles reach their final decision. On the other hand, if $\delta^{13}C$ is more than 3 ‰, a final decision based on the stable isotopic investigation is not possible. Similar to this, group "**B2a**" can be subdivided into two subgroups: Marbles with $\delta^{13}C$ values lower than 0 ‰, belong to the quarries of Babadağ [BBD], while a $\delta^{13}C$ value higher than 0 ‰ does not allow for further distinction. Group "**B2b**" can also be subdivided into two subgroups: Marbles from Babadağ [BBD] have $\delta^{13}C$ value higher than 1.5 ‰, but both Babadağ [BBD] and Ayazma [AYA] marbles are characterised by $\delta^{13}C$ values lower than 1.5 ‰.

The next decision level – ***Phase V*** – is based on $^{87}Sr/^{86}Sr$ isotopic ratios. Serhat [SRH] and Altınoluk [ALT], which make up the group "**A2a**", and one of the subgroups of "**A2b**" reach they final decision based on the $^{87}Sr/^{86}Sr$ isotopic ratios: Marbles from Serhat [SRH] have $^{87}Sr/^{86}Sr$ ratios lower than 0.7076, while marbles from Altınoluk [ALT] have $^{87}Sr/^{86}Sr$ ratios higher than 0.7077. The marbles with $\delta^{13}C$ values between 2 ‰ and 3 ‰ of the group "**A2b**" can also subdivided into two smaller groups: Marbles from Ayazma [AYA] and Serhat [SRH] are characterised by $^{87}Sr/^{86}Sr$ ratios lower than 0.7076 and marbles from Marmara [MRM] and Orhangazi [ORH] by $^{87}Sr/^{86}Sr$ ratios higher than 0.7076.
In the other branch of the decision tree, Milas [MLS] and Afyon [AFY] can be distinguished based on the $^{87}Sr/^{86}Sr$ ratios. Milas [MLS] marbles have $^{87}Sr/^{86}Sr$ ratios lower than 0.7077, while Afyon [AFY] marbles have $^{87}Sr/^{86}Sr$ ratios higher than 0.7077. The rest-group of "**B2a**" can also be refined: Babadağ [BBD] and Muğla [MGL] have $^{87}Sr/^{86}Sr$ ratios higher than 0.7070, while Karabiga [KB] marbles have $^{87}Sr/^{86}Sr$ ratios lower than 0.7070. Additionally, marbles from the group "**B2b**", with $\delta^{13}C$ values lower than 1.5 ‰, reach their final decision: Marbles from Ayazma [AYA] have $^{87}Sr/^{86}Sr$ ratios lower than 0.7076, while marbles from Babadağ [BBD] are higher than 0.7076.

Finally, only some pairs have not reached their final decision. Ayazma [AYA] and Serhat [SRH], both from the same geological unit, namely the North Kazdağ Range cannot be distinguished yet. However, investigations of cathodoluminescence microfacies help to reach their final stage. In the other branch, some overlapping occurs between the marbles from Babadağ [BBD] and Muğla [MGL]. In this case, cathodoluminescence microfacies can be used to make the final decision as well. One open decision cannot be answered: I have not found a criterion that can distinguish marbles from Marmara [MRM] and Orhangazi [ORH].

15. Determination of the Provenance of Trojan marbles using the Decision Tree

15.1. Prehistoric marbles

15.1.1. Kumtepe marbles

A comparison of the multiple results of the marbles from Kumtepe with Anatolian and Greek marbles (that are investigated in the framework of this study and stem from the literature), based on stable isotopic investigation ($\delta^{18}O$ and $\delta^{13}C$ values), $^{87}Sr/^{86}Sr$ ratios, Mn and Sr concentrations and the maximum grain size determination determined by eye, led to the following conclusion: The raw material of the Kumtepe objects originated from the Hierapolis, Denizli and Thiountas regions in south-west Anatolia (Figure 107 and Figure 108).

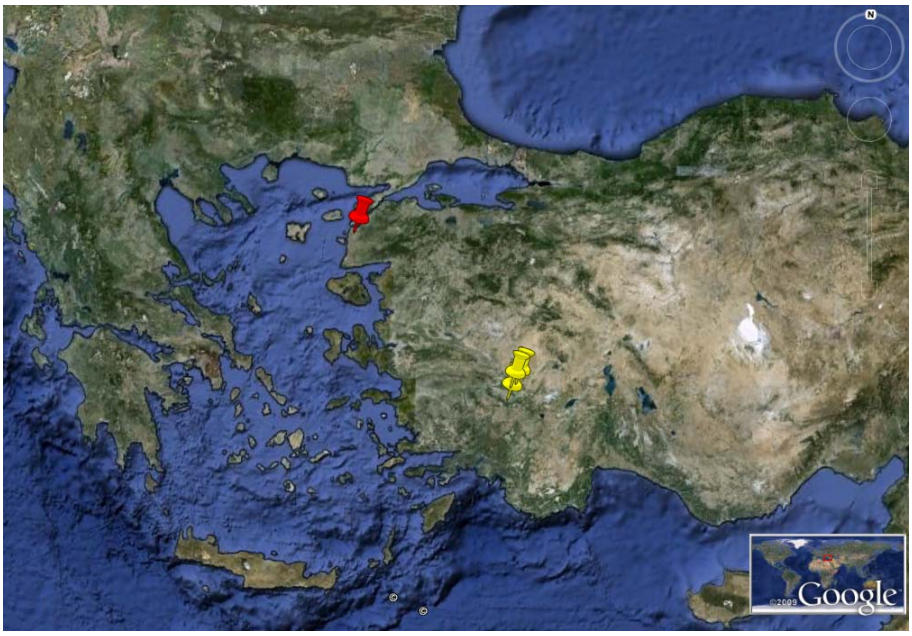

Figure 107: Geographic locations (yellow pins) of the raw materials used for the production of the Kumtepe marbles (red pin)

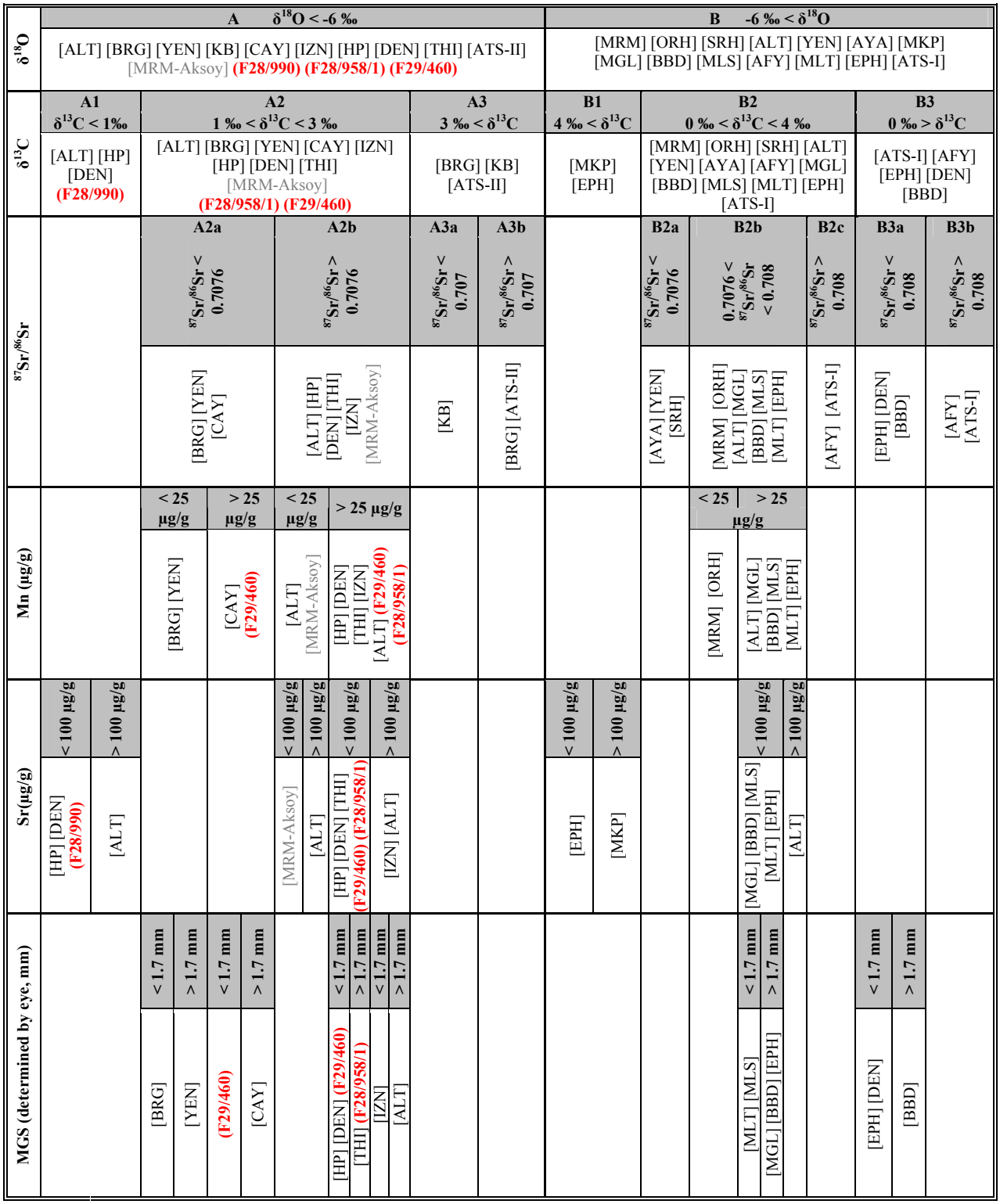

Figure 108: Determination of the Provenance of Kumtepe marbles using the Decision Tree

15.1.2. Bronze Age marbles

Unfortunately, only few of the Trojan marbles could be related with certainty to single stratigraphic periods, especially to the periods Troia IV and Troia VI.

Figure 110 shows the decision tree comparing the marble objects belonging to the Troia IV period (with red) to Anatolian and Greek marbles. The raw material of two of the objects, D3/449 and D8/1844, originated from Paros (Greece). In addition, the raw material of D8/1755 was made of marble from Thiountas or Naxos. Because the grain size of the marble of object D8/1755 can be observed with the naked eye (ca. 3.5 mm), the origin is most probably Naxos. Figure 110 shows the marbles of the Troia VI period with green letters. I9/393 and Z7/732 originate from Naxos, and A8/491 comes from the region of Hierapolis and Denizli. Orange colour designates the remaining Trojan marbles that cannot be related to one of the Trojan stratigraphic periods. Even if, in some cases, it was not possible to identify a single marble quarry, it can be concluded that the raw material predominantly came from Paros and Naxos, but some of the objects were made of marble from Denizli, Hierapolis and Thiountas.

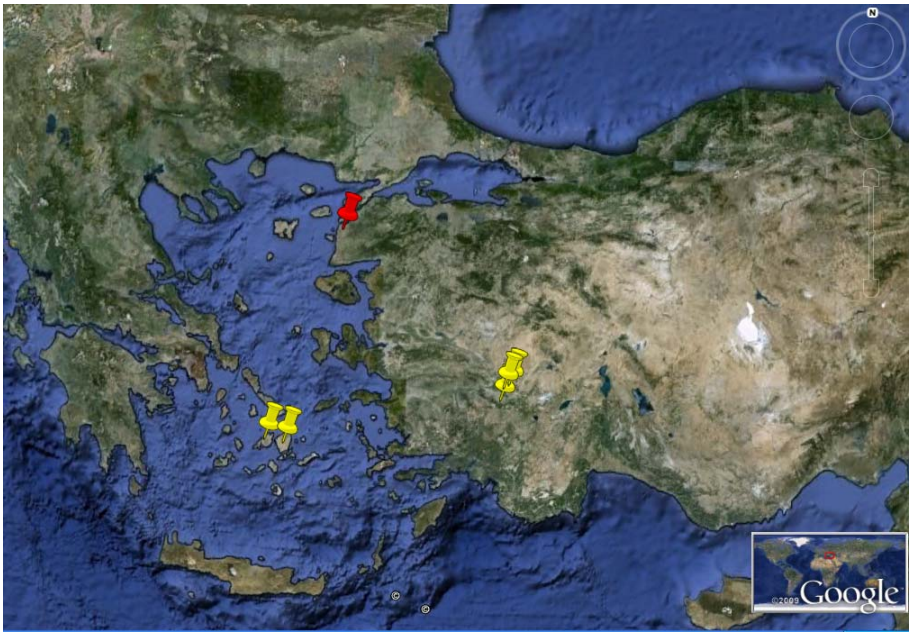

Figure 109: Geographic locations (yellow pins) of the raw materials that were used to produce the Bronze Age marbles of Troia (red pin).

Figure 110: Decision tree of the Bronze Age marbles (red = Troia IV, green = Troia VI, yellow = unknown context.

15.2. Hellenistic marbles

The following conclusion resulted from the comparison of the Hellenistic marbles from Troia with Western Anatolian and Greek marbles, based on QTA/FA analysis, stable isotopic investigation ($\delta^{18}O$ and $\delta^{13}C$ values), $^{87}Sr/^{86}Sr$ ratios, the following conclusion could be drawn: The raw material of the architectural elements of the Hellenistic Period in Troia originated mainly from Marmara, but raw material from Paros and Thasos were also observed. In addition, it is obvious that different raw materials were used to build different monuments; the ***Athena Temple*** was build of marble from Marmara, while the ***Athena Temple Portico*** was built with marble from Marmara, Paros and Thasos. For the Sanctuary "Roman Altar", marble from Marmara and Thasos were used. The raw material of the ***Bath***, ***Blue Marble Building*** also originated from Marmara, but they are different from the marbles that were used in former periods. The marble of the ***Sanctuary***, ***North Building Threshold***, from Marmara Island, is very similar to that of Athena Temple. Marbles from Marmara, Paros and Thasos were used for the construction of the ***Bouleuterion***.

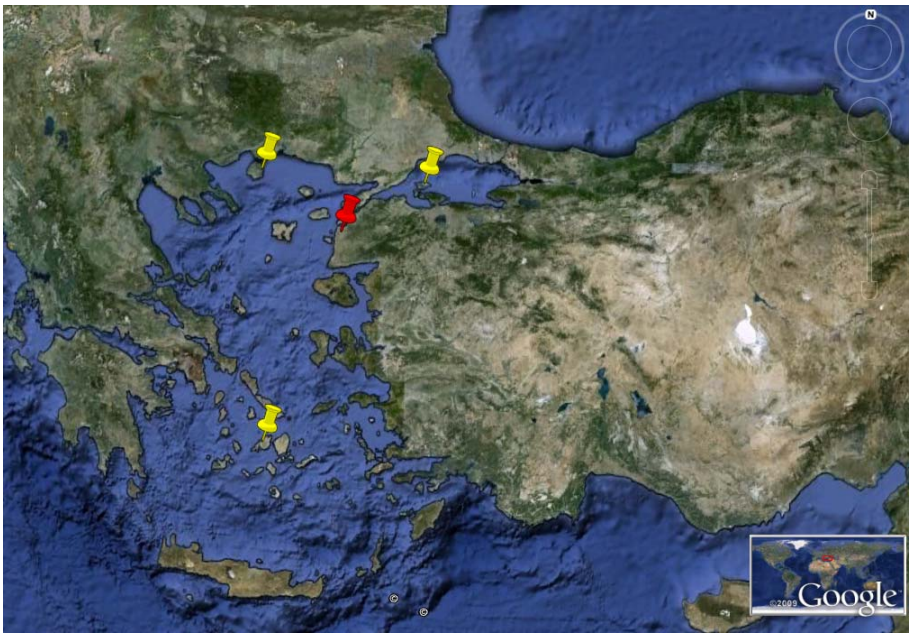

Figure 111: Geographic locations (yellow pins) of the raw materials that were used to produce the Hellenistic marbles of Troia (red pin).

15.3. Roman marbles

Based on the QTA/FA analysis, stable isotopic investigation ($\delta^{18}O$ and $\delta^{13}C$ values) and $^{87}Sr/^{86}Sr$ ratios, the origin of the raw materials of the ***Inscription "Children of Claudius"*** was Marmara or Thasos. Because the marble did not develop a strong odour during sampling (which is very typical for Marmara marbles), it is very probable that the marble came from Thasos.

The architectonical elements and columns of the ***Odeion*** have very similar raw materials that came from Marmara. Therefore, raw materials from one certain quarry were probably transported to Troia for the construction of this monument and no recycled materials were used. In order to build the ***Nymphaeum base of the Bath***, different materials were used: Marble from Marmara and marble from Paros were both newly transported to Troia or recycled. However, one new marble type can be recognized, which originated from Karabiga very close to Troia on the mainland of the Karabiga Peninsula on the opposite side of Marmara Island.

Figure 112: Geographic locations of the raw materials (yellow pins) that were used to produce the Roman marbles of Troia (red pin).

PART VI

CONCLUSION

16. Methodological advancements resulting from this study

- Systematic sampling is unavoidable to determine the provenance of marble. Systematic sampling was carried out in western Anatolia in order to determine the provenance of archaeological marble objects that were excavated in the Troad and neighbouring areas, but outside of this region as well.
- Western Anatolian marbles are calcitic with the exception of marbles from Bergaz. Apart from dolomite, many accessory minerals can be observed such as feldspar, muscovite, quartz, epidote, flogopite, graphite, apatite, perovskite, rutile, gypsum and opaque minerals, but the distribution of the accessory minerals did not allow for a differentiation between the Anatolian marble quarries.
- The parameters of the fractal analysis (FA) such as D_{box} and SD_{box} and of the quantitative fabric analysis, such as MGS, $MGS_{99\%}$, the ratio $MGS/MGS_{99\%}$, MGA, $MGA_{99\%}$, $MGA/MGA_{99\%}$ allowed the differentiation between the major tectonic units in West Anatolia. Quantitative texture analysis (QTA) is extremely laborious considering not only the fact that the images must be converted into drawings but also since the statistical treatment of data requires that many samples for each provenance site are available. The importance of QTA lies in the fact that it has given a rigorous numerical character to textural information. The construction of a meaningful database is therefore extremely arduous.
- The most commonly applied method for the determination of the origin of marble, the isotopic ratios of carbon and oxygen, is due to the discriminating ability of the two variables and owing to their simplicity in terms of interpretation and use. However, with an increasing number of measurements, it gets more and more difficult to determine the origin of marble based on these two parameters alone, although a selection of the possible provenance is feasible in most of the cases. The intra-quarry distribution of the carbon and oxygen isotopic ratios can help in the provenance determination of marble objects.
- The distinguishing power of the $^{87}Sr/^{86}Sr$ isotopic ratios between the marble occurrences in West Anatolia became obvious in this study.
- The trivariate assignment methods using isotopic signatures ($^{87}Sr/^{86}Sr$, $\delta^{13}C$ and $\delta^{18}O$) of Anatolian, Greek and Trojan marbles was used in this study to establish their provenance

among of bivariate plots ($\delta^{13}C$ vs. $\delta^{18}O$). Comparing the two methods, the trivariate method allows a better selectivity and a much more secure assignment of provenance.

17. Petroarchaeological studies versus archaeological theories

The provenance of marble raw material used during the long history of Troia, have been determined in this study. There are significant differences between the raw materials that were used during different historical periods:

- The raw material of the Late Chalcolithic objects from Kumtepe originated in the quarries from the Hierapolis, Denizli and Thiountas regions in south-west Anatolia;
- The raw material of the Bronze-Age objects predominantly came from the Cyclades (Paros and Naxos), but some of the objects were made of marble from Denizli, Hierapolis and Thiountas in south-west Anatolia;
- The raw material of the architectural elements of the Hellenistic Period in Troia originated mainly from Marmara, but raw material from Paros and Thasos were also observed;
- The raw material of the architectural elements of the Roman Period in Troia originated mainly from Marmara, but marble from Paros was also observed, similarly to the Hellenistic Period. However, one new marble type can be recognized, which originated from Karabiga very close to Troia on the mainland of the Karabiga Peninsula on the opposite side of Marmara Island.

My results are in good accordance with former archaeological studies and with the archaeological theories of the cultural and exchange contact of Troia.

The provenance of the marble objects of Kumtepe indicates that the Chalcolithic community of the Troad was part of wider northwestern and southwestern Anatolian cultural settings. The provenance of the marble objects, belonging to the Bronze-Age period in Troia, clearly demonstrates that exchange systems were well developed between Troia and other cities in Anatolia, but also the Cyclades and the Greek mainland. Troia had trade partners from all directions of the compass. In the Hellenistic Period, as Troia were re-settled by Greeks, the main building materials were limestone and marl, but marble were used for the construction of the sacral monuments, and the raw material were transported from Marmara and the Greek Islands. In the Roman period, Troia was part of the famous roman trade system and the prominent buildings were constructed of the famous marbles from Marmara and the Cycladic

Islands. In the case of Nymphaeum base of the Bath, Karabiga marble was used. It is likely that the raw material from Karabiga were used because the marble quarries on Marmara Island were not reachable during some weeks and months of the year due to the specific properties of wind and streaming in the Bosporus. On the other hand, the different impression of the stone (bluish colour) may also have been a reason for its use. The Trojan people did not use the marbles from the local sources of the quarries of the Kazdağ Region. The only marble sources near Troia that were used came from Marmara Island and, in one specific case, from Karabiga in the Roman period.

18. Open questions resulting from this study

There is no question that that the identification of provenance of the white marbles used in Antiquity remains an issue of fundamental interest for archaeologists and art historians and continues to engage scientists of various disciplines. Despite the efforts of mineralogists, petrographers, geochemists, statisticians and physicists, who, as we have seen, have used an extraordinary variety of analytical methods over the last century and more, the problem can still not be considered in every respect and satisfactorily resolved.

An important task for the near future is the systematic entering of the existing data into databases, e.g., MissMarble, in order to figure out the topics that we have to pursue. One of them is the expansion of the geographical territory, at least to the territory of the Empire of Alexander the Great. The next one is to refill or restock the database with the missing information, e.g. by selected methods that are new or re-estimated in marble provenancing (such as qualitative textural analyses, analyses of the fluid inclusion, small angle neutron scattering and $^{87}Sr/^{86}Sr$).

Looking at the chemical composition of marble, maybe the analyses of calcium- and/or magnesium-isotopes could help in answering provenance questions, because calcium and magnesium are major components both in calcitic and dolomitic marbles.

Even now, not one non-destructive analytical technique exists that can quickly and explicitly determine the provenance of most white marbles.

In consideration of Troia, further investigations are recommendable:

- The investigation of marble findings from Prehistoric times has to be extended, especially to include the marble figurines and vessels of the Chalcolithic and Bronze Age, preferably on findings with certain context.
- On the other hand, in this work, the archaeometric study on the architectonical elements of the Hellenistic and Roman period were carried out. It would be interesting to see the results of provenance analyses of the sculptures and sarcophagus that were excavated in Troia.

19. References

AKCAY, H., DEMIR, C., OZER, U. & GUCER, S. 1999. Chemometric characterization studies of marbles by atomic absorption spectrometry. *Chemia Analityczna,* 44 (3B)**,** 577-589.

AKKÖK, R. 1983. Structural and metamorphic evolution of the northern part of the Menderes Massif: new data from the Derbent area and their implication for the tectonics of the massif. *J Geol,* 91**,** 342-350.

ANDREAE, B., OEHLSCHLEGEL, G. & WEBER, K. 1972. Zusammenfügung der Fragmente eines Meleager Sarkophags in Frankfurt und Kassel. *Jahrbuch des Deutschen Archäologischen Instituts,* 87**,** 388-432.

ASGARI, N. 1977. Die Halbfabrikate kleinasiatischen Girlanden-Sarkophage und ihre Herkunft. *Archäologischer Anzeiger***,** 329-380.

ASGARI, N. & MATTHEWS, K. 1995. The stable isotope analysis of marble from Proconnesus. *In:* MANIATIS, Y., HERZ, N. R. & BASIAKOS, Y. (eds.) *The study of marble and other stones used in Antiquity. Proceedings of the III Asmosia Conference, Athens, May 1993*. London: Archetype Books. 123-129.

ASHWORTH, J. R. & EVIGREN, M. M. 1985. Plagioclase relations, central Menderes Massif, Turkey. II. Perturbation of garnet-plagioclase geobarometers. *J. metamorph Geol,* 3**,** 219-229.

ASLAN, R., BLUM, S., KASTL, G., SCHWEIZER, F. & THUMM, D. 2002. *Mauerschau. Festschrift für Manfred Korfmann,* Remshalden-Grunbach, Greiner pp.

ATTANASIO, D. 1999. The use of electron spin resonance spectroscopy for determining the provenance of classical marbles. *Applied Magnetic Resonance,* 16**,** 383-402.

ATTANASIO, D. 2003. *Ancient white marbles. Analysis and identification by paramagnetic resonance spectroscopy.,* Roma, L´erma di Bretschneider. 284 pp.

ATTANASIO, D., ARMIENTO, G., BRUNO, M., EMANUELE, M. C., PENSABENE, P. & PLATANIA, R. 2002a. The re-establishment of an electron spin resonance database for the provenancing of white and greyish marbles: new data for Italian and Greek quarries. *In:* HERRMANN, J. (ed.) *Asmosia.*

ATTANASIO, D., ARMIENTO, G., BRUNO, M., EMANUELE, M. C., PENSABENE, P. & PLATANIA, R. 1998. The re-establishment of an electron spin resonance database for the provenancing of white and greyish marbles: new data for Italian and Greek quarries. *In:* HERZ, N. (ed.) *A history of the Association for the Study of Marble and Other Stones in Antiquity, Abstracts.* Boston: Museum of Fine Arts.

ATTANASIO, D., BRILLI, M. & BRUNO, M. 2008a. The properties and identification of marble from Proconnesos (Marmara Island, Turkey): a new database including isotopic, EPR and petrographic data. *Archaeometry,* 50**,** 747-774.

ATTANASIO, D., BRILLI, M. & OGLE, N. 2006. *The Isotopic Signature of Classical Marbles,* Roma, L'Erma di Bretschneider pp.

ATTANASIO, D., BRILLI, M. & ROCCHI, P. 2008b. The marbles of two early Christian churches at Latrun (Cyrenaica, Libya). *Journal of Archaeological Science,* 35**,** 1040-1048.

ATTANASIO, D., CONTI, L., PLATANIA, R. & TURI, B. 2002b. Multimethod provenance determinations: isotopic, ESR and petrographic discrimination of fine-grained white marbles. *In:* LAZZARINI, L. (ed.) *Interdisciplinary studies on ancient stone.* Padova: Bottega d`Erasmo. 141-148.

ATTANASIO, D. & PLATANIA, R. 2002. Refinement and assessment of the classification rule for an update of the EPR petrograhic marble database. *In:* LAZZARINI, L. (ed.) *Interdisciplinary studies on ancient stone.* Padova: Bottega d`Erasmo. 149-156.

AYDIN, Y. 1974. *Etude petrographique et geochimique de la partie centrale du Massif d´Istranca (Turkuie). PhD Thesis,* Nancy, University of Nancy pp.

BARBIN, V., BURNS, S. J., DECROUEZ, M., ODDONE, M. & ZEZZA, U. 1992a. Cathodoluminescence, REE and stable isotopes charcterisation of marbles from Crevola, Candoglia, Lasa (Italy) and Pteleos (Greece). *In:* D. DECROUEZ, CHAMAY, J. & ZEZZA, F. (eds.) *The conversation of monuments in the Mediterranean basin. Proceedings of 2nd International Symposium.* Geneva. 47-62.

BARBIN, V., RAMSEYER, K., BURNS, S. J., DECROUEZ, D., MAIER, J. L. & CHAMAY, J. 1991a. Cathodoluminescence signature of white marble artefacts. *Materials Research Society Symp. Proc.,* 185**,** 299-308.

BARBIN, V., RAMSEYER, K. & DEBENAY, J. P. U. A. 1991b. Cathodoluminescence of Recent biogenic carbonates: an environmental and ontogenetic fingerprint. *Geol. Mag.,* 128**,** 19-26.

BARBIN, V., RAMSEYER, K., DECROUEZ, D., BURNS, S. J., CHAMAY, J. & MAIER, J. L. 1992b. Cathodoluminescence of White Marbles - an Overview. *Archaeometry,* 34**,** 175-183.

BARBIN, V., RAMSEYER, K., DECROUEZ, D. & HERB, R. 1989. Marbres blancs: characterisation par cathodoluminescence. *C. R. Acad. Sci. Paris,* 308**,** 861-866.

BARBIN, V., REEDER, E. & DRAYMAN-WEISSER, T. 1999. An unidentified but probably identical origin of several white marble artefacts from the Walters Art Gallery (Baltimore, USA): Evidence from petrographic, cathodoluminescence and stable isotope studies. *In:* SCHVOERER, M. (ed.) *Archeomateriaux.* Bordeaux: CRPAA-PUB. 39-44.

BARBIN, V., ZEZZA, U. & PARDO, E. S. 1995. The cathodoluminescence of Macael white marbles (Almeria, Spain). *In:* MANIATIS, Y., HERZ, N. & BASIAKOS, Y. (eds.) *The study of Marble and other Stones Used in Antiquity.* London: Archetype Press. 131-136.

BASARIR, E. 1970. *Bafa gölü dagunsunda kalan Menderes Masifi kanadini jeolojisi ve petrografisi,* Izmir. 102 pp.

BASARIR, E. 1975. *Cine güneyindeki metamorfilterin petrografisi be bireysel indeks minerallerin doku icerisindeki geliseimleri,* Izmir. 79 pp.

BEQUEREL (ed.) 1859. *Ann. de Chimie et de Physique*. 40 pp.

BEQUEREL (ed.) 1867. *La Lumiere*. 354 pp.

BIRICOTTI, F. & SEVERI, M. 2004. A nondestructive methodology for the characterization of white marble of artistic and archaeological interest. *Journal of Cultural Heritage*.

BOZKURT, E. 1996. Metamorphism of Paleaozoic schist in the southern Menderes Massif: field, petrographic, textural and microstructural evidence. *Turk J Earth Sci,* 5**,** 105-121.

BOZKURT, E. & SATIR, M. 2000. The southern Menderes Massif (western Turkey): geochronology and exhumation history. *Geological Journal,* 35**,** 285-296.

BRILLI, M., CAVAZZINI, G. & TURI, B. 2005. New data of Sr-87/Sr-86 ratio in classical marble: an initial database for marble provenance determination. *Journal of Archaeological Science,* 32**,** 1543-1551.

BRUNO, M., CONTI, L., LAZZARINI, L., PENSABENE, P. & TURI, B. 2002. The marble quarries of Thasos: an archaeometric study. *In:* LAZZARINI, L. (ed.) *Interdisciplinary studies on ancient stone.* Padova: Bottega d`Erasmo. 157-162.

BRUNO, M., ELCI, H., YAVUZ, A. B. & ATTANASIO, D. 2009. Unknown marble quarries of Western Asia Minor. *IX ASMOSIA International Conference, Tarragona 2009, Abstract Book.* Tarragona: ICAC. 69.

BRUNO, M., LAZZARINI, L., SOLIGO, M., TURI, B. & VARTI-MATARANGAS, M. 2000. The ancient quarry at Karavas (Paros) and the characterization of its marble. *In:* SCHILARDI, D. U. & KATSONOPOULOU, D. (eds.) *Paria Lithos: Parian quarries, marble and workshops of sculpture.* Athens. 95-103.

CAGLAYAN, M. A., ÖZTÜRK, E. M., ÖZTÜRK, Z., SAV, H. & U., A. 1980. Menderes Masifi güneyine ait bulgular ve yapisal yorum. *Geological enginnering, Turkey,* 10**,** 9-17.

CAGLAYAN, M. A., SENGÜN, M. & YURTSEVER, A. 1988. Main fault system shaping the Istranca Massif, Turkey. *Yournal of Pure and Applied Science, Series A `Geosciences´,* 21**,** 145-154.

CAMPANELLA, L., GREGORI, E., TOMASSETTI, M. & VISCO, G. 2001. Identification of different types of imperial age marble finds using instrumental chemical analysis and pattern recognition analysis. *Annali Di Chimica,* 91 (11-12)**,** 701-718.

CANDAN, O. & KUN, N. 1991. Possible Pan-African volcanics in the Ödemis submassif of the Menderes Massif, western Turkey. *Mineral Res Explor Inst Bull,* 122**,** 1-16.

CAPEDRI, S. & VENTURELLI, G. 2004. Accessory minerals as tracers in the provenancing of archaeological marbles, used in combination with isotopic and petrographic data. *Archaeometry,* 46**,** 517-536.

CARERI, G., LAZZARINI, L. & MAZZACURATI, V. 1992. Angular distribution of light diffused from laserirradiated craystalline marbles. Potential use for identification purposes. *In:* WAELKENS, M., HERZ, N. & MOENS, L. (eds.) *Ancient Stones: Quarrying, Trade and Provenance Determination.* Leuven, Belgium: Leuven University Press. 237-242.

CASTORINA, F., PREITE MARTINEZ, M. & TURI, B. 1997. Provenance determination of classical marbles by the combined use of oxygen, carbon, and strontium isotopes: a preliminary study. *Sci. Technol. Cultural Heritage,* 6**,** 145-150.

CASTRO, E. 1995. The interest of pore-size distribution in the identification of marbles - suction tests. 379-386.

CHATALOV, G. A. 1988. Recent development in the geology of the Strandzha Zone in Bulgaria. *Bulletin of the Technical University of Istanbul,* 41**,** 433–465.

COLI, M. 1989. Litho-structural assemblage and deformation history of "Carrara marble". *Bollettino della Società Gelologica Italiano* 108**,** 581–590.

CONFORTO, L., FELICI, M., MONNA, D., SERVA, L. & TEDDEUCCI 1975. A preliminary evaluation of chemical data (trace element) from classical marble quarries in the Mediterranean. *Archaeometry,* 17**,** 201-213.

CORDISCHI, D., MONNA, D. & SEGRE, A. L. 1983. ESR analysis of marble samples from mediterranean quarries of archaeological interest. *Archaeometry,* 25**,** 68-76.

CRAIG, H. & CRAIG, V. 1972. Greek Marbles: Determination of provenance by isotopic analysis. *Science,* 176**,** 401-403.

CRAMER, T. 1998. Die Marmore des Telephosfrieses am Pergamonaltar. *Berliner Beiträge zur Archäometrie,* 15**,** 95-198.

CRAMER, T. 2004. *Multivariate Herkunftsanalyse von Marmor auf petrographischer und geochemischer Basis. ,* Berlin, Doctoral Thesis, Technical University Berlin pp.

DE GRACIANSKY, P. C. 1972. *Recherches geologiques dans le Taurus Lycien occidental,* Orsay. 570 pp pp.

DELALOYE, M. & BINGÖL, E. 2000. Granitoids from western and northwestern Anatolia: Geochemistry and modelling of geodynamic evolution. *International Geology Review,* 42**,** 241-268.

DORA, O. Ö., KUN, N. & CANDAN, O. 1992. Menderes Masifinin metamorphic tarihcesi ve jeotektonik konumu. *Bull Geol Soc Turkey,* 35.

DULIU, O. G., DINESCU, L. C. & SKLIROS, D. 1999. INAA study of the distribution of some major and trace elements in Greek limestones and marbles. *Journal of Trace and Microprobe Techniques,* 17**,** 165-175.

DÜRR, S. 1975. *Über Alter und geotektonische Stellung des Menderes-Kristallins/ SW-Anatolien und seine Äequivalente in der mittleren Ägäis,* Germany. -107 pp pp.

DÜRR, S., ALTHERR, R., KELLER, J., OKRUSCH, M. & SEIDEL, E. 1978. *The median Aegean crystalline belt: stratigraphy, structure, metamorphism and magmatism*. 455-477 pp.

ELMAS, A. & YIGITBAS, E. 2005. Comment on "Tectonic evolution of the Intra-Pontide suture zone in the Armutlu Peninsula, NW Turkey" by Robertson and Ustaömer. *Tectonophysics,* 405**,** 213–221.

EVIGREN, M. M. & ASHWORTH, J. R. 1984. Andalusitic and kyanitic facies series in the central Menderes Massif, Turkey. *N Jahrb Mineral Geol Paläontol Beil,* 5**,** 219-227.

FILGIS, M. N. & MAYER, W. (eds.) 1992. *Troia - Sicherung und Konservierung der prähistorischen und historischen Bausubstanz* Mainz: Zabern. 83-104 pp.

FOSTER, G. V. & HERZ, N. R. 1985. Identification of Marble Provenance by Pattern-Recognition of Xeroradiographs. *American Journal of Archaeology,* 89**,** 331-331.

FRANK, J. R., CARPENTER, A. B. & OGLESBY, T. W. 1982. Cathodoluminescence and composition of calcite cement in the Taum Sauk limestone (Upper Cambrian), southeatern Missouri. *J. Sediment. Petrol.,* 52**,** 631-638.

FRANZINI, M., GRATZIU, C. & SPAMPINATO, M. 1984. Degradazione del marmo per effetto. *Rendiconti della Societa Italiana di Mineralogia e Petrologia,* 39**,** 47-57.

FRANZINI, M., LEZZERINI, M. & ORIGLIA, F. in print. The ancient marbles from the Campiglia Marittima area (Tuscany, Italy). *European Journal of Mineralogy*.

GEORGIEV, G., DABOVSKI, C. & STANISHEVA-VASSILEVA, G. 2001. East Srednogorie–Balkan rift Zone. *In:* ZIEGLER, P. A., CAVAZZA, W., ROBERSTSON, A. H. F. & CRASQUIN-SOLEAU, S. (eds.) *Peri-Tethys Memoir: 6. Peri-Tethyan Rift/Wrench Basins and Passive Margins*. . Me´moires du Muse´um d'Histoire Naturelle de Paris. 259– 293.

GERMANN, K. & CRAMER, T. 2005. Methoden der Herkunftsbestimmung für Naturwerksteine. Das Beispiel des Marmors. *Zeitschrift der Deutschen Gesellschaft für Geowissenschaften,* 156**,** 25-31.

GERMANN, K., GRUBEN, G., KNOLL, H., VALIS, V. & WINKLER, F. J. 1988. Provenance characteristics of Cycladic (Paros and Naxos) marbles. A multivariate geological approach. *In:* HERZ, N. & WAELKENS, M. (eds.) *Classical Marble: Geochemistry, Technology, Trade.* Dordrecht: Kluwer Academic Publishers. 251-262.

GERMANN, K., HOLZMANN, G. & WINKLER, F. J. 1980. Determination of marble provenance: limits of isotopic analysis. *Archaeometry,* 22**,** 99-106.

GOETTE, H. R., POLIKRETI, K., VACOULIS, T. & MANIATIS, Y. 1999. Investigation of the greyish-blue marble of Pentelikon and Hymettus. *In:* SCHVOERER, M. (ed.) *Archeomateriaux.* Bordeaux: CRPAA-PUB. 83-90.

GÖNCÜOGLU, C. & ERENDIL, M. 1990. Pre-Late Cretaceous tectonic units of Armutlu Peninsula. *8. Petroleum Congress of Turkey . Proceedings.* 161-168.

GORGONI, C., KOKKINAKIS, I., LAZZARINI, L. & MARIOTTINI, M. 1992. Geochemical and petrographic characterization of "rosso antico" and other white-grey marbles of Mani (Greece). *In:* WAELKENS, M., HERZ, N. & MOENS, L. (eds.) *Ancient Stones: Quarrying, Trade and Provenance Determination.* Leuven, Belgium: Leuven University Press. 155-166.

GORGONI, C., LAZZARINI, L., PALLANTE, P. & TURI, B. 2002a. An updated and detailed mineropetrographic and C-O stable isotopic reference database for the main Mediterranean marbles used in antiquity. *In:* HERRMANN, J. & HERZ, N. (eds.) *Interdisciplinary Studies on Ancient Stone.* London: Archetype Publications. 115-131.

GORGONI, C., LAZZARINI, L., PALLANTE, P. & TURI, B. 2002b. An updated and detailed mineropetrographic and C-O stable isotopic reference database for the main Mediterranean marbles used in antiquity. *In:* HERRMANN, J., HERZ, N. & NEWMAN, R. (eds.) *Interdisciplinary Studies on Ancient Stone.* London: Archetype Publications.

GREEN, W. A., YOUNG, S. M. M., VAN DER MERWE, N. & HERRMANN, J. J. J. 2002. Source tracing marble: trace element analysis with inductively coupled plasma-mass spectrometry. *In:* HERRMANN, J. & HERZ, N. (eds.) *Interdisciplinary Studies on Ancient Stone.* London: Archetype Publications. 132-142.

GRIMANIS, A. P. & VASSILAKI-GRIMANI, M. 1988. Provenance studies of Greek marbles by instrumental neutron activation analysis. *In:* HERZ, N. R. & WAELKENS, M. (eds.) *Classical marble: geochemistry, technology, trade.* Dordrecht. 275-282.

GRUNDY, P. J. & JONES, G. A. 1976. *Electron microscopy in the study of materials.,* New York, Crane, Russak pp.

GÜNGÖR, T. & ERDOGAN, B. 2001. Emplacement age and direction of the Lycian nappes in the Söke-Selcuk region, western Turkey *International Journal of Earth Sciences,* 89**,** 874-882.

GÜNGÖR, T. & ERDOGAN, B. 2002. Tectonic significance of mafic volcanic rocks in a Mesozoic sequence of the Menderes Massif, West Turkey. *International Journal of Earth Sciences,* 91**,** 386-397.

HABERMANN, D., NEUSER, R. D. & RICHTER, D. K. 1996. REE-activated cathodoluminescence of calcite and dolomite: high-resolution spectrometric analysis of CL emission (HRS-CL). *Sedimentary Geology,* 101**,** 1-7.

HABERMANN, D., NEUSER, R. D. & RICHTER, D. K. 1998. Low limit of Mn2+-activated cathodoluminescence of calcite: state of the art. *Sedimentary Geology,* 116**,** 13-24.

HEINRICHS, H. & HERRMANN, A. G. 1990. *Praktikum der analytischen Geochemie,* Berlin, Springer pp.

HERRMANN, J. J. & BARBIN, V. 1993. The exportation of marbles from the quarries on Thasos; cathodoluminescence of samples from Turkey and Italy. *Amer. J. Archaeology,* 97**,** 91-103.

HERZ, N. 1985. Isotopic analysis of marble. *In:* RAPP, G. J. & GIFFORD, J. A. (eds.) *Archaeological Geology.* New Haven: Yale Univ. Press. 331-351.

HERZ, N. 1987. Carbon and oxygen isotopic ratios: a data base for classical Greek and Roman marble. *Archaeometry,* 29**,** 35-43.

HERZ, N. 1988. The oxygen and carbon isotopic data base for classical marble. *In:* HERZ, N. & WAELKENS, M. (eds.) *Classical Marble: Geochemistry, Technology, Trade.* Dordrecht: Kluwer Academic Publishers. 305-314.

HERZ, N. 2000. The classical marble quarries of Paros: Paros I, II and III. *In:* SCHILARDI, D. U. & KATSONOPOULOU, D. (eds.) *Paria Lithos: Parian quarries, marble and workshops of sculpture.* Athens. 27-32.

HERZ, N. & DEAN, N. E. 1986. Stable isotopes and archaeological geology: the Carrara marble, northern Italy. *Applied Geochemistry,* 1**,** 139-151.

HERZ, N. & GARRISON, E. 1998. *Geologycal methods for Archaeology*, Oxford University Press pp.

HERZ, N., MOSE, D. G. & WENNER, D. B. 1982. 87Sr/86Sr ratios: a possible discriminant for classical marble provenance. *Geological Society of America, Abstracts with Program.* 514.

HETZEL, R., ROMER, R., CANDAN, O. & PASSCHIER, C. W. 1998. Geology of the Bozdag area, central Menderes massif, SW Turkey. *Geologische Rundschau,* 87**,** 394-406.

JAKOBSHAGEN 1986.

JONGSTE, P. F. B., JANSEN, J. B., MOENS, L. & DEPAEPE, P. 1995. A multivariate provenance determination of white marbles using ICPAES and stable isotope analysis. *In:* MANIATIS, Y., HERZ, N. & BASIAKOS, Y. (eds.) *The study of Marble and other Stones Used in Antiquity.* London: Archetype. 143-150.

JONGSTE, P. F. B., JANSEN, J. B., MOENS, L., PEAPE, P. & WAELKENS, M. 1992. The use of marble in latium between 70 and 150 A.D. ICP-AES for determination of the provenance of white marbles. *In:* WAELKENS, M., HERZ, N. & MOENS, L. (eds.) *Ancient Stones: Quarrying, Trade and Provenance Determination.* Leuven, Belgium: Leuven University Press. 263-268.

KOLLER, K., DEPEAPE, P. & MOENS, L. 2009. The Ephesian marble quarries. Topography, analysis, conlcusions. *In:* MANIATIS, Y. (ed.) *ASMOSIA VII. Proceedings of the 7th International Conference of Association for the Study of Marble and Other Stones in Antiquity.* Athen: École française d'Athènes.

KORFMANN, M. 1994. Troia - Ausgrabungen 1993. *In:* KORFMANN, M. (ed.) *Studia Troica.* Mainz: Zabern. 1-50.

KORFMANN, M. (ed.) 2006. *Troia. Archäologie eines Siedlungshügels und seiner Landschaft,* Mainz am Rhein: von Zabern. IX, 419 S. pp.

KORFMANN, M. & MANNSPERGER, D. 1998. *Troia, ein historischer Überblick und Rundgang,* Darmstadt, Konrad Theiss Verlag GmbH pp.

KRITSOTAKIS, K., PERDIKATSIS, V. & LASKARDIS, K. 2003. An attempt for Greek marble discrimination based on trace- and isotope- analyses combined with mineralogical and petrographical analysis. *ASMOSIA VII - 7th International Conference - Thassos, Greece, 15-20 September, Book of Abstracts.*

KRÖGER, F. A. 1948. *Some aspects of the luminescence 1,2 of solids,* Amsterdam, Elsevier. - 310 pp.

KUMAR, B., DASSHAMRA, S., SREENIVAS, B., DAYAL, A. M., RAO, M. N., DUBEY, N. & CHAWLA, B. R. 2002. Carbon, oxygen and strontium isotope geochemistry of Proterozoic carbonate rocks of the Vindhyan Basin, central India. *Precambrian Research,* 113**,** 43-63.

LAPUENTE, M. P., TURI, B. & BLANC, P. 2000. Marbles from Roman Hispania: stable isotope and cathodoluminescence characterization. *Applied Geochemistry,* 15**,** 1469-1493.

LAPUENTE, P., TURI, B., LAZZARINI, L. & NOGALES, T. 1999. Provenance investigation of white marble sculptures from Augusta Emerita, Hispania. *In:* SCHVOERER, M. (ed.) *Archeomateriaux.* Bordeaux: CRPAA-PUB. 111-116.

LAZZARINI, L. 2002. The origin and characterization of breccia nuvolata, marmor Sagarium, and marmor Triponticum. *In:* HERRMANN, J. & HERZ, N. (eds.) *Interdisciplinary Studies on Ancient Stone.* London: Archetype Publications. 58-67.

LAZZARINI, L. & ANTONELLI, F. 2003. Petrographic and isotopic characterization of the marble of the island of Tinos (Greece). *Archaeometry,* 45**,** 541-552.

LAZZARINI, L. & CANCELLIERE, S. 2000a. Characterisation of the white marble of two unpublished Roman quarries on the Islands of Fourni and Skyros (Greece). *Periodico di Mineralogia,* 69**,** 49-62.

LAZZARINI, L. & CANCELLIERE, S. 2000b. Characterisation of white marble of two unpublished ancient Roman quarries on the Island of Fuorni and Skyros (Greece). *Periodico di Mineralogia,* 69**,** 49-62.

LAZZARINI, L. & MARIOTTINI, M. 1987. La provenienza dei marmi cristallini usati in antico: un nuovo contributo al problema del rapporto calcite/dolomite. *Estratto da "Materiali Lapidei", Supplemento al n. 41/1987 del "Bolletino dArte" del Ministerio per i Beni Culturali e Ambientali,.* 69-72.

LAZZARINI, L., MARIOTTINI, M., PECORARO, M. & PENSABENE, P. 1988. Determination of the provenance of marbles used in some ancient monuments in Rome. *In:* HERZ, N. & WAELKENS, M. (eds.) *Classical Marble: Geochemistry, Technology, Trade.* Dordrecht: Kluwer Academic Publishers. 399-410.

LAZZARINI, L., MOSCHINI, G. & STIEVANO, B. M. 1980a. A contribution to the identification of italian, greek and anatolian marble through a petrological study and the evaluation of Ca/Sr ratio. *Archaeometry,* 22**,** 173-183.

LAZZARINI, L., MOSCHINI, G. & STIEVANO, B. M. 1980b. *Some examples of identification of ancient marbles through a petrological study and the evaluation of Ca/Sr ratio*. -35- pp.

LAZZARINI, L., PICCIOLOI, C. & TURI, B. 2002a. Identification of the constituent marble of some scukptures of the Farnese Collection at the National Archaeological Museum of Naples. *In:* LAZZARINI, L. (ed.) *Interdisciplinary studies on ancient stone.* Padova: Bottega d`Erasmo. 363-368.

LAZZARINI, L., PONTI, G., MARTINEZ, P. M., ROCKWELL, P. & TURI, B. 2002b. Historical, technical, petrographic, and isotopic features of Aphrodisian marble. *In:* HERRMANN, J. & HERZ, N. (eds.) *Interdisciplinary Studies on Ancient Stone.* London: Archetype Publications. 163-168.

LEN, A. 2006. A kisszögű neutronszórás archeometriai alkalmazási lehetőségei / Possible Applications of Neutron Small Angle Scattering in Archaeology *Archeometriai Műhely,* 3**,** 27-31.

LEPSIUS, G. R. 1890. *Griechische Marmorstudien,* Berlin, Reimer. 57 pp.

LIU, Y., BERNER, Z., MASSONE, H.-J. & ZHONG, D. 2006. Carbonatite-like dykes from the eastern Himalayan syntaxis: geochemical, isotopic, and petrogenetic evidence for melting of metasedimentary carbonate rocks within the orogenic crust. *Journal of Asian Earth Sciences,* 26**,** 105-120.

LLOYD, R. V., SMITH, P. W. & HASKELL, H. W. 1985. Evaluation of the manganese ESR method of marble characterization. *Archeometry,* 27**,** 108-116.

LLOYD, R. V., TRANH, A., PEARCE, S., CHEESEMAN, M. & LUMSDEN, D. N. 1988. ESR spectroscopy and X-ray powder diffractometry for marble provenance determination. *In:* HERZ, N. & WAELKENS, M. (eds.) *Classical Marble: Geochemistry, Technology, Trade.* Dordrecht, Boston: Kluwer 369-378.

LONG, J. V. P. & AGRELL, S. O. 1965. The cathodoluminescence of minerals in thin section. *Mineralogical Magazine,* 34**,** 318-326.

MACHEL, H. G., MASON, R. A., MARIANO, A. N. & MUCCI, A. 1991. Causes and emission of luminescence in calcite and dolomite. *In:* BARKER, C. E. & KOPP, O. C. (eds.) *Luminescence Microscopy and Spectroscopy: Qualitative and Quantitative Applications SEPM Short Course.* 9-25.

MANDI, V., VASSILIOU, A., MANIATIS, Y. & GRIMANIS, A. P. 1995. An evaluation of the contribution of trace elements to the determination of marble provenance. *In:* MANIATIS, Y., HERZ, N. & BASIAKOS, Y. (eds.) *The study of Marble and other Stones Used in Antiquity.* London: Archetype Press. 207-214.

MANFRA, L., MASI, U. & TURI, B. 1975. Carbon and oxygen isotope rations of marbles from ancient quarries of western Anatolia and their archaeological significance. *Archaeometry,* 17**,** 215-221.

MANIATIS, Y. & MANDI, V. 1992. Electron-Paramagnetic-Resonance Signals and Effects in Marble Induced by Working. *Journal of Applied Physics,* 71**,** 4859-4867.

MANIATIS, Y., MANDI, V. & NIKOLAOU, A. 1995. Provenance investigation of marbles from Delphi with ESR spectroscopy. *In:* MANIATIS, Y., HERZ, N. & BASIAKOS, Y. (eds.) *The study of Marble and other Stones Used in Antiquity.* London: Archetype Press. 443-452.

MARGOLIS, S. V. & SHOWERS, W. 1988. Weathering characteristics, age, and provenance determinations on ancient Greek and roman marble artifacts. *In:* HERZ, N. & WAELKENS, M. (eds.) *Classical Marble: Geochemistry, Technology, Trade.* Dordrecht: Kluwer Academic Publishers. 233-242.

MARSHALL, D. J. (ed.) 1988. *Cathodoluminescence of geological materials,* Boston: Unwin-Hyman. -143 pp.

MATTHEWS, K. J. 1997. The establishment of a data base of neutron activation analyses of white marble. *Archaeometry,* 39**,** 321-332.

MATTHEWS, K. J., LEESE, M. N., HUGHES, M. J., HERZ, N. & BOWMAN, S. G. E. 1995. Establishing the provenance of marble using statistical combinations of stable isotope

and neutron activation analysis data. *In:* MANIATIS, Y., HERZ, N. & BASIAKOS, Y. (eds.) *The study of Marble and other Stones Used in Antiquity.* London: Archetype Press. 171-180.

MATTHEWS, K. J., MOENS, L., WALKER, S., WAELKENS, M. & PEAPE, P. 1992. The re-evaluation of stable isotope data for Pentelic marble. *In:* WAELKENS, M., HERZ, N. & MOENS, L. (eds.) *Ancient Stones: Quarrying, Trade and Provenance Determination.* Leuven, Belgium: Leuven University Press. 203-212.

MAXWELL, J. A. 1968. *Rock and mineral analysis,* New York, Interscience Publishers pp.

MCCONNELL, J. D. C. 1977. Electron microscopy and electron diffraction. *In:* ZUSSMAN, J. (ed.) *Physical Methods in Determinative Mineralogy.* New York: Academic Press. 475-527.

MCCREA, J. M. 1950. On the isotopic chemistry of carbonates and a palaeotemperature scale. *J. Phys. Chem.,* 18**,** 849-857.

MCLAUGHLIN, S. 1977. Electrostatic potentials at membrane-solution interfaces. *Current Topics in Membranes and Transport,* 9**,** 71–144.

MELLO, E. 1983. Studio della provenienza di marmi bianchi mediante analisi degli elementi in trace e uso della pattern recognition all'elaboratore elettronico. *In:* DOLCI, E. (ed.) *Marmo restauro.* Carrara: Museo del Marmo. 150-162.

MELLO, E., MELONI, S., MONNA, D. & ODDONE, M. 1988a. A computer-based pattern recognition approach to the provenance study of Mediterranean marbles through trace elements analysis. *In:* HERZ, N. & WAELKENS, M. (eds.) *Classical Marble: Geochemistry, Technology, Trade.* Dordrecht: Kluwer Academic Publishers. 283-292.

MELLO, E., MONNA, D. & ODDONE, M. 1988b. Discriminating sources of Mediterranean marbles: a pattern recognition approach. *Archaeometry,* 30**,** 102-108.

MELONI, S., ODDONE, M., GENOVA, N., CRESPI, V. C., MELLO, E., TANDA, G., ARIAS, C., BUONAMICI, M. & BERZERO, A. 1993. Provenance Studies of Ancient Etruscan Marble Monuments and Sardinian Pottery by Neutron-Activation Analysis and Data Reduction. *Journal of Radioanalytical and Nuclear Chemistry-Articles,* 168**,** 273-286.

MELONI, S., ODDONE, M. & ZEZZA, U. 1995. Rare-earth element patterns of white marble samples from ancient quarries in Carrara (Italy). *In:* MANIATIS, Y., HERZ, N. & BASIAKOS, Y. (eds.) *The study of Marble and other Stones Used in Antiquity.* London: Archetype Press. 181-186.

MEYERS, W. J. 1974. Carbonate cement stratigraphy of the Lake Valley Formation (Mississippian), Sacramento Mountains, New Mexico. *J. Sediment. Petrol.,* 44**,** 837-861.

MOENS, L., PEAPE, P. & WAELKENS, M. 1992. Multidisciplinary research and cooperation: keys to a succesful provenance determination of white marble. *In:* WAELKENS, M., HERZ, N. & MOENS, L. (eds.) *Ancient Stones: Quarrying, Trade and Provenance Determination.* Leuven, Belgium: Leuven University Press. 247-254.

MOENS, L., ROOS, P., DERUDDER, J., DEPEAPE, P. & WAELKENS, M. 1987. Identification of archaeologically interesting white marbles by instrumental neutron activation analysis (INAA) and petrography: comparison between samples from Afyon and Usak (Turkey). *J. Trace and Microprobe Techniques,* 5**,** 101-114.

MOENS, L., ROOS, P., RUDDER, J., PEAPE, P., VAN HENDE, J. & WAELKENS, M. 1988. A multi-method approach to the identification of white marbles used in Antique artifacts. *In:* HERZ, N. & WAELKENS, M. (eds.) *Classical Marble: Geochemistry, Technology, Trade.* Dordrecht: Kluwer Academic Publishers. 243-250.

MOLLI, G. & HEILBRONNER, R. 1999. Microstructures associated with static and dynamic recrystallization of Carrara marble (Alpi Apuane, NW Tuscany, Italy) *Geologie en Mijnbouw,* 78**,** 119-126.

MONOD, O., KOZLU, H., GHIENNE, J. F., DEAN, W. T., GÜNAY, Y., HERISSE, A. L., PARIS, F. & ROBARDET, M. 2003. Late Ordovician glaciation in southern Turkey. *Terra Nova,* 15**,** 249-257.

MORBIDELLI, P., TUCCI, P., IMPERATORI, C., POLVORINOS, A., MARTINEZ, M. P., AZZARO, E. & HERNANDEZ, M. J. 2007. Roman quarries of the Iberian peninsula: "Anasol" and "Anasol"-type. *European Journal of Mineralogy,* 19**,** 125-135.

MÜLLER, H. W., SCHWAIGHOFER, B., BEBEA, M., PISO, I. & DIACONESCU, A. 1999. Marbles in the roman province Dacia. *In:* SCHVOERER, M. (ed.) *Archeomateriaux.* Bordeaux: CRPAA-PUB. 131-140.

MÜLLER, H. W., SCHWAIGHOFER, B., BENEA, M., PISO, I. & DIACONESCU, A. 1996. Greek marbles in the Roman province of Dacia. *Greek Society for Archaeometry Conference Athens 1996 - Abstracts Athens.*

NICHOLS, E. L., HOWES, H. L. & WILBER, D. T. 1928. *Cathodo-luminescence and the luminescence of incandescent solids,* Washington. -350 pp.

NORRISH, K. & CHAPPELL, B. W. 1977. X-ray fluorescence spectrography. *In:* ZUSSMAN, J. (ed.) *Physical Methods of Determinative Mineralogy.* London: Academic Press. 201-272.

ODDONE, M., MELONI, S. & MELLO, E. 1985. Provenance Studies of the White Marble of the Cathedral of Como by Neutron-Activation Analysis and Data Reduction. *Journal of Radioanalytical and Nuclear Chemistry,* 90**,** 373-381.

OESTERLING, N., HEILBRONNER, R., STÜNITZ, H., BARNHOORN, A. & MOLLI, G. 2007. Strain dependent variation of microstructure and texture in naturally deformed Carrara marble *Journal of Structural Geology,* 29**,** 681-696

OKAY, A. I. 1989a. Alpine-Himalayan Blueschists. *Annual Review of Earth and Planetary Sciences,* 17**,** 55-87.

OKAY, A. I. 1989b. An Exotic Eclogite Blueschist Slice in a Barrovian-Style Metamorphic Terrain, Alanya Nappes, Southern Turkey. *Journal of Petrology,* 30**,** 107-132.

OKAY, A. I. 2000. Was the Late Triassic orogeny in Turkey caused by the collosion of an oceanic plateau. *In:* BOZKURT, E., PIPER, J. D. A. & WINCHESTER, J. A. (eds.) *Tectonics and magmatism in Turkey and the surrounding area.* London: Geological Society. 25-42.

OKAY, A. I. 2001. Stratigraphic and metamorphic inversions in the central Menderes Massif: a new structural model. *International Journal of Earth Sciences,* 89**,** 709-727.

OKAY, A. I. 2008. Geology of Turkey: A Synopsis. *In:* YALCIN, Ü. (ed.) *Anatolian Metal IV.* Bochum: Deutsches Bergbau-Museum.

OKAY, A. I. & ALTINER, D. 2007. A condensed mesozoic succession north of Izmir: A fragment of the anatolide-tauride platform in the Bornova Flysch zone. *Turkish Journal of Earth Sciences,* 16**,** 257-279.

OKAY, A. I., BOZKURT, E., SATIR, M., YIGITBAS, E., CROWLEY, Q. G. & SHANG, C. K. 2008. Defining the southern margin of Avalonia in the Pontides: Geochronological data from the Late Proterozoic and Ordovician granitoids from NW Turkey. *Tectonophysics,* 461**,** 252-264.

OKAY, A. I. & KELLEY, S. P. 1994. Tectonic Setting, Petrology and Geochronology of Jadeite Plus Glaucophane and Chloritoid Plus Glaucophane Schists from North-West Turkey. *Journal of Metamorphic Geology,* 12**,** 455-466.

OKAY, A. I. & MONIE, P. 1997. Early Mesozoic subduction in the Eastern Mediterranean: Evidence from Triassic eclogite in northwest Turkey. *Geology,* 25**,** 595-598.

OKAY, A. I., MONOD, O. & MONIE, P. 2002. Triassic blueschists and eclogites from northwest Turkey: vestiges of the Paleo-Tethyan subduction. *Lithos,* 64**,** 155-178.

OKAY, A. I. & SATIR, M. 2000. Coeval plutonism and metamorphism in a latest Oligocene metamorphic core complex in northwest Turkey. *Geological Magazine,* 137**,** 495-516.

OKAY, A. I. & SATIR, M. 2006. Geochronology of Eocene plutonism and metamorphism in northwest Turkey: evidence for a possible magmatic arc. *Geodinamica Acta,* 19**,** 251-266.

OKAY, A. I., SATIR, M., MALUSKI, H., SIYAKO, M., MONIE, P., METZGER, V. & AKYÜZ, S. 1996. Paleo- and Neo-Tethyan events in north-western Turkey. *In:* YIN, A. & HARRISON, T. M. (eds.) *The tectonic evolution of Asia.* 420-441.

OKAY, A. I., SATIR, M., TUYSUZ, O., AKYUZ, S. & CHEN, F. 2001. The tectonics of the Strandja Massif: late-Variscan and mid-Mesozoic deformation and metamorphism in the northern Aegean. *International Journal of Earth Sciences,* 90**,** 217-233.

OKAY, A. I., SENGÖR, A. M. C. & GORUR, N. 1994. Kinematic History of the Opening of the Black-Sea and Its Effect on the Surrounding Regions. *Geology,* 22**,** 267-270.

OKAY, A. I. & TÜYSÜZ, O. 1999. Tethyan sutures of Northern Turkey. *Geol. Soc. Long. Spec. Publ.,* 156**,** 475-515.

OKAY, A. I., TUYSUZ, O., SATIR, M., OZKAN-ALTINER, S., ALTINER, D., SHERLOCK, S. & EREN, R. H. 2006. Cretaceous and Triassic subduction-accretion, high-pressure-low-temperature metamorphism, and continental growth in the Central Pontides, Turkey. *Geological Society of America Bulletin,* 118**,** 1247-1269.

ÖZCAN, A., GÖNCÜOĞLU, M. C., TURAN, N., UYSAL, S., SENTÜRK, K. & ISIK, A. 1988. Late Paleozoic evolution of the Kütahya-Bolkardag belt. *Middle East Technical University:Journal of Pure and Applied Sciences,* 21**,** 211-220.

ÖZER, S., ÖZKAR, I., TOKER, V. & SARI, B. A. S. H. 2001. *Stratigraphy of the upper Cretaceous-Paleocene sequences in the southern sector of the Menderes Massif*. 288 pp.

PENTIA, M., HERZ, N. & TURI, B. 2002. Provenance determination of classical marbles: a statistical test based on 87Sr/86Sr, 18O/16O and 13C/12C isotopic ratios. *In:* LAZZARINI, L. (ed.) *Interdisciplinary studies on ancient stone.* Padova: Bottega d`Erasmo. 219-226.

PENTIA, M., HERZ, N. & TURI, B. 2003. Provenance determination of classical marbles: a statistical test based on 87Sr/86Sr, 18O/16O and 13C/12C isotopic ratios. *In:* LAZZARINI, L. (ed.) *Interdisciplinary studies on ancient stones.* Padova: Bottega D´Erasmo. 219-226.

PERUGINI, D., MORONI, B. & POLI, G. 2003. Characterization of marble textures by image and fractal analysis. *In:* LAZZARINI, L. (ed.) *ASMOSIA VI Sixth International Conference, Venice, June 15-18 2000.* 241-246.

PESCHLOW-BINDOKAT, A. & GERMANN, K. 1981. Die Steinbrüche von Milet und Herakleia am Latmos. *JDJ,* 96**,** 157-235.

PIERI, M., BURLINI, L., KUNZE, K., STRETTON, I. & L. OLGAARD, D. 2001. Rheological and microstructural evolution of Carrara marble with high shear strain: results from high temperature torsion experiments *Journal of Structural Geology,* 23**,** 1393-1413

PIKE, S. 1999. Preliminary results of a systematic characterisation study of Mount Pentelikon, Attica, Greece. *In:* SCHVOERER, M. (ed.) *Archeomateriaux.* Bordeaux: CRPAA-PUB. 165-170.

POLIKRETI, K. & MANIATIS, Y. 2002. A new methodology for the provenance of marble based on EPR spectroscopy. *Archaeometry,* 44**,** 1-21.

POLIKRETI, K. M. Y. 2003. Micromorphology, composition and origin of the orange patina on the marble surfaces of Propylaea (Acropolis, Athens). *The Science of the Total Environment,* 308**,** 111-119.

PROCHASKA, W. & ATTANASIO, D. 2009. Tracing the origin of marbles by inclusion fluid chemistry. *IX ASMOSIA International Conference, Tarragona 2009, Abstract Book.* Tarragona: ICAC. 57.

RENFREW, C. & SPRINGER PEACEY, J. 1968. Aegean Marble: A petrological study. *Annual of the British School at Athens,* 63**,** 45-64.

ROOS, P., MOENS, L., DERUDDER, J., DEPEAPE, P., VAN HENDE, J. & WAELKENS, M. 1995. Chemical and petrographical characterization of greek marbles from Pentelikon, Naxos, Paros and Thasos. *In:* MANIATIS, Y., HERZ, N. & BASIAKOS, Y. (eds.) *The study of Marble and other Stones Used in Antiquity.* London: Archetype Press. 263-272.

ROSE, C. B. 1992. The 1991 Post-Bronze Age Excavations at Troia. *In:* KORFMANN, M. (ed.) *Studia Troica II.* Mainz: Zabern. 43-60.

ROSE, C. B. 1993. The 1992 Post-Bronze Age Excavations at Troia. *In:* KORFMANN, M. (ed.) *Studia Troica III.* Mainz: Zabern. 97-116.

ROSE, C. B. 1994. The 1993 Post-Bronze Age Research and Excavations at Troia. *In:* KORFMANN, M. (ed.) *Studia Troica IV.* Mainz: Zabern. 75-104.

ROSE, C. B. 1995. The 1994 Post-Bronze Age Research and Excavations at Troia. *In:* KORFMANN, M. (ed.) *Studia Troica V.* Mainz: Zabern. 81-106.

RYBACH, L. & NISSEN, H. U. 1965. Neutron activation of Mn and Na traces in marbles worked by the ancient Greeks. *Radiochemical methods of analysis,* 1**,** 105-117.

SATIR, M. & FRIEDRICHSEN, H. 1986. The Origin and Evolution of the Menderes Massif, Western Turkey - a Rubidium Strontium and Oxygen Isotope Study. *Geologische Rundschau,* 75**,** 703-714.

SATIR, M. & TAUBALD, H. 2001. Hydrogen and oxygen isotope evidence for fluid-rock interactions in the Menderes massif, western Turkey. *International Journal of Earth Sciences,* 89**,** 812-821.

SCHMID, J., AMBÜHL, M., DECROUEZ, D., MULLER, S. & RAMSEYER, K. 1999a. A quantitative fabric analysis approach to the discrimination of white marbles. *Archaeometry,* 41**,** 239-252.

SCHMID, J., DECROUEZ, D. & RAMSEYER, K. 1999b. A new element for the provenance determination of white marbles: Quantitative Fabric Analysis. *In:* SCHVOERER, M. (ed.) *Archeomateriaux.* Bordeaux: CRPAA-PUB. 171-176.

SCHMID, J., RAMSEYER, K. & DECROUEZ, D. 1995. A new element for the provenance determination of white marbles: qualitative fabric analysis. *ASMOSIA IV, Actes de la IV ème Conference Internationale.* Bordeaux,. 171-175.

SCHUSTER, R., MOSHAMMER, B. & ABART, R. 2005a. Tectonic and Stratigraphic Information on Greenschist to Eclogite Facies Metamorphic Austroalpine Units by a Sr–C–O Isotope Study on Marbles. *In:* TOMLJENOVIC, B., BALEN, D. & VLAHOVIC, I. (eds.) *7th Workshop on Alpine Geological Studies, Abstract book. Croatian Geological Society.* Opatija. 87-88.

SCHUSTER, R., MOSHAMMER, B. & ABART, R. 2005b. Tectonic and Stratigraphic Information on Greenschist to Eclogite Facies Metamorphic Austroalpine Units by a Sr–C–O Isotope Study on Marbles. *In:* TOMLJENOVIĆ, B., BALEN, D. & VLAHOVIĆ, I. (eds.) *7th Workshop on Alpine Geological Studies. Abstracts book.* Opatija. 87-88.

SENGÖR, A. M. C., SATIR, M. & AKKÖK, R. 1984. Timing of Tectonic Events in the Menderes Massif, Western Turkey - Implications for Tectonic Evolution and Evidence for Pan-African Basement in Turkey. *Tectonics,* 3**,** 693-707.

SENGÖR, A. M. C. & YILMAZ, Y. 1981. Tethyan Evolution of Turkey - a Plate Tectonic Approach. *Tectonophysics,* 75**,** 181-241.

SENGÖR, A. M. C., YILMAZ, Y. & KETIN, I. 1982. Remnants of a Pre Late Jurassic Ocean in Northern Turkey - Fragments of Permian-Triassic Paleo-Tethys - Reply. *Geological Society of America Bulletin,* 93**,** 932-936.

SIPPEL, R. F. & GLOVER, E. D. 1965. Structures in carbonate rocks made visible by luminescence petrography. *Science,* 150**,** 1283-1287.

SMITH, J. V. & STENSTROM, R. C. 1965. Electron-excited luminescence as a petrologic tool. *J. of Geology,* 73**,** 627-635.

SUNAL, G., NATAL'IN, B. A., SATIR, M. & TORAMAN, E. 2006. Paleozoic magmatic events in the Strandja Massif, NW Turkey. *Geodinamica Acta,* 19**,** 283-300.

SUNAL, G., SATIR, M., NATAL'IN, B. A. & TORAMAN, E. 2008. Paleotectonic position of the Strandja massif and surrounding continental blocks based on zircon Pb-Pb age studies. *International Geology Review,* 50**,** 519-545.

SZÉKELY, B. & ZÖLDFÖLDI, J. 2009. Fractal analysis and quantitative fabric analysis database of West Anatolian white marbles. *In:* MANIATIS, Y. (ed.) *ASMOSIA VII. Proceedings of the 7th International Conference of Association for the Study of Marble and Other Stones in Antiquity.* Athenes: École française d'Athènes. 719-734.

TANAKA, T. 1924. *Journal Optical Society of America,* 8**,** 287-318.

TOPUZ, G., ALTHERR, R., KALT, A., SATIR, M., WERNER, O. & SCHWARZ, W. H. 2004a. Aluminous granulites from the Pulur complex, NE Turkey: a case of partial melting, efficient melt extraction and crystallisation. *Lithos,* 72**,** 183-207.

TOPUZ, G., ALTHERR, R., SATIR, M. & SCHWARZ, W. H. 2004b. Low-grade metamorphic rocks from the Pulur complex, NE Turkey: implications for the pre-Liassic evolution of the Eastern Pontides. *International Journal of Earth Sciences,* 93**,** 72-91.

TOPUZ, G., ALTHERR, R., SCHWARZ, W. H., DOKUZ, A. & MEYER, H. P. 2007. Variscan amphibolite-facies rocks from the Kurtoglu metamorphic complex (Gumushane area, Eastern Pontides, Turkey). *International Journal of Earth Sciences,* 96**,** 861-873.

TOPUZ, G., OKAY, A. I., ALTHERR, R., MEYER, H. P. & NASDALA, L. 2006. Partial high-pressure aragonitization of micritic limestones in an accretionary complex, Tavsanli Zone, NW Turkey. *Journal of Metamorphic Geology,* 24**,** 603-613.

TOPUZ, G., OKAY, A. I., ALTHERR, R., SATIR, M. & SCHWARZ, W. H. 2008. Late Cretaceous blueschist facies metamorphism in southern Thrace (Turkey) and its geodynamic implications. *Journal of Metamorphic Geology,* 26**,** 895-913.

TÜRKECAN, A. & YURTSEVER, A. 2002. Geological map of Turkey Istanbul: Ankara, Turkey, General Derectorate of Mineral Researc and Exploration.

UNTERWURZACHER, M., POLLERES, J. & MIRWALD, P. 2005. Provenance study of marble artefacts from the Roman burial area of faschendorf (Carinthia, Austria). *Archaeometry,* 47**,** 265-273.

USTAÖMER, T. & ROBERTSON, A. H. F. 1994. Late Paleozoic marginal basin and subduction-accretion: the Paleotethyan Küre Complex, Central Pontides, northern Turkey. *Journal of the Geological Society London,* 151**,** 291-305.

WIMMENAUER, W. 1985. *Petrographie der magmatischen und metamorphen Gesteine.,* Stuttgart, Enke Verlag pp.

ZEZZA, U. 1999. Non-destructive colour parameters applied to provenance studies of archaeological mediterranean white marbles. *In:* SCHVOERER, M. (ed.) *Archeomateriaux.* Bordeaux: CRPAA-PUB. 185-190.

ZÖLDFÖLDI, J. 2009. Database of white marble from the Indian Subcontinent: a review. *Asmosia IX, Abstracts.* Tarragona: ICAC.

ZÖLDFÖLDI, J., HEGEDÜS, P. & SZÉKELY, B. 2008a. Interdisciplinary data base of marble for archaeometric, art historian and restoration use. *In:* YALCIN, Ü., ÖZBAL, H. & PASAMEHMETOGLU, G. (eds.) *Ancient Mining in Turkey and the Eastern Mediterranean.* Ankara: Atilim University. 225-251.

ZÖLDFÖLDI, J., HEGEDÜS, P. & SZÉKELY, B. 2008b. MissMarble: egy archeometriai, müvészettörténeti és müemlékvédelmi célú, internet-alapú, interdiszciplinális adatbázis. *Archeometriai Műhely,* 5**,** 41-49.

ZÖLDFÖLDI, J., HEGEDÜS, P. & SZÉKELY, B. 2009. MissMarble: Online Datenbanksystem über Marmor für Naturwissenschaftler, Archäologen, Denkmalpfleger, Kunsthistoriker und

Restauratoren. *In:* HAUPTMANN, A. & STEGE, H. (eds.) *Archäometrie und Denkmalpflege 2009. Kurzfassungen. Metalla Sonderheft 2.* . München. 161-163.

ZÖLDFÖLDI, J., PINTÉR, F., SZÉKELY, B., TAUBALD, H., T. BIRÓ, K., MRÁV, Z., TÓTH, M., SATIR, M., KASZTOVSZKY, Z. & SZAKMÁNY, G. 2004a. Római márványtöredékek vizsgálata a Magyar Nemzeti Múzeum gyűjteményéből. / Provenance Studies on marble fragments in the Hungarian National Museum. *Archeometriai Műhely,* 1**,** 39-45.

ZÖLDFÖLDI, J. & SATIR, M. 2003. Provenance of the White Marble Building Stones in the Monuments of Ancient Troia. *In:* G.A. WAGNER, PERNICKA, E. & UERPMANN, H. P. (eds.) *Troia and the Troad.* Berlin: Springer. 203-223.

ZÖLDFÖLDI, J. & SZÉKELY, B. 2003. A case study of combining quantitative fabric analysis (QFA) and fractal analysis (FA) on white marbles with conventional analytical techniques for provenance analysis. *In:* SNETHLAGE, R. & MEINHARDT-DEGEN, J. (eds.) *Proceedings of the 13th Workshop of EU 496 EUROMARBLE.* Munich: Bavarian State Department of Historical Monuments 141-149.

ZÖLDFÖLDI, J. & SZÉKELY, B. 2004. Kísérlet a nyugat-anatóliai tektonikai egyégek kvantitatív textúraelemzésen alapuló szétválasztására régészeti származásvizsgálati szempontból. / An attempt to separate Western Anatolian tectonic units based on Quantitative Textural Analysis for archaeological marble provenance. *Archeometriai Műhely,* 1**,** 22-26.

ZÖLDFÖLDI, J. & SZÉKELY, B. 2005a. Provenance of Roman and Greek marble building stones of Troy. *Proceedings of the 33rd International Symposium on Archaeometry, 22-26 April 2002, Amsterdam. Geoarchaeological and Bioarchaeological Studies 3.* Amsterdam. 123-129.

ZÖLDFÖLDI, J. & SZÉKELY, B. 2005b. Quantitative Fabric Analysis (QFA) and Fractal Analysis (FA) on Marble from West-Anatolia and Troy. *Proceedings of the 33rd International Symposium on Archaeometry, 22-26 April 2002, Amsterdam. Geoarchaeological and Bioarchaeological Studies 3.* Amsterdam. 113-119.

ZÖLDFÖLDI, J. & SZÉKELY, B. 2008. Quantitative Fabric Analysis (QFA) on marble from West Anatolia: Application of raster- (fractal) and vector-based (geometric) approaches. *British Archaeological Reports Int. 1746.* 413-420.

ZÖLDFÖLDI, J. & SZÉKELY, B. 2009. Carbon, oxygen and strontium isotopic systematics of white marbles used in the Antiquity. *Asmosia IX, Abstracts.* Tarragona: ICAC.

ZÖLDFÖLDI, J., SZÉKELY, B. & FRANZEN, C. 2004b. Interdisciplinary data base of historically relevant marble material for archaeometric, art historian and restoration use. *In:* G. GRASSEGGER-SCHÖN & G. PATITZ (eds.) *Natursteinsanierung Stuttgart 2004, Neue Natursteinsanierungsergebnisse und messtechnische Erfassungen.* München: Siegl. 79-86.

ZÖLDFÖLDI, J., TAUBALD, H., PINTÉR, F., TÓTH, M., T. BIRÓ, K., SATIR, M., MRÁV, Z., KASZTOVSZKY, Z., SZAKMÁNY, G. & DEMÉNY, A. 2005. Provenance Studies on Roman Marble Fragments in the Hungarian National Museum, Budapest. *Proceedings of the 33rd International Symposium on Archaeometry, 22-26 April 2002, Amsterdam. Geoarchaeological and Bioarchaeological Studies 3.* Amsterdam. 119-123.

ZÖLDFÖLDI, J. & WEIGELE, J. 2007. Kampf um die Erhaltung der Marmorskulpturen des Stuttgarter Lapidariums. *In:* GRASSEGGER-SCHÖN, G., PATITZ, G. & WÖLBERT, O. (eds.) *Natursteinsanierung Stuttgart 2007, Neue Natursteinsanierungsergebnisse und messtechnische Erfassungen.* München. 49-63.

APPENDIX A: INVESTIGATED ARCHAEOLOGICAL OBJECTS

(All pictures: © Troia Project)

Investigated archaeological objects of the Prehistoric times

Areal	Archaeological unit	Year of excavation	Description	Context	Figure
Kumtepe					
F28	990	1995	Marble bowl fragment		Fig 1-A
F29	460	1995	Marble bowl fragment		Fig 1-B
F28	958/1	1995	Marble bowl fragment		n.d.
Korfmann					
D8	1844	1994	Polish stone	Troia IV	Fig 1-C
D8	1755	1994	Polish stone	Troia IV	Fig 1-D
D9	106	1989	Fragment		Fig 1-E
E8	354(44)	1996	Bracelet fragment	Troia VIIb2	Fig 1-F
K8	730	1992	Fragment		Fig 1-G
D3	30	1988	Polish stone fragment		Fig 1-H
G6	42(1)	1997	Fragment		Fig 1-I
D7	48	1990	Pendant fragment		Fig 1-J
E4/5	95	1988	Polish stone		Fig 1-K
E4	640(149)	1993	Marble disc fragment		Fig 1-L
E9	1297	1997	Marble fragment	Troia VII	Fig 1-M
D3	449	1995	Bowl fragment		Fig 1-N
Z7	732	1994	Round stone	Troia VI / VII ?	Fig 1-P
K17	1138	19xx	Disc		Fig 1-Q
I9	393	1993	Marble pendant	Troia VI	Fig 1-R
A8	491	1995	Marble knob	Troia VI	Fig 1-S
K12	B38	1989	Marble fragment of a bowl		n.d.
Y8 (1)	100	1998	Pendant		n.d.
Blegen					
91/44 (7)			Idol fragment		
T-44/58 (4)			Fragment		
T-8/14 (3)			Polish stone		
T23 (5)			Fragment		

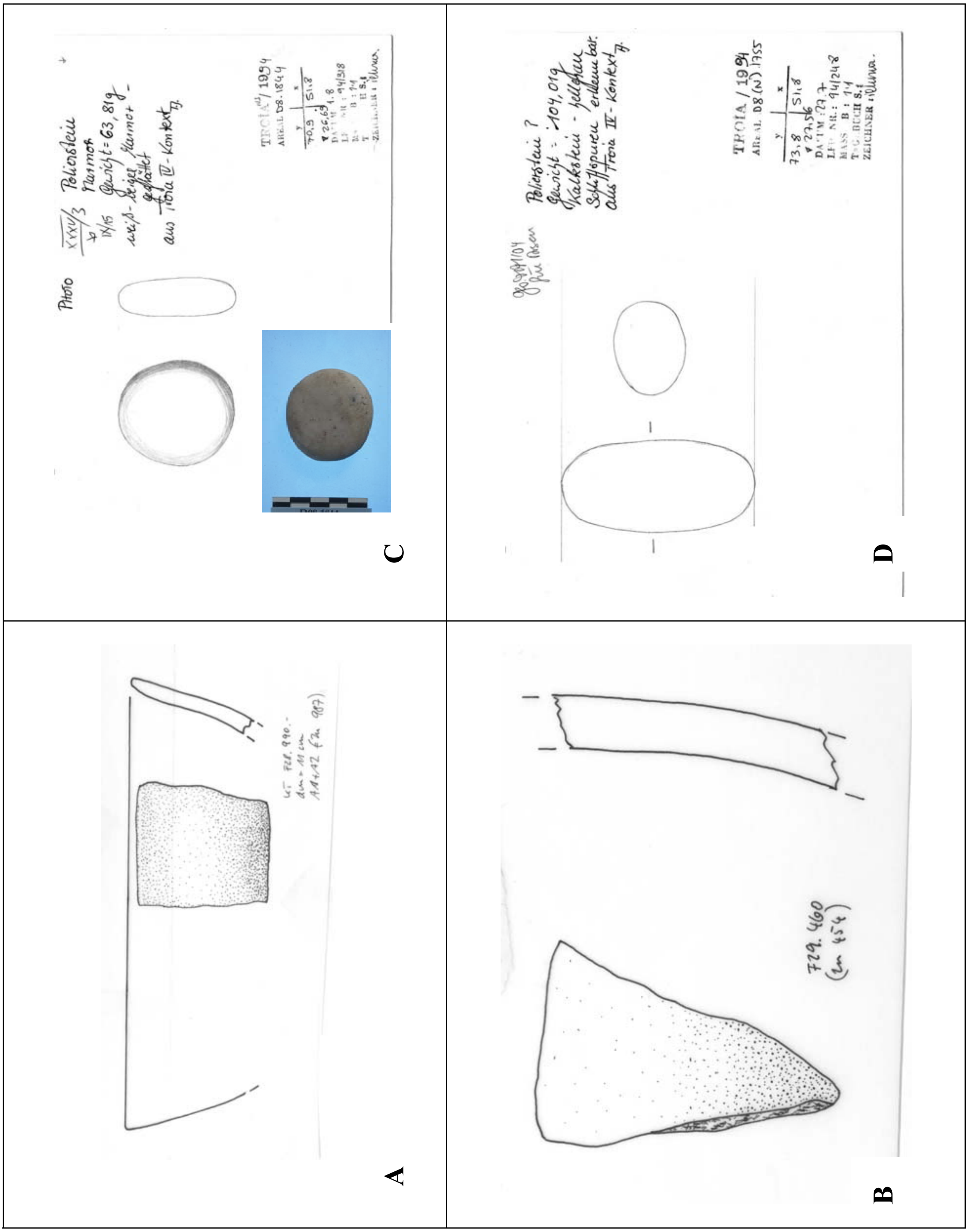
A
B
C
D

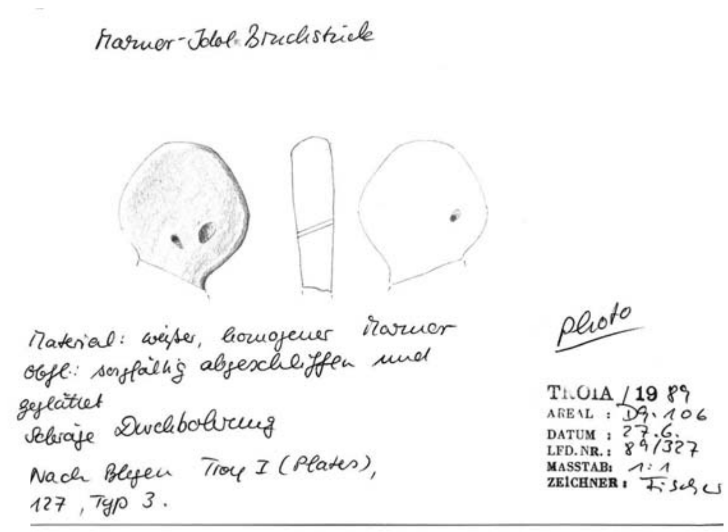
Marmor-Idol-Bruchstück
Material: weißer, homogener Marmor
Obfl.: sorgfältig abgeschliffen und geglättet
Schräge Durchbohrung
Nach Blegen Troy I (Plates), 127, Typ 3.
photo
TROIA / 19 89
AREAL : D9.106
DATUM : 27.6.
LFD. NR. : 89/327
MASSTAB: 1:1
ZEICHNER : Fischer
E

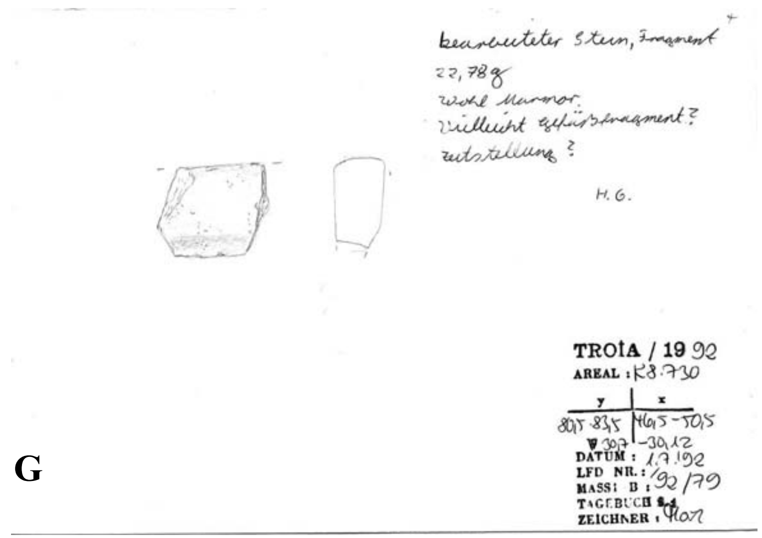
bearbeiteter Stein, Fragment
22,78 g
wohl Marmor
vielleicht Gefäßfragment?
Zeitstellung?
H.G.
TROIA / 19 92
AREAL : K8.730
y
x
805-835
46,5-50,5
▼30,7-30,12
DATUM : 1.7.92
LFD NR. : 92/79
TAGEBUCH S.
ZEICHNER : Mor
G

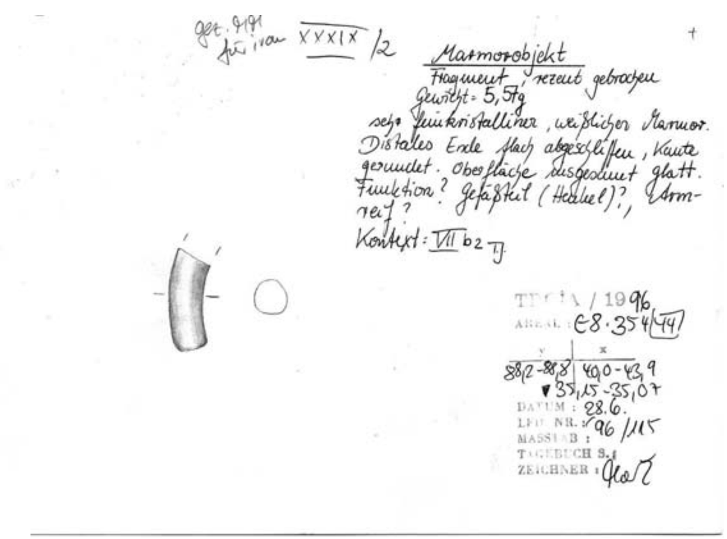
gez. 9.91 für von XXXIX/2
Marmorobjekt
Fragment, rezent gebrochen
Gewicht: 5,57 g
sehr feinkristalliner, weißlicher Marmor.
Distales Ende flach abgeschliffen, Kante gerundet. Oberfläche insgesamt glatt.
Funktion? Gefäßteil (Henkel)?, Armreif?
Kontext: VII b2 TJ.
TROIA / 1996
AREAL : E8.354 (44)
y
x
88,2-88,8
49,0-43,9
▼35,15-35,07
DATUM : 28.6.
LFD. NR. : 96/115
TAGEBUCH S.
ZEICHNER : Mor
F

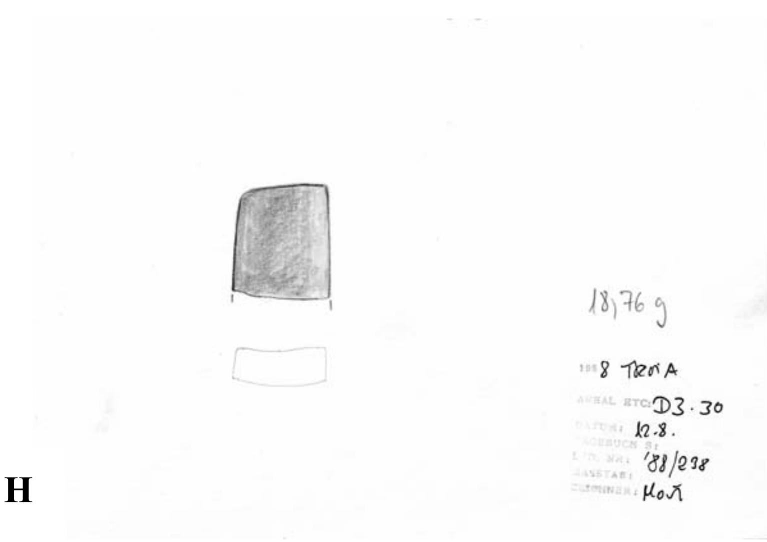
18,76 g
1988 TROIA
AREAL ETC: D3.30
DATUM: 12.8.
LFD. NR.: 88/238
ZEICHNER: Mor
H

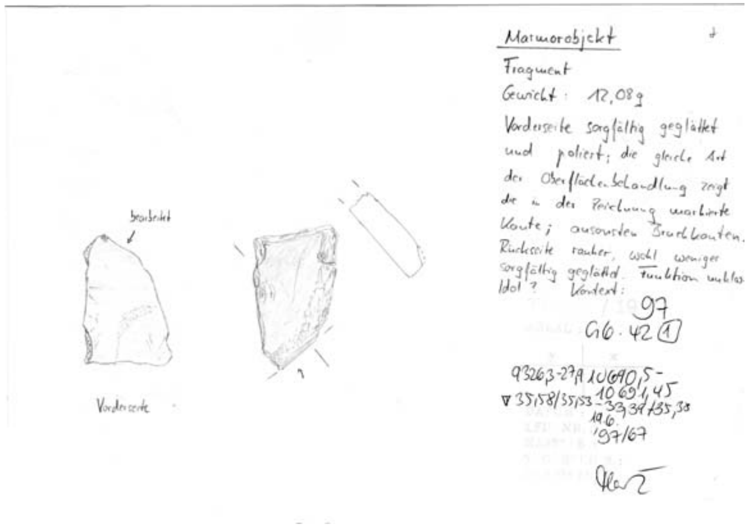
Marmorobjekt
Fragment
Gewicht: 12,08g
Vorderseite sorgfältig geglättet und poliert; die gleiche Art der Oberflächenbehandlung zeigt die in der Zeichnung markierte Kante; ansonsten Bruchkanten. Rückseite rauher, wohl weniger sorgfältig geglättet. Funktion unklar Idol?
97
G6.42 1
Vorderseite

I

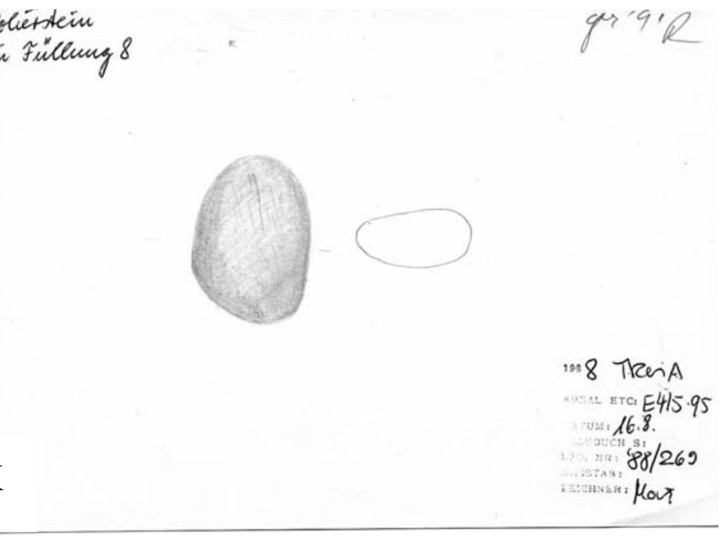
Polierstein
in Füllung 8
1988 TROIA
E4/5.95
16.8.
88/269

K

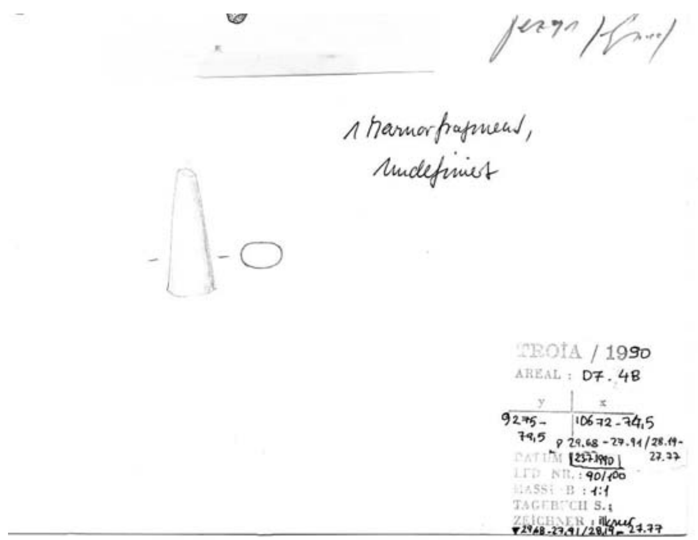
1 Marmorfragment,
undefiniert
TROIA / 1990
AREAL: D7.48
y
x
LFD NR.: 90/100
MASS: B: 1:1
TAGEBUCH S.:
ZEICHNER:

J

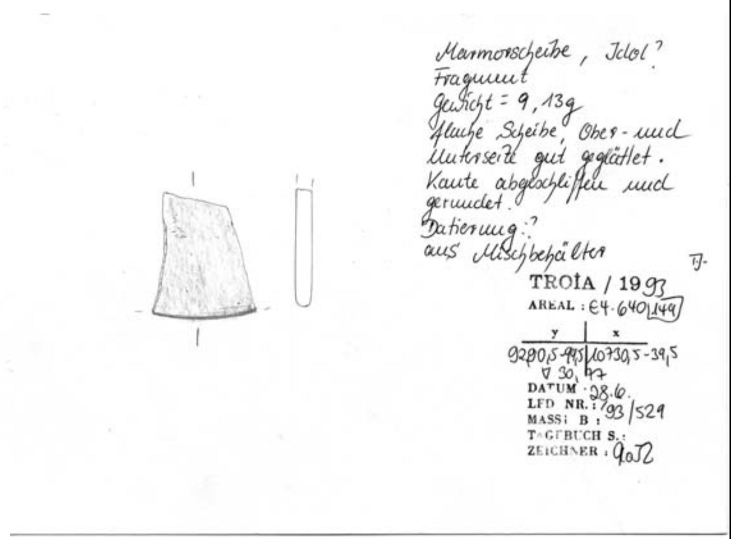
Marmorscheibe, Idol?
Fragment
Gewicht = 9,13g
flache Scheibe, Ober- und Unterseite gut geglättet.
Kante abgeschliffen und gerundet.
Datierung:?
aus Mischbehälter
TROIA / 1993
AREAL: E4.640
y
x
DATUM: 28.6.
LFD NR.: 93/529
MASS: B:
TAGEBUCH S.:
ZEICHNER:

L

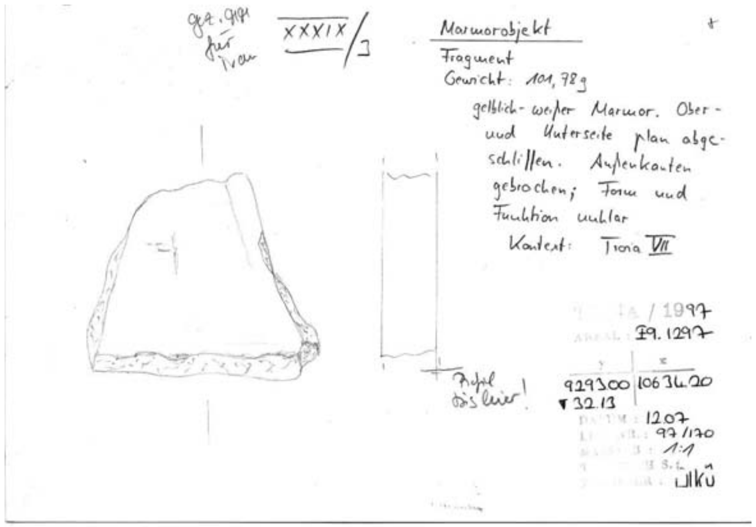
XXXIX
Marmorobjekt
Fragment
Gewicht: 101,78g
gelblich-weißer Marmor. Ober- und Unterseite plan abgeschliffen. Außenkanten gebrochen; Form und Funktion unklar
Kontext: Troia VII
/ 1997
I9.1297
929300 | 10634.20
32.13
1207
97/170
1:1
Profil bis hier!

M

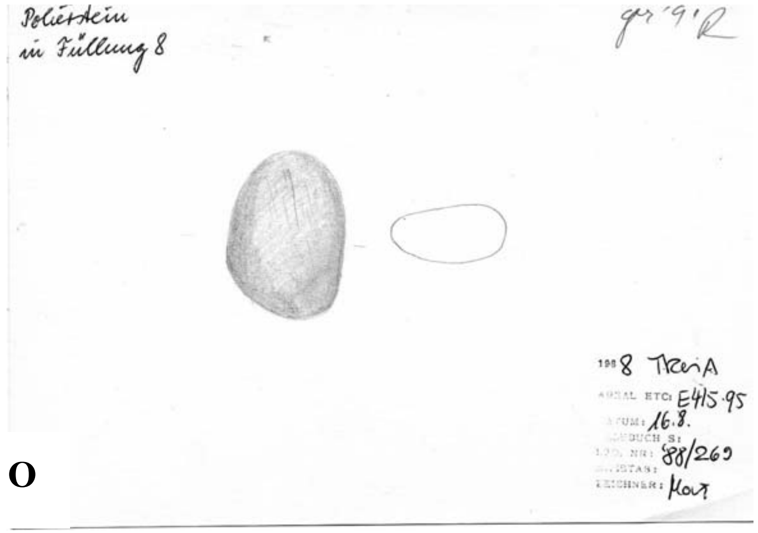
Polierstein
in Füllung 8
1988 TROIA
E4/5.95
16.8.
88/269
Korf

O


Photo
Ø 9cm
Marmorschälchen
fragmentiert
Gewicht. 101,3g
TROIA / 1995
AREAL : D3.449
y | x
~92.67 | ~107.56
22.60
DATUM : 5.7.95
LFD NR. : 95/166
MASSTAB : 1:1
TAGEBUCH S.:
ZEICHNER :
Flache runde Schale aus weißem, grobkristallinem Marmor.
Innen- und Außenseite geglättet, Innenseite aber deutlich sorgfältiger
Kontext: Störung
D03.0449

N

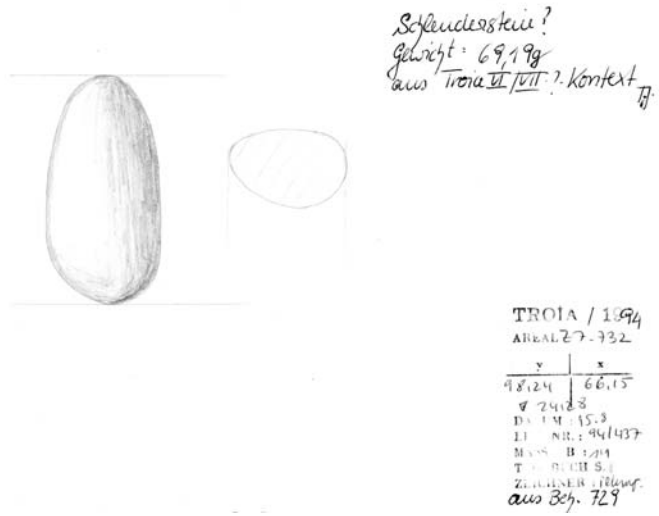
Schleuderstein?
Gewicht: 69,19g
aus Troia VI/VII ?. Kontext
TROIA / 1994
AREAL Z7.732
y | x
98,24 | 66,15
24,28
15.8
94/437
1:1
aus Bef. 729

P

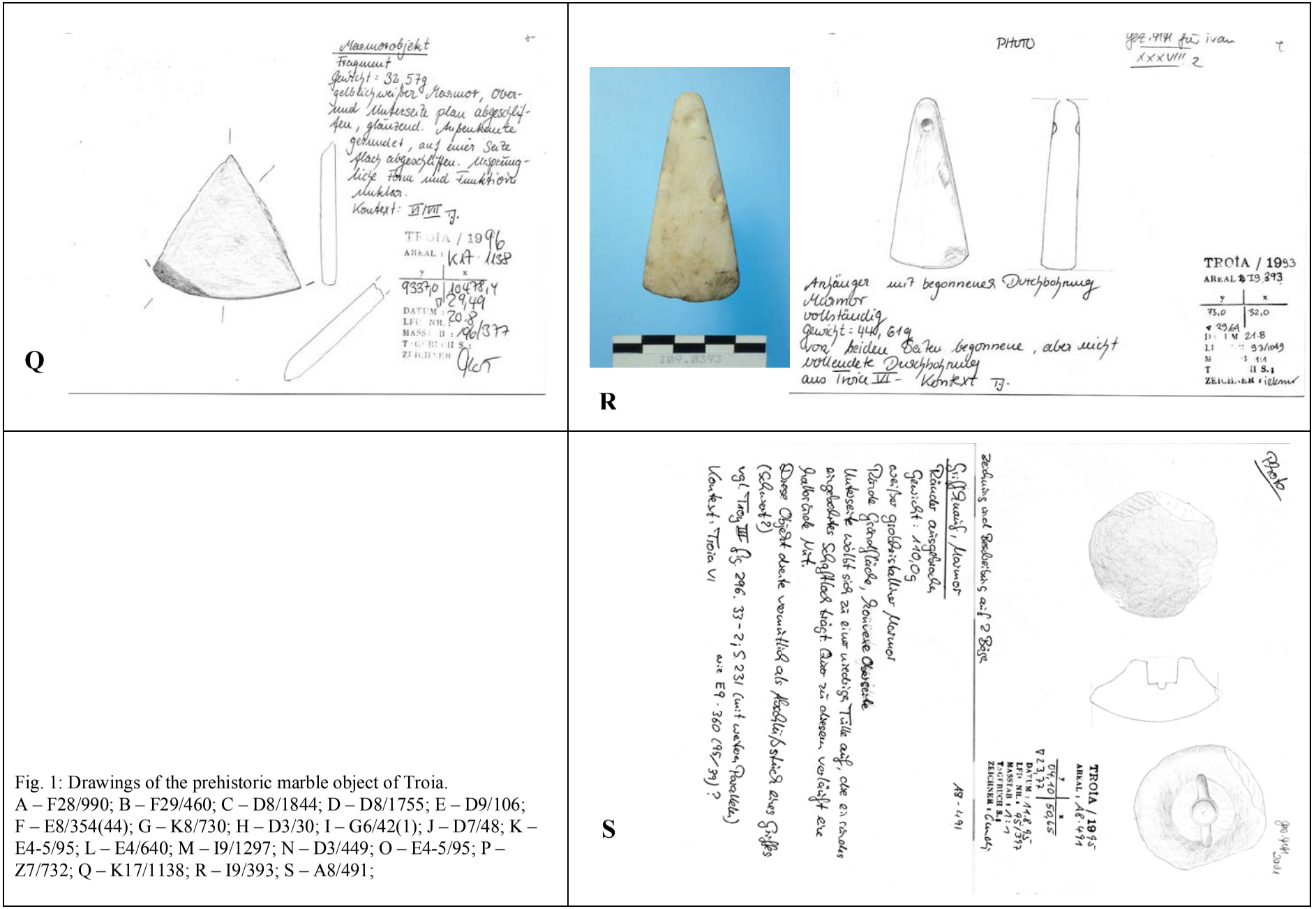

Fig. 1: Drawings of the prehistoric marble object of Troia.
A – F28/990; B – F29/460; C – D8/1844; D – D8/1755; E – D9/106; F – E8/354(44); G – K8/730; H – D3/30; I – G6/42(1); J – D7/48; K – E4-5/95; L – E4/640; M – I9/1297; N – D3/449; O – E4-5/95; P – Z7/732; Q – K17/1138; R – I9/393; S – A8/491;

Investigated archaeological objects of the Hellenistic and Roman periods

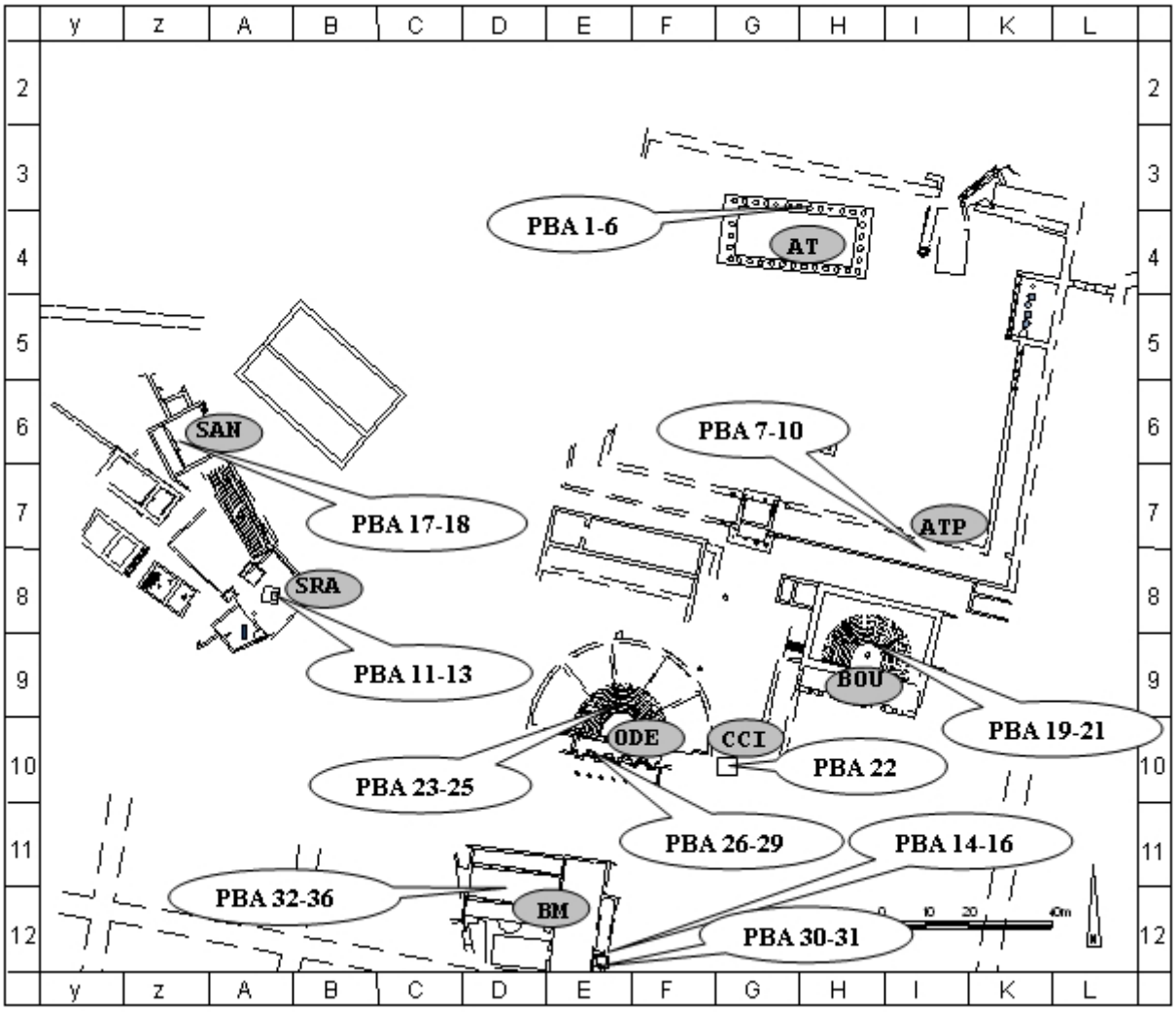

Fig. 2: Plan of Troia VIII and IX (after Troia project) with sampling. AT = Athena temple; ATP = Athena Temple Portico; BOU = Bouleuterion; SAN = Sanctuary; SRA = Sanctuary Roman Altar; BM = Bath moulding; ODE = Odeion; CCI = Children of Claudius Inscription

Fig. 3. a-b): Reconstruction of Athena Temple, 280 B.C. c) The platform of the Temple and d) fragment 'in situ' of coffered ceiling of the Athena Temple © Troia Project and CERHAS.

Fig. 5. Reconstruction and remains of Bouleuterion, 2nd century B.C. © Troia Project and CERHAS.

Fig. 4. Reconstruction of Athena Temple Porticus, 230 B.C. © Troia Project and CERHAS.

Fig. 6. Reconstruction of the Bath, Nympheum base moulding, late 2nd c. A.D. © Troia Project and CERHAS.

Fig. 7. Reconstruction and remains of the Odeion, early 2nd century A.D. © Troia Project and CERHAS.

APPENDIX B: BASICS OF THE ANALYTICAL METHODS

1. Quantitative fabric analysis (QFA)

For the QFA-technique, according to the classic approach of SCHMID *et al. (SCHMID et al. 1995; SCHMID et al. 1999a; SCHMID et al. 1999b)*, scanned thin sections were manually outlined for the grain boundaries. The grain boundary data set serves as the input of the numerical processing.

The main problem is that the computer programmes presently used are incapable of recognising the outlines of calcite crystal grains with the required accuracy. The starting point of the analysis is therefore the manual transformation of macroscopic images into a drawing produced from a statistically significant number of grains (at least 400), as shown in Figure 1.

Furthermore it is important to note that QFA technique (and also FA, see later) are influenced via the creation of the data set at the smallest grain scale: by the outlining of the crystal boundaries a cut-off effect exists, because below a given size the observer cannot follow the boundary lines; furthermore the automated processing filters out the very small crystals (Figure 2). The grain size histograms should be evaluated having this fact in mind.

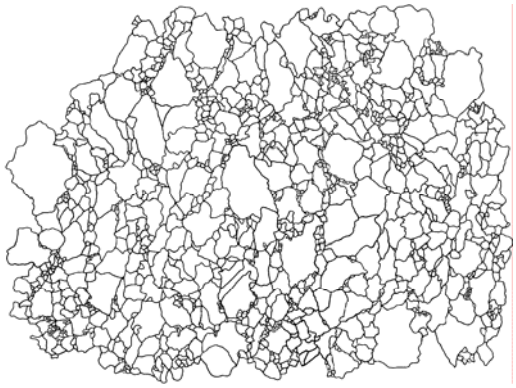

A

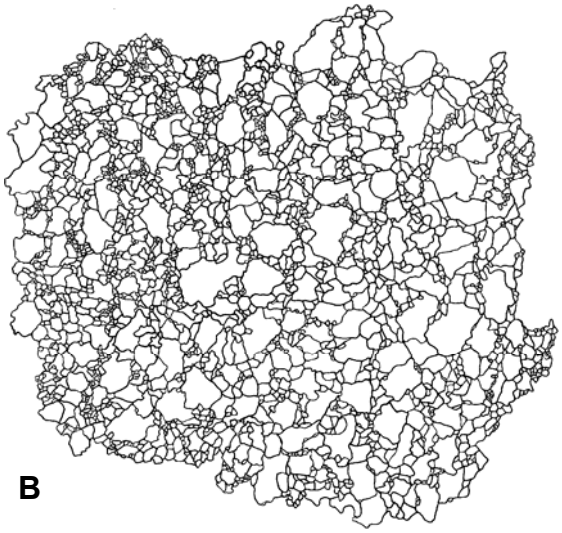

B

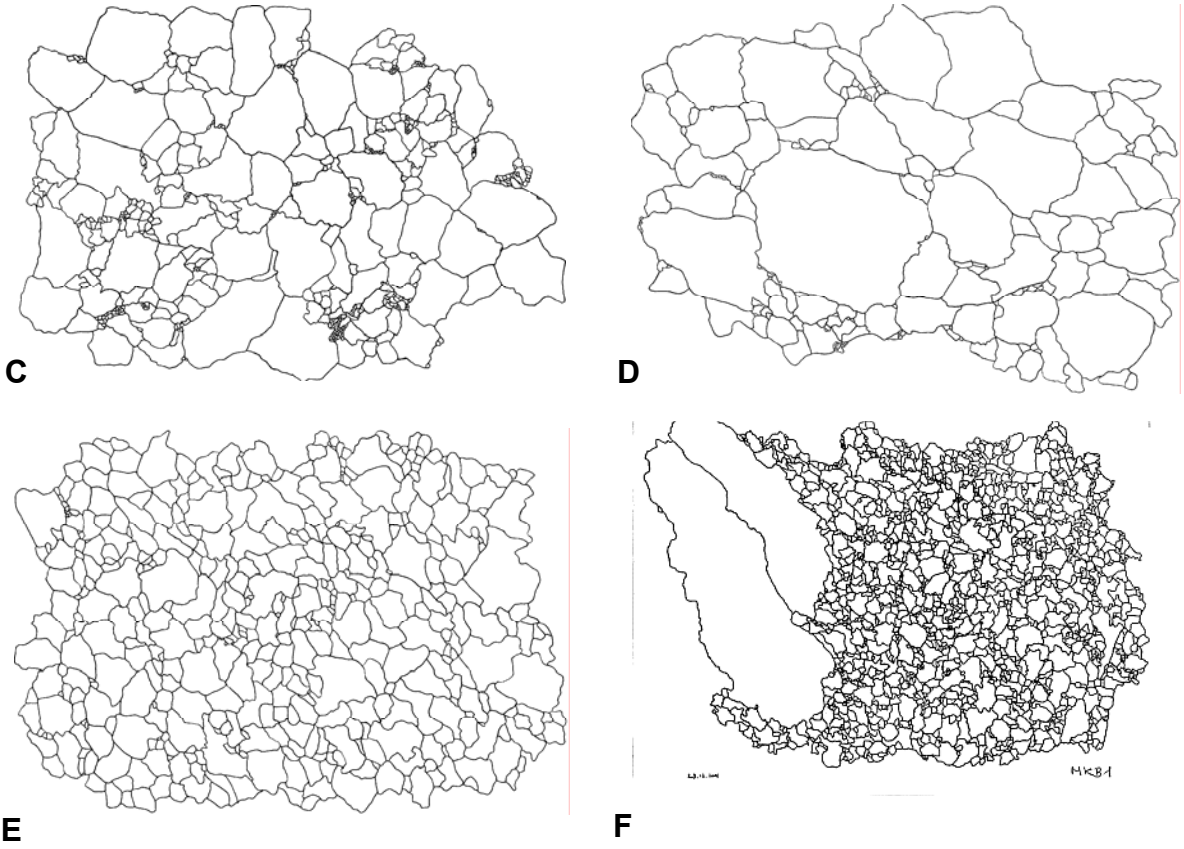

Figure 1: Examples of scanned thin sections which were manually outlined for the grain boundaries

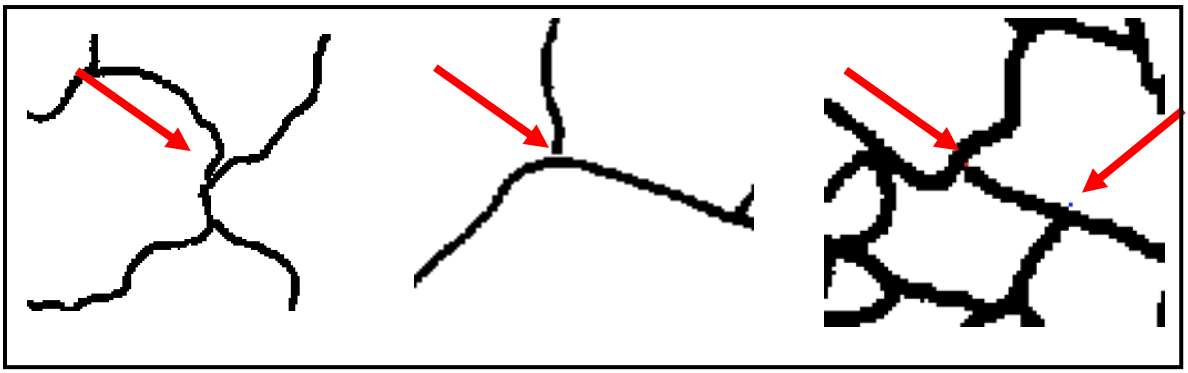

Figure 2: Results are influenced via the creation of the data set at the smallest grain scale

1.1. Grain size distribution and grain orientation

Similarly, to the method of PERUGINI *et al.* (2003) the grain boundaries were determined in an automated manner to avoid manual bias. To determine the most commonly used property, the *maximum grain size* (MGS; e.g., MOENS *et al.* 1988) the extents of all individual grains have to be calculated. The automatic derivation of geometric properties of the grains is more or less self-explanatory; however, the calculation of some parameters is needed to be explained in more detail. To determine the *maximum grain size (MGS)* the extents of all individual grains

have to be calculated. To this end, the maximum extent (*long axis*) is measured in the following way: The geometric shape of the grain is rotated with all possible angles and the bounding co-ordinate box is determined. The maximum length of this co-ordinate box defines the long axis. The appropriate rotation angle to maximise this extent is done by using the Brent method (BRENT 1973; PRESS *et al.* 1989). The *short axis* is given by the other (smaller) extent of the aforementioned bounding box, i.e., the short axis equals to the extent of the grain perpendicular to the direction in which the largest extent is measured. The *axial difference* is difference of the long axis and the short axis (SCHMID *et al.* 1995). The *shape factor* is the ratio of the convex hull perimeter to the grain perimeter. The direction of the long axis defines the *orientation* of the individual grain. Unfortunately, this direction cannot be fixed to an external reference, since the samples are not oriented. To make *orientation distribution* of the grains comparable to those of other samples a common reference should be defined. In our method we calculate the *mode of the orientation distribution* and this direction is treated as *reference orientation* for the individual sample. Having all the reference orientations and the orientation distribution of all samples, the distributions become comparable. However, if the grain pattern is dominated by less elongated grains, or the distribution is bimodal, the mode of the orientation distribution is not well defined, or may happen to be aligned with other maxima. Therefore, the reference orientation may become biassed or completely disorientated. In these cases the distributions, of course, are not comparable.
In the case of heteroblastic samples, which represent a considerable part of the studied sample set, the small grains are overrepresented in the grain distribution. Since the smaller grains are typically more rounded than larger ones because of geometrical reasons, their long axis determining the orientation is not well defined. Because of their numerical overrepresentation in the distribution this rather stochastic behaviour may cause a bias in the orientation distribution. Therefore, in case of heteroblastic samples the orientation distribution is less definite; consequently instead of the grain boundary approach a raster based fractal analysis is more feasible.

Here an important remark has to be made: although MGS is widely used in marble provenance, unfortunately, in some heteroblastic samples extraordinary big grains occur being not typical for the general fabric. A typical problem of the maximum grain size (MGS) determination is shown in Figure 1F. In such a case MGS is highly dependent on the selection of the thin section. To be statistically more robust, the lower 99 % range of the data (the interval that contains the smallest 99 %) is calculated, termed as $MGS_{99\%}$ (ZÖLDFÖLDI &

SZÉKELY 2004; ZÖLDFÖLDI & SZÉKELY 2005, 2008). There is typically a considerable difference between MGS and the more robust $MGS_{99\%}$ (sometimes a factor of 2!, see also Table 14). Since the MGS turned to be a good provenance indicator, it is important to make statistically more reliable (to minimise the effect of the random selection). Figure 3 demonstrates the statistical usefulness of the $MGS_{99\%}$ as the conventional MGS and the $MGS_{99\%}$ values are plotted versus the box dimension. There is a correlation between the MGS and box dimension, but the correlation is much better if we use $MGS_{99\%}$; the latter point data set form a more compact cluster around the trend line. The reason for that is the effective maximum grain size is slightly influenced by the random sample selection, therefore the spread of the examination points increases.

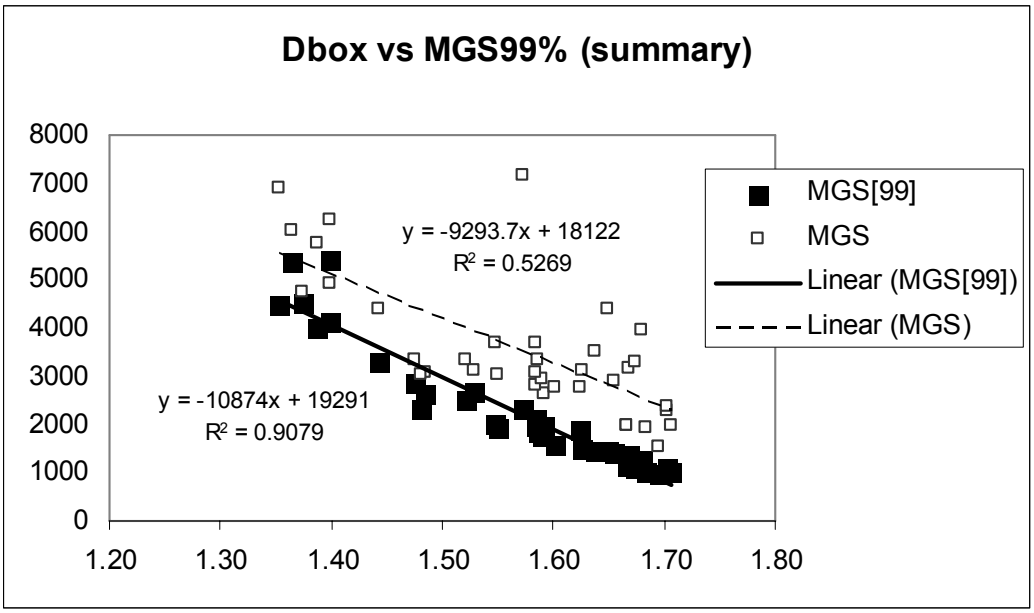

Figure 3: Conventional MGS and the MGS99% values versus the box dimension

The same consideration led to the definitions of 99% quantile of the grain area distribution, $MGA_{99\%}$, analogous to $MGS_{99\%}$. Similarly to the $MGS_{99\%}$, MGA and the $MGA_{99\%}$ values are plotted versus the box dimension. As we see also in the case of maximum grain size analysis, there is also a correlation between the MGA and box dimension, but the correlation is much better if we use $MGA_{99\%}$; the latter point data set form a more compact cluster around the trend line (Figure 4). PERUGINI *et al.* (2003) found of basic importance the distribution of the grain area. To characterize this distribution they introduced its standard deviation. (In their paper they denote it as σ, but to avoid confusion we denote it as σ_A.) To complete this

descriptive approach the *average grain area* (*AGA*) is considered as a reciprocal of the average grain density.

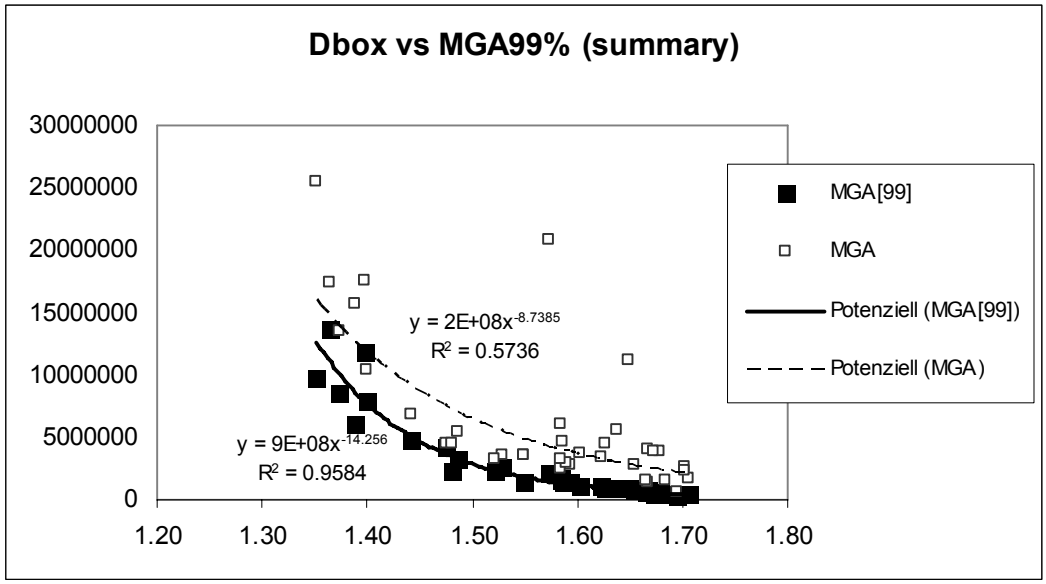

Figure 4: MGA and $MGA_{99\%}$ values versus the box dimension

1.2. Derivation of the fractal dimension related data

Fractal analysis is a new mathematical approach to the quantification of structural information on natural object. When applied to marble textures the method enables rigorous characterisation of textural relationships of calcite grains, and makes it possible to incorporate the spatial interconnections among grains and the geometrical features of the single grain in the fractal dimension calculation. In combination with quantitative fabric analysis (QFA), fractal analysis is a powerful tool in the discrimination of marbles from various occurrences given its high capability to resolve the convolution of the grain boundaries, which is a distinguishing textural feature of marbles.

Fractal geometry represents a major advance over previous methods for quantifying the complex patterns encountered in nature that where previously described only qualitatively (ROACH & FOWLER 1993). In contrast with classical Euclidean geometry, made up of regular and smooth shapes undergoing rigid laws of order and symmetry, fractal geometry applies to the description of complex and irregular phenomena and, in this respect, it is far closer to nature than Euclidean geometry. Many natural patterns are better characterized using fractal geometry and the importance of fractals has been recognized at every spatial scale in biotic

and abiotic processes (KENKEL & WALKER 1996). Some definitions are given to understand fractals and how fractal geometry can be used in studying natural objects.

Table 14: Some examples of the determined parameters. Note the factor more than 2 in the column MGS/MGS$_{99\%}$

	Sample name	*N*	*MGS (µm)*	*MGS$_{99\%}$ (µm)*	*MGS]/ MGS$_{99\%}$*	*MGA (µm²)*	*MGA$_{99\%}$ (µm²)*	*MGA/ MGA$_{99\%}$*
Afyon	A13	973	2756	1869	1.474	3393431	1088909	3.116
	A14	834	2655	1972	1.346	2792827	1358491	2.056
	A2	430	3138	2677	1.172	3550173	2652886	1.338
	A4-1	191	6881	4504	1.528	25440748	9755672	2.608
	A4-2	193	4744	4528	1.048	13476376	8481968	1.589
	A6-2	789	2816	2103	1.339	2436874	1615257	1.509
	A8	3061	1761	1158	1.521	1051255	541836	1.940
Babadag	BD1	237	3323	2868	1.159	4438615	4156647	1.068
	BD4	790	3070	2620	1.172	5397256	3201846	1.686
	BD6	459	3021	2325	1.300	4517816	2364587	1.911
Milas	Mi2	1013	3077	2000	1.539	3215470	1531565	2.099
	Mi3-2	1247	3018	1940	1.556	3509450	1467468	2.392
Mugla	M2-1	248	5777	4008	1.441	15627284	6114207	2.556
	M2-2	140	6004	5384	1.115	17421016	13708807	1.271
	M4	697	3324	2485	1.338	3228381	2293828	1.407
	M7	189	4929	4125	1.195	10468921	7893137	1.326
	M8	945	3683	2025	1.819	3644703	1386704	2.628
Kazdag-South	K15	1408	3357	1835	1.829	4586329	1380164	3.323
	K18	2471	3516	1464	**2.401**	5600829	916444	**6.111**
	K21	2763	2269	1016	**2.233**	2677303	388794	**6.886**
Kazdag-Nord	K1	1948	2942	1759	1.673	3000754	1373589	2.185
	K2	2260	3938	1260	**3.125**	3813369	563370	**6.769**
	K3	1347	7164	2325	**3.082**	20834267	2172188	**9.591**
	K4	514	4390	3303	1.329	6785673	4878332	1.391
	K7	634	6246	5397	1.157	17633107	11802889	1.494
	AyazmaA	2589	4415	1462	**3.019**	11115754	947649	**11.730**
Marmara	Ma3	1605	3695	2072	1.783	6093962	1734591	3.513
	Mar1a	1475	2757	1566	1.761	3762435	1118193	3.365
	BAN1b	2512	1990	1143	1.741	1383168	545388	2.536
	ZTM2-2	3952	3160	1360	**2.323**	4023047	810518	**4.964**
	ORH2c	4002	3290	1113	**2.956**	3871332	542595	**7.135**

A fractal is an ´object´ whose shape is irregular and/or fragmented at all scales. Mathematically, a fractal is defined as a set for which the Hausdorff-Besicovich dimension (or fractal dimension D) strictly exceeds the Euclidean dimension, D_E, which is always an integer (MANDELBROT 1982). A basic property of fractals is their ´scaling´ behaviour (self similarity). Self similarity implies that every part of the object is a reduced version of the whole. Two classes of fractals exist: ´mathematical` and `natural` fractals. In mathematical fractals, theirs self similarity property is assumed to hold good for the entire spectrum of time or space scales. In natural fractals, which are encourted in nature and which are the primary

concern of this chapter, small- and large-scale constrains usually confine the self similarity property to a finite range of scales.

Analyses of fractal natural objects are carried out by estimating their fractal dimension (e.g. MANDELBROT 1982; TURCOTTE 1997). From this point of view fractals are helpful to quantify "object" that cannot be adequately quantified using classical concepts such as marble textures. Conventionally the result of the fractal analysis is a single number, the fractal dimension. There are several methods to determine its value, e.g., box dimension, mass dimension and information dimension methods (TURCOTTE 1997). However, in our experience not all the samples behave as a simple fractal, some of them show tendency to multifractality (e.g., (TURCOTTE 1997). It seems feasible to evaluate the individual points on the log-log plot and determine further parameters. A common problem of the box dimension calculation comes from the limited size of the sample; larger boxes sometimes do not fit into the framework of the sample. To avoid this problem PERUGINI *et al.* (2003) applied a thoroidal approach linking the opposite side of the sample together. We overcome this problem in a more sophisticated way: during the box counting the sample is rotated to increase the number of fitted boxes. The result of this calculation phase is the maximum number of boxes which constitutes one point for the log-log plot. A further advantage of this calculation that the tendency for multifractality can be better observed. From a single fractal calculation three parameters are determined: D, k, σ_D. D is the fractal dimension derived from the slope of the regression line; k is the coefficient of the expression: $M(L) = k \cdot L^D$; e.g., PERUGINI *et al.* (2003); and σ_D the standard deviation of D. The latter parameter is found to be important (e.g. ZÖLDFÖLDI & SZÉKELY 2008), because it shows the tendency towards multifractality, the higher the value the stronger the multifractality (Figure 5).

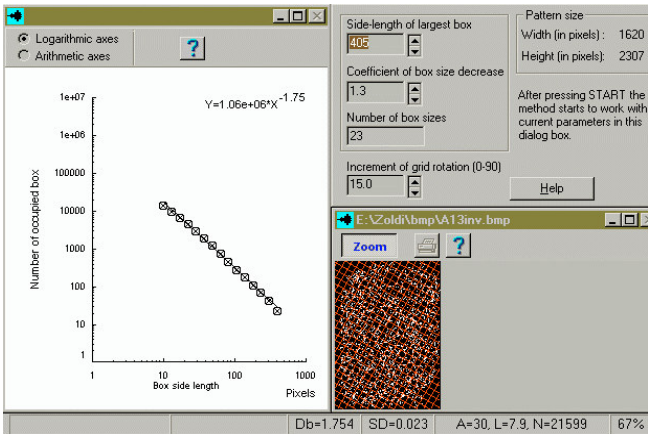

Figure 5: The calculation of the simplest fractal dimension type, the box counting method was used (*e.g.*, (TURCOTTE 1997): the number of black pixels is calculated for increasingly big squares. These numbers are plotted in a log-log plot; usually we get a straight line (simple fractal distribution). The parameter of this line gives the fractal dimension of the image.

2. Cathodoluminescence investigation (CL)

2.1. The principles of the method

Many minerals display luminescence when excited with different type of radiation, such as electron beam, (cathodoluminescence = CL), X-rays (radioluminescence = RL), visible or ultraviolet light (photoluminescence = PL), heat (thermoluminescence = TL), or an ion beam (ionoluminescence = IL). This chapter will focus on CL, because most carbonate geologists use these excitation methods.

2.1.1. Excitation and luminescence

Excitation and luminescence involve electronic transitions between energy levels of atoms or ions. The fundamental excitation and emission process is illustrated in Figure 1. The horizontal lines represent energy states of electrons in an atom or ion of a hypothetical host crystal, or in an impurity hosted in the crystal, functioning as an activator of luminescence. Thereby, E-0 is the ground state, and E-1 to E-4 represent higher, unoccupied energy states. In case of insulators, such as carbonates, E-0 corresponds to a filled electron band, and all the elevated energy states are above the valence band but below the conduction band. In insulators, the energy gap between the valence and conduction bands is large, i.e., greater than about 3.0 eV. In case of semiconductors and photoconductors, the band gap is narrow, i.e., smaller than about 3.0 eV, and the elevated states are below and/or within the conduction band.

If the energy gap between the excited level and an adjacent lower level is small, the electron in the excited state tends to decay non-radiatively by phonon emission (releasing energy as heat). Luminescence, i.e., radiative decay, is caused by a transition from a higher to a lower energy level accompanied by emission of a photon (light). Luminescence only occurs if the gap to the adjacent lower level is larger than a ´critical value´.

In case of most insulators, such as calcite or dolomite, the band gap between the filled electron band (E-0) and the adjacent unfilled electron band corresponds to the energy of an ultraviolet photon. Hence, visible light is not absorbed, and visible luminescence is not expected from the pure, optically inert crystals. The pure substance, therefore, is colorless, transparent, and non-luminescent (in short: optically inert). Such is the case for pure calcite. However, pure insulators may display ´intrinsic´ luminescence that is caused by lattice defects. In case of calcite, it is an extremely faint blue luminescence. Intrinsic luminescence is

visible only with high excitation energy and/or at low temperature, and if there are no activators in appreciable amounts in the lattice to mask it.

Fehler! Es ist nicht möglich, durch die Bearbeitung von Feldfunktionen Objekte zu erstellen.

Figure 1: The process of excitation (absorption) and emission (luminescence) in a hypotethycal substance having the electronic energy levels (energy increasing from E-0 to E-4, not to scale). (After MACHEL *et al.* 1991)

Numerous optically inert substances host optically active impurities. Many impurities are optically active because they have ground states that have only partially filled electron bands (orbitals), and the adjacent electronic levels are separated by gaps that correspond to photons of visible or infrared light. Such is the case for transition elements, e.g., Mn^{2+} or Cr^{3+}. Hence, visible luminescence is expected from these impurities. In general, the luminescence of insulators is usually caused by excitation and emission by impurities and, subordinately, lattice defects (collectively called luminescence centres).

2.1.2. Activation by transition and rare earth elements

Generally, if an impurity is an activator in one mineral, it is an activator in every mineral. Common activators in binary oxides are Mn^{2+}, Mn^{4+}, Ag^{+}, Sn^{2+}, Sb^{3+}, Tl^{+}, Pb^{2+}, Cr^{3+}, and a large number of rare earth elements (NICHOLS *et al.* 1928; CURIE 1963; JOHNSON 1966; IMBUSCH 1978). The exact position of the energy bands of an activator depends on the symmetry of coordination of the activator, which depends on the nature and distance of the coordinating atoms/ions. In oxygen-dominated hosts, the coordination of activators usually is octahedral.

In contrast to luminescence activated by transition element, the emission spectra of rare earth elements do not depend, or only an insignificant degree, on their coordination. This is because luminescence of rare earth elements is caused by energy transitions of shielded electrons in the inner, unfilled 4f shell, not by transitions of the outer shell electrons.

2.1.3. Sensitization

Sensitization can be considered as the absorption of energy by an impurity (sensitizer) with subsequent transfer of absorbed energy to an activator (Figure 2).When all of the energy absorbed by the sensitizer ions is transferred to activator ions, the sensitizer is spectroscopically unrecognizable. On the other hand, a sensitizer may itself be an activator and emit its own characteristic luminescence (e.g., Ce3+ in calcite; GIES 1975; BLASSE &

AGUILAR 1984) if not all of the excited sensitizer ions transfer their activation energy to the activator ions. Sensitization occurs by two basic mechanisms: i) resonance transfer between atoms/ions and ii) reabsorption of emission. Sensitization may occur following any type of excitation because resonance transfer does not depend on the initial mode of excitation.

Fehler! Es ist nicht möglich, durch die Bearbeitung von Feldfunktionen Objekte zu erstellen.

Figure 2: A senzitizer (S) absorbs excitation energy and becomes excited. Because of the electromagnetic coupling between senzitizer and activator (A), the senzitizer transmits ist excitation energy to the activator, which become excited and emits luminescence with ist own, characteristic wavelength(s). (After (MACHEL *et al.* 1991).

2.1.4. Quenching

Quenching is the suppression of activator luminescence by impurities (quenchers) that ´trap´part or all of the absorbed energy. Energy is transferred from activators to quenchers in a manner similar to that illustrated in Figure 3 for closely spaced activators. Excited quenchers decay by multiphonon or infrared emission, rather than by emission of visible light. This occurs because the energy levels of these ions, particularly the energy gap between the ground state and the first excited state, are too close to one another to facilitate radiative transitions in the visible range. Elements that act as quenchers in carbonates and most other oxygen-dominated minerals are Fe^{2+}, Co^{2+}, Ni^{2+}, and others. Fe^{3+} is a quencher in some minerals, including carbonate, but an activator in others. Quenching, as activation and sensitization, involves intracrystalline energy transfer that is independent of the type of excitation.

Fehler! Es ist nicht möglich, durch die Bearbeitung von Feldfunktionen Objekte zu erstellen.

Figure 3: When activator concentration is low, excitation/absorption and emission take place on the same ion (left). When the activator concentration is high, the absorbing ion may transfer ist excitation energy to another similar ion rather than emit luminescence. The excitation energy may be transferred to many ions, and eventually may be trapped at a sink (black) where it is dissipated as heat. (After (MACHEL *et al.* 1991).

2.1.5. Emission intensity

Emission intensities depend mainly on two factors: i) the concentration of activators, sensitizers, and quenchers; and ii) the type of excitation. CL, RL, and PL result in different emission intensities, and long-wavelength to visible light generally will not lead to luminescence. This is because the absorption bands of pure insulators and many activators and sensitizers are in the ultraviolet part of the spectrum, and/or the absorption band is extremely weak for low-energy ultraviolet light because the corresponding transition is

forbidden (as in the case of Mn^{2+}). Consequently, in carbonate, only short-wave ultraviolet light excitation of less than about 260 nm yields all emission lines, excitation with wavelengths between 260-285 nm will yield most emission lines, and excitation with wavelengths longer than about 285 nm will yield few or none. This is in accordance with observation that non-sensitized Mn^{2+}-activated luminescence in calcite is weak with intermediate to long-wave ultraviolet light excitation, whereas non-sensitized Mn^{2+}-activation is strong with electron excitation.

Where several activators are present, CL will have not only a different intensity, but also a difference in the visible colour. This is caused by the relative redistribution of emission band/peak heights.

The activator concentration is important to luminescence intensity in two ways:

i) Firstly, it determines the luminescence detection limit. There has to be a certain minimum activator concentration for luminescence to be detectable by the human eye because the emission intensity depends on the number of activator ions raised to an excited state, and on the probability that an ion raised to an excited state will decay by emission of light. Intensities below this threshold cannot be seen (or instrumentally detected). The effective minimum concentration varies from activator to activator and from host crystal to host crystal, from instrument to instrument, and from eye to eye.

ii) Secondly, the activator concentration determines concentration quenching and extinction. Generally, the higher the concentration of an activator, the higher the luminescence intensity (if other variables, such as temperature, beam current and density, are held constant). This is because emission intensities are additive, at least where the luminescence centers are spaced widely enough so that they act independently, without significant energy transfer between them.

There are two types of traps. One is similar activator ions whose electron states are ´perturbed´ by presence of an adjacent impurity or by lattice defects (IMBUSCH 1978). If sufficiently perturbed activator ions may no longer have an energy gap larger than the critical value, thus the energy transferred to them is lost as heat. This constitutes concentration quenching. The other type of trap is dissimilar impurities, i.e., quencher elements.

2.1.6 Experimental evidence for CL of calcite and dolomite

It is generelly acknowledged that the most important activator of luminescence in natural calcite and dolomite is Mn^{2+}, and the most important quencher of Mn^{2+}-activated luminescence is Fe^{2+} (MACHEL 1985; MARSHALL 1988).

i) the minimum concetration of each activator sufficient to produce visually detectable emission;

ii) the quantitative relationship between activator concentration and intensity (in the absence of quanchers);

iii) the importance of activators other than Mn^{2+} in natural carbonates;

iv) the importance of sensitizers in natural carbonates;

v) the role of lattice defects in causing or modifying emission;

vi) the quantitative effects of Fe^{2+} and Fe^{3+} in quenching;

vii) the concentrations of Fe^{2+} and Fe^{3+} at which visual extinction of Mn^{2+}-activated luminescence in carbonates occurs.

2.1.7. The roles of Mn and Fe in natural calcite and dolomite

Although it appears that Mn^{2+} and Fe^{2+} are the main elements involved in the luminescence of natural carbonates, the quantitative dependence of CL on their concentrations is controversal. There has been little, and partially inconsistent, quantitative work demostrating the dependence of emission intensity on Fe/Mn-ratio, or on the absolute Mn and Fe-concentration (MACHEL 1985; MASON 1987). Other studies (PAGEL *et al.* 2000; GÖTZE 2000) suggest how spectrophotometric determination can aid in obtaining this information (Figure).

The necessary first step in constraining CL fields to establish Mn-Fe compositions at which luminescence may be expected was done by MACHEL *et al.* (1991).

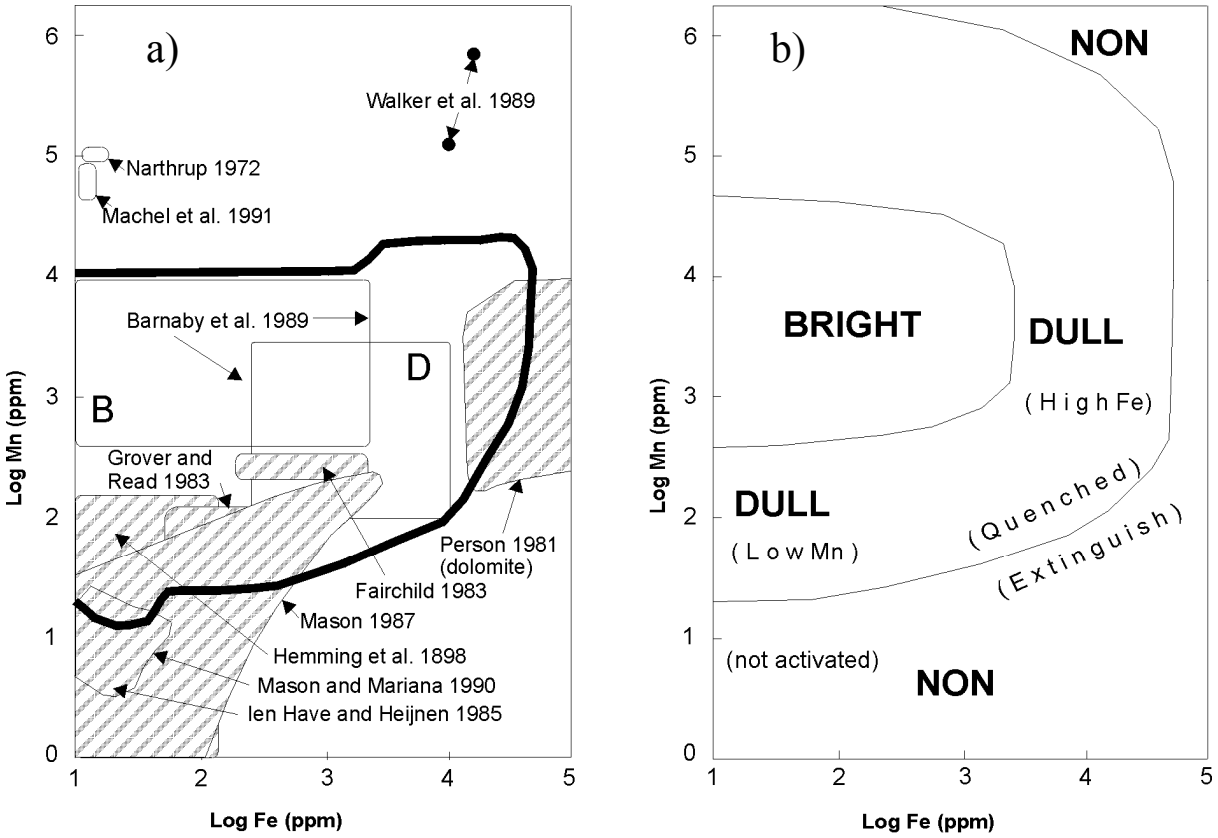

Figure 4: The diagram on the left side (a) is compiled from the sources noted on the figure. The heavy solid line encloses a field denoting Fe-Mn compositions where luminescing calcite and dolomite have been observed. The shaded fields (labelled by author) denote Fe-Mn compositions where the absence of CL has been observed. B and D denote BRIGHT and DULL CL ranges compiled by BARNABY & RIMSTIDT (1989). Diagram b shows the interpretation of the data in diagram a showing the regions for NON, BRIGHT and DULL CL.

Figure 4 is a compilation of data from the literature pertaining mostly to CL, and assuming that only Fe and Mn are involved in controlling the luminescence – obviously, this assumption is a gross oversimplication of CL in natural carbonates, but it is appropriate in the absence of sufficient experimental data on the other elements. Figure 4 is an interpretation by MACHEL *et al.* (1991) of the data presented in Figure . The heavily outlined unshaded region in Figure 4 encloses the composition of natural calcite and dolomite in which CL emission was observed. The shaded regions enclose composition in which NON luminescence was recorded (labelled with author). The regions in Figure 4 can be used to define approximately the position of fields of NON, BRIGHT, and DULL CL. At Mn concentration around 15-20 ppm and Fe concentration below approximately 200 ppm, it is not yet clear whether the Fe content exerts an observable influence on the intensity of luminescence, or whether the Mn content is more important. MACHEL *et al.* (1991) suspect that the latter is true, and that Fe-quenching of Mn2+-activated CL begins near 200 ppm. Accordingly, the lower limiting line for luminescence, separating the NON and DULL fields at ca. 15 ppm, is shown as being

almost independent of Fe up to approximately 200 ppm Fe. This is consistent with the CL observations of MASON (1987) that Mn content has more influence on CL than Fe content when the latter is below about 1000 ppm. With increasing Fe content, the limiting line for luminescence is shown sloping upwards, as though it was a function of the Fe/Mn ratio, coincident with the boundary of the data in Figure . This type of behaviour is consistent with the views of MACHEL (1979), PIERSON (1979, 1981), and FRANK *et al.* (1982) who asserted that the Fe/Mn ratio (rather than an absolute Fe concentration) controls the intensity of carbonate luminescence, and its extinction. There do not appear to be any data for calcite or dolomite with only a few tens of ppm Mn and several hundreds to thousand of ppm Fe, probably because of the common positive correlation between these elements in natural carbonates. With increasing Mn content, DULL CL changes to BRIGHT CL due to an increase in the activator concentration without significant quenching. The data plotted in Figure 4 suggest that the DULL to BRIGHT boundary is located at about 400 ppm Mn and nearly independent of Fe content up to about 2000 ppm Fe.

3. Carbon and oxygen isotope analyses

Like most elements, carbon and oxygen consist of mixtures of isotopes, one of which is greatly prevalent with respect to the others. Carbon consists of isotopes ^{12}C and ^{13}C in the average proportions of 98.89% and 1.11%, while oxygen is made up of a mixture of three isotopes ^{16}O, ^{17}O and ^{18}O with proportions of 99.76%, 0.037% and 0.204% respectively. Radioactive isotopes, although not relevant in this context, are often present alongside stable isotopes, ^{14}C being a well-known example. They have different half-lives and concentrations that depend, in a quite complex manner, on nuclear formation processes and the age of the material. They form the basis of many dating methods.

3.1. The principles of stable isotope analysis

The isotopic ratio (δ) obtained is given in parts per mil (‰ i.e. per thousend) relative to the PDB standard (CRAIG 1957), where

$$d = \frac{(R_{Sample} - R_{PDB}) \times 1000}{R_{PDB}}$$

and

$$R = {}^{13}C/{}^{12}C \text{ or } {}^{18}O/{}^{16}O$$

Controls of the isotopic composition of oxygen and carbon in a rock are principally through temperature, chemical composition, and isotopic ratios of water. The processes involved are after HERZ (1988a) and FAURE (1986) the following:

i. mode of origin, either as a chemical precipitate or as a „hash“ of organic shell fragments or a mixture of both, and composition of the cements;
ii. isotopic composition of water associated with the carbonate minerals during their formation and later history;
iii. temperature of metamorphism which converted the limestone into marble and the extent of reactions and fractionation with adjacent rocks and with pore waters; and
iv. later weathering history.

In this way marble from a given region formed at a particular time with ist own geological history may develop unique isotopic characteristics.

Uniform isotopic compositions, necessary for viable geochemical signatures, should obtain over a wide area if

i. the protolith was deposited and underwent diagenesis in a uniform environment;
ii. isotopic equilibrium was attained and maintained during formation for metamorphism;
iii. the marble unit is homogeneous – preferably almost pure carbonate – and thick;
iv. the metamorphic gradient was not too steep.

High $\delta^{13}C$ values in limestone and marble indicate a substantial contribution by inorganic CaCO3, either detrital or as a chemical precipitate. Values over 4 ‰ in Paros and Ephesos marbles are attributable to an inorganic mode of origin. The high translucency and uniform texture of the Parian is consistent with such an origin. A high variation in $\delta^{13}C$ values in many marbles may be largely due to their being origin and their geological history. A difference of over –6‰ is seen in carbonates forming at near 0 ºC at the ocean bottom compared to 30 ºC close to the surface (FAURE 1986).

Large isotopic variations in marble appear to be due to:

(i) exchange between the carbonate minerals and silicates or oxides within the marble or near its contact with other formations;
(ii) a steep metamorphic gradient; or
(iii) weathering.

With pure white marble, (i) is not a common problem except near formation contacts. With metamorphism of the limestone to marble, $\delta^{18}O$ decreases, the amount depending on the temperatures reached. Where metamorphism was widespread, the marble bed thick and pure carbonate, temperatures uniform, and equilibrium attained, $\delta^{18}O$ values will be relatively uniform. When the metamorphic gradient was very steep, as on Naxos with a horizontal gradient of 30 ºC per km (RYE *et al.* 1976), values will vary widely and may fall into separate $\delta^{18}O$ fields. The effects of equilibration between carbonates and silicate minerals in adjacent schist beds is seen around Apollonas (HERZ 1988b): differences in $\delta^{18}O$ of about –6‰ obtained from the centre of a 20 m thick marble bed to its contact with schist.

Weathering, especially in a humid environment, can affect isotopic ratios. Pieces with different weathering histories (e.g., one buried in a well, another in soil, and a third used in a wall) will exchange oxygen with water of different compositions and show quite different

values. Fresh marble compared to material weathered for less than 50 years in the same block shows differences of up to 0.7‰ in oxygen, but less than 0.2 ‰ in carbon (HERZ 1987).

Oxygen isotopic compositions of the oceans changed through geological time. Limestones will have isotopic compositions, which reflect the seawater composition of the time of deposition. In a quarry where marble beds of different ages are in contact, separate isotopic data fields may result, inherited from their original limestone. This might be the explanation for the two distinct fields for Doliana in a region of extensive tectonism.

4. $^{87}Sr/^{86}Sr$ isotope ratio analyses

4.1. Basics of radiogenic isotope geochemistry

The basic equation of radioactive decay is:

$$\frac{dN}{dt} = -\lambda N$$

λ is the decay constant, which we defined as the probability that a given atom would decay in some time dt. It has units of time^{-1}. Let´s rearrange equation before and integrate:

$$\int_{N_0}^{N} \frac{dN}{N} = \int_{0}^{t} -\lambda dt$$

Where N_0 is the number of atoms of the radioactive, or parent, isotope present at time t=0. Integrating, we obtain:

$$\ln \frac{N}{N_0} = -\lambda t$$

This can be expressed as:

$$\frac{N}{N_0} = e^{-\lambda t}$$

Suppose we want to know the amount of time for the number of parent atoms to decrease to half the original number, i.e. t when N/N_0 = ½. Setting N/N_0 to ½, we can rearrange the last equation to get:

$$t_{1/2} = \frac{\ln 2}{\lambda}$$

This is the definition of the *half-life*, $t_{1/2}$.

Now the decay of the parent produces some daugther, or *radiogenic*, nuclides. The number of daughters produced is simply the difference between the initial number of parents and the number remaining after time t.

$$D=N_0-N$$

Rearranging to isolate N_0 and substituting that, we obtain:

$$D=Ne^{\lambda t}-N=N\,(e^{\lambda t}-1)$$

This tells us that the number of daughters produced is a function of the number of parents present and time. Since in general there will be some atoms of the daughter nuclide around to begin with, i.e., when t=0, a more general expression is:

$$D=D_0+N(e^{\lambda t}-1)$$

Where D_0 is the number of daughters originally present.
Let´s now write equation using the example of ^{87}Rb to ^{87}Sr:

$$^{87}Sr = {}^{87}Sr_0 + {}^{87}Rb(e^{\lambda t} - 1)$$

As it turns out, it is generally much easier, and usually more meaningful, to measure to ratio of two isotopes than the absolute abundance of one. Therefore, it will measure the ratio of ^{87}Sr to a non-radiogenic isotope, which by convention is ^{86}Sr. Thus the useful form is:

$$\frac{^{87}Sr}{^{86}Sr}=\left(\frac{^{87}Sr}{^{86}Sr}\right)_0+\frac{^{87}Rb}{^{86}Sr}\left(e^{\lambda t}-1\right)$$

This equation is a concise statement of Sr isotope geochemistry.

4.2. High-resolution stratigraphy with strontium isotopes

At any instant in time the ^{87}Sr/ ^{86}Sr ratio is essentially uniform throughout the world ocean, the average ^{87}Sr/ ^{86}Sr ratio is 0.7094 ± 0.0012 at the present time (at the 95 % confidence level), but over the course of geologic time the isotopic composition of marine strontium has varied in resonance to changing inputs of the two isotopes (BRASS 1976).
In a given chemical system the isotopic ratio of ^{87}Sr/ ^{86}Sr is determined by four parameters:

(i) the isotopic abundance at the time of calcite formation,
(ii) the Rb/Sr ratio of the system,
(iii) the decay constant of ^{87}Rb to ^{87}Sr, and
(iv) the time elapsed since the formation of calcite.

Local differences in the Rb/Sr will, with time, result in local differences in the abundance of ^{87}Sr. Mixing of material during recrystallisation will tend to homogenise these local variations (GAST 1955, 1960).

One interesting and useful feature of this system arises from the long residence time of Sr in seawater and its ready substitution in calcium carbonate. Because of its long residence time, the $^{87}Sr/^{86}Sr$ ratio of seawater is homogeneous at any given time. The $^{87}Sr/^{86}Sr$ ratio of seawater is controlled by the relative input of Sr from the continents and ridge-crest hydrothermal activity. The ratio of these will vary with mean spreading rate, erosion rates, and plate geometry. The variation of $^{87}Sr/^{86}Sr$ in seawater through the Phanerozoic has been determined from the analysis of carbonate and phosphate fossils (PETERMAN *et al.* 1970; PALMER & ELDERFIELD 1985; HESS *et al.* 1986), so that ages can be determined simply by determining the $^{87}Sr/^{86}Sr$ ratio of marine carbonate precipitated from seawater and comparing these values to the published Sr-evolution curves.

ANDERSON, T. F. & ARTHUR, M. A. 1983. Stable Isotopes of oxygen and their application to sedimetologic and paleoenviromental problems. *Stable Isotopes in Sedimentary Geology, SEPM Short Course. No10, Dallas.*
BARNABY, R. J. & RIMSTIDT, D. J. 1989. Redox conditions of calcite cementation interpreted from Mn and Fe contents of authigenic calcites. *Geological Society of America Bullettin,* 101**,** 795-804.
BLASSE, G. & AGUILAR, M. 1984. Luminescence of natural calcite (CaCO3). *J. of Luminescence,* 29**,** 239-241.
BRASS, G. W. 1976. The variation of the marine 87Sr/86Sr ratio during the Phanerozoic time: interpretation using a flux model. *Geochimica et Cosmochimica Acta,* 40**,** 721-730.
BRENT, R. P. 1973. Algorithms for Minimization without Derivates. *In:* ENGLEWOOD CLIFFS, N. J. (ed.) *Prentice-Hall.*
CRAIG, H. 1957. Isotopic standards for carbon and oxygen and correction factors for mass-spectrometric analysis of carbon dioxide. *Geochimica et Cosmochimica Acta,* 12**,** 133-149.
CURIE, D. 1963. *Luminescence in crystals,* New York, Wiley. -332 pp.
FAURE, G. 1986. *Principles of Isotope Geology,* New York, John Wiley & Sons. 589 pp.
FRANK, J. R., CARPENTER, A. B. & OGLESBY, T. W. 1982. Cathodoluminescence and composition of calcite cement in the Taum Sauk limestone (Upper Cambrian), southeatern Missouri. *J. Sediment. Petrol.,* 52**,** 631-638.
GAST, P. W. 1955. Abundance of 87Sr during geologic time. *Bull. Geol. Soc. Am.,* 66**,** 1449-1454.
GAST, P. W. 1960. Alkali metals in stone meteorites. *Geochimica et Cosmochimica Acta,* 19**,** 1-4.
GIES, H. 1975. Activation possibilities and geochemical correlations of photoluminescing carbonates, particularly calcites. *Mineralogy Deposita,* 10**,** 216-227.
GÖTZE, J. 2000. *Cathodoluminescence microscopy and spectroscopy in applied mineralogy,* Freiberg, TU Bergakademie Freiberg pp.
HERZ, N. 1987. Carbon and oxygen isotopic ratios: a data base for classical Greek and Roman marble. *Archaeometry,* 29**,** 35-43.
HERZ, N. 1988a. Geology of Greece and Turkey: Potential marble source regions. *In:* HERZ, N. & WAELKENS, M. (eds.) *Classical Marble: Geochemistry, Technology, Trade.* Dordrecht: Kluwer Academic Publishers. 7-10.
HERZ, N. 1988b. The oxygen and carbon isotopic data base for classical marble. *In:* HERZ, N. & WAELKENS, M. (eds.) *Classical Marble: Geochemistry, Technology, Trade.* Dordrecht: Kluwer Academic Publishers. 305-314.
HESS, J., BENDER, M. L. & SCHILLING, J. G. 1986. Evolution of the ratio of strontium 87 to strontium 86 in seawater from Cretaceous to present. *Science,* 231**,** 979-984.
IMBUSCH, G. F. 1978. *Inorganic luminescence*. 1-92 pp.
JOHNSON, P. D. 1966. *Oxygen-dominated lattices*. -287-337 pp.
KENKEL, N. C. & WALKER, D. J. 1996. Fractals in the biological sciences. *Coenoses,* 11**,** 77-100.
MACHEL, H. G. 1985. Cathodoluminescence in calcite and dolomite and its chemical interpretation. *Geoscience Canada,* 12**,** 139-147.
MACHEL, H. G., MASON, R. A., MARIANO, A. N. & MUCCI, A. 1991. *Causes and measurements of luminescence in calcite and dolomite*. -172-173 pp.
MANDELBROT, B. 1982. *Fractal Geometry of Nature,* New York, W.H. Freeman & Co pp.
MARSHALL, D. J. (ed.) 1988. *Cathodoluminescence of geological materials,* Boston: Unwin-Hyman. -143 pp.
MASON, R. A. 1987. Ion microprobe analysis of trace elements in calcite with an application to the cathodoluminescence zonation of limestone cements from the lower carboniferous of south wales. *Chem. Geol.,* 64**,** 209-224.
MOENS, L., ROOS, P., RUDDER, J., PEAPE, P., VAN HENDE, J. & WAELKENS, M. 1988. A multi-method approach to the identification of white marbles used in Antique artifacts. *In:* HERZ, N. & WAELKENS, M. (eds.) *Classical Marble: Geochemistry, Technology, Trade.* Dordrecht: Kluwer Academic Publishers. 243-250.
NICHOLS, E. L., HOWES, H. L. & WILBER, D. T. 1928. *Cathodo-luminescence and the luminescence of incandescent solids,* Washington. -350 pp.
PAGEL, M., BARBIN, W., BLANC, P. & OHNENSTETTER, D. (eds.) 2000. *Cathodoluminescence in Geosciences,* Berlin - Heidelberg - New York: Springer. 514 pp.
PALMER, M. R. & ELDERFIELD, H. 1985. Sr isotopic composition of sea water over the past 75 Myr. *Nature,* 314**,** 526-528.
PERUGINI, D., MORONI, B. & POLI, G. 2003. Characterization of marble textures by image and fractal analysis. *In:* LAZZARINI, L. (ed.) *ASMOSIA VI Sixth International Conference, Venice, June 15-18 2000.* 241-246.
PETERMAN, Z. E., HEDGE, C. E. & TOURTELOT, H. A. 1970. Isotopic composition of strontium in sea water throughout Phanerozoic time. *Geochimica et Cosmochimica Acta,* 34**,** 105-120.
PRESS, W. H., FLANNERY, B. P., TEUKOLSKY, S. A. & VETTERLING, W. T. 1989. *Numerical recipes in Pascal,* Cambridge, Cambridge University Press pp.

ROACH, D. E. & FOWLER, A. D. 1993. Dimensionality analysis of patters: Fractal measurements. *Comput. Geosci.,* 19**,** 849-869.

RYE, R. O., SCHUILING, R. D., RYE, D. M. & JANSEN, J. B. H. 1976. Carbon, hydrogen, and oxygen isotope studies of the regional metamorphic complex at Naxos, Greece. *Geochimica et Cosmochimica Acta,* 40**,** 1031-1049.

SCHMID, J., AMBÜHL, M., DECROUEZ, D., MULLER, S. & RAMSEYER, K. 1999a. A quantitative fabric analysis approach to the discrimination of white marbles. *Archaeometry,* 41**,** 239-252.

SCHMID, J., DECROUEZ, D. & RAMSEYER, K. 1999b. A new element for the provenance determination of white marbles: Quantitative Fabric Analysis. *In:* SCHVOERER, M. (ed.) *Archeomateriaux.* Bordeaux: CRPAA-PUB. 171-176.

SCHMID, J., RAMSEYER, K. & DECROUEZ, D. 1995. A new element for the provenance determination of white marbles: qualitative fabric analysis. *ASMOSIA IV, Actes de la IV ème Conference Internationale.* Bordeaux,. 171-175.

TURCOTTE, D. L. 1997. *Fractals and chaos in geology and geophysics,* Cambridge, Cambridge University Press pp.

ZÖLDFÖLDI, J. & SZÉKELY, B. 2004. Kísérlet a nyugat-anatóliai tektonikai egyégek kvantitatív textúraelemzésen alapuló szétválasztására régészeti származásvizsgálati szempontból. / An attempt to separate Western Anatolian tectonic units based on Quantitative Textural Analysis for archaeological marble provenance. *Archeometriai Műhely,* 1**,** 22-26.

ZÖLDFÖLDI, J. & SZÉKELY, B. 2005. Quantitative Fabric Analysis (QFA) and Fractal Analysis (FA) on Marble from West-Anatolia and Troy. *Proceedings of the 33rd International Symposium on Archaeometry, 22-26 April 2002, Amsterdam. Geoarchaeological and Bioarchaeological Studies 3.* Amsterdam. 113-119.

ZÖLDFÖLDI, J. & SZÉKELY, B. 2008. Quantitative Fabric Analysis (QFA) on marble from West Anatolia: Application of raster- (fractal) and vector-based (geometric) approaches. *British Archaeological Reports Int. 1746.* 413-420.

APPENDIX C: INFORMATION AND INTRODUCTION TO THE MISSMARBLE DATABASE

ZÖLDFÖLDI J, HEGEDÜS P & SZÉKELY B (2008): Interdisciplinary data base of marble for archaeometric, art historian and restoration use. In: *Yalcin, Ü., Özbal, H. and Pasamehmetoglu, G.(eds.): Ancient Mining in Turkey and the Eastern Mediterranean.* Atilim University, Ankara. 225-251.

Interdisciplinary Data Base of Marble for Archaeometric, Art Historian and Restoration Use

Judit Zöldföldi[1], Péter Hegedüs[2] & Balázs Székely[3,4]

[1]University of Tübingen, Institute of Geoscience
Wilhelmstrasse 56, D-72074 Tübingen
zoeldfoeldi@yahoo.de
[2] Arany János út 1, H-7754 Bóly, Hungary
[3] Christian Doppler Laboratory for Spatial Data from Laser Scanning and Remote Sensing, Institute of Photogrammetry and Remote Sensing, Vienna University of Technology, Vienna, Austria
[4] Department of Geophysics and Space Science, Institute of Geography and Earth Sciences, Eötvös University, Budapest, Hungary

Abstract

Marble material is widely used for artistic, sculptural and architectural work all over the history of Europe. Marble masterpieces are known from Greek temples, busts of Roman noblemen, and baroque figures to modern facade material, to mention only a few examples. The multitude of raw material and the various creation techniques raise several questions concerning the analysis, provenance, restoration of the objects. A number of proposals have been recently published to unify the data content of data bases concerning marble artefacts and samples. Our approach is similar to the previous workers, however, we renew our earlier concept that a common interface is needed for the data management and query. In this paper we give an account on the state of the art of our project that intends to provide an integrated, scalable and extendable data management and analysis system.

The project aims to characterise historic and recent marble quarries, as well specific marble objects, and makes the information available to all other people involved in the field of research and preservation of marble artefacts. We have developed a software solution for the problem based on client/server architecture. The server-side engine can be installed both on Windows and Linux systems, while the client software is Windows-based. The client software connects to the server via internet connection in a way that the user does not need to install any additional software. The client-side software can be easily updated: the user receives a message to automatically update the software and the update is done by a single mouse click.

The data content of our data base follows the principles laid down previously. Beside of the sample description (geographic location and catalogue data) the data base includes information on colour and fabric, physical properties, chemical composition, mineralogical composition (both macroscopic and instrumental), isotopic data, and textural analyses like fractal analytical and quantitative textural properties. Most of these properties are suitable as filtering criteria to provide query tools and data grouping possibilities. Furthermore there is a sophisticated geographical hierarchy defined in the system, so the samples can be organised into a logical geographic context as well. This context later can be used for larger scale studies, e.g., for provenance determination.

Introduction

During each archaeological research project a lot of data are compiled by literature research, evaluation of resources, field studies, surveys, measurements and simulations. After the termination of the project the vast majority of these data typically remains unpublished. The data themselves are stored by the research institutions often decentralised, analogously or digitally, using various media and in databases of different formats. All these data would be, in principle, ready for dissemination for any scientific purposes on request; however, only the author has the information about the storage and code system of the data. This makes it difficult to verify the conclusions of the publications in the light of the gathered data; and this makes it almost impossible to prepare the data for later use in other projects to answer other research-related questions involving third research parties. Sometimes unnecessarily repeated work is done; consequently the resources of the applied research equipment are needlessly used. To avoid duplicated research, the researchers are expected to publish the data together with the scientific contributions to provide public access to the original information.

Nevertheless, it is often difficult to fulfil this demand. The standards for raw data publication are quite different from the requirements for research publications. Most of the editorial boards discourage the publication of voluminous raw data; only some journals provide data repository functions. Even if such a repository is provided, the storage must be organised in such a way that the structure and format are conceivable for the researchers worldwide. Furthermore, the data must be filed in reliable data centres where they are maintained and are put into archives for long time and remain available even if the IT solutions change.

There is a general agreement in the scientific community that the co-ordinated and free availability of the research data serves all scientists fosters interdisciplinary studies and helps international efforts. Via the availability of the raw data the original research results gain also importance and become valuable.

The demand for data integration generated by provenance studies

Determining the source area of white marbles used in antiquity for sculptures and buildings is still an important problem in archaeology and art history. Deciphering the source of an artefact is a multidisciplinary–multi-method approach whereby disciplines like art history and archaeology have to supply from stylistic characteristics and the original location the most likely time frame and place of fabrication, but also locations of quarries in use at this time period. Natural science disciplines such as physics, chemistry or earth sciences, on the other hand, have to apply physical, chemical, mineralogical and petrographical analysis techniques which unequivocally assign the artefact's marble to comparable material from a unique quarry. Simply based on individual parameters, however, reliable determinations are

questionable and only a multi-method approach may reach a high confidence level. Moreover, almost all techniques applied to date are destructive for the artefact, i.e., they consume material. Thus, the size extractable from an archaeological artefact sets limits on the quantitative use of certain techniques. Therefore, it is important to apply a set of techniques which encompass the whole characteristics of the extracted material, i.e., not only the bulk chemical fingerprint, but also chemical, mineralogical and petrological heterogeneities as well as preferred orientations/accumulations. From this viewpoint a combination of cathodoluminescence texture, fabric analysis and geochemical parameters such as stable isotopes, is an ideal, low cost multi-method approach which satisfies the demand for 2D characterization of the material.

Still, large uncertainties exist on the assignment to a source as not all ancient quarries are known; certain quarries used in antiquity were reopened later or are still in use and thus the exact location of the ancient quarry is unclear; often only small, randomly oriented chips from ancient dumps are available which are not necessarily representative for the quarry and the marble in the quarry is heterogeneous. Thus, the knowledge at quarry level is limited and depends on the quality of the sampling method, i.e., random extraction/collection or well defined location and orientation. Therefore, any substantial improvement in the determination reliability of the source area of white marble used for a specific artefact needs detailed studies of the 3D variability at each ancient quarry site. Furthermore, a search for still unknown sites is required.

The provenance approach

The marble provenance studies have a long tradition in the archaeology; for science historic reasons the roots of marble provenance studies lay in the Mediterranean (e.g., Herz & Waelkens 1988; Waelkens *et al.* 1992; Maniatis *et al.* 1995; Schvoerer 1999; Herrmann *et al.* 2002; Lazzarini 2002). Beyond studies on the famous occurrence of Carrara marble, there are studies on the Aegean marbles, however, only a few investigations of other European marble occurrences have been carried out. These studies typically are of pure geological or petrographical nature, systematic interdisciplinary investigations are often lacking. Some new initiative exists from several authors and research groups, dealing first of all with the stable isotope characteristic of the white marbles from Austria (e.g., Müller & Schwaighofer 1999; Unterwurzacher 2005; Zöldföldi *et al.* 2004a, 2005) and Romania (e.g., Benea et al. 1995; Müller *et al.* 1995; Benea 1996; Benea *et al.* 1998).

Previous comprehensive systems

Restorers, researchers working in various fields of humanities, museologists and specialists managing collections, are basically interested in the construction of data retrieval system of primary data. Thus, the storage, access and safety of scientific data can be assured via co-ordinated activity of the data producers. Summarizing the users' requirements, in our previous work (Zöldföldi *et al.* 2004b, Zöldföldi & Weigele 2007) we laid down some principles that we found necessary to follow in designing such a system. A list of properties that the data base necessarily should contain was also provided. Although some design elements were previously set, this conceptual paper can be considered as the launch date of our current project.

Somewhat later, Cramer (2004) developed an expert system "MarbExpert" for marble provenance determination. A wide range of analytical techniques has been included:

Macroscopic and microscopic petrographic analysis including thin-sections, calcite/dolomite characterization by means of XRD, quantification of the acid-soluble carbonate-hosted Mg, Fe, Sr and Mn by means of ICP-OES, and of Sr and the REE by means of ICP-MS, isotopic composition ($\delta^{13}C$ and $\delta^{18}O$), cathodoluminescence spectra, EPR-spectra and gas chromatographic analysis of the volatile phases. The database and a set of questions were implemented into an easy-to-use expert system shell which on one hand forces the user to "ask the right questions" – i.e. to make precise observations –, on the other hand, it allows him/her to get hints for a marble provenance determination with a high degree of reliability. The Knowledge Acquisition with a database of actually 17 marble quarry districts together with the Question Editor are capable of processing 30 questions on petrographic, geochemical and archaeologically relevant properties. The use of "fuzzy logic" also allows the processing of "diffuse" answers. The whole "MarbExpert" system may be modified and completed by the user according to specific marble quarries or characteristics.

In his recently published book Attanasio *et al.* (2006) using case studies, extends the scope of the data introducing a new isotopic, EPR and petrographic database of Mediterranean white marbles which includes 1346 samples from 20 different historical quarrying sites. 12 variables from three different techniques (isotope analysis, EPR, and petrography) were measured for each sample. This conceptual framework, depending on the specific problem under investigation and on the user's experience, can be used at various levels of complexity, from simple bidimensional graphs to full multi-method statistical analysis.
Attanasio *et al.* (2006), concerning the general issue, wrote: "*Although future work in this direction is already planned, it seems important to point out once again that the establishment of a truly comprehensive collection of data relies critically on the possibility to share results and samples within the archaeometrical community"*.

A short review of common data types in marble analysis

The first attempts to apply scientific methods to the study of marble go back to the work of G.R. Lepsius, which was published in 1890. He introduced the methods of petrography into the field and in particular the microscopic study of thin sections (Lepsius 1890). This was the only method utilised until the mid 20th century and it still remains important today. In the first half of the twentieth century it was gradually accompanied by the use of X-ray diffraction spectra, with which the identification of the most significant mineral phases could be made. Spectroscopic techniques for the identification of trace elements, those with a presence of the order of 0.1% or below, then began to be introduced. Chemical fingerprinting of different materials and samples is possible with this technique, and for this reason it has become the most commonly used analytical method in archaeological research.

The determination of the type and quantity of trace elements is one of the most frequently used analytical methods in archaeometry. Without going into the technical details many different methods have been developed for trace analysis. They include optical emission spectroscopy (OES), atomic absorption spectroscopy (AAS), X-ray fluorescence (XRF), electron microprobe (EMP) and neutron activation analysis (NAA). More recently techniques using a torch of argon plasma to ionize samples in solution have became more common. The most important of these techniques are inductively coupled plasma spectroscopy (ICPS), inductively coupled plasma atomic emission spectroscopy (ICP-AES) and inductively coupled plasma mass spectroscopy (ICP-MS). Leaving aside older and less frequently used methods, the various techniques obviously have different levels of sensibility and accuracy. This means

that the comparison of data obtained by different methods is often problematic, as can also be the case when the same techniques are used by different laboratories.

The quantitative study of texture (Quantitative Textural Analysis or QTA) is in essence the numerical analysis of microscopic images obtained with thin sections evaluating the textural properties on the marble samples by means of quantitative fabric analysis (QFA) and fractal analysis (FA). Fractal analysis is a mathematical approach to the quantification of structural information on natural object. When applied to marble textures the method enables rigorous characterisation of textural relationships of calcite grains, and makes it possible to incorporate the spatial interconnections among grains and the geometrical features of the single grain in the fractal dimension calculation. In combination with quantitative fabric analysis (QFA), fractal analysis is a powerful tool in the discrimination of marbles from various occurrences given its high capability to resolve the convolution of the grain boundaries, which is a distinguishing textural feature of marbles.

The isotope geochemistry of carbon and oxygen applied to the study of marble provenance commenced in 1970s (Craig & Craig 1972). The method was proposed as the most powerful among the techniques already in use, which were, essentially, chemical and petrographic. The isotopic compositions of carbon and oxygen measured in marble samples collected from four different quarry areas of Greece (Naxos, Paros, Mt. Pentelicon and Mt. Hymettos) were remarkably different. The initial results were very promising and encouraged many other researchers to take the same route. The new data, plotted on the usual $\delta^{18}O/\delta^{13}C$ diagram, already gave a more confused frame for the growing database of marble isotopic compositions. Herz (1985) presented much new data and summarized the existing results. About the same time the most important subsequent contribution was a more detailed investigation of the marbles of the Carrara and Seravezza (Herz & Dean 1986). These authors also noticed the possibility of distinguishing the two sites isotopically, while intra-site discrimination was found to be difficult. After the above mentioned studies the marble isotopic reference diagram has been enlarged and updated several times, in the last two decades. A comprehensive account was published by Moens *et al.* (1992). More recently Gorgoni *et al*. (2002) published an extensive diagram of the Greek quarries and Zöldföldi & Satır (2003), Zöldföldi & Székely (2004; 2005b) of the white marble quarries in Anatolia.

On examination of the more recent diagrams the main limits of isotopic analysis become quite evident. Owing to the ever growing number of sampled sites, as well as to the growing number of samples available per quarry, site superposition has become almost a rule, with the results that multiple provenances are a common outcome of isotopic assignments.
The $\delta^{18}O$-$\delta^{13}C$ plots are widely used today to determine provenance but, unfortunately, with so many quarries in the data bank, many quarry fields overlap in values. Clearly ancillary data banks are needed to obtain a more certain determination of provenance. Because of great advantage of isotopic ratio analysis, principally the need for only small samples and homogeneity over large areas, we decided to include the $^{87}Sr/^{86}Sr$ isotopic ratios along with $\delta^{18}O$ and $\delta^{13}C$ and to do a trivariate analysis to improve the discriminating powers of the $\delta^{18}O$-$\delta^{13}C$ plot.

In the last twenty years the already existing methods have been accompanied by a further series of even more sophisticated techniques, these include magnetic resonance, cathodoluminescence, laser reflectance and the quantitative analysis of texture.

Recently a new database of white marbles, based primarily on EPR (Electron Paramagnetic Resonance or ESR) spectroscopy and including some of the most important Greek, Turkish and Italian historical quarrying sites, has been introduced (Armiento *et al.* 1997; Attanasio 1999). In the field of marble provenance the use of ESR spectroscopy, which detects, among others, the Mn^{2+} impurity ubiquitously present in marbles, dates back to the early 1980s (Cordischi *et al.* 1983). Since then much more work has been carried out (Lloyd *et al.* 1988; Maniatis *et al.* 1988, Maniatis & Polikreti 1998), but the use of EPR spectroscopy has remained relatively limited.
This is partly due to the intrinsic characteristics of the method which is not particularly suited for quantitative analytical determinations, but also to the fact different variables have been measured and used by different authors and to the lack of generally accepted standards for both signal intensity and magnetic field strength. In spite of these difficulties the amount of information that EPR spectroscopy of marbles may provide is remarkable.

In addition, and being aware of the fact that reliable assignments may be often obtained only by the combined use of different analytical methods. (Matthews *et al.* 1995; Moens *et al.* 1992), the database was conceived from the beginning as a starting data set to be extended to other measuring techniques. It is obvious, in fact, that the data processing step and the statistical analysis of the experimental information require the various measurements to be carried out on the same quarry samples.

Since its first introduction the marble database has been considerably enlarged and updated. New samples, mainly from Anatolian quarries, have been collected and measured. New, more suitable, standardization procedures have been adopted and also the measuring process has been modified and improved, particularly in the case of the petrographic or morphological variables, which were previously estimated simply on a qualitative basis and given as categorical variables (Attanasio *et al.* 1999). The classification rule, based on discrimination function analysis and taking into account the new experimental results, has been optimized and validated using standard statistical techniques, as well a set of test samples. This last point, i.e. the validation step, is particularly important in that development of a reliable classification method depends upon the ability to estimate realistically its error bar. Extension of the database to other techniques was introduced in the paper of Attanasio and Platania (2003), where morphological variables have been included, but more substantially reported elsewhere, where isotopic data have been taken into account to improve discrimination within a single, large quarrying site (Attanasio *et al.* 2000) or among a properly selected subset of sites (Attanasio 2003). On the basis of the above outline, an updated account of the EPR and petrographic marble database, covering all aspects of data collection, standardization and analysis seemed appropriate and is given in Attanasio (2003).

It is important to remark on the combined use of different methods. This is because all previous studies have unequivocally revealed that no single analytical technique is capable of resolving all the problems related to provenance. Quite frequently one of the techniques, although extremely sophisticated, will produce data that does not discriminate some of the possible provenance sites, which are instead easily distinguished by using a different technique, and vice versa. It is commonly agreed that an approach that integrates two or three different methods and measures is necessary to determine reliable provenances.

The results produced using integrated methods, or occasionally with single techniques, go far beyond simply assigning the provenance of artefacts. Most known marble localities, including renowned sites such as Dokimeon, Proconessos, or Carrara, are extensive regions that include numerous districts and quarries. In favourable conditions particular areas of the locality can

be distinguished, at least partially, and further analyses may sometimes reveal the district or even the exact quarry of provenance. The data can also be utilised to determine whether different parts or fragments of a work originate from the same quarry and even if they originate from the same single block of marble.

This is of great interest since such information, when available, may allow us to recognise forgeries (Polikreti 2007) and later restorations, detect different stages of the manufacturing process, and monitor the reassembly of large artefacts. Furthermore, if a number of samples from the same large work are available; the use of disparate or homogeneous materials can be verified, providing information regarding the building history and manufacturing process of the artefact. The former result would suggest that the construction material had been acquired at different times or from different places, whereas homogeneous materials can originate only from a single quarrying project, which may have planned specifically within the context of a single construction project.

Motivation of our project

In accordance with Attanasio's (2006) cited opinion, we intended to create a common interface to collect, share and, possibly to comment or criticize the existing results. Similarly to other authors, we have collected a number of own measurement data especially in Anatolia (Zöldföldi & Székely 2003; 2004; 2005a; 2005b) and in Austria (Zöldföldi *et al.* 2004a; 2005). These data and the requirement of comparison to other marbles with different provenance involved an imminent need for such an approach. Since the informal replies to our requests to the community were positive, the development has been started.

The aim of this project was to develop a scientifically and technologically interdisciplinary and easily accessible data base management system with user friendly interfaces for data entry, quality control, storage, continuous dissemination, and exchange. This is needed to develop innovative, efficient and practical ways of processing, archiving, and disseminating the large volume of data. Furthermore, the system should provide practical hints to understand the techniques applied on various samples and relate them to other literature data.

Conceptual elements and general properties of the system

The rapid pace of information technology development in the last years makes it possible to create a general information system including already existing analyses and results not only of marble occurrences but of archaeological objects and architectural elements. Conceptually we intend to manage the results of analyses of both type of material together to handle the data in the same manner. It enhances the overlaps and the gaps in the analytical results defining the further analyses to be done. On the other hand the integration makes it possible to spare expensive and time consuming measurements, if the data are already available from the material with the same provenance.

General properties

As any such software (or IT) solution, the system should fulfil the following criteria:
- User friendliness: the typical (trained) user should be able to use the system effectively, including, among others, data input, retrieval and update.
- Scalability: the system should provide means for the extension in scope, number of users, increasing access, and amount of data.

- Data security: the system should be tailored to prevent unwanted, incidental data loss as well as intruder attacks or malicious access.

Our system provides a user-friendly interface for those users who are familiar with the principles of the sampling and various types of marble investigations. The menu structure follows the logic of the sample identification, processing and measurements, therefore it is easy to understand and use. The system is designed to be scalable, especially extendable to include new methods that are developed. The data base from the server side can be extended to include new fields for each record; the client-side application can be easily updated by the user if the system administration sends a message to do so. The access is password protected, however, there no need for more protection since major attacks are not expected.
And last but not least the system is designed to perform user defined filtering operations practically on any combination of logical "AND" criteria, i.e., restricting the selection set by multiple selection.

Conceptual issues

The goal of the developed system is to provide help for data comparison, provenance analyses and to reveal missing analytical results. It integrates data on raw material (hereafter referred to as geological samples) and results on archaeological (art historical and/or architectural) objects (referred to as archaeological samples). The system manages both type of data using the same concept, and most of the data entries are the same for both object types. However, because of the nature of the stored data, in some aspects the two data structures differ.

The data entries are organized in the following scheme. All records contain the following entries: Sample identification; Methods applied on the sample; Colour and fabric; Mineralogical composition; Textural properties; Chemical composition; Isotope geochemical data; Electron paramagnetic resonance; Engineering physical properties. Dependencies on the type of the sample are the following. (a) in case of *geological sample*: geological classification (age, facies); (b) in case of *archaeological samples*: Archaeological description of the objects; Probable provenance if determined; Conservational and restoration experience.
The system is designed so that further amendments and extensions are possible without data loss. It will be updated and tailored according to the experience gathered during its use. It is planned to revise the system functionalities, data structure and data content regularly according to the requirements of the users and data providers. However, the amendments should be done so that the changes do not hamper the comparisons with the previous data and applied methods.

The design of the system

Implementation

From the point of view of the implementation our software solution is based on client/server architecture. The server-side engine is based on the freeware PostgresSQL-technique that can be installed both on Windows and Linux systems, while the client software is Windows-based. The client software connects to the server via a standard internet connection layer in a way that the user does not need to install any additional software. (A firewall-protection may be an issue, but can be solved by an experienced user.) The client-side software can be easily updated: the user receives a message to automatically update the software and the update is

done by a single mouse click. This solution ascertains that the whole community has the same interface and no outdated access tools exist.

The data content

The data content of our data base follows the principles laid down previously. The data base is designed so that it should form an effective means of data exchange between (a) the data producers and (b) the data users.

(a) From our point of view the data producers are those researchers, who carry out any type of measurements on marble material regardless of its purpose, e.g., geoscientific, physical, chemical, material scientific, archaeological and art historical analyses;
(b) The data users are expected to be interested in any type of comparison, classification, query of the aforementioned data set.

The development of the data base had two major aspects. At the first place the structure of the records had to be defined; the structure is expected to be basically unchanged, though the feedback of the users should be taken into account continuously. To foster the exchange of ideas and experiences a notice board is included in the system.

In the following the data base structure is outlined. The structure is determined by all possible features of marbles which may be useful in the distinction of their different types.
The data entries are organized in the following scheme:

1. Sample identification
2. Methods applied on the sample
3. Colour and fabric
4. Mineralogical composition
5. Textural properties
6. Chemical composition
7. Isotope geochemical data
8. Electron paramagnetic resonance
9. Engineering physical properties
10. Depending on the type of the sample
    a. In case of geological sample: geological classification (age, facies)
    b. In case of archaeological or art historical samples : archaeological description of the objects; probable provenance if determined
11. Conservational and restoration experience

(a) Sample identification
In order to be able to handle the archaeological and geological samples in the same manner, the data of the sample and the locality/artefact properties are stored in separate relational data base. However, they are connected via unique key field entries. Each sample is assigned to one of the categories; consequently the samples inherit properties from the ancestor category. Some of the identifying properties are compulsory, to avoid any indetermination in the data base. These properties basically belong to the identification data block (Figure 2), so the analytical result can be added later.

(b) Geographic identification
It is important to emphasize that the data of the localities and the artefacts are entered and managed separately to allow any number of samples in the data base for a given

locality/artefact. To this end a nesting concept has been applied for the determination of the geographic location (somewhat sloppily, hereafter referred to as georeference). It is assumed that the sample (whatsoever it is) has an approximate localization (e.g., continent). This is then the top level of georeference; consequently, all samples must have this property. (In the vast majority of the cases the continent of origin can be determined. If the artefact is found e.g., in a shipwreck and the provenance cannot be determined, then a special "region" can also be introduced.)

Having defined the region of origin, the user may define deeper level of georeference. It is possible to give any level of geographic identification (region, country, locality, mountains, island, quarry, etc.) without any restriction. The logical structure is maintained by the property named "upward nesting" that is, the geographic entity that completely contain the entity to be defined (Figure 1). Since all samples have the continent property defined, all sampling localities can be assigned to at least one higher geographic entity. As it was mentioned above, the geographic entities are managed separately from the samples, since the geographic context does not depend on the actual sample.

This way a geographic structure pyramid can be built. This structure is collected dynamically as the data base grows, and the users do not have to do extra effort for its maintenance, since all new entries are defined by their first occurrence. Even if the geographical assignment has an error, later it can be corrected, and the samples themselves should not be modified.

The structure allows to store unlimited nested features, e.g. within in a quarry several raw materials can be present, and the system allows this separation, e.g., western wall, NE pit, etc. If the user later decides to split up a locality, it can be done by introduction of new geographic level, and the samples belonging to the new geographic units can be reordered accordingly.
Similarly the buildings/artefacts can be handled in this manner. The larger unit (e.g., a sculpture) can be later divided into sampling units. In this sense the artefact is the geographical entity, which can be split according to the needs

(c) Method summary sheet
In this part of the data base the measurement history of the sample is summarized. Beside of the date and type of the carried out measurements and related information (e.g. laboratory, instrument type), the external references (sample identification) of the measuring laboratories are stored. Ample space is provided for further investigation types and other bookkeeping information.
Of course, the different measurements can be summarized on the very same sheet only if the measurement was made on the very same specimen. If not, the measurements will be separated to different samples with their own sample ID. This approach assures that artefacts mosaicked of various materials can be separately stored in the scheme.

(d) Macroscopic properties
This sheet summarizes all the observations which are done without instrumentations, made during field work or in the lab, for example colour and smell, distinguishing between calcitic and dolomitic marble (reaction with HCl), fabric, foliation, minerals detected by naked eyes.

(e) Microscopic properties
This group sums up the results of different observations methods:

1. Microscopic and microprobe investigation;
2. Quantitative Textural Analysis (QTA) including quantitative Fabric Analysis (QFA) and Fractal Analysis (FA) for statistical evaluation of grain size analyses. Additional to the

conventional grain size determination, the statistical distribution (histogram) of other grain size-properties, like axial difference (long axis – short axis), ratio perimeter/surface, shape factor etc., Fractal Analysis (FA, mass dimension method) is used to extract pattern related parameters in order to characterise the different samples (Zöldföldi & Székely 2005b);
3. Staining technique;
4. Cathodoluminescence imaging.

(f) Instrumental data
Detailed description of samples is given based on instrumental studies, which include:
1. X-ray diffraction (XRD) in order to determine the mineralogical composition;
2. X-ray fluorescence (XRF), inductively coupled plasma mass spectrometry (ICP-MS), instrumental neutron activation analyses (INAA), and prompt gamma activation analyses (PGAA) in order to determine the chemical composition of the sample;
3. Carbon and oxygen isotope geochemistry;
4. $^{87}Sr/^{86}Sr$ isotope geochemistry.

Examples of applications

This internet accessible database forms the scientific basis and background of provenance analyses of historical monuments and marble masterpieces. Here a few application examples are provided.

(a) Authenticity of "antique" marble objects
In one of our projects the authenticity of some marble artefacts said to be authentic Cycladic Neolithic sculptures had to be determined. Conceptually the decision was made based on several factors, including macroscopic, microscopic, cathodoluminescence investigation, isotopic analyses. First of all the results measured on the raw material were compared to the data base values. In a part of the cases this comparison immediately showed that the assumed provenance can be excluded because of several discrepancies in the mineralogical and stable isotopic composition.
One of the sculptures showed almost identical values in all analysed aspects with the assumed raw material of Naxos, i.e., we could conclude that the material is very probably Cycladic marble. On the other hand this study proved the importance and necessity of the weathering studies of the material because despite of the similarity of the bulk rock material the surface of the analysed sculpture did not show the weathering properties which would be expected of an artefact with the corresponding age. This way it was possible to conclude that this piece is also a modern forgery, though of original material.

(b) Provenance determination of building material in Troy (Turkey)
Marble is an important building material in Troy, from the Greek period, Ilion (Troy VIII, shortly before 700 BC - 85 BC) and Roman period, Ilium (Troy IX, 85 BC - c. 500 AD). These phases of construction left their fingerprints on the buildings and monuments of Troy. The materials of the monuments could have been shipped from various areas because of the occupation history of Troy and the surrounding area. This example has already been published in detail (Zöldföldi & Satir 2003; Zöldföldi & Székely 2005a), here we summarize it briefly as a successful application example to identify geographic locality of quarries of possible provenance.

There are abundant marble material resources in the near vicinity and in the farther surrounding of Troy (Zöldföldi & Satır 2003): various white marble occurrences can be found

in Asia Minor (Sakarya Zone tectonic unit: Marmara, Orhangazi, Bergaz, Mustafa Kemalpasa, Altınoluk; Menderes Massif tectonic unit: Muğla, Afyon, Uşak, Babadağ). Furthermore archaic quarries are well-know in the archipelago of the Aegean: Naxos, Paros, Thasos, Lesbos etc. Because of the extended commercial connection in the Roman times other marble sources come into consideration. On the other hand, the recycling of the already readily available material cannot be excluded. This wide variety of white marble material sets up a challenging problem of the origin(s) of the architectural and sculptural stone-works. The analysis of the building material can explain the commercial and political connections via the determination of the possible shipment sources.
In this study the following architectural elements were considered: Athena Temple (280 BC), Athena Temple Portico (230 BC), Sanctuary of "Roman Altar" (3rd century BC), Bouleuterion and Bath moulding (both 2nd century BC), Odeion (2nd century AD).

The textural analysis of the fabric (maximum grain size and fractal properties) excludes most of the occurrences of the Menderes Massif and some of the Aegean Islands like Thasos and Naxos. Based on microscopic investigation and stable isotopic geochemistry the material used for construction of the Athena Temple dated at 280 BC could have come from the Marmara and/or Orhangazi area. Some samples of the Temple (PBA1-2) can be clearly referred to Marmara and/or Orhangazi, based on their $^{87}Sr/^{86}Sr$ ratios, but the rest of them fall also into the $^{87}Sr/^{86}Sr$ ranges of Marmara and/or Orhangazi. More specific reference to provenance cannot be made presently, because the geological samples from these areas, Marmara and Orhangazi are indistinguishable. The investigation of the Athena Temple Porticoes shows that, in part, the same building material has been used such as for the Athena Temple (new shipping from the same quarries or recycling). However, a new group of material, certainly from Pentelikon, Greece was also found. According to the stable isotopic geochemistry the "Sanctuary" of Roman Altar dated from the 3rd century BC, was built of marble from Serhat or Altınoluk, but Marmara and/or Orhangazi can not be excluded. The building material of Bouleuterion dated from the 2nd century BC was derived from Marmara, which is proved based on microscopic, cathode-luminescence investigation, stable isotope geochemistry, and Sr-isotope ratios. Concerning the next construction period (Troy IX) fragments of several architectural elements and columns of Odeion were investigated. Based on microscopic investigation and isotopic geochemical constrains, the marble for this construction phase came from Marmara/Orhangazi, Serhat, Ayazma, or Altınoluk.

The fragments of the Bath moulding dated from the late 2nd century BC can be sharply separated into three groups. One of them stems from Marmara and/or Orhangazi, the second from Bergaz, while the 3rd one shows affinity to Paros (Greece) on the basis of stable isotope geochemistry and cathode-luminescence features. This complex provenance pattern demonstrates that this architectural feature was constructed of material from various shipments (including marble from Greece) or, more probably, partly of recycled material already present at Troy. In summary the majority of marbles used for construction of the Trojan architectural elements is derived from Marmara and/or Orhangazi areas, with minor percentages of other Northwest Anatolian and Greek shipment at various historical periods.

(c) Importance of provenance analyses in restoration
It has been shown by Recheis et al. (2001) that in certain cases the *in situ* analytical techniques may fail to provide appraisable results in the lack of provenance information. These authors analysed the portals of Schloss Tirol (Tyrol, Austria) dated to the 12th century.
The two marble portals of "Schloss Tirol" show differences, both in material and in weathering state. As the building history of the portals is still not clear – historians suppose that some parts of the portals are older and completed by different masters – it is of significant

interest whether the differences are due to a different weathering history or due to marble materials of different provenance. Based on isotopic analysis, trace element analysis and grain size determination, Recheis *et al.* (2001) conclude that there is a difference between the two portals in the whole and a difference between some parts of the palace portal in particular. Furthermore these authors draw the conclusion that "*for a reliable interpretation of ultrasonic results with respect to weathering effects the knowledge of the exact origin of the marbles is necessary*". Our data base is intended to serve for such purposes.

Conclusions

A data management system has been developed for storage and manipulation of various properties of marble rock samples and artefacts. The system applies the client-server architecture, allowing multiuser access. A novel conceptual approach, to handle the geological samples similarly to the archaeological artefacts, has been found advantageous to manage the data records and to make provenance decisions using various filtering criteria.

Acknowledgements

This project has been initiated in the framework of the Graduate College 442 of the Deutsche Forschungsgemeinschaft, called "*Anatolien und seine Nachbarn*" at the University of Tübingen (led by M. Korfmann, later P. Pfälzner) and of the DAAD-MÖB project (led by M. Satır and K.T. Biró). For a given period earlier in the project Balázs Székely received support from University of Tübingen, later contributed partly as a Békésy György Postdoctoral Fellow. All help is gratefully acknowledged.

Bibliography

ARMIENTO, G., ATTANASIO, D. & PLATANIA, R.
1997 Electron spin resonance study of white marbles from Tharros Sardinia): A reappraisal of the technique, possibilities and limitations. *Archaeometry* 39, 2, 309-319.

ATTANASIO, D.
1999 The use of electron spin resonance spectroscopy for determining the provenance of classical marbles. *Applied magnetic resonance*, 16, 3, 383-402.

ATTANASIO, D., EMANUELE, M.C. & PLATANIA R.
1999 ESR and Petrographic Determination of the Provenance of Classical Marble: Evaluation and Assessment of the Classification Rules. In: 2nd International Congress on Science and Technology for the Safeguard of Cultural Heritage in the Mediterranean Basin. Paris, 5-9 July 1999, Vol. 1, 477-48.

ATTANASIO, D., ARMIENTO, G., BRILLI, M., EMANUELE, M., PLATANIA R. & TURI, B.
2000 Multi-method marble provenance determinations: the Carrara marbles as a case study for the combined use of isotopic, ESR and petrographic data. *Archaeometry* 42, 2, 257-272.

ATTANASIO, D. & PLATANIA R.
2000 ESR Spectroscopy as a Tool for Identifying Joining Fragments of Antique Marbles: The Example of a Pulpit by Donatello and Michelozzo. *Journal of Magnetic Resonance* 144, 322-329.

ATTANASIO, D.
2003 Ancient white marbles: analysis and identification by paramagnetic resonance spectroscopy, "L'Erma" di Bretschneider, Roma, pp. 283.

ATTANASIO, D. & PLATANIA, R.
2003 Refinement and assessment of the classification rule for an updated version of the EPR and petrographic marble database. In: L. Lazzarini (ed.): *Interdisciplinary studies on ancient stone*, Bottega d'Erasmo, Padova, 149-155.

ATTANASIO, D., BRILLI, M. & OGLE, N.
2006 The Isotopic Signature of Classical Marbles. L'Erma di Bretschneider, Roma.

BENEA, M.
1996 Carbon and Oxygen Isotopic Ratios in Bucova Marble (Souht Carpathians); In: *Proc. of the 90th Anniversary of the Geol. Inst. of Romania, June 12-19, 1996*, Bucharest.

BENEA, M., MÜLLER, H.W. & SCHWAIGHOFER, B.
1995 Comparison between some marble quarries from Romania using petrochemical features; *Studia Univ.Babes-Bolyai, Ser.geol.*, XL, 1, 229-234.

BENEA, M., MÜLLER, H.W. & SCHWAIGHOFER, B.
1998 The single Roman marble quarry in Romania. In: *Proc. of the 31st International Symposium on Archaeometry, 27 April -2 May 1998*, Budapest.

CORDISCHI, D., MONNA, D. & SEGRE, A.L.
1983 ESR analysis of marble samples from Mediterranean quarries of archaeological interest. *Archaeometry* 25, 1, 68-76.

CRAIG, V., & CRAIG H.
1972 Greek Marbles: Determination of provenance by isotopic analysis. *Science* 176, 401-403.

CRAMER, T.
2004 *Multivariate Herkunftsanalyse von Marmor auf petrographischer und geochemischer Basis.* 334 pp. URL: http://opus.kobv.de/tuberlin/volltexte/2004/742/.

HERRMANN, J., HERZ, N. & NEWMAN, R. (eds.)
2002 *Interdisciplinary Studies on Ancient Stone – Proceedings of the Fifth International Conference of the Association for the Study of Marble and Other Stones in Antiquity, Museum of Fine Arts, Boston, June 1998*; Archetype Publications, London.

HERZ, N.
1985 *Isotopic analysis of marble*. In: G. JR. Rapp & J. A. Gifford (eds.), *Archaeological Geology*, Yale Univ. Press, New Haven, United States, 331-351.

HERZ, N. & DEAN, N.E.

1986 Stable isotopes and archaeological geology: the Carrara marble. *Applied Geochemistry*, **1, 139-151.**

HERZ, N. & WAELKENS, M. (eds.)
1988 *Classical Marble: Geochemistry, Technology, Trade*; NATO ASI Series E, Applied Sciences, Vol. 153**.** Kluwer Academic Publishers, Dordrecht, Boston.

LAZZARINI, L. (ed.)
2002 *Interdisciplinary Studies on Ancient Stone – ASMOSIA VI, Proceedings of the Sixth International Conference of the Association for the Study of Marble and Other Stones in Antiquity, Venice, June 15-18, 2000*; Bottega d'Erasmo Aldo Ausilio Editore, Padova.

LEPSIUS, R.
1890 *Griechische Marmorstudien,* Abhandlungen Königl. Akademie der Wissenschaften, Phil.-Hist. Kl, Berlin.

LLOYD, R. V., SMITH, P.W. & HASKELL, H.W.
1988 Evaluation of the manganese ESR method of marble characterization. *Archaeometry*, 27, 1, 108-116.

MANIATIS, Y., MANDI, V. & NIKOLAU, A.
1988 Provenance investigation of marbles from Delphi with ESR spectroscopy. In N. Herz & M. Waelkens (eds.): *Classical marble: geochemistry, technology, trade.* Kluwer Publications, Dordrecht, 443-452.

MANIATIS, Y. & POLIKRETI, K.
1998 Provenance of white marble with EPR spectroscopy: further developments. In: *Proc. of the V ASMOSIA Conference, Boston, June 1998, Abstracts*.

MANIATIS, Y., HERZ, N. & BASIAKOS, Y. (eds.)
1995 *The Study of Marble and Other Stones Used in Antiquity.* Archetype Publications, London.

MATTHEWS, K.J., LEESE, M.N., HUGHES, M.J., HERZ, N. & BOWMAN, S.G.E.
1995 Establishing the provenance of marble using statistical combinations of stable isotope and neutron activation data In: Y. Maniatis, N. Herz & Y. Basiakos (eds.), *The study of marble and other stones used in the antiquity*, Archetype Publisher, London, 181-186.

MOENS, L., ROOS, P., DE PAEPE, P. & LUNSINGH SCHEURLEER, R.
1992 Provenance determination of white marble sculptures from the Allard Pierson Museum in Amsterdam, based on chemical, microscopic and isotopic criterias. In: M. Waelkens, N. Herz & L. Moens (eds.) *Ancient stones: quarrying, trade and provenance: interdisciplinary studies on stones and stone technology in Europe and Near East from the prehistoric to the early Christian period*, Leuven University Press, Leuven, 269-276.

MÜLLER, H.W., SCHWAIGHOFER, B., BENEA, M., PISO, I. & DIACONESCU, A.

1995 Marbles in the Roman Province of Dacia; In: *Actes d'ASMOSIA IV^eme Conference Internationale, 9-14 oct.1995*, Bordeaux/Talence, France, Abstract Book.

MÜLLER, H.W.& SCHWAIGHOFER, B.
1999 Die römischen Marmorsteinbrüche in Kärnten, *Carinthia II*, 549-572.

PINTÉR, F. & ZÖLDFÖLDI, J.
2005 A szombathelyi Isis-szentélyből származó két márványminta eredethatározása stabilizotóp-geokémiai és petrográfiai módszerekkel / Provenancing two marble samples from the Savaria Iseum by stable isotope geochemistry and petrography. *Archeometriai Műhely*, 2, 1, 57-59. www.ace.hu/am

POLIKRETI, K.
2007 Detection of ancient marble forgery: techniques and limitations. *Archaeometry* 49, 4, 603-619.

RECHEIS, A., BIDNER, T. & MIRWALD, P.W.
2001 The ultrasonic differences of the two marble portals of Schloss Tirol / South Tyrol - a case of weathering or of marble? *Acta Universitatis Carolinae - Geologica* 45, 1, 29-30.

SCHVOERER, M. (ed.)
1999 *Archéomatériaux – Marbres et Autres Roches. Actes de la IVème Conférence Internationale de l'Association pour l'Étude des Marbres et Autres Roches Utilisés dans le Passé;* Centre de Recherche en Physique Appliquée à l'Archéologie et Presses Universitaires de Bordeaux (Bordeaux-Talence).

UNTERWURZACHER, M., POLLERES, J. & MIRWALD, P.
2005 Provenance study of marble artefacts from the roman burial area of Faschendorf (Carinthia, Austria). *Archaeometry* 47, 2, 265-273.

WAELKENS, M., HERZ, N. & MOENS, L. (eds.)
1992 *Ancient Stones: Quarrying, Trade and Provenance – Interdisciplinary Studies on Stones and Stone Technology in Europe and Near East from the Prehistoric to the Early Christian Period*; Leuven University Press (Leuven) and Katholieke Universiteit Leuven Acta Archaeologica Lovaniensia, Monographiae 4.

ZÖLDFÖLDI, J. & SATIR, M.
2003 Provenance of white marble building stones in the monuments of the ancient Troia. In: G.A. Wagner, E. Pernicka & H.P. Uerpmann (eds.), *Troia and the Troad,* Springer, Berlin, 203-223.

ZÖLDFÖLDI, J. & SZÉKELY, B.
2003 A case study of combining quantitative fabric analysis (QFA) and fractal analysis (FA) on white marbles with conventional analytical techniques for provenance analysis. In: R. Snethlage & J. Meinhardt-Degen (eds.), *Proceedings of the 13th Workshop of EU 496 EUROMARBLE*, Bavarian State Department of Historical Monuments Munich, 141-149.

ZÖLDFÖLDI, J. & SZÉKELY, B.
2004 Kísérlet a nyugat-anatóliai tektonikai egyégek kvantitatív textúraelemzésen alapuló szétválasztására régészeti származásvizsgálati szempontból (An attempt to separate Western Anatolian tectonic units based on Quantitative Textural Analysis for archaeological marble provenance). *Archeometriai Műhely* 1, 1, 22-26. www.ace.hu/am

ZÖLDFÖLDI, J., PINTÉR, F., SZÉKELY,B., TAUBALD, H., BIRÓ, K., MRÁV, ZS., TÓTH, M., SATIR, M., KASZTOVSZKY, ZS. & SZAKMÁNY, GY.
2004a Római márványtöredékek vizsgálata a Magyar Nemzeti Múzeum gyűjteményéből (Provenance Studies on marble fragments in the Hungarian National Museum). *Archeometriai Műhely* 1, 1, 39-45. www.ace.hu/am

ZÖLDFÖLDI, J., SZÉKELY, B., & FRANZEN, Ch.
2004b Interdisciplinary data base of historically relevant marble material for archaeometric, art historian and restoration use. In: G. Grassegger-Schön & G. Patitz (eds.), *Natursteinsanierung Stuttgart 2004, Neue Natursteinsanierungsergebnisse und messtechnische Erfassungen,* Siegl, München, 79-86.

ZÖLDFÖLDI, J. & SZÉKELY, B.
2005a Provenance of Roman and Greek marble building stones of Troy. Proceedings of the 33rd International Symposium on Archaeometry, 22-26 April 2002, Amsterdam. *Geoarchaeological and Bioarchaeological Studies* 3, 123-129.

2005b Quantitative Fabric Analysis (QFA) and Fractal Analysis (FA) on Marble from West-Anatolia and Troy. Proceedings of the 33rd International Symposium on Archaeometry, 22-26 April 2002, Amsterdam. *Geoarchaeological and Bioarchaeological Studies* 3, 113-119.

ZÖLDFÖLDI, J., TAUBALD, H., PINTÉR, F., TÓTH, M., T. BIRÓ, K., SATIR, M., MRÁV, ZS., KASZTOVSZKY, ZS., SZAKMÁNY, GY. & DEMÉNY, A.
2005 Provenance Studies on Roman Marble Fragments in the Hungarian National Museum, Budapest. Proceedings of the 33rd International Symposium on Archaeometry, 22-26 April 2002, Amsterdam. *Geoarchaeological and Bioarchaeological Studies* 3, 119-123.

ZÖLDFÖLDI, J. & WEIGELE, J.
2007 Kampf um die Erhaltung der Marmorskulpturen des Stuttgarter Lapidariums, Teil 1: Bestandsaufnahme, Schadenskartierung, naturwissenschaftliche Untersuchungen, In: G. Grassegger-Schön, G. Patitz, & O. Wölbert (eds.), *Natursteinsanierung Stuttgart 2007, Neue Natursteinsanierungsergebnisse und messtechnische Erfassungen,* Siegl, München, 49-64.

Entity	Upward nesting
Tectonic unit Z	[Continent]
Locality C	Tectonic unit Z
Quarry R	Tectonic unit Z
Formation Y	Tectonic unit Z
Formation W	Tectonic unit Z
Locality A	Formation W
Locality B	Formation W
Locality D	Formation Y
Quarry Q	Locality B
Quarry P	Locality B

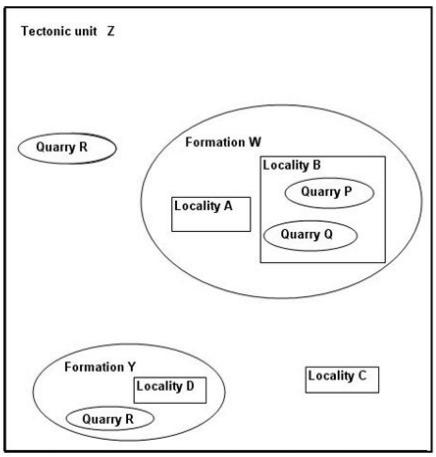

Figure 1: The logical structure is maintained by the property named "upward nesting" that is, the geographic entity that completely contain the entity to be defined.

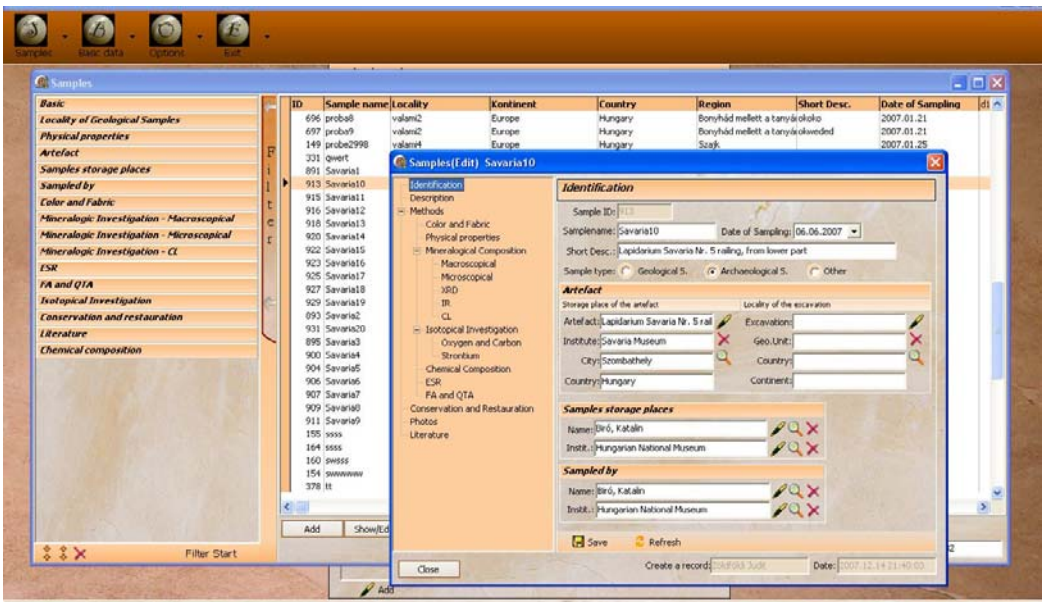

Figure 2: Each sample is assigned to one of the categories (archaeological/geological/other); consequently the samples inherit properties from the ancestor category. Some of the identifying properties are compulsory, to avoid any indetermination in the data base. These properties basically belong to the identification data block, so the analytical result can be added later.

APPENDIX D: RESULTS OF ANALYTICAL INVESTIGATION

1. Macroscopical and microscopical description

1.1. Kumtepe marbles

Areal	Container	Material	Grain size	Solubility with HCl
Kumtepe				
F28	990	greyish white marble	fine-grained	+
F29	460	white marble	medium- to corse grained	+
F28	958/1	reddish white marble	fine- to medium-grained	+

1.2. Bronze Age marbles

Areal	Container	Material	Grain size	Solubility with HCl
Troia				
1999				
D8	1844	white marble	fine- to mediumgrained	+
K8	730	white marble	fine-grained, strongly weathered surface	+
Z7	732	greyish white marble	medium-grained	+
D3	30	white marble	corse-grained	+
D9	106	reddish white marble	corse-grained (Kirklareli)	+
E8	354(44)	white marble	fine-grained	+
E4	640(149)	white marble	fine-grained	+
G6	42(1)	milky-white marble	fine-grained	+
D7	48	greyish white marble	medium- to fine-grained	+
E4/5	100	white marble	fine-grained, high amount of micas	+
D8	1755	greyish white marble	medium- to corse-grained, geedert	+
E4/5	95	white marble	medium-grained	+
K12	B38	white marble	corse-grained	+
E9	1297	white marble	fine-grained, strongly wethered surface	+
Y8 (1)	100	yellowish white marble	fine-grained	+
K17	1138	white marble	fine-grained	+
A8	491	white marble	corse-garined	+
D3	449	white marble	corse- to very corse-grained	+
I9	393	yellowish white marble	medium-grained	+
Blegen				
91/44 (7)		yellowish white marble	fine- medium-grained	+
T-44/58 (4)		yellowish white marble	fine- medium-grained	+
T-8/14 (3)		greyish white marble	corse-grained	+
T23 (5)		white marble	fine- to medium-grained	+

1.3. Hellensitic marbles

	Areal	Material	Grain size and texture	Odour	Solubility with HCl
Athena Temple Portico	PBA1	white marble	fine- to medium-grained heteroblastic	light	+
	PBA2	white marble	fine- to medium-grained heteroblastic	strong	+
	PBA3	white marble	fine- to medium-grained heteroblastic	strong	+
	PBA4	white marble	fine- to medium-grained heteroblastic	strong	+
	PBA5	greyish white marble	medium-grained heteroblastic	strong	+
	PBA6	white marble	medium- to corse-grained heteroblastic	strong	+
	PBA7	greyish white marble	medium-grained heteroblastic	strong	+
	PBA8	white marble	medium- to corse-grained heteroblastic	strong	+
	PBA9	white marble	fine- to medium-grained heteroblastic	no	+
	PBA10	greyish white marble with red veins	medium-grained heteroblastic	no	+
Sanctuary „Roman Altar“	PBA11	white marble	medium-grained heteroblastic	strong	+
	PBA12	white marble	medium- to corse-grained heteroblastic	strong	+
	PBA13	yellowish white marble	medium- to corse-grained heteroblastic	strong	+
Bath, Blue Marble Building	PBA14	dark grey marble	fine-grained heteroblastic	no	+
	PBA15	dark grey marble	fine-grained heteroblastic	no	+
	PBA16	dark grey marble	fine grained heteroblastic	no	+
Sanctuary, North Building Treshold	PBA17	white marble	corse-grained heteroblastic	strong	+
	PBA18	white marble	fine- to medium-grained heteroblastic	strong	+
Bouleuterion	PBA19	white marble	medium- to corse-grained heteroblastic	light	+
	PBA20	grey marble	fine-grained homeoblastic	strong	+
	PBA21	white/grey marble with foliation	medium- to corse-grained heteroblastic	strong	+

1.4. Roman marbles

	Areal	Material	Grain size and texture	Odour	Solubility with HCl
Children of Claudius	PBA22	white marble	fine- to medium-grained heteroblastic	light	+
Odeion	PBA23	white marble	medium-grained heteroblastic	strong	+
	PBA24	greyish white marble	medium-grained heteroblastic	strong	+
	PBA25	white marble	fine- to medium grained heteroblastic	strong	+
	PBA26	greyish white marble	medium grained heteroblastic		+
	PBA27	grey marble	fine- to medium grained heteroblastic		+
	PBA28	dark grey marble	fine- to medium-grained heteroblastic	light	+
	PBA29	dark grey marble	fine- to medium-grained heteroblastic	no	+
Bath, Nymphaeum base and moulding	PBA30	white marble	fine- to medium grained heteroblastic	no	+
	PBA31	greyish white marble	medium-grained heteroblastic	light	+
	PBA32	white marble	medium- to corse-grained heteroblastic	strong	+
	PBA33	greyish white marble	fine- to medium grained heteroblastic	no	+
	PBA34	grey marble	medium-grained	no	+
	PBA35	white marble	medium-grained heteroblastic	strong	+

2. XRD-Analysis

Mineralogical composition of the investigated marbles is listed in the following tables. The tables list the major and accessory minerals based on powder XRD measurements. The column "file" is the intern ID of the sample at the Institute for Geochemical Research, Hungarian Academy of Sciences.

2.1. Anatolian marbles

2.1.1. Rhodope-Stradja Massif

	Sample	Major mineral components	Accessory minerals	File
Bergaz	BE1	calcite	dolomite, quartz	21765
	BE2	dolomite, calcite	quartz	21620
Karabiga	KB1	calcite	dolomite, quartz	21767
	KB3	dolomite, calcite	quartz, dolomite	21668

2.1.2. Sakarya Zone

2.1.2.1. Kazdağ range

	Sample	Major mineral components	Accessory minerals	File
Altinoluk	ALT1A	calcite	quartz	21726
	ALT1C	calcite	kaolinite, quartz, dolomite	21727
	ALT1D	dolomite, calcite	quartz, kaolinite	21728
	ALT1E	calcite	quartz	21729
	ALT1F	calcite	quartz	17828
	ALT1G	calcite	quartz	21730
	ALT2A	dolomite, calcite	quartz, kaolinite, mica	21731
	ALT2B	calcite	dolomite, quartz, mica, chlorite	21732
	ALT2C	calcite	dolomite, quartz, mica	21733
	ALT2D	calcite	quartz, mica, kaolinite	21734
	ALT2E	calcite	dolomite, quartz, kaolinite	21736
	ALT2F	calcite	quartz, mica	21737
	ALT2G	calcite	quartz	21738
	ALT1I	calcite	quartz	17827
	ALT1J	calcite		21742
	ALT1K	calcite, dolomite	mica, quartz, chlorite	21743
	K12	calcite	dolomite, quartz	18574
	K15	calcite	quartz	18575
	K18	calcite	quartz	18576
	K22	calcite	quartz	17831
Serhat	K3	calcite	quartz, mica, dolomite	21773
	K4	calcite	quartz	21774
Ayazma	AyazmaD	calcite	quartz	21783
	AyazmaB	calcite	mica	17829
	K2	calcite	quartz, mica	18571

	K6	calcite	quartz	18572
	K9	calcite	mica	18573
	ZTM6	calcite	quartz	21614
Yenice	KAR1	calcite	quartz	21759
	KAR5	calcite	dolomite, quartz	21781
	KAR12	calcite	quartz	21779
	K1	calcite	quartz, dolomite	21772
	KR1	dolomite, calcite	kaolinite, quartz	21895

2.1.2.2. Karakaya Complex

	Sample	Major mineral components	Accessory minerals	File
Manyas	MAN3	calcite	quartz	21767
Mustafa Kemalpasa	KE4	calcite	quartz	18577
	KE1	calcite	dolomite, quartz, plagioclase	21763
	MKB1	calcite	quartz	21630
Bandirma				
Marmara	MA1	calcite	quartz, dolomite	21805
	MA11	calcite	quartz, dolomite	21894
	MA1b	calcite	dolomite, mica, quartz, plagioclase, hematite	17830
	ZTM2	calcite	dolomite, quartz	21755

2.1.2.3. Armutlu-Ovacık Zone

	Sample	Major mineral components	Accessory minerals	File
Orhangazi	ORH1	calcite	quartz	17825
	ORH2B	calcite	dolomite	21744
	ORH2C	calcite	dolomite, quartz	21745
	ORH2D	calcite	dolomite, quartz, plagioclase, hematite	17826
	ORH2E	calcite	quartz, mica	21755
	ORH2F	calcite	dolomite, quartz	21756
Iznik	no data			

2.1.3. Anatolide Tauride block

2.1.3.1. Menderes Massif

	Sample	Major mineral components	Accessory minerals	File
Milas	MI1	calcite, dolomite	quartz	21896
	MI2	calcite	dolomite	21629
	MI3	calcite, dolomite	mica, quartz	21784
	MI4	calcite	quartz	21804
	MI11	calcite, dolomite	quartz	18605
Yatagan	ZTM4	calcite	plagioclase, quartz, mica	18612
	ZTM5	calcite	quartz	21613
Mugla	M4	calcite	quartz	18606

	M6	calcite	quartz	21782
	M7	calcite	quartz	
	M8	calcite	quartz, dolomite	18589
	M11	calcite	quartz	18604
	M12	calcite, dolomite	quartz	21803
Mugla-Leylak	M10	calcite	dolomite, quartz	18597
	M9	calcite, dolomite	quartz	18596
	M2			

2.1.3.2. Central-Anatolide-Tauride block

	Sample	Major mineral components	Accessory minerals	File
Afyon	ZTM1	calcite	quartz	21718
	ZTM3	calcite	quartz, mica, plagioclase	21612
	A1	calcite	quartz	21757
	A2	calcite	quartz	18565
	A3	calcite	quartz	21769
	A4	calcite	quartz	21768
	A13	calcite	quartz	18568
	A16	calcite	quartz, mica, chlorite	21771
Usak	ZTM8	calcite	quartz	21619
Babadag	BD4	calcite	quartz	18569
	BD6	calcite	quartz	18570

2.2. Trojan marbles

2.2.1. Kumtepe marbles

Areal	Container	Major mineral components	Accessory minerals	File
F28	990	calcite		
F29	460	calcite	dolomite, quartz, chlorite	21657
F28	958/1	calcite, dolomite		21671

2.2.2. Bronze Age marble

Areal	Container	Major mineral components	Accessory minerals	File
D8	1844	calcite	dolomite, quartz	21663
K8	730	calcite		
Z7	732	calcite	dolomite, hematite?	21658
D3	30	calcite	quartz	21662
D9	106	calcite	dolomite	21665
E8	354(44)	calcite		
E4	640(149)	calcite		21711
G6	42(1)	calcite	quartz	21674
D7	48	calcite		
E4/5	100	calcite		
D8	1755	calcite		
E4/5	95	dolomite, calcite	plagioclase, quartz	21667

K12	B38	calcite	quartz	21664
E9	1297	calcite		
Y8 (1)	100	calcite	dolomite, quartz, chlorite	21673
K17	1138	calcite	dolomite, quartz, plagioclase	21710
A8	491	calcite	dolomite, quartz	21656
D3	449	calcite	dolomite, quartz, christobalite	21661
I9	393	calcite	dolomite, quartz	21725
A0	70	calcite	quartz, kaolinite and/or chlorite	21675
Blegen		calcite		
91/44 (7)		calcite		
T-44/58 (4)		calcite		
T-8/14 (3)		calcite	dolomite	21672
T23 (5)		dolomite, calcite	quartz	21666

2.2.3. Hellenistic marbles

	Sample	Major mineral components	Accessory minerals	File
Athena Temple	PBA1	calcite	quartz	21631
	PBA2	calcite, dolomite	quartz	21632
	PBA3	calcite, dolomite	quartz, mica, hematite	17836
	PBA4	calcite	quartz	21636
	PBA5	calcite	dolomite, chlorite, quartz	18607
	PBA6	calcite	dolomite, mica, quartz	17837

	Sample	Major mineral components	Accessory minerals	File
Athena Temple Portico	PBA7	calcite, dolomite	quartz	21637
	PBA8	calcite	dolomite, quartz	18608
	PBA9	calcite, dolomite		21638
	PBA10	calcite	quartz, mica, dolomite	17839

	Sample	Major mineral components	Accessory minerals	File
Sanctuary „Roman Altar“	PBA11	calcite	dolomite, quartz	21639
	PBA12	calcite		21640
	PBA13	calcite	quartz, dolomite	21641

	Sample	Major mineral components	Accessory minerals	File
Bath, Blue Marble Building	PBA14	calcite	quartz, mica, dolomite	17840
	PBA15	calcite		21642
	PBA16	calcite	quartz, dolomite	17841

	Sample	Major mineral components	Accessory minerals	File
Sanctuary, North Building Treshold	PBA17	calcite	quartz, dolomite	21645
	PBA18	calcite		21646

	Sample	Major mineral components	Accessory minerals	File
Bouleuterion	PBA19	calcite	quartz, dolomite, mica	18609

	PBA20	calcite	dolomite	n.k.
	PBA21	calcite	dolomite	21654

2.2.4. Roman marbles

Claudius Inscrip.	Sample	Major mineral components	Accessory minerals	File
	PBA22	calcite	quartz, dolomite	21649

	Sample	Major mineral components	Accessory minerals	File
Odeion architectural elements	PBA23	calcite, dolomite	quartz, mica	21650
	PBA24	calcite, dolomite	quartz	18610
	PBA25	n.d.	n.d.	-
	PBA26	calcite	dolomite, quartz, plagioclase	21655
Odeion columns	PBA27	calcite	quartz, dolomite	17842
	PBA28	calcite	quartz, dolomite	17847
	PBA29	calcite	dolomite	21651

Bath, nympheum base moulding	Sample	Major mineral components	Accessory minerals	File
	PBA30	calcite	dolomite, quartz	21652
	PBA31	calcite	dolomite, quartz, plagioclase	17848
	PBA32	calcite	quartz	18611
	PBA33	calcite	amphibole, quartz	21653
	PBA34	calcite	quartz, dolomite	17849
	PBA35	calcite	quartz	17850

3. XRF-Analysis

		CaO (%)	SiO_2 (%)	TiO_2 (%)	Al_2O_3 (%)	Fe_2O_3 (%)	MnO (%)	MgO (%)	Na_2O (%)	K_2O (%)	P_2O_5 (%)	Ba ppm	Cr ppm	Nb ppm	Ni ppm	Rb ppm	V ppm	Y ppm	Zn ppm	Zr ppm	Sr ppm
Afyon	A13	49.494	0.000	0.003	0.000	0.065	0.000	0.040	0.000	0.000	0.031	0	0	2	0	5	6	2	2	8	48
	A2	49.593	0.000	0.000	0.000	0.059	0.000	0.112	0.000	0.000	0.030	0	0	1	0	6	6	2	5	8	102
	A6	49.647	0.000	0.000	0.000	0.064	0.000	0.097	0.000	0.000	0.022	0	14	1	2	4	6	2	2	7	57
Assos	AST1	49.129	0.000	0.000	0.000	0.059	0.000	0.517	0.000	0.000	0.027	6	13	0	0	4	6	2	8	8	202
Babadag	BD4	49.055	0.000	0.000	0.000	0.088	0.000	0.464	0.000	0.000	0.027	0	0	2	0	4	6	2	8	8	118
	BD5	49.046	0.000	0.000	0.000	0.090	0.000	0.451	0.000	0.000	0.283	2	0	2	0	4	8	2	26	7	184
	BD6	49.126	0.000	0.000	0.000	0.076	0.000	0.473	0.000	0.000	0.104	0	23	0	2	4	6	2	10	8	150
Bergaz	BE1	48.802	0.000	0.000	0.000	0.077	0.000	0.742	0.000	0.003	0.035	0	0	2	0	5	6	3	59	8	110
Kazdag South	K12	48.451	0.000	0.008	0.004	0.092	0.000	1.496	0.000	0.018	1.106	0	0	1	0	8	6	2	8	10	181
	K15	48.760	0.000	0.000	0.000	0.068	0.000	1.290	0.000	0.000	0.038	0	0	0	0	6	6	9	5	9	157
	K18	49.510	0.000	0.000	0.000	0.058	0.000	0.449	0.000	0.000	0.017	0	102	1	1	5	6	2	5	8	181
	K21	46.315	0.000	0.003	0.000	0.100	0.000	4.323	0.000	0.026	0.178	0	258	2	1	5	8	3	6	10	126
Kazdag North	K2	48.956	0.000	0.008	0.139	0.099	0.000	0.577	0.000	0.073	0.074	20	11	2	2	7	6	2	4	8	98
	K6	49.145	0.000	0.001	0.000	0.082	0.000	0.357	0.000	0.007	0.032	0	16	0	0	6	6	3	4	6	90
	K7	49.077	0.000	0.000	0.000	0.061	0.000	0.510	0.000	0.000	0.040	0	0	0	0	5	8	2	8	6	135
	K9	49.238	0.000	0.000	0.000	0.060	0.000	0.523	0.000	0.010	0.067	5	16	0	0	6	6	2	12	8	121
Kemalpasa	KE4	49.501	0.000	0.000	0.000	0.053	0.000	0.262	0.000	0.000	0.020	0	0	2	0	4	6	2	7	8	135
Mugla	M11	49.777	0.000	0.000	0.000	0.068	0.000	0.051	0.000	0.000	0.030	0	39	0	0	3	6	2	5	7	71
	M7	49.458	0.000	0.000	0.000	0.162	0.000	0.158	0.000	0.000	0.017	0	0	0	0	4	6	2	6	7	64
	M8	49.288	0.000	0.006	0.000	0.086	0.001	0.543	0.000	0.000	0.041	0	4	0	2	6	6	4	2	9	93
	M9	44.879	0.000	0.000	0.000	0.512	0.025	6.171	0.000	0.000	0.019	0	108	2	8	5	6	3	8	6	92
Manyas	MAN3	49.182	0.000	0.000	0.000	0.067	0.000	0.660	0.000	0.000	0.043	0	0	2	0	6	6	5	8	7	117
Milas	Mi1	46.916	0.000	0.000	0.000	0.109	0.000	3.832	0.000	0.000	0.028	0	0	1	6	6	6	5	6	7	82
	Mi4	49.307	0.000	0.000	0.000	0.102	0.000	0.323	0.000	0.000	0.064	0	0	1	1	5	12	3	3	7	175
Mustafa - kemalpasa	MKB1	48.862	0.141	0.011	0.000	0.056	0.000	0.617	0.000	0.000	0.022	6	0	1	0	4	6	2	6	8	113

4. AAS-Analysis

	Mg (w%)	Fe (µg/g)	Mn (µg/g)
Altinoluk			
ALT1A	3.33	388.14	45.42
ALT1C	3.39	894.22	20.92
ALT1J	3.02	295.09	7.72
ALT2C	15.92	716.58	31.67
ALT2f	4.69	521.73	24.43
Ayazma			
AYAZMA A	9.89	641.83	10.34
AYAZMAc	5.43	560.90	10.39
Bandirma			
BAN1a	3.97	257.19	6.71
BAN1b	5.86	164.63	6.51
Babadag			
BD4	3.24	584.04	18.30
BD7	3.99	846.69	112.20
Bergaz			
BE1	4.71	395.34	10.63
BE2	95.66	809.44	34.30
Cay			
CAY1A	2.64	408.06	26.61
CAY3C	1.92	1101.69	344.53
Afyon			
ISC1F	1.69	501.62	28.34
ISC1J	2.72	590.05	62.05
ISC2B	1.99	338.12	30.17
Iznik			
IZNIK1A	1.22	847.68	46.55
IZNIKb	1.65	890.71	80.55
Serhat			
K22	3.37	329.27	12.43
K3	3.23	544.92	3.23
K4	2.68	275.00	25.98
Yenice			
KAR1	2.89	294.41	1.14
KAR5	9.29	370.59	10.21
Karabiga			
KB1D	0.81	562.68	25.78
KB1F	0.47	572.35	68.06
KB3	3.76	278.28	10.46
Marmara			
MA1	5.67	359.12	7.43
MAR1Awhite	3.24	284.56	10.27
MAR1Ablack	3.35	2659.35	113.31
Milas			
MI2	6.22	465.76	63.27
MI3	18.85	466.39	55.29

	Mg (w%)	Fe (µg/g)	Mn (µg/g)
Orhangazi			
ORH1B	1.13	326.72	14.47
ORH1C	1.27	180.13	18.31
ORH2a	10.10	323.44	6.20
ZTM6	3.12	128 8.07	6.72
Troia Bronze Age			
A8/491	11.56	1076.13	25.99
D3/449	0.68	471.67	14.22
D8/1844	14.69	675.32	20.15
D9/106	12.22	1692.67	486.36
E4/640	3.04	205.63	8.52
E9/1297	1.46	586.47	1.98
F28/958	18.38	790.97	57.65
F29/460	9.63	775.85	25.54
G6/42(1)	3.07	412.63	7.74
I9/343	15.27	441.42	26.34
Troia Hellenistic Period			
PBA1	3.14	305.94	16.05
PBA11	3.15	209.53	5.15
PBA13	3.95	326.87	11.86
PBA18	3.84	278.86	1.73
PBA2	39.23	363.58	1.96
PBA21blau	9.26	360.62	6.32
PBA22	3.59	318.79	4.68
Troia Roman Period			
PBA24	26.58	373.09	3.17
PBA29	3.60	362.27	1.23
PBA3	20.97	421.17	0.1
PBA32	2.64	380.91	9.77
PBA33	2.10	342.35	24.71

5. Isotopic ratios measured in this study ($\delta^{13}C$, $\delta^{18}O$, $^{87}Sr/^{86}Sr$)

sample_name	sample_short_description	locality_name	continent	country	geological_unit	d13c	d18o	87Sr/86Sr
A3	Geological Sample Afyon	Afyon	Asia	Turkey	Taurides	2.69	-2.56	
A3b	Geological Sample Afyon	Afyon	Asia	Turkey	Taurides	2.63	-2.45	
A6b	Geological Sample Afyon	Afyon	Asia	Turkey	Taurides	1.03	-4.41	0.7081520
A6	Geological Sample Afyon	Afyon	Asia	Turkey	Taurides	1.10	-4.46	0.7081520
A4b	Geological Sample Afyon 3	Afyon	Asia	Turkey	Taurides	3.64	-4.40	
A4	Geological Sample Afyon 3	Afyon	Asia	Turkey	Taurides	3.61	-4.41	
ZTM3	Geological Sample Afyon Bal	Afyon	Asia	Turkey	Taurides	1.93	-4.26	
A12	Geological Sample Afyon Sari	Afyon	Asia	Turkey	Taurides	0.84	-5.17	
A13b	Geological Sample Afyon Sari bencekli	Afyon	Asia	Turkey	Taurides	1.04	-5.35	
A13	Geological Sample Afyon Sari bencekli	Afyon	Asia	Turkey	Taurides	1.05	-5.53	0.7080090
ZTM1	Geological Sample Afyon Seker	Afyon	Asia	Turkey	Taurides	-0.16	-6.65	
A14	Geological Sample Afyon Seker	Afyon	Asia	Turkey	Taurides	1.01	-5.45	0.7080090
A3	Geological sample Afyon/Turkey	Afyon	Asia	Turkey	Taurides	2.92	-2.89	
A8	Geological Sample Afyon1	Afyon	Asia	Turkey	Taurides	3.77	-4.57	
A16	Geological Sample Afyon-Kaplan Postu	Afyon	Asia	Turkey	Taurides	-1.19	-5.49	
A1	Geological Sample Afyon-Oniks	Afyon	Asia	Turkey	Taurides	-1.44	-5.44	
A1b	Geological Sample Afyon-Oniks	Afyon	Asia	Turkey	Taurides	-1.08	-4.72	
A2	Geological Sample Afyon-Sarisi	Afyon	Asia	Turkey	Taurides	1.32	-3.25	
A2b	Geological Sample Afyon-Sarisi	Afyon	Asia	Turkey	Taurides	1.33	-3.26	
BD1	Geological Sample BabaDag	Babadag	Asia	Turkey	Taurides	3.77	-4.57	
A1	Geological Sample Afyon	Afyon	Asia	Turkey	Taurides	4.69	-14.32	
A12	Geological Sample Afyon	Afyon	Asia	Turkey	Taurides	1.29	-4.91	
A4	Geological Sample Afyon	Afyon	Asia	Turkey	Taurides	3.64	4.40	
AKH2	Geological Sample Afyon	Akhisar	Asia	Turkey	Akhisar	2.59	-1.16	
A 2	Geological sample, Aphrodisias	Aphrodisias	Asia	Turkey	Taurides	1.17	-2.64	0.7076500
AFR 12	Geological sample, Aphrodisias	Aphrodisias	Asia	Turkey	Taurides	2.53	-3.03	0.7076040
A 20	Geological sample, Aphrodisias	Aphrodisias	Asia	Turkey	Taurides	2.38	-3.21	0.7076000
AFR 13	Geological sample, Aphrodisias	Aphrodisias	Asia	Turkey	Taurides	2.51	-3.18	0.7076710
AFR 14	Geological sample, Aphrodisias	Aphrodisias	Asia	Turkey	Taurides	1.03	-3.82	0.7075510
AFR 21*	Geological sample, Aphrodisias	Aphrodisias	Asia	Turkey	Taurides	0.74	-4.17	0.7080580
AFR 27	Geological sample, Aphrodisias	Aphrodisias	Asia	Turkey	Taurides	1.97	-3.64	0.7076560
AFR 30	Geological sample, Aphrodisias	Aphrodisias	Asia	Turkey	Taurides	2.20	-3.95	0.7081960
AFR 31	Geological sample, Aphrodisias	Aphrodisias	Asia	Turkey	Taurides	1.44	-3.82	0.7078560
AFR 5	Geological sample, Aphrodisias	Aphrodisias	Asia	Turkey	Taurides	2.12	-3.32	0.7076830
AFR 22,21	Geological sample, Aphrodisias	Aphrodisias	Asia	Turkey	Taurides	1.74	-3.91	0.7077200
AFR 6	Geological sample, Aphrodisias	Aphrodisias	Asia	Turkey	Taurides	1.97	-3.73	0.7078910
AFR I b *	Geological sample, Aphrodisias	Aphrodisias	Asia	Turkey	Taurides	1.65	-2.59	0.7078780
AFR 9	Geological sample, Aphrodisias	Aphrodisias	Asia	Turkey	Taurides	1.76	-3.53	0.7076300
A 8	Geological sample, Aphrodisias, Turkey	Aphrodisias	Asia	Turkey	Taurides	0.60	-2.54	0.7075400
BD4	Geological Sample BabaDag	Babadag	Asia	Turkey	Taurides	1.54	-2.38	0.7075290
BD6	Geological Sample BabaDag	Babadag	Asia	Turkey	Taurides	-0.03	-2.72	0.7075190
BD5	Geological Sample BabaDag	Babadag	Asia	Turkey	Taurides	0.66	-4.45	0.7075290
AyazmaA	Geological sample Ayazma	Ayazma	Asia	Turkey	Sakarya Zone	2.12	-2.53	
ZTM6	Geological Sample Ayazma	Ayazma	Asia	Turkey	Sakarya Zone	1.72	-1.88	
K2	Geological Sample Kazdag-Ayazma	Ayazma	Asia	Turkey	Sakarya Zone	2.10	-2.80	
Ayazma C	Geological Sample Ayazma	Ayazma	Asia	Turkey	Sakarya Zone	2.12	-2.53	
Ayazma D	Geological Sample Ayazma	Ayazma	Asia	Turkey	Sakarya Zone	1.61	-3.33	
Ayazma B	Geological Sample Ayazma	Ayazma	Asia	Turkey	Sakarya Zone	2.13	-2.87	
K21	Geological Sample Altinoluk	Altinoluk	Asia	Turkey	Sakarya Zone	1.49	-2.89	0.7077280

K15b	Geological Sample Altinoluk	Altinoluk	Asia	Turkey	Sakarya Zone	2.26	-0.51	
K18b	Geological Sample Altinoluk	Altinoluk	Asia	Turkey	Sakarya Zone	2.72	-0.86	
K15	Geological Sample Altinoluk	Altinoluk	Asia	Turkey	Sakarya Zone	2.32	-0.51	
K18	Geological Sample Altinoluk	Altinoluk	Asia	Turkey	Sakarya Zone	2.72	-0.86	
K12	Geological Sample Altinoluk	Altinoluk	Asia	Turkey	Sakarya Zone	1.36	-7.45	0.7078994
K12b	Geological Sample Altinoluk	Altinoluk	Asia	Turkey	Sakarya Zone	1.41	-7.64	0.7078994
ALT 1A	Geological Sample Altinoluk	Altinoluk	Asia	Turkey	Sakarya Zone	1.68	-2.46	
ALT 1C	Geological Sample Altinoluk	Altinoluk	Asia	Turkey	Sakarya Zone	-0.51	-17.88	
ALT 1F	Geological Sample Altinoluk	Altinoluk	Asia	Turkey	Sakarya Zone	2.09	-5.88	
ALT 1H	Geological Sample Altinoluk	Altinoluk	Asia	Turkey	Sakarya Zone	0.45	-10.34	
ALT 1I	Geological Sample Altinoluk	Altinoluk	Asia	Turkey	Sakarya Zone	2.62	-0.82	
ALT 1J	Geological Sample Altinoluk	Altinoluk	Asia	Turkey	Sakarya Zone	1.12	-4.75	
ALT 2C	Geological Sample Altinoluk	Altinoluk	Asia	Turkey	Sakarya Zone	2.08	-5.02	
ALT 2F	Geological Sample Altinoluk	Altinoluk	Asia	Turkey	Sakarya Zone	2.14	-2.48	
Ban1a	Geological Sample, Bandirma, Turkey	Bandirma	Asia	Turkey	Sakarya Zone	3.45	-2.86	
Ban1b	Geological Sample, Bandirma, Turkey	Bandirma	Asia	Turkey	Sakarya Zone	3.32	-2.72	
KB 3	Geological Sample, Karabiga, Turkey	Karabiga	Asia	Turkey	Sakarya Zone	3.66	-5.54	
			Asia	Turkey		3.46	-6.64	
			Asia	Turkey		3.26	-7.35	
			Asia	Turkey		3.40	-9.04	
KB 1-F	Geological Sample, Karabiga, Turkey	Karabiga	Asia	Turkey	Sakarya Zone	2.87	-10.98	
Be1	Geological Sample Bergaz	Bergaz	Asia	Turkey	Sakarya Zone	1.92	-10.35	
Be1b	Geological Sample Bergaz	Bergaz	Asia	Turkey	Sakarya Zone	1.93	-10.35	
Be2b	Geological Sample Bergaz	Bergaz	Asia	Turkey	Sakarya Zone	3.57	-10.71	
Be2	Geological Sample Bergaz	Bergaz	Asia	Turkey	Sakarya Zone	3.60	-10.69	
K1	Geological Sample Kazdag-Kapikaya, Turkey	Kapikaya	Asia	Turkey	Sakarya Zone	1.04	-10.24	
Kar1	Geological Sample Karadoru	Karadoru	Asia	Turkey	Sakarya Zone	2.19	-5.16	
K7	Geological Sample Kazdag-Nord	Kazdag-Nord	Asia	Turkey	Sakarya Zone	2.36	-9.72	0.7075330
K6	Geological Sample Kazdag-Nord	Kazdag-Nord	Asia	Turkey	Sakarya Zone	1.41	-2.81	0.7075186
K7b	Geological Sample Kazdag-Nord	Kazdag-Nord	Asia	Turkey	Sakarya Zone	2.41	-9.90	0.7075330
K9	Geological Sample Kazdag-Nord	Kazdag-Nord	Asia	Turkey	Sakarya Zone	1.52	-4.82	0.7075937
K9b	Geological Sample Kazdag-Nord	Kazdag-Nord	Asia	Turkey	Sakarya Zone	1.60	-4.97	0.7075937
K1	Kazdag-North, Turkey	Kazdag-Nord	Asia	Turkey	Sakarya Zone	1.46	-10.66	
K3	Kazdag-North, Turkey	Kazdag-Nord	Asia	Turkey	Sakarya Zone	1.99	-2.51	
K4	Kazdag-North, Turkey	Kazdag-Nord	Asia	Turkey	Sakarya Zone	3.03	-5.10	
Ma3	Geological Sample Marmara	Marmara	Asia	Turkey	Sakarya Zone	3.14	-1.52	
ZTM2	Geological Sample Marmara	Marmara	Asia	Turkey	Sakarya Zone	3.18	-1.52	
ZTM2-2	Geological Sample Marmara	Marmara	Asia	Turkey	Sakarya Zone	3.14	-1.61	
Nas 34	Marmara	Marmara	Asia	Turkey	Sakarya Zone	3.14	-1.63	0.7079800
Nas 35	Marmara	Marmara	Asia	Turkey	Sakarya Zone	2.22	-2.53	0.7077500
Nas 36	Marmara	Marmara	Asia	Turkey	Sakarya Zone	2.67	-1.80	0.7080300
Nas 37	Marmara	Marmara	Asia	Turkey	Sakarya Zone	3.09	-0.71	0.7080700
Mar1a(schwarz)	Marmara, Turkey	Marmara	Asia	Turkey	Sakarya Zone	3.14	-1.61	0.7076150
Ke1	Geological Sample Kemalpasa	Mustafa Kemalpasa	Asia	Turkey	Sakarya Zone	5.01	-2.78	
Ke1	Geological Sample Kemalpasa	Mustafa Kemalpasa	Asia	Turkey	Sakarya Zone	5.00	-2.76	
Ke2	Geological Sample Kemalpasa	Mustafa Kemalpasa	Asia	Turkey	Sakarya Zone	3.52	-1.73	
Ke2	Geological Sample Kemalpasa	Mustafa Kemalpasa	Asia	Turkey	Sakarya Zone	3.52	-1.73	
Ke2b	Geological Sample Kemalpasa	Mustafa Kemalpasa	Asia	Turkey	Sakarya Zone	3.53	-1.76	
MKB1	Geological Sample Mustafa-Kemalpasa (Beyaz)	Mustafa Kemalpasa	Asia	Turkey	Sakarya Zone	4.50	-2.81	
MKB1b	Geological Sample Mustafa-Kemalpasa (Beyaz)	Mustafa Kemalpasa	Asia	Turkey	Sakarya Zone	4.53	-2.78	
ORH2c	Geological Sample, Orhangazi, Turkey	Orhangazi	Asia	Turkey	Sakarya Zone	3.05	-6.98	0.7076520
orh2a	Geological Sample, Orhangazi, Turkey	Orhangazi	Asia	Turkey	Sakarya Zone	3.31	-3.13	0.7076580
ORH 1B	Geological Sample, Orhangazi, Turkey	Orhangazi	Asia	Turkey	Sakarya Zone	2.13	-5.53	
ORH 1-B	Geological Sample, Orhangazi, Turkey	Orhangazi	Asia	Turkey	Sakarya Zone	2.46	-2.23	

ORH 1C	Geological Sample, Orhangazi, Turkey	Orhangazi	Asia	Turkey	Sakarya Zone	3.14	-2.16	
ORH 2A	Geological Sample, Orhangazi, Turkey	Orhangazi	Asia	Turkey	Sakarya Zone	3.31	-3.13	
ORH 2B	Geological Sample, Orhangazi, Turkey	Orhangazi	Asia	Turkey	Sakarya Zone	4.01	-3.44	
ORH 2C	Geological Sample, Orhangazi, Turkey	Orhangazi	Asia	Turkey	Sakarya Zone	3.00	-4.78	
ORH 2-C	Geological Sample, Orhangazi, Turkey	Orhangazi	Asia	Turkey	Sakarya Zone	3.05	-3.20	
ORH 2D	Geological Sample, Orhangazi, Turkey	Orhangazi	Asia	Turkey	Sakarya Zone	3.76	-2.58	
ORH 2E	Geological Sample, Orhangazi, Turkey	Orhangazi	Asia	Turkey	Sakarya Zone	3.43	-2.80	
ORH 2-E	Geological Sample, Orhangazi, Turkey	Orhangazi	Asia	Turkey	Sakarya Zone	3.30	-2.83	
ORH 2F	Geological Sample, Orhangazi, Turkey	Orhangazi	Asia	Turkey	Sakarya Zone	2.83	-2.82	
IZNIK A	Geological Sample, Iznik, Turkey	Iznik	Asia	Turkey	Sakarya Zone	1.78	-7.29	
IZNIK B	Geological Sample, Iznik, Turkey	Iznik	Asia	Turkey	Sakarya Zone	2.42	-8.49	
CAY 1A	Geological Sample, Cay, Turkey	Cay	Asia	Turkey	Sakarya Zone	1.07	-7.77	
CAY 3A	Geological Sample, Cay, Turkey	Cay	Asia	Turkey	Sakarya Zone	1.64	-8.16	
CAY 3B	Geological Sample, Cay, Turkey	Cay	Asia	Turkey	Sakarya Zone	1.37	-7.79	
CAY 3C	Geological Sample, Cay, Turkey	Cay	Asia	Turkey	Sakarya Zone	1.15	-8.22	
K3	Geological Sample Kazdag-Serhat	Serhat	Asia	Turkey	Sakarya Zone	2.00	-2.49	
K4	Geological Sample Kazdag-Serhat	Serhat	Asia	Turkey	Sakarya Zone	2.65	-4.93	
Man3	Geological Sample Manyas	Manyas	Asia	Turkey	Manyas	3.70	-2.16	
Man3b	Geological Sample Manyas	Manyas	Asia	Turkey	Manyas	3.66	-2.00	
El1	Geological Sample Elazi	Elazig	Asia	Turkey	Elazi	0.93	-10.84	
T1	Takaoglu/Harmandali	Harmandali	Asia	Turkey	Harmandali	1.58	-2.54	
T2	Takaoglu/Harmandali	Harmandali	Asia	Turkey	Harmandali	-1.68	-11.39	
T2b	Takaoglu/Harmandali	Harmandali	Asia	Turkey	Harmandali	-1.70	-11.41	
T3	Takaoglu/Harmandali	Harmandali	Asia	Turkey	Harmandali	-1.25	-11.58	
Mi2b	Geological Sample Milas	Milas	Asia	Turkey	Menderes Massif	3.72	-3.73	
Mi4	Geological Sample Milas	Milas	Asia	Turkey	Menderes Massif	3.44	-6.88	
Mi4	Geological Sample Milas	Milas	Asia	Turkey	Menderes Massif	3.41	-6.87	
Mi2	Geological Sample Milas	Milas	Asia	Turkey	Menderes Massif	3.72	-3.75	0.7077610
Mi3	Geological Sample Milas	Milas	Asia	Turkey	Menderes Massif	3.44	-6.88	
Mi1	Geological Sample Milas-Sedef	Milas	Asia	Turkey	Menderes Massif	3.78	-4.60	0.7077606
Mi1b	Geological Sample Milas-Sedef	Milas	Asia	Turkey	Menderes Massif	3.80	-4.53	0.7077606
M12	Geological Sample Mugla	Mugla	Asia	Turkey	Menderes Massif	3.94	-5.90	
M12b	Geological Sample Mugla	Mugla	Asia	Turkey	Menderes Massif	3.83	-5.50	
M7b	Geological Sample Mugla	Mugla	Asia	Turkey	Menderes Massif	1.22	-3.86	
M8b	Geological Sample Mugla	Mugla	Asia	Turkey	Menderes Massif	2.96	-4.64	
M7	Geological Sample Mugla	Mugla	Asia	Turkey	Menderes Massif	1.25	-3.71	0.7075370
M4	Geological Sample Mugla	Mugla	Asia	Turkey	Menderes Massif	3.06	-5.86	
M8	Geological Sample Mugla	Mugla	Asia	Turkey	Menderes Massif	2.93	-4.68	
M11	Geological Sample Mugla	Mugla	Asia	Turkey	Menderes Massif	0.32	-5.93	0.7078520
M11b	Geological Sample Mugla	Mugla	Asia	Turkey	Menderes Massif	0.21	-5.76	0.7078520
ZTM4	Geological Sample Mugla/Yatagan	Mugla Yatagan	Asia	Turkey	Menderes Massif	2.46	-0.71	
ZTM5	Geological Sample Mugla/Yatagan	Mugla Yatagan	Asia	Turkey	Menderes Massif	3.65	-0.26	
M6	Geological Sample Mugla-Ege Beyaz	Mugla-Ege Beyaz	Asia	Turkey	Menderes Massif	1.53	-3.59	
M6b	Geological Sample Mugla-Ege Beyaz	Mugla-Ege Beyaz	Asia	Turkey	Menderes Massif	1.52	-3.65	
M10	Geological Sample Mugla-Leylak	Mugla-Leylak	Asia	Turkey	Menderes Massif	3.06	-5.86	
M10b	Geological Sample Mugla-Leylak	Mugla-Leylak	Asia	Turkey	Menderes Massif	3.07	-5.96	
M9	Geological Sample Mugla-Leylak	Mugla-Leylak	Asia	Turkey	Menderes Massif	3.87	-6.49	
M9b	Geological Sample Mugla-Leylak	Mugla-Leylak	Asia	Turkey	Menderes Massif	3.87	-6.37	
M2-1	Geological Sample Mugla-Lila	Mugla-Lila	Asia	Turkey	Menderes Massif	3.94	-5.90	
M2-2	Geological Sample, Mugla-Lila, Turkey	Mugla-Lila	Asia	Turkey	Menderes Massif	3.83	-5.50	
ZTM7	Geological Sample Suepren/Eskisehir	Suepren/Eskisehir	Asia	Turkey	Suepren/Eskisehir	2.37	-3.87	
TR1	Geological Sample Tire	Tire	Asia	Turkey	Tire	1.55	-5.87	
TR2	Geological Sample Tire	Tire	Asia	Turkey	Tire	1.55	-5.80	
GUS1	Geological Sample, Quarry Gummern, Austria	Gummern	Europe	Austria	Weissenstein Marbles	0.10	-5.19	

GUS2	Geological Sample, Quarry Gummern, Austria	Gummern	Europe	Austria	Weissenstein Marbles	1.88	-8.08
GUS3	Geological Sample, Quarry Gummern, Austria	Gummern	Europe	Austria	Weissenstein Marbles	0.89	-5.43
GUS5	Geological Sample, Quarry Gummern, Austria	Gummern	Europe	Austria	Weissenstein Marbles	1.08	-5.53
GUS6	Geological Sample, Quarry Gummern, Austria	Gummern	Europe	Austria	Weissenstein Marbles	0.64	-5.00
GUS2_10_1	Geological sample, Quarry Gummern, Austria	Gummern	Europe	Austria	Weissenstein Marbles	1.80	-9.75
GUS2_10_2	Geological sample, Quarry Gummern, Austria	Gummern	Europe	Austria	Weissenstein Marbles	1.80	-9.75
GUS2_10_3	Geological sample, Quarry Gummern, Austria	Gummern	Europe	Austria	Weissenstein Marbles	1.80	-9.75
GUS3_10_2	Geological sample, Quarry Gummern, Austria	Gummern	Europe	Austria	Weissenstein Marbles	1.00	-5.61
GUS6_10_1	Geological sample, Quarry Gummern, Austria	Gummern	Europe	Austria	Weissenstein Marbles	0.64	-5.00
GUS6_10_2	Geological sample, Quarry Gummern, Austria	Gummern	Europe	Austria	Weissenstein Marbles	0.64	-5.00
GUS6_10_3	Geological sample, Quarry Gummern, Austria	Gummern	Europe	Austria	Weissenstein Marbles	0.64	-5.00
TRS1	Geological Sample, Quarry Treffen, Austria	Treffen	Europe	Austria	Weissenstein Marbles	0.45	-6.17
TRS2	Geological Sample, Quarry Treffen, Austria	Treffen	Europe	Austria	Weissenstein Marbles	0.32	-7.26
TRS3	Geological Sample, Quarry Treffen, Austria	Treffen	Europe	Austria	Weissenstein Marbles	-0.07	-6.22
TRS4	Geological Sample, Quarry Treffen, Austria	Treffen	Europe	Austria	Weissenstein Marbles	1.40	-7.00
TRS5	Geological Sample, Quarry Treffen, Austria	Treffen	Europe	Austria	Weissenstein Marbles	0.87	-6.10
POS1	Geological Sample, Quarry Poels, Austria	Poels	Europe	Austria	Poels	3.43	-3.43
POS2	Geological Sample, Quarry Poels, Austria	Poels	Europe	Austria	Poels	1.31	-5.71
POS3	Geological Sample, Quarry Poels, Austria	Poels	Europe	Austria	Poels	3.71	-6.56
POS3A	Geological Sample, Quarry Poels, Austria	Poels	Europe	Austria	Poels	1.02	-5.51
POS3B	Geological Sample, Quarry Poels, Austria	Poels	Europe	Austria	Poels	1.88	-7.08
POS4a	Geological Sample, Quarry Poels, Austria	Poels	Europe	Austria	Poels	2.13	-8.22
POS4b	Geological Sample, Quarry Poels, Austria	Poels	Europe	Austria	Poels	3.09	-4.77
POS5	Geological Sample, Quarry Poels, Austria	Poels	Europe	Austria	Poels	1.93	-4.94
PUS1	Geological Sample, Quarry Pupitsch, Austria	Puppitsch	Europe	Austria	Puppitsch	1.21	-14.18
PUS2	Geological Sample, Quarry Pupitsch, Austria	Puppitsch	Europe	Austria	Puppitsch	1.90	-14.34
PUS3	Geological Sample, Quarry Pupitsch, Austria	Puppitsch	Europe	Austria	Puppitsch	2.09	-14.75
PUS4	Geological Sample, Quarry Pupitsch, Austria	Puppitsch	Europe	Austria	Puppitsch	1.90	-13.99
bLES3	Geological Sample, Quarry Schwarzviertel, Austria	Schwarzviertel	Europe	Austria	Schwarzviertel	1.77	-5.70
bLES1	Geological Sample, Quarry Schwarzviertel, Austria	Schwarzviertel	Europe	Austria	Schwarzviertel	2.10	-5.17
bLES2	Geological Sample, Quarry Schwarzviertel, Austria	Schwarzviertel	Europe	Austria	Schwarzviertel	2.03	-3.88
LES3	Geological Sample, Quarry Schwarzviertel, Austria	Schwarzviertel	Europe	Austria	Schwarzviertel	1.76	-4.48
bLES4	Geological Sample, Quarry Schwarzviertel, Austria	Schwarzviertel	Europe	Austria	Schwarzviertel	0.97	-6.06
LES7	Geological Sample, Quarry Schwarzviertel, Austria	Schwarzviertel	Europe	Austria	Schwarzviertel	3.37	-5.30
SS1	Geological Sample, Quarry Sekull, Austria	Sekull	Europe	Austria	Sekull	0.36	-12.05
ST2a	Geological Sample, Quarry Sekull, Austria	Sekull	Europe	Austria	Sekull	0.50	-8.75
ST2b	Geological Sample, Quarry Sekull, Austria	Sekull	Europe	Austria	Sekull	1.02	-11.00
bSt2e	Geological Sample, Quarry Sekull, Austria	Sekull	Europe	Austria	Sekull	1.09	-8.49
ST2f	Geological Sample, Quarry Sekull, Austria	Sekull	Europe	Austria	Sekull	0.63	-8.04
ST2g	Geological Sample, Quarry Sekull, Austria	Sekull	Europe	Austria	Sekull	0.61	-10.90
TIS1	Geological Sample, Quarry Tiffen, Austria	Tiffen	Europe	Austria	Tiffen	-0.91	-15.08
TIS2	Geological Sample, Quarry Tiffen, Austria	Tiffen	Europe	Austria	Tiffen	-0.68	-14.84
TIS3	Geological Sample, Quarry Tiffen, Austria	Tiffen	Europe	Austria	Tiffen	0.25	-15.27
TIT1	Geological Sample, Quarry Tiffen, Austria	Tiffen	Europe	Austria	Tiffen	0.37	-13.99
TOS1	Geological Sample, Quarry Töschling, Austria	Toeschling	Europe	Austria	Toeschling	0.75	-11.17
TOS3A	Geological Sample, Quarry Töschling, Austria	Toeschling	Europe	Austria	Toeschling	0.41	-12.06
TOS3b	Geological Sample, Quarry Töschling, Austria	Toeschling	Europe	Austria	Toeschling	0.65	-11.14
TOS4	Geological Sample, Quarry Töschling, Austria	Toeschling	Europe	Austria	Toeschling	0.29	-10.55
TOS2		Toeschling	Europe	Austria	Toeschling	-0.11	-10.84
BSB1A	Geological Sample Slovenska Bistrica (Slovenia)	Slovenska Bistrica	Europe	Slovenia	Slovenska Bistrica	0.02	-7.79
BSB1B	Geological Sample Slovenska Bistrica (Slovenia)	Slovenska Bistrica	Europe	Slovenia	Slovenska Bistrica	0.64	-8.36
BSB2	Geological Sample Slovenska Bistrica (Slovenia)	Slovenska Bistrica	Europe	Slovenia	Slovenska Bistrica	0.01	-6.63
POLT2	Polgardi	Polgardi	Europe	Hungary	Polgardi	0.04	-10.99
POLT3	Polgardi	Polgardi	Europe	Hungary	Polgardi	1.18	-6.16

POLT4	Polgardi	Polgardi	Europe	Hungary	Polgardi	1.85	-8.71	
Hy 1a	Hymettos	Hymettos	Europe	Greece	Hymettos	1.17	-2.87	0.7071700
Hy 1b	Hymettos	Hymettos	Europe	Greece	Hymettos	2.53	-2.21	0.7072500
Hy 1c	Hymettos	Hymettos	Europe	Greece	Hymettos	2.17	-3.00	0.7072200
Hy 2	Hymettos	Hymettos	Europe	Greece	Hymettos	2.05	-2.74	0.7074300
M 413	Geological sample, Pentelikon, Greece	Pentelikon	Europe	Greece	Pentelikon	2.48	-2.29	0.7075410
Pe 3	Pentelikon	Pentelikon	Europe	Greece	Pentelikon	2.64	-6.66	0.7083800
Pe 7	Pentelikon	Pentelikon	Europe	Greece	Pentelikon	2.94	-7.90	0.7088200
Pe 1	Pentelikon	Pentelikon	Europe	Greece	Pentelikon	2.47	-6.68	0.7083500
Pe 2	Pentelikon	Pentelikon	Europe	Greece	Pentelikon	2.54	-6.13	0.7083000
Pe-Spilia	Pentelikon	Pentelikon	Europe	Greece	Pentelikon	2.49	-8.26	0.7081360
Pe-Dyon.	Pentelikon	Pentelikon	Europe	Greece	Pentelikon	2.74	-7.04	0.7082160
NA 17	Naxos Melanes	Naxos	Europe	Greece	Naxos	1.92	-3.21	0.7079100
NA 19	Naxos Melanes	Naxos	Europe	Greece	Naxos	2.02	-2.52	0.7079800
NA 20	Naxos Melanes	Naxos	Europe	Greece	Naxos	1.77	-4.89	0.7078800
NA-Mel	Naxos Melanes	Naxos	Europe	Greece	Naxos	2.06	-3.34	0.7076310
PA-LY	Paros Lychnites	Paros Lychnites	Europe	Greece	Paros Lychnites	4.57	-3.48	0.7075340
PA-PL/C	Paros Lychnites	Paros Lychnites	Europe	Greece	Paros Lychnites	5.05	-3.76	0.7073690
PL 12	Paros Lychnites	Paros Lychnites	Europe	Greece	Paros Lychnites	5.17	-2.98	0.7075000
PL 15	Paros Lychnites	Paros Lychnites	Europe	Greece	Paros Lychnites	4.90	-3.50	0.7073800
PL 13	Paros Lychnites	Paros Lychnites	Europe	Greece	Paros Lychnites	4.93	-3.74	0.7077400
PL 4	Paros Lychnites	Paros Lychnites	Europe	Greece	Paros Lychnites	5.36	-2.90	0.7075700
8312	Geological sample, Thasos Aliki, Greece	Thasos Aliki	Europe	Greece	Thasos Aliki	3.75	-2.74	0.7078100
8317	Geological sample, Thasos Aliki, Greece	Thasos Aliki	Europe	Greece	Thasos Aliki	3.71	-2.59	0.7075200
8321	Geological sample, Thasos Aliki, Greece	Thasos Aliki	Europe	Greece	Thasos Aliki	3.63	-3.38	0.7078100
TA-AIW	Thasos Aliki	Thasos Aliki	Europe	Greece	Thasos Aliki	2.44	-2.89	0.7080190
TH 2	Thasos Aliki	Thasos Aliki	Europe	Greece	Thasos Aliki	3.33	-2.64	0.7079200
TH 20	Thasos Aliki	Thasos Aliki	Europe	Greece	Thasos Aliki	3.13	0.39	0.7077600
TH 9	Thasos Aliki	Thasos Aliki	Europe	Greece	Thasos Aliki	3.55	-0.09	0.7076900
BKUKUL	Geological Sample Kukul (Macedonia)	Kukul	Europe	Macedonia	Kukul	2.82	-2.49	
CAFOR65	Carrara	Carrara	Europe	Italy	Carrara	2.62	-1.80	0.7077330
ARCO 2	Geological sample, Carrara, Italy	Carrara	Europe	Italy	Carrara	2.11	-1.37	0.7079000
ARCO 2e	Geological sample, Carrara, Italy	Carrara	Europe	Italy	Carrara	2.20	-2.26	0.7078200
ARCO 4b	Geological sample, Carrara, Italy	Carrara	Europe	Italy	Carrara	2.46	-1.48	0.7079800
ARCO 5	Geological sample, Carrara, Italy	Carrara	Europe	Italy	Carrara	2.06	-3.48	0.7078000
CA 51213	Geological sample, Carrara, Italy	Carrara	Europe	Italy	Carrara	2.04	-2.15	0.7077980
CA 541	Geological sample, Carrara, Italy	Carrara	Europe	Italy	Carrara	2.32	-2.16	0.7077560
CA-R	Geological sample, Carrara, Italy	Carrara	Europe	Italy	Carrara	2.48	-0.95	0.7077360
CAMC6035	Geological sample, Carrara, Italy	Carrara	Europe	Italy	Carrara	2.37	-1.71	0.7078300
Fa1	CNRgiu97, Carrara, Miseglia, Fantiscritti	Fantiscritti	Europe	Italy	Carrara	2.16	-2.05	
C1	CNRgiu97, Carrara, Miseglia, Canalgrande	Canalgrande	Europe	Italy	Carrara	2.06	-1.93	
P1.1	CNRgiu97, Carrara, Torano, Polvaccio	Polvaccio	Europe	Italy	Carrara	2.29	-1.35	
R1	CNRgiu97, Carrara, Torano, Ravaccione	Ravaccione	Europe	Italy	Carrara	2.04	-2.41	
Tr2	CNRgiu97, Carrara, Torano, Sponda1	Sponda1	Europe	Italy	Carrara	2.17	-1.64	
Tr2.7	CNRgiu97, Carrara, Torano, Sponda2	Sponda2	Europe	Italy	Carrara	2.48	-1.56	
PR1	Viana do Alentejo, Portugal	Viana do Alentejo	Europe	Portugal	Viana do Alentejo	2.40	-6.25	0.7098000
PR2	Viana do Alentejo, Portugal	Viana do Alentejo	Europe	Portugal	Viana do Alentejo	2.32	-6.30	0.7097200
PR3	Viana do Alentejo, Portugal	Viana do Alentejo	Europe	Portugal	Viana do Alentejo	2.18	-6.10	0.7097500
PR4	Viana do Alentejo, Portugal	Viana do Alentejo	Europe	Portugal	Viana do Alentejo	2.85	-6.35	0.7095000
PR5	Viana do Alentejo, Portugal	Viana do Alentejo	Europe	Portugal	Viana do Alentejo	2.90	-6.21	0.7089600
PR6	Viana do Alentejo, Portugal	Viana do Alentejo	Europe	Portugal	Viana do Alentejo	2.55	-6.40	0.7088500
PR7	Viana do Alentejo, Portugal	Viana do Alentejo	Europe	Portugal	Viana do Alentejo	2.21	-6.44	0.7099200
PR8	Viana do Alentejo, Portugal	Viana do Alentejo	Europe	Portugal	Viana do Alentejo	2.73	-6.27	0.7099000
PR9	Vilavicosa, Portugal	Vilavicosa	Europe	Portugal	Vilavicosa	2.38	-5.65	0.7094900

PR10	Vilavicosa, Portugal	Vilavicosa	Europe	Portugal	Vilavicosa	2.16	-5.66	0.7093500
PR11	Vilavicosa, Portugal	Vilavicosa	Europe	Portugal	Vilavicosa	1.66	-5.91	0.7092800
PR12	Vilavicosa, Portugal	Vilavicosa	Europe	Portugal	Vilavicosa	1.95	-5.88	0.7091000
PR13	Vilavicosa, Portugal	Vilavicosa	Europe	Portugal	Vilavicosa	2.00	-5.73	0.7089000
PR14	Vilavicosa, Portugal	Vilavicosa	Europe	Portugal	Vilavicosa	2.43	-5.68	0.7094500
SP11	Las Cabreras, Spain	Las Cabreras	Europe	Spain	Las Cabreras	1.52	-9.46	0.7092600
SP12	Las Cabreras, Spain	Las Cabreras	Europe	Spain	Las Cabreras	1.45	-9.57	0.7093900
SP13	Las Cabreras, Spain	Las Cabreras	Europe	Spain	Las Cabreras	0.10	-11.04	0.7094600
SP14	Las Cabreras, Spain	Las Cabreras	Europe	Spain	Las Cabreras	0.35	-10.90	0.7134200
SP15	Las Cabreras, Spain	Las Cabreras	Europe	Spain	Las Cabreras	0.53	-10.75	0.7114000
SP20	Los Covachos, Spain	Los Covachos	Europe	Spain	Los Covachos	2.72	-5.90	0.7090000
SP18	Los Covachos, Spain	Los Covachos	Europe	Spain	Los Covachos	2.90	-6.20	0.7090200
SP19	Los Covachos, Spain	Los Covachos	Europe	Spain	Los Covachos	2.44	-6.09	0.7086500
SP21	Los Covachos, Spain	Los Covachos	Europe	Spain	Los Covachos	2.86	-6.11	0.7089000
SP17	Los Covachos,Spain	Los Covachos	Europe	Spain	Los Covachos	2.64	-5.78	0.7091600
SP1	Macael, Spain	Macael	Europe	Spain	Macael	1.59	-9.37	0.7077500
SP2	Macael, Spain	Macael	Europe	Spain	Macael	1.04	-7.92	0.7079000
SP3	Macael, Spain	Macael	Europe	Spain	Macael	2.02	-8.40	0.7077600
SP4	Macael, Spain	Macael	Europe	Spain	Macael	1.95	-6.71	0.7077900
SP5	Macael, Spain	Macael	Europe	Spain	Macael	0.04	-8.52	0.7083200
SP6	Macael, Spain	Macael	Europe	Spain	Macael	1.96	-7.62	0.7077400
SP7	Macael, Spain	Macael	Europe	Spain	Macael	1.75	-7.21	0.7080100
SP8	Macael, Spain	Macael	Europe	Spain	Macael	1.97	-8.03	0.7078600

F28/990	Marmorgefässbruchstück	Kumtepe				2.67	-6.31	
F29/460	Marmorgefässbruchstück	Kumtepe				2.85	-5.49	
F28/958/1	Marmorgefässbruchstück	Kumtepe				0.54	-13.55	
Z7/732	Round stone	Toia BA				1.10	-6.23	
D3/30	Polish stone fragment	Toia BA				1.89	-5.07	
D9/106	Fragment	Toia BA				3.55	-8.22	
E8/354(44)	Bracelet fragment	Toia BA						
E4/640(149)	Marbledisc Fragment	Toia BA				3.40	-4.17	
G6/42(1)	Fragment	Toia BA				-0.43	-5.63	
D7/48	Pendant fragment	Toia BA						
E4/5/100	Alabaster bowl fragment	Toia BA						
D8/1755	Polish stone	Toia BA				1.97	-6.56	
E4/5/95	Polish stone	Toia BA				2.74	-4.36	
K12/B38	Marblefragment of a bowl	Toia BA				2.31	-0.99	
E9/1297	Marblefragment	Toia BA				1.38	-4.61	
Y8(1)/100	Pendant	Toia BA				2.31	-12.56	
K17/1138	Disc	Toia BA				3.13	-6.42	
A8/491	Marbleknob	Toia BA				1.12	-8.03	
D3/449	Bowlfragment	Toia BA						
D2/190		Toia BA						
I9/393	Marble pendant	Toia BA				2.27	-6.85	
Blegen		Toia BA						
91/44 (7)	Idolfragment	Toia BA						
T-44/58 (4)	Fragment	Toia BA						
T-8/14 (3)	Polish stone	Toia BA				2.50	-3.90	
T23 (5)	Fragment	Toia BA				2.96	-3.24	
PBA1	Athena Temple Metope, Troia	Toia				3.59	-2.06	
PBA2	Athena Temple, Metope with giant (A236)Troia	Toia				2.88	-5.09	
PBA3	Athena Temple, Cornice with palmette, Troia	Toia				2.54	-1.66	
PBA4	Athena Temple, Doric capital (A231), Troia	Toia				2.50	-0.94	

PBA5	Athena Temple, Ceiling coffer, Troia	Toia	2.50	-3.13	
PBA6	Athena Temple, Ceiling coffer (A226) Troia	Toia	3.41	-2.28	
PBA7	Athena Temple Portico, Doric frieze, Troia	Toia	3.22	-2.29	
PBA8	Athena Temple Portico, Doric frieze, Troia	Toia	2.38	-2.73	0.7076460
PBA9	Athena Temple Portico, Doric frieze, Troia	Toia	4.64	-6.08	
PBA10	Athena Temple Portico, Doric frieze, Troia	Toia	4.26	-7.80	
PBA11	Sanctuary, "Roman altar", base molding, Troia	Toia	2.38	-6.70	
PBA12	Sanctuary, "Roman altar", base molding, Troia	Toia	2.72	-1.60	
PBA13	Sanctuary, "Roman altar", base molding, Troia	Toia	2.84	0.21	
PBA14	Bath, Blue marble building, Troia	Toia	4.24	-2.80	
PBA15	Bath, Blue marble building, Troia	Toia	4.22	-2.56	
PBA16	Bath, Blue marble building, Troia	Toia	3.91	-3.17	
PBA17	Sanctuary, North building threshhold, Troia	Toia	2.92	-0.84	
PBA18	Sanctuary, North building threshhold, Troia	Toia	2.17	-1.99	0.7076100
PBA19	Bouleuterion, Seats, Troia	Toia	3.43	-2.80	0.7075210
PBA20	Bouleuterion, Seats, Troia	Toia	5.45	-5.19	
PBA21BLAU	Bouleuterion, Seats, Troia	Toia	3.38	-1.65	
PBA21WEISS	Bouleuterion, Seats, Troia	Toia	2.95	-2.22	0.7076400
PBA22	Children of Claudius, Dedicatory Inscription, Troia	Toia	2.37	-1.73	
PBA23	Odeion, Architectural element, Troia	Toia	2.82	-3.09	
PBA24	Odeion, Architectural element, Troia	Toia	2.45	-2.74	0.7076600
PBA25	Odeion, Architectural element, Troia	Toia	2.48	-1.85	
PBA26	Odeion, column, Troia	Toia	2.51	-2.94	0.7076490
PBA27	Odeion, column, Troia	Toia	2.18	-1.69	
PBA28	Odeion, column, Troia	Toia	2.16	-2.31	
PBA29	Odeion, column, Troia	Toia	2.23	-3.68	
PBA30	Bath, Nymphaeum base molding, Troia	Toia	5.45	-5.19	
PBA31	Bath, Nymphaeum base molding, Troia	Toia	5.25	-3.62	
PBA32	Bath, Molding, Troia	Toia	3.31	-2.12	0.7077190
PBA33	Bath, Molding, Troia	Toia	3.60	-11.20	
PBA34	Bath, Molding, Troia	Toia	3.09	-10.92	
PBA35	Troia	Toia	3.23	-1.20	